A MODEL AND CALCULATIONS FOR THE PROPERTIES OF AN EXPLODING PLASMA SPHERE

By

RUFUS ELBRIDGE BRUCE, JR.

Bachelor of Science
Louisiana State University
Baton Rouge, Louisiana
1949

Master of Science
Oklahoma State University
Stillwater, Oklahoma
1962

Submitted to the Faculty of the Graduate School of
the Oklahoma State University
in partial fulfillment of the requirements
for the degree of
DOCTOR OF PHILOSOPHY
May, 1966

OKLAHOMA
STATE UNIVERSITY
LIBRARY

NOV 8 1966

A MODEL AND CALCULATIONS FOR THE PROPERTIES

OF AN EXPLODING PLASMA SPHERE

Thesis Approved:

Francis C. Todd
Thesis Adviser

H Harrington

Leon W. Schroeder

W. J. Lewis

R B Leal

J W Boggs
Dean of the Graduate School

621470

PREFACE

This work was undertaken at the suggestion of Dr. F. C. Todd who acted as the author's advisor and project supervisor. The purpose of the study was to investigate some of the phenomena associated with the plasma resulting from the impact of a hypervelocity particle on an aluminum target.

The specific problem undertaken was intended to yield an analytical method for determining the properties of an exploding sphere of an alumnium plasma. The calculated properties were to form a basis for confirming laboratory experiments. The analytical model was to be applicable to a more detailed analysis.

The assistance and guidance of Dr. Todd have been invaluable in the completion of this work. The author is grateful to Mr. B. A. Sodek for the many discussions concerning the formulation and construction of the digital computer program. The author is also indebted to Dr. Jerry MacIntire for his extensive aid in reviewing the material in the first six chapters of the thesis.

The work was carried out under NASA Contract Number NASr-7 administered through the Research Foundation, Oklahoma State University.

TABLE OF CONTENTS

TABLE OF CONTENTS (Continued)

LIST OF TABLES

LIST OF TABLES (Continued)

LIST OF FIGURES

LIST OF FIGURES (Continued)

LIST OF FIGURES (Continued)

LIST OF FIGURES (Continued)

LIST OF FIGURES (Continued)

CHAPTER I

INTRODUCTION

When a small particle with a hypersonic speed strikes a stationary plane metallic target, several interesting phenomena are observed (Charters, 1960). Within the first microsecond of the impact, a very brief, but intense, light flash is emitted. The impact results in an almost perfectly hemispherical crater which is many times larger than the projectile. In addition, the crater may have a small curled lip around the periphery. During the crater formation, ultra-high speed photography shows the emanation of a fine, high velocity spray from the crater region which is in the form of a cylinder.

High speed particles occur, naturally, in the region above the atmosphere of the earth. They are called micrometeoroids while in space. The NASA project, which has supported the research for this thesis, began as an analytical study of micrometeoroid impact with emphasis on aluminum as a target material. Lake (1962) reported on a theoretical solution to the impact problem which was based upon a model proposed by Dr. F. C. Todd, project director. The essential features of this model consist of the formation of a plasma from the projectile and impacted target material and the propagation of a shock wave radially outward from the point of initial contact. Subsequently, Sodek (1965) devised a theoretical determination of the essential properties of the impact of a spherical micrometeoroid on a semi-infinite plane.

Lake and Sodek confirm, in detail, the broader assumptions of this impact model. With aluminum as a target material and a micrometeoroid of normal mass and velocity, peak material pressures in the order of tens of megabars were predicted. Such pressures are sufficient to convert the impacted material into a hot, dense plasma. Experimental evidence of such a plasma has been confirmed by Alexander (1962). Project work is now directed toward the evaluation of the properties of such a plasma.

The subject of paramount interest and of this study is the relation of the thermodynamic properties of the plasma with the energy and size of the impacting micrometeoroid. In theory, the properties of the plasma spray may be studied through a detailed, experimental examination of the spectra of the emitted light. This examination must include intensity-time measurements on the spectra. The interpretation of the experimental results is, however, very difficult. The emitted light is a very complicated function of the temperature, density, ionization and speed of the plasma spray. Before the light can be related to the thermodynamic properties of the plasma, the physical characteristics of the spray must be understood. Furthermore, the interpretation of the plasma spray properties in terms of the initial state parameters is more difficult. In order to partially resolve this difficulty, a theoretical solution was sought for the following problem which is a simplification of the actual phenomena.

Statement of the Problem

Consider an isolated aluminum sphere which has the radius, R_o. At times $t = 0$, let the energy density in the sphere be E_o, a constant value

throughout the sphere, sufficient in magnitude to cause the aluminum to be a hot plasma at solid density. Since solid density is assumed, the value of the energy density, E_o, may also be expressed in terms of the initial energy content per atom of aluminum in the solid state. In addition, a radial electric field is imposed between the sphere and an external, concentric, spherical electrode. Thermodynamic equilibrium is assumed to exist initially and during the subsequent expansion of the sphere of plasma. The immediate objectives of the problem is to obtain values, throughout the plasma during its expansion, for the pressure, temperature, density, flow velocity and ionization of the plasma as a function of several values for E_o.

The problem was designed to determine the characteristics of the continuous spectra that is emitted as the plasma sphere expanded into a vacuum. In order to determine these characteristics, it was necessary (1) to construct an improved equation of state for aluminum, and (2) to use the improved equation of state to analytically determine the pressure temperature, density, flow velocity and ionization of the plasma as a function of time and of spatial coordinates with E_o as a parameter. From the analytically determined, spatial distributions, the basic properties of the emitted light may be predicted. In this manner, it is possible to correlate the characteristics of the emitted spectra with the original energy input.

To summarize, the solution to the proposed problem that is presented in this thesis may be divided into three parts: (1) development of an improved equation of state for a rapidly expanding sphere of plasma, (2) the use of this equation of state to predict the values of the listed

variables throughout the plasma as a function of E_o when a sphere of plasma expands into a vacuum, and (3) the presentation of the equations to calculate the spectral energy distribution of the continuum radiation from the sphere of plasma as it rapidly expands. In this list of the parts of the thesis, the first two have been investigated with a digital computer and numerical solutions are given for a range of values of E_o. The equations and the techniques are given for the third part of the thesis, but the digital computer calculations are not yet complete.

Treatment of the Problem

A solution to the proposed problem is sought in terms of quantities that may be observed in experiments, or checked against prior analytical studies. The analytical problem introduces several unknown constants, several approximations and some equations of limited pressure-temperature range. In order to investigate these uncertainties and the validity of the assumption of local thermodynamic equilibrium, the equation of state for the analytical solution must be checked. For low densities and high temperatures, the check on the analytical predictions is provided by the assumption that the equation of state for the plasma approaches to the perfect gas law. An experimental check on the analytical solution is necessary, and practically essential, for high densities and relatively low temperatures. For this range, a convenient laboratory experiment is the application of the "exploding wire" techniques to short wires. If a part of the "exploding wire" expands into an evacuated portion of a hollow sphere, this portion may be employed to simulate very closely to an "exploding sphere" of plasma. This experiment may be employed as a

calibration point provided the energy input to the exploding wire is accurately known. For higher temperatures and pressures, a second experimental approximation is the "hemispherical plasma" which forms when the giant pulse of light from a laser is incident on a slab of aluminum. Both of these experiments are being assembled.

From the similarity between the exploding wire and the analytical problem as stated, one concludes that many of the expansion and spectral characteristics will be the same. Among these similar characteristics are the following:

a) Exploding wires appear to explode as hollow cylinders

b) Shortly after the expansion begins, the wire appears to be covered with a darkened shell which quickly disappears

c) The emitted light indicates a temperature substantially lower than that corresponding to the energy content.

The above characteristics indicate that:

1) The new equation of state must account for all important energy components;

2) The most important energy transfer and loss mechanisms must be included in a conservation of energy equation.

The problem has been formulated incorporating the above features. In Chapters II and III the theory of a modified semi-classical equation of state is developed. The numerical method used to compute the equation of state is reviewed in Chapter IV. The flow problem is formulated in Chapter V and the numerical method is outlined in Chapter VI. Equations to calculate the emitted continuous spectra are determined in Chapter IX. Results and interpretations of the results of the study comprise the remainder of the text.

CHAPTER II

CONFIGURATION INTEGRAL

1. Introduction

For calculation of the expansion of a plasma, an equation of state is required that is valid over the entire pressure range for which the calculation is to be valid. Deviation from the perfect gas law is large at high pressures and the deviation decreases to negligible values as the pressure decreases. The historic problem for obtaining the equation of state is the evaluation of the interaction forces between the particles in the plasma. These forces have been stated in mathematical terms and their determination requires the evaluation of the interaction partition function, or configuration integral. The partition function consists of the product of several terms in which each term is simply related to the Helmholtz free energy for each component in the plasma. Through the evaluation of this function, one may obtain the thermal and ionic properties of non-ideal gases. The approximation by the perfect gas law with no interaction forces is not applicable for a high density plasma. In the discussion in this thesis, the configuration integral is evaluated for two body interactions. In another thesis, that is in preparation, the interaction forces are calculated for three body interactions, which are then added to the two body interactions.

This chapter is devoted to the solution of the configuration integral and to its effect upon thermodynamic and ionization properties. Its evaluation, using cluster integral theory, forms the basis for the development of a consistant classical equation of state for a real plasma. The term, consistant, indicates that the methods and approximations in evaluating the thermal properties are the same as those used in the ionization part of the problem. The term, "real", implies that the theory is developed for a plasma that is composed of electrons, ions and neutral atoms of finite sizes which interact with relative position-dependent potentials. The theory is rigorous to the extent of the rigor of the cluster expansion method and is valid within the limits of classical statistics. Radially symmetric forces are assumed to exist around the atoms, ions and electrons.

The theory of plasma equations of state will be developed in a straight-forward statistical manner. Starting with the partition function for the system, it will be shown that solutions both of the ionization properties and of the thermodynamic properties depend upon the evaluation of the excess Helmholtz free energy: the contribution to the free energy from the interaction potentials. Some of the main approximation methods to evaluate this interaction are outlined. Finally it will be shown that the same method for evaluating the interaction free energy may be used to produce a consistent theory.

In Section 2, the configuration integral shall be introduced and it will be shown that thermodynamic terms arising from its evaluation may be considered as additive corrections. In Section 3, the form of the Helmholtz free energy correction resulting from different approximations

will be given. Several methods of evaluating ionization properties of a plasma are considered in Section 4. A consistent theory will be presented in Section 5.

The development of the complete equation of state is in Chapter III. The numerical method used to tabulate the equation of state is in Chapter IV. A comparison of the equation of state resulting from the various approximations is given in Chapter VII.

2. Formulation--The Configuration Integral

A generalized form of the partition function is expressable as the product of separate components. It follows that the resulting thermodynamic properties of the system components are additive. Consider a partition function, expressible as a product:

$$Z_T = Z_A Z_B Z_C \cdots\cdots Z_N , \tag{2.1}$$

where the Z_I's are partition functions for separable subsystems of the entire system. The Helmholtz free energy is related to the partition function by

$$A_T = -kT \ln Z_T , \tag{2.2}$$

in which k is the Boltzmann constant and T is the temperature. Combining 2.1 and 2.2, one determines that

$$A_T = A_A + A_B + A_C + \cdots + A_N , \tag{2.3}$$

where

$$A_i = -kT \ln Z_i . \tag{2.4}$$

By the usual thermodynamic relations, it follows that the remaining thermodynamic properties are also separable and additive. The principal relations are summarized below:

$$S_i = -\left(\frac{\partial A_i}{\partial T}\right)_{V,N_i} = \text{Entrophy Component}\ ; \tag{2.5}$$

$$P_i = -\left(\frac{\partial A_i}{\partial V}\right)_{T,N_i} = \text{Pressure Component}\ ; \tag{2.6}$$

$$\mu_i = \left(\frac{\partial A_i}{\partial N_i}\right)_{T,V,N_j} = \text{Component Chemical Potential}\ ; \tag{2.7}$$

$$E_i = -T^2\left(\frac{\partial}{\partial T}\left[A_i/T\right]\right)_{V,N_i} = \text{Component Internal Energy}\ ; \tag{2.8}$$

in which V is the volume, and N_i is the density of the i^{th} species.

The interaction partition function, configuration integral, can be represented by one of the Z_I's of Equation 1. In the formation of the classical canonical ensemble, the volume in phase space that is occupied by the system is called the partition function, Z:

$$Z = \frac{1}{N!\ h^{3N}} \int dp\, dr\ \exp\left[-H(p,r)/kT\right]. \tag{2.9}$$

In 2.9, H(p,r) is the N-particle (identical particle) Hamiltonian

$$H(p,r) = \sum_{i=1}^{N} \frac{p_i^2}{2m} + U(N)\ , \tag{2.10}$$

in which p_i is momentum of the i^{th} particle and U(N) is the interaction

potential energy of the system*. U(N) is expressed as the sum of all 2-body potentials of the form

$$U(N) = \sum_{pairs} w(r_{ij}) \; ; \quad w(r_{ij}) = w(|\vec{r}_i - \vec{r}_j|) . \tag{2.11}$$

The integration of 2.9 is over the 3N position and the 3N momentum coordinates. Thus

$$dp = \prod_{j=1}^{N} d^3p \tag{2.12}$$

and

$$dr = \prod_{j=1}^{N} d^3r \; . \tag{2.13}$$

The integral is immediately separable into two parts:

$$Z = \frac{1}{N!\, h^{3N}} \left[\int \exp\left[-\sum_i \frac{p_i^2}{2m} / kT \right] dp \right] \left[\int \exp\left[-\sum_{i \neq j} w_{ij} / kT \right] dr \right] . \tag{2.14}$$

If all of the potentials are identically zero, the last integral on the right of 2.14 yields a factor, V^N, which results from N, independent vector coordinates which are integrated over the volume. This yields the ideal, or transitional partition function, Z_{TR}:

---

*Strictly speaking, U(N) is not the system's potential energy but the potential of average force. (See Appendix II).

$$Z_{TR} = \frac{V^N}{N!\, h^{3N}} \int \exp\left[-\sum_i \frac{p_i^2}{2m} / kT\right] dp . \tag{2.15}$$

For indistinguishable particles, this integral becomes

$$Z_{TR} = \frac{V^N}{N!\, \lambda^{3N}} , \tag{2.16}$$

where λ is the mean thermal de Broglie wavelength:

$$\lambda = \frac{h}{(2\pi m kT)^{1/2}} . \tag{2.17}$$

Thus, 2.14 may be written as

$$Z = Z_{TR}\, Z_{IN} \tag{2.18}$$

where Z_{IN} is called the configuration integral, or interaction partition function, and is defined by

$$Z_{IN} = \frac{1}{V^N} \int \exp\left[-\sum_{i \neq j} v_{ij} / kT\right] dr . \tag{2.19}$$

The configuration integral is simply the expectation value of the interaction potential. Its evaluation leads directly to the excess Helmholtz free energy, A_{IN} using

$$A_{IN} = -kT \ln Z_{IN} . \tag{2.20}$$

Knowledge of A_{IN}, or the evaluation of Z_{IN}, is needed for specification of thermodynamic and ionization properties.

3. Effect of Interaction on the Thermodynamic Properties

To determine the effect of the interaction potentials on the thermodynamic properties, one has the choice of evaluating $\ln Z_{IN}$, or of calculating F_{IN} directly. In the following parts of this section, various methods are outlined for this evaluation.

a. Debye-Huchel Approximation

The classic solution of interest is the Debye and Huckel's theory for calculating the electrostatic contribution to the thermodynamic properties of ionic solutions (P. Debye, et al 1923). Roseland, in 1924, suggested the application of this theory to ionized gases. A very brief sketch of the theory is given here; and more detailed treatments may be found in standard statistical mechanics texts (R. H. Fowler, 1936; R. Fowler and E. A. Guggenheim, 1956; R. A. Robinson and R. H. Stokes, 1955).

Following Fowler and Guggenheim (1956), the excess Helmholtz free energy is related to the average electrostatic microfield, $\bar{\psi}_\alpha$ by

$$\epsilon \bar{\psi}_\alpha = \frac{\partial A_{IN}}{\partial \epsilon_\alpha} \, , \tag{2.21}$$

where ϵ is the electronic charge, ϵ_α is the charge on the species, α, and the A_{IN} can be placed in the Pfaffian form: $dA_{IN} = \sum_\alpha \left(\frac{\partial A_{IN}}{\partial \epsilon_\alpha}\right) d\epsilon_\alpha$.

This leads to the relation,

$$A_{IN} = \int \sum_\alpha \epsilon \bar{\psi}_\alpha \, d\epsilon_\alpha \, . \tag{2.22}$$

The average field is obtained by linearizing the Poisson-Boltzmann equation,

$$\nabla^2 \bar{\psi}_\alpha(r) = \frac{-4\pi}{DV} \sum_\beta \epsilon_\beta \exp\left[-\epsilon_\beta \bar{\psi}_\alpha(r)/kT\right] \tag{4.23}$$

to obtain

$$\nabla^2 \bar{\psi}_\alpha(r) = \kappa^2 \bar{\psi}_\alpha(r), \tag{2.24}$$

where

$$\kappa^2 = 4\pi \sum_i C_i \epsilon_i^2 / kTD. \tag{2.25}$$

C_i is the particle number density of the i^{th} species in the gas and D is the dielectric constant. The solution of 2.24 is,

$$\bar{\psi}_\alpha = \frac{A'}{r} e^{-\kappa r} \tag{2.26}$$

where A' is determined by matching potentials at the surface of the atom, which is presumed to be a sphere of radius "a". This potential is the Debye, or Yukawa potential. Its range is designated the Debye length, and is the recripical of κ; i.e. $\lambda_D = 1/\kappa$. Completing the integration of 2.22 by using 2.26 and neglecting the product κa, leads to the Debye Limiting Law for the interaction free energy per unit volume:

$$F_{IN}^{DH} = -\frac{kT\kappa^3}{12\pi} = -\kappa \sum_i C_i \epsilon_i^2 / 3D \tag{2.27}$$

The pressure and internal energy density corrections for the limiting law are obtained from Equations 2.6, 2.8 and 2.27). These give

$$P_{IN}^{DH} = -\frac{\kappa}{6D} \sum_i C_i \epsilon_i^2 \tag{2.28}$$

and

$$E_{IN}^{DH} = -\frac{\chi}{2D} \sum_i C_i \epsilon_i^2 . \tag{2.29}$$

The negative sign in Equations 2.27 thru 2.29 reflects the ordering, or the collective polarization effect, which results from the interaction of the electrostatic microfields.

This theory would be valid for high density if χ were not dependent upon the density. For the statistical argument to apply, a large number of particles must be within the potential range, λ_D. This dependence of λ_D upon C_i makes the theory a low density approximation.

The second limitation of the theory arises from the linearization of 2.23. For higher order terms to be negligible, the average electrostatic energy must be smaller than the thermal energy. If A_{ij} is the distance at which the thermal and electrostatic static energies are equal, then

$$|A_{ij}| = \frac{|\epsilon_i \epsilon_j|}{DkT} \leq (3/4\pi C)^{1/3} . \tag{2.30}$$

In the regions of validity for the theory, the resulting corrections are usually very small when compared to the ideal gas theory and can usually be neglected without serious error.

Various extensions and validity criteria of the theory are reviewed by Duclos and Cambel (1962).

b. Mayer-Ursell Cluster Expansions

The technique for obtaining the properties of an imperfect gas was solved, in principal, by Mayer and Mayer (1940) in the sense that

any, selected virial coefficient could be expressed explicitly as a multiple integral provided that the interactions were position dependent with respect to each other. The use of coulomb potentials created divergences in the integrals and prevented their application to ionized media. J. E. Mayer (1950) devised a method for using coulomb potentials in the theory. He obtained the Debye correction as the first term of an expansion.

The theory provides a mathematically rigorous method for evaluating the configuration integral

$$Z_{IN} = V^{-N} \int \exp\left[-\sum_{i \neq j} w_{ij}/kT\right] dr \qquad (2.19)$$

by expanding the exponential in terms of the cluster function,

$$f_{ij} = \exp(-w_{ij}/kT) - 1 \qquad (2.31)$$

This procedure converts Equation 2.19 to a series of integrals (of which the first few are reasonably easy to evaluate).

No attempt is made to outline Mayer's method in this report. An outline of the cluster theory which is based upon the development by H. L. Friedman (1962) is given in Appendix II. For details, references in that appendix should be consulted. By necessity, some of the terminology introduced in Appendix II will be used in this chapter.

In formulating his theory of ionic solutions, Mayer (1950) evaluates the second order cluster integrals, when u = 2, for the primative, short-range potential (rigid spheres) combined with the Yukawa potential. This potential is expressed as

$$u(r_{ij}) = u^{+}(r_{ij}) + (\epsilon_i \epsilon_j / D r_{ij}) e^{-\chi r_{ij}}, \qquad (2.32)$$

where $u^{+}(r_{ij})$ is the short range potential specified by

$$u^{+}(r_{ij}) = \infty \quad ; \quad r_{ij} \leq a_{ij} \,,$$
$$u^{+}(r_{ij}) = 0 \quad ; \quad r_{ij} > a_{ij} \,. \tag{2.33}$$

"a_{ij}" is the distance of closest approach. After showing that the ring graph contribution was the Debye correction, Mayer collected the remaining two body interactions as a sum of integrals. J. C. Poirier (1952) has tabulated the integrals in terms of convenient parameters. The results have been summarized by Duclos and Cambel (1962). The interaction free energy per unit volume from the Mayer solution is given by

$$F_{IN}^{MA} = -\frac{kT\varkappa^3}{12\pi} - \frac{kT}{2\sum_i c_i z_i} \sum_{\lambda} \sum_{j} \sum_{\nu} c_i c_j z_i^{\nu} z_j^{\nu} (-1)^{\nu} \alpha_{ij}^{1-\nu} \left[b_{\nu}(\phi_{ij}) + g_{\nu}(\phi_{ij}) \right]. \tag{2.34}$$

In 2.34

c_k = number density of k^{th} ionic species

z_k = dimensionless charge of k^{th} ionic species

$b_{\nu}(\phi)$ = integral evaluated by Poirier for various values of ϕ

$g_{\nu}(\phi)$ = integral evaluated by Poirier for various values of ϕ

k = Boltzmann constant

T = temperature

$\varkappa$ = Debye parameter

α_{ij} = a_{ij} DkT/e^2

ϕ_{ij} = a_{ij}/λ_D

e = electron charge

λ_D = $1/\varkappa$ = Debye length

ν = parameter indicating additional Coulomb bond chains between the two particles.

For plasmas, the usual procedure is to fix the distance of closest approach as that distance for which thermal and electrostatic energies of the i^{th} and j^{th} particles are equal, Equation 2.30. Duclos and Cambel (1961) suggest that a better approximation may be given by

$$a_{ij} = C_a \left[-\frac{\lambda_D}{2} + \left(\frac{\lambda_D^2}{4} + A_{ij} \lambda_D \right)^{1/2} \right], \tag{2.35}$$

where C_a is arbitrary and

$$A_{ij} = \left| z_i z_j \right| e^2 / DkT. \tag{2.30}$$

A reasonable validity criteria for Mayer's solution is given by

$$a_{ij} \leq (C_T)^{-1/3}. \tag{2.36}$$

This simply states that the distance of closest approach must be smaller than the average distance between particles.

Thus, within the separation limits in Equation 2.36, the imperfect-gas, free-energy correction is specified by Equations 2.30, 2.34 and 2.35. Combining these with 2.5 thru 2.8 allows one to determine the corrections to the other thermodynamic properties of the plasma.

c. Exact Formulism

In 1957, Meeron (1957) showed that Mayer's sum of integrals for the 2nd order term could be converted to a single integral of a closed form. Further improvements in the formalism are included in the discussion in Appendix II. Using the set notation shown in Appendix I, the interaction free energy per unit volume is

$$F_{IN} = -kT \left[\frac{\kappa^3}{12\pi} + \sum_{\underline{u}}^{11} c^{\underline{u}} B_{\underline{u}}(\kappa) \right] \tag{2.37}$$

where $\underline{C}$ is the concentration set, κ is the Debye parameter and the $B_{\underline{u}}(\kappa)$ are cluster integrals. The symbol $\sum_{\underline{u}}''$ indicates the sum over all subsets of the composition set, starting with u = 2 and

$$\underline{C}^{\underline{u}} = C_1^{u_1} C_2^{u_2} \cdots C_\sigma^{u_\sigma}$$

where C_i is concentration of the i^{th} component and u_i is the element of the concentration subset $\underline{u}$ (the number of i^{th} species in the subset $\underline{u}$). The integrand for any order cluster integral can be expressed in the formalism of ϕ-bonds (Equations A2.62 thru A2.65 in Appendix II). The integrals for the second order terms take the following form:

$$B_{ab}(\kappa) = \left[V(1+\delta_{ab})\right]^{-1} \int_V \left\{ \left[1+k_{ab}\right] \exp(q_{ab}) - 1 - q_{ab} - q_{ab}^2/2 \right\} d\{a,b\}, \qquad (2.38)$$

where

$$k_{ab} \equiv \exp\left[-u_{ab}^{+}/kT\right] - 1 \qquad (2.39)$$

and

$$q_{ab} \equiv -\left[(4\pi\varepsilon^2/DkT)\, z_a z_b \exp(-\kappa r)\right]/4\pi r. \qquad (2.40)$$

In the preceeding equations:

δ_{ab} = kronocker delta

u_{ab}^{+} = is an arbitrary short range potential

ε = electron charge

D = dielectric constant

z_a = dimensionless charge parameter

r = distance between two bodies

κ = Debye parameter.

In terms of the cluster integral, Equation 2.38, the free energy per unit volume becomes (through the 2nd order terms only)

$$F_{IN} = -kT\left[\frac{\chi^3}{12\pi} + \sum_{a\leq b}^{\sigma} \frac{C_a C_b}{V(1+\delta_{ab})} \int_V \left\{\left[\left[1+k_{ab}\right]e^{q_{ab}} - 1 - q_{ab} - q_{ab}^2/2\right\} d\{a,b\}\right]. \quad (2.41)$$

The above expression is rigorous within the limits of classical statistics (Friedman, 1962). In 2.37, accuracy is limited only by the validity of the short range potentials (u^+_{ab}) and the number of terms considered (maximum value of $\underline{u}$ in the summation). This latter point is one of the uncertainties of the theory. While convergence of the series is accepted, the speed of convergence is not known. When the theory is used for ionic solutions, the general procedure is to use sufficient terms to give agreement with experimental data. Unfortunately, there are no experimental data yet available for very high density plasmas, thus other means must be devised to check the numerical results. This will be discussed in the next section.

d. Exact Primitive Potential Formalism and Extensions to Arbitrary Short Range Potentials

In view of the preceeding discussion, the most reasonable course of action appears to be the following:

1. Develop the theory for an arbitrary, short-range potential in a form that is suitable for manipulation of the potentials;
2. Evaluate the free energy through the second order terms;
3. Fit to reasonable approximations, by variation of the potential parameters.

The Thomas-Fermi model for an equation of state is chosen as a reasonable, high-density, high-temperature approximation. An ideal gas is chosen as the best approximation for low densities. The problem of fitting the calculated results at these two extremes, immediately presents two requirements:

1. The short range potentials must be expressable in terms of convenient parameters;
2. The integrals (2.41) must be cast into a form that allows convenient manipulation of these parameters.

In the remainder of this section it will be shown how the primitive potential solution may be used to satisfy the above requirements.

The exact solution for the primitive potential is obtained from 2.38. By transforming to relative coordinates and integrating over the center of mass coordinate, a factor of V is found, which cancels the V in 2.38. Converting to spherical coordinates and integrating over the angular part, the relation yields

$$B_{ab}(x) = \frac{4\pi}{(1+\delta_{ab})} \int_0^\infty \left\{ \left[1 + k_{ab} \right] e^{q_{ab}} - Q_{ab} \right\} r^2 dr \qquad (2.42)$$

where r is the relative distance between particles and q_{ab} is defined by 2.40. Q_{ab} is defined by

$$Q_{ab} \equiv 1 + q_{ab} + q_{ab}^2/2 \,. \qquad (2.43)$$

The primitive potential specifies

$$\begin{aligned} u_{ab}^{+} &= \infty \quad ; \quad r \leq r_{ab} \\ u_{ab}^{+} &= 0 \quad ; \quad r > r_{ab} \end{aligned} \qquad (2.44)$$

which, of course, is a rigid sphere. Substitution of 2.43 and 2.44 into 2.42 leads immediately to

$$B_{ab}(\chi) = \frac{4\pi}{(1+\delta_{ab})}\left[\int_{r_{ab}}^{\infty} e^{q_{ab}} r^2 dr - \int_{0}^{\infty} Q_{ab} r^2 dr\right] . \qquad (2.45)$$

Break the second integral into two integrals, and the integral becomes

$$B_{ab}(\chi) = \frac{4\pi}{(1+\delta_{ab})}\left[\int_{r_{ab}}^{\infty} (e^{q_{ab}} - Q_{ab}) r^2 dr - \int_{0}^{r_{ab}} Q_{ab} r^2 dr\right] . \qquad (2.46)$$

For the primitive potential, the interaction free energy is given by

$$F_{IN} = -kT\left[\frac{\chi^3}{12\pi} + \sum_{a\le b}^{\sigma} c_a c_b \, Q_{ab}^{r_{ab}}\right] \qquad (2.47)$$

where

$$Q_{ab}^{r_{ab}} = \frac{4\pi}{(1+\delta_{ab})}\left[\int_{r_{ab}}^{\infty} (e^{q_{ab}} - Q_{ab}) r^2 dr - \int_{0}^{r_{ab}} Q_{ab} r^2 dr\right] . \qquad (2.46)$$

The distance of closest approach, r_{ab}, may be defined by 2.30 or 2.35.

The preceeding results will now be used to solve the arbitrary potential problem. It is assumed that the short range potentials can be written in the form

$$u_o^{\dagger}(r_{ab}) = u_{ab}^{\dagger}(u_o, r_o, r_{ab}) \qquad (2.48)$$

where u_o and r_o are two parameters which describe the potential. Define a sequence of sectionally uniform step functions

$$f_{ab}(u_o, r_o, r) = \infty \;, \quad 0 \le r < (r_2 - \tfrac{\Delta r}{2}) \;;$$
$$= t_2 \;, (r_2 - \tfrac{\Delta r}{2}) \le r < (r_2 + \tfrac{\Delta r}{2}) \;;$$
$$\vdots$$
$$= t_n \;, (r_n - \tfrac{\Delta r}{2}) \le r < (r_n + \tfrac{\Delta r}{2}) \;;$$
$$= 0 \;, (r_n + \tfrac{\Delta r}{2}) \le r < \infty \;; \tag{2.49}$$

where

$$(r_k - \tfrac{\Delta r}{2}) = (r_{k-1} + \tfrac{\Delta r}{2}) .$$

Further let the sequence be represented by

$$\left\{ f_{ab}(u_o, r_o, r_i), \Delta r \right\} .$$

This may be defined such that for a set of selected r_i's,

$$f_{ab}(u_o, r_o, r_i) = u^{\dagger}(u_o, r_o, r_i). \tag{2.50}$$

This function is defined so the sequence equals the original potential function in the limit

$$u^{\dagger}(u_o, r_o, r_i) = \lim_{\substack{n \to \infty \\ \Delta r \to 0}} \left\{ f_{ab}(u_o, r_o, r_i), \Delta r_i \right\} \tag{2.51}$$

Substitution of this sequence for $u^{+}(r_{ab})$ in 2.38, using 2.38, leads to

$$B_{ab}(x) = \frac{4\pi}{(1+\delta_{ab})} \left\{ \sum_{k=1}^{\infty} \left[\exp\left[-f_{ab}(u_o, r_o, r_k)/kT \right] \int_{r_k - \frac{\Delta r}{2}}^{r_k + \frac{\Delta r}{2}} e^{q_{ab}} r^2 dr - \int_{r_k - \frac{\Delta r}{2}}^{r_k + \frac{\Delta r}{2}} Q_{ab} r^2 dr \right] \right\} . \tag{2.52}$$

For simplification of notation, define the following

$$f_k = \exp\left[-f_{ab}(u_o, r_o, r_k)/kT \right] . \tag{2.53}$$

Using this notation,

$$B_{ab}(x) = \frac{4\pi}{(1+\delta_{ab})}\left\{\sum_{k=1}^{\infty}\left[f_k\int_{r_k-\frac{\Delta r}{2}}^{r_k+\frac{\Delta r}{2}} e^{g} r^2 dr - \int_{r_k-\frac{\Delta r}{2}}^{r_k+\frac{\Delta r}{2}} \rho r^2 dr\right]\right\}. \tag{2.54}$$

To convert 2.54 to the desired form, first add and subtract $f_k\int_{r_k-\frac{\Delta r}{2}}^{r_k+\frac{\Delta r}{2}} \rho r^2 dr$:

$$B_{ab}(x) = \frac{4\pi}{(1+\delta_{ab})}\left\{\sum_{k}\left[\left[f_k\int_{r_k-\frac{\Delta r}{2}}^{r_k+\frac{\Delta r}{2}} (e^{g}-\rho) r^2 dr + f_k\int_{r_k-\frac{\Delta r}{2}}^{r_k+\frac{\Delta r}{2}} \rho r^2 dr - \int_{r_k-\frac{\Delta r}{2}}^{r_k+\frac{\Delta r}{2}} \rho r^2 dr\right]\right]\right\}. \tag{2.55}$$

Regrouping terms and rewriting the ranges of the integrations,

$$B_{ab} = \frac{4\pi}{(1+\delta_{ab})}\sum_{k}\left\{f_k\left[\left(\int_{r_k-\frac{\Delta r}{2}}^{\infty}(e^{g}-\rho)r^2dr - \int_{0}^{r_k-\frac{\Delta r}{2}}\rho r^2 dr\right) - \left(\int_{r_k+\frac{\Delta r}{2}}^{\infty}(e^{g}-\rho)r^2dr - \int_{0}^{r_k+\frac{\Delta r}{2}}\rho r^2 dr\right)\right] + \int_{0}^{r_k-\frac{\Delta r}{2}}\rho r^2 dr - \int_{0}^{r_k+\frac{\Delta r}{2}}\rho r^2 dr\right\}. \tag{2.56}$$

The notation of 2.56 can be simplified by noting that the bracketted integral, i.e.,

$$\left(\int_{r_k-\frac{\Delta r}{2}}^{\infty}(e^{g}-\rho)r^2dr - \int_{0}^{r_k-\frac{\Delta r}{2}}\rho r^2 dr\right) \equiv \frac{1+\delta_{ab}}{4\pi}\,\rho_{ab}^{r_k-\frac{\Delta r}{2}}, \tag{2.57}$$

are the primitive potential solutions. Using this notation, 2.56 is simplified to

$$B_{ab} = \sum_{k}\left\{f_k\left[\rho_{ab}^{r_k-\frac{\Delta r}{2}} - \rho_{ab}^{r_k+\frac{\Delta r}{2}}\right] + \frac{4\pi}{1+\delta_{ab}}\int_{0}^{r_k-\frac{\Delta r}{2}}\rho r^2 dr - \frac{4\pi}{1+\delta_{ab}}\int_{0}^{r_k+\frac{\Delta r}{2}}\rho r^2 dr\right\}. \tag{2.58}$$

By examining the first and last terms of the sum in 2.58, further simplification can be realized. For k = 1, $f_k = 0$, $r_1 + \frac{\Delta r}{2} = r_2 - \frac{\Delta r}{2}$ and $r_1 - \frac{\Delta r}{2} \equiv 0$. The last term k = n+1, $f_{n+1} = 1$, $r_{n+1} + \frac{\Delta r}{2} \equiv \infty$ and $r_{n+1} - \frac{\Delta r}{2} = r_n + \frac{\Delta r}{2}$. Separating the first and last terms of the sum yields

$$B_{ab} = -\frac{4\pi}{(1+\delta_{ab})}\int_0^{r_2-\frac{\Delta r}{2}} \rho r^2 dr + \sum_{k=2}^{n}\left\{ f_k\left[\rho_{ab}^{r_k-\frac{\Delta r}{2}} - \rho_{ab}^{r_k+\frac{\Delta r}{2}}\right] + \frac{4\pi}{1+\delta_{ab}}\int_0^{r_k-\frac{\Delta r}{2}} \rho r^2 dr \right.$$

$$\left. - \frac{4\pi}{1+\delta_{ab}}\int_0^{r_k+\frac{\Delta r}{2}} \rho r^2 dr \right\} + \frac{4\pi}{1+\delta_{ab}}\int_{r_n+\frac{\Delta r}{2}}^{\infty} (e^q - \rho) r^2 dr \quad . \qquad (2.59)$$

The last term is obtained by regrouping the integrals in their original form (2.55). All of the integrals,

$$\int_0^{r_k-\frac{\Delta r}{2}} \rho r^2 dr$$

cancel since $r_k + \frac{\Delta r}{2} = r_{k+1} - \frac{\Delta r}{2}$. Thus 2.59 reduces to

$$B_{ab} = \sum_{k=2}^{n} f_k\left[\rho_{ab}^{r_k-\frac{\Delta r}{2}} - \rho_{ab}^{r_k+\frac{\Delta r}{2}}\right] + \rho_{ab}^{r_n+\frac{\Delta r}{2}} \quad . \qquad (2.60)$$

The interaction free energy for arbitrary potentials is, therefore

$$F_{IN} = -kT\left[\frac{\chi^3}{12\pi}\right.$$

$$\left. + \sum_{a\neq b}^{\sigma} c_a c_b \left\{ \sum_{k=2}^{n} f_{k;ab}\left[\rho_{ab}^{r_k-\frac{\Delta r}{2}} - \rho_{ab}^{r_k+\frac{\Delta r}{2}}\right] + \rho_{ab}^{r_n+\frac{\Delta r}{2}} \right\}\right] , \qquad (2.61)$$

where

$$f_{k;a,b} = \exp\left[-f_{ab}(u_o, r_o, r_k)/kT\right]; \; r_{k+1} = r_k + \Delta r. \qquad (2.62)$$

In this way the evaluation of a very complicated sum of integrals, 2.41, is converted to a double sum of less involved integrals. Given a suitable table of values for the P^r_{ab}, matching the model to experimental data is possible. As Δr is made smaller, the more exact becomes the evaluation.

Outside of a suitable evaluation of the $f_{k;ab}$, the only undetermined quantities are the C_i's. This problem will be discussed in the next section.

4. Ionization Properties

The specifications for the ordinary thermodynamic properties of a plasma are dependent upon the concentration of the various species which compose the plasma. The equation of state must specify ionization consistent with the thermodynamic properties. The usual procedure for plasmas from ideal gases is to use Saha's equation, 2.71. For plasmas with interacting particles, changes must be made in this procedure to account for the observed reduction of the ionization potential. It is desirable that the approximations used in determining the ionization modifications are consistent with those for the thermodynamic properties.

In this section, Saha's equation will be derived and its application discussed. The interaction partition function modifies this equation. These modifications and some of the approximations that are employed to calculate the "effective ionization potential" will be reviewed in the remainder of this section.

a. Saha Equation - Ideal Plasmas

Saha's equation may be derivable from the partition functions for each species. Ecker and Kröll (1962) give the partition function of the a^{th} species as

$$Z_a = \left[Z_a(T)\, Z_a(E) \right]^{N_a} / N_a! = Z_{aT}^{N_a} / N_a! \,, \qquad (2.63)$$

where

$Z_a(T)$ = translational partition function;

$Z_a(E)$ = electronic excitation function;

$Z_{aT} = Z_a(T)\, Z_a(E)$;

N_a = number of the a^{th} ionic species.

The electronic partition is designated by Z_e. The partition function for the system is defined as

$$Z_T \equiv Z_e \prod_a Z_a \,. \qquad (2.64)$$

The relation

$$A = -kT \ln Z \qquad (2.65)$$

may be evaluated using Stirling's approximation for $N!$. This leads to

$$A = -kT \left[\sum_a N_a \left(\ln Z_{aT}/N_a + 1 \right) + \sum_a a N_a \left(\ln \frac{Z_e}{\sum_a a N_a} + 1 \right) \right] \qquad (2.66)$$

since $N_e = \sum_a a\, N_a$. For equilibrium

$$\frac{\partial A}{\partial N_a} = \frac{\partial A}{\partial N_{a+1}} \qquad (2.67)$$

Completing the specified partial derivatives, and, after simplification, it is found that

$$\frac{N_a N_e}{N_{a+1}} = \frac{Z_{aT} Z_e}{Z_{(a+1)T}} \quad . \tag{2.68}$$

By noting that $Z_a(T) \approx Z_{a+1}(T)$ and that $Z_e = 2V(2\, m_e kT)^{3/2}/h^3$, the above equation is reduced to

$$\frac{C_{a+1} C_e}{C_a} = 2\left(\frac{2\pi m_e kT}{h^2}\right)^{3/2} \frac{Z_{a+1}(E)}{Z_a(E)} \quad , \tag{2.69}$$

where m_e is the mass of the electron, h is Planck's constant and all of the other symbols are as previously defined.

The electronic excitation partition functions are defined by

$$Z_i(E) = \sum_j g_{ij} \exp(-E_{ij}/kT) \tag{2.70}$$

in which g_{ij} is the j^{th} level degeneracy and E_{ij} is the energy of the j^{th} level of the i^{th} species. The energy levels are measured from the same reference point, thus the E_{ij} of the a + 1^{th} species have a common factor if the ground level of the a^{th} species is the reference point. The common factor is the ionization energy of the a^{th} species. Separation of this common factor produces Saha's Equation:

$$\frac{C_{a+1} C_e}{C_a} = 2\left(\frac{2\pi m_e kT}{h^2}\right)^{3/2} \frac{Z'_{a+1}(E)}{Z'_a(E)}\, e^{-I_a/kT} \tag{2.71}$$

If the plasma is composed of an element with σ electrons, each possible species of ionization must be considered. To determine the concentration of the various species, one must solve the system of equations

$$C_{a+1} = \frac{C_a}{C_e} \cdot 2\left(\frac{2\pi m_e kT}{h^2}\right)^{3/2} \frac{Z'_{a+1}(E)}{Z'_a(E)}\, e^{-I_a/kT}, \quad a = 1, 2, \cdots, \sigma. \tag{2.72}$$

Except for the simplest cases, the only practical method for solving this system is by iterative, numerical techniques. This is discussed in Chapter III.

b. Effective Ionization Potentials

The system of equation in 2.72 is only valid for an ideal plasma. If there is an interaction potential between the plasma particles, the system must be modified. In practice, this is usually accomplished by replacing I_a with an effective ionization potential that agrees with the experimental observations. This requirement to employ an effective ionization potential follows from the insight that is gained from the Debye-Hückel theory. The microfields of a plasma interact to produce a collective polarization of the plasma. When an atom is ionized by absorption of the energy, I_a, the free electron can go to a lower energy state in the continuum. This lower energy state arises from the partial ordering of the plasma. The energy regained may be considered as a reduction of the ionization potential, ΔI. The effective ionization potential, I_a^*, is defined by

$$I_a^* = I_a - \Delta I_a \quad . \tag{2.73}$$

There are many methods devised to approximate the effective ionization potential. Most of the methods are based, to some degree on the Debye-Hückel theory; and consequently, have limited ranges of validity.

The simplest approximation is to assume that no bound electron can exist in a state which has a radius greater than the Debye radius. Using Balmer-like functions, one is able to determine a maximum bound quantum number and an effective ionization potential. In a somewhat more

sophisticated manner, D. Kelly (1959) used a modified Debye potential with a screening factor as a variable parameter in conjunction with hydrogen state functions. He solved Schroedinger's equation. This procedure resulted in the maximum quantum number, g_i^*, which is given by

$$g_i^* = .804 \lambda_D z_i / a_o \tag{2.74}$$

where λ_D is the Debye radius, z_i is the dimensionless core charge of the i^{th} species and a_o is the 1st Bohr radius. C. A. Rouse (1962) used Kelly's equation for g_i^* and a Balmer-type expression to calculate effective ionization potentials:

$$\Delta I_i = I_i / (g_i^* + 1)^2 \tag{2.75}$$

A slightly different procedure was reported by Bruce, et al, (1964). For hydrogen, a direct solution for I* was obtained from Schroedinger's equation with the Debye (Yukawa) potential. The effective ionization potential was calculated for various values of the Debye radius, by utilizing Hülthen and Laurikainen's (1936) eigenvalue problem study. The variation of I* with λ_D is shown in Figure 2.1. In high density regions, much higher ionizations were calculated than were predicted by any of the preceeding methods. Deviations from the predictions of the next method to be outlined were insufficient to warrant further effort in this direction.

c. Method of Ecker and Kröll

The preceeding methods become somewhat questionable beyond the validity limits of the Debye-Huckel theory. It may be shown (Ecker, 1962) that the upper limit of particle density for a valid application

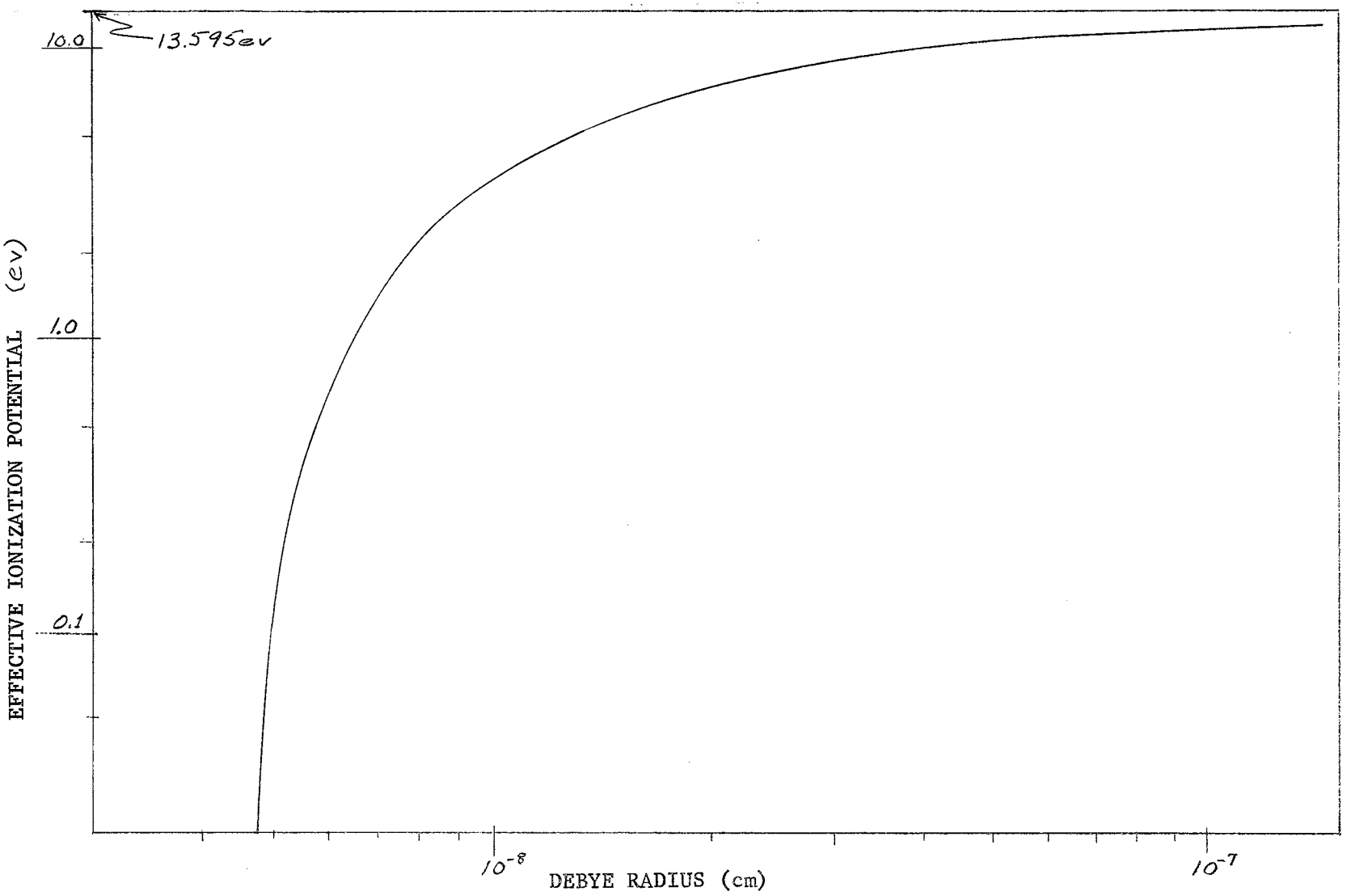

Figure 2.1. Effective Ionization Potential for Hydrogen as a Function of the Debye Length.

of the Debye-Huckel theory is given by

$$C_{CR} = \left(\frac{3}{4\pi}\right)\left[\frac{kT}{\epsilon^2_{i_{max}}}\right]^3 \tag{2.76}$$

where C_{cr} is called the critical density and $\epsilon_{i_{max}}$ is the maximum ionic core charge in the plasma. In 1962, Ecker and Kröll (ibid.) reported a method for calculating ΔI that is valid beyond the above limit and to the semiclassical limit

$$C_e < \left[\frac{2\pi m_e kT}{h^2}\right]^{3/2} \tag{2.77}$$

Ecker and Kröll introduce an interaction partition function and find the extent to which this modifies the Saha equation. Assuming the Coulomb interactions are responsible for this interaction, they develop equations for ΔI in density regions both above and below the critical density.

In arriving at their result, they introduce an interaction partition function, Z_{IN}, in Equation 2.64. The new, total partition function, Z'_T, is defined by

$$Z'_T = Z_T Z_{IN}\,, \tag{2.78}$$

where Z_T is defined by 2.64. The Helmholtz free energy becomes

$$A = -kT \ln Z_T + A_{IN}\,. \tag{2.79}$$

Using Stirling approximation, this is evaluated as

$$A = -kT\left[N_e\left[\ln \frac{Z_{eT}}{N_e} + 1\right] + \sum_a N_a\left[\ln \frac{Z_{aT}}{N_a} + 1\right]\right] + A_{IN}\,. \tag{2.80}$$

substituting

$$N_e = \sum_{a=0}^{\sigma} a N_a \tag{2.81}$$

and completing the partial differentiation, the following relation is found

$$\frac{C_{a+1} C_e}{C_a} = 2 \left[\frac{2\pi m_e k T}{h^2} \right]^{3/2} \frac{Z_{a+1}(E)}{Z_a(E)} \exp\left[-(I_a - \Delta I_a)/kT \right], \tag{2.82}$$

where

$$\Delta I_a = - \frac{\partial A_{IN}}{\partial N_{a+1}} + \frac{\partial A_{IN}}{\partial N_a} - \frac{\partial A_{IN}}{\partial N_e} . \tag{2.83}$$

In order to evaluate ΔI, Ecker and Kröll note that the excess chemical potential, defined by

$$\mu_a^{IN} = \left(\frac{\partial A_{IN}}{\partial N_a} \right)_{T, V, N_b}, \tag{2.84}$$

may be evaluated (following Fowler and Guggenheim) by the relation

$$\mu_a^{IN} = \int_0^1 \epsilon_a \bar{\psi}_a (\lambda, \epsilon_a) \, d\lambda , \tag{2.85}$$

where λ is the variable of integration; this parameter is a dimensionless charge parameter (Fowler, et al, 1956). The authors evaluate the average electrostatic micropotential, $\bar{\psi}_a$, for each of the regions of interest. For number densities below the critical density, the Debye theory is used. For densities greater than C_{cr}, a closest neighbor approximation is used. Their result is stated as follows:

$C \leq C_{cr}$

$$\Delta I_a = (\kappa / 2D) \left(\epsilon_{a+1}^2 - \epsilon_a^2 + \varepsilon^2 \right) ; \tag{2.86a}$$

$$C \geq C_{CR}$$
$$\Delta I_a = (\mathcal{C}/2Dr_0)(\epsilon_{a+1}^2 - \epsilon_a^2 + \varepsilon^2); \tag{2.86b}$$

where

$$\mathcal{C} = 2.2\left[\sum_\beta C_{\beta CR}\epsilon_\beta^2/kT\right]^{1/2} C_{CR}^{1/3}, \tag{2.87}$$

$$r_0 = [3/4\pi C]^{1/3} \tag{2.88}$$

$$C = C_e + \sum_a C_a \tag{2.89}$$

and

ϵ_i = charge of the i^{th} species (esu),

$\varkappa$ = Debye parameter,

D = Dielectric constant,

ε = Charge of electron (esu),

$C_{\beta CR}$ = Density of β^{th} species at critical density.

The purpose of the constant, $\mathcal{C}$, is to match the two approximations at the critical density; r_0 is the radius of the average volume for a particle; and C is the total number density of the particles.

In application, one must solve the system of 2.72 in which the ionization potentials, I_a, are replaced with I_a^*, 2.73, using 2.86 for ΔI_a. The method is readily applicable to all species, including mixtures. The most unsatisfactory feature of the method is that the approximations are not entirely consistent with those for the thermal properties. Of greater importance, however, ΔI_a is dependent only upon the Coulomb potential interaction: none of the other possible interaction potentials enter into the calculation. A method that appears more consistent is introduced in the next section.

5. Consistent Theory

For most regions of interest, a non-ideal equation of state for a plasma may be easily formulated which does not have entirely consistent approximations for the thermodynamic and the ionic properties. Such an equation of state may be constructed from Mayer's approximation for the thermal properties and Ecker and Kröll's approximation for the ionic properties. The primary objection to this procedure (in addition to lack of consistency) is the neglect of the more complex interactions of the particles. A more consistent and complete model may be constructed from the ionization properties in a manner which is consistent with cluster integral theory. This procedure is described in the next few paragraphs.

According to Ecker and Kröll, the reduction in ionization potential may be expressed by the relation

$$\Delta I_a = -\mu_{a+1} - \mu_e + \mu_a \tag{2.83}$$

in which the μ_a's are the excess chemical potentials. After conversion to per unit volume units, ΔI is expressible in closed form for arbitrary potentials through the chemical potentials:

$$\mu_a = -kT \frac{\partial}{\partial C_a}\left[\frac{\kappa^3}{12\pi} + \sum_{a\le b}^{\sigma} C_a C_b \left\{\sum_{k=2}^{n} f_{kjab}\left[\rho_{ab}^{r_k-\frac{\Delta r}{2}} - \rho_{ab}^{r_k+\frac{\Delta r}{2}}\right] + \rho_{ab}^{r_n+\frac{\Delta r}{2}}\right\}\right], \tag{2.90}$$

where the first term yields a purely Debye correction: compare 2.27 and 2.86a.

In this manner, the same approximations are used in solving for the thermodynamic and ionization parts of the equation of state problem. Solutions should be valid throughout the classical region. The accuracy

of the equation of state, in its validity region, should be dependent only upon the accuracy of the short range potential and the number of terms which are included in the cluster expansion. The disadvantage with the model is the number of terms that are required for the calculations. With large, high-speed computors this difficulty is not of great importance.

6. Summary

The primary problem which arises in obtaining an equation of state for real plasmas is the evaluation of the Helmholtz free energy for their interaction forces. This quantity enters into both the thermodynamic and the ionization properties of the plasma. Approximations for determining F_{IN} and the related ΔI have been outlined. Methods involving reasonably consistent approximations have been shown and these range from the ideal gas theory to complicated interaction potentials. These models are summarized below:

1. Ideal Gas Theory: F_{IN} is approximated as zero. Ionization properties are determined by the system of equation 2.72. The approximation is valid for low density and high temperatature.
2. Debye Approximation: Valid in slightly higher density and lower temperature regions. F_{IN} is given by 2.27 and the I_a in 2.72 is replaced by I_a^*. ΔI_a is given by 2.86a, or by some other Debye approximations.
3. Rigid Sphere Model: Reasonably valid to the semiclassical limit. F_{IN} given by either Mayer's approximation, 2.34, or by the more exact approximation, 2.47. Without total inconsistency, ΔI_a is given by Ecker and Kröll's method, 2.86.

4. Arbitrary Potential Model: Valid to the semiclassical limit. F_{IN} given by 2.61. ΔI_a determined from 2.83 by the use of 2.90.

With the acquirement of more experimental data for high density plasmas the Arbitrary Potential Model should be the most useful. Until more experimental data is available, extensive work with the model is not warranted. Only the development of the model and the demonstration of its feasibility is undertaken in this thesis.

CHAPTER III

ALUMINUM PLASMA EQUATION OF STATE

1. Introduction

For compatability with the flow problem, the best choice for the independent variables of the equation of state are internal energy, density and mass density. This cannot be accomplished with closed analytic expressions. In fact, it is impossible to express the equation of state in closed form for any choice of independent variables; thus, a tabular form is necessary. The equations for the thermodynamic and the ionization properties of the plasma will be presented in this chapter in the following form:

I Internal Energy

$$E = E(T, C_e, C_1, \cdots, C_{14}) \tag{3.1}$$

II Ionization Properties

$$C_i = C_i(T, \rho) \; ; \quad i = 2, \cdots, 14 \tag{3.2}$$

$$C_e = \sum_{i=2}^{14} (i-1) C_i \tag{3.3}$$

III Other Thermodynamic Properties

$$X_i = X_i(T, C_e, C_1, \cdots, C_{14}) \tag{3.4}$$

The numerical method of calculation will be presented in Chapter IV. In this chapter, only expressions defining the internal energy and the pressure are given. In Section 4, complete specifying equations are reviewed.

a. Phenomenological Considerations

As the energy content of a real gas is increased, the total energy increase does not appear in kinetic energy of the components of the gas. Other modes of storing energy exist. As the energy content of the gas increases, ionization increases. The kinetic energy of the particles is reduced by the energy required to ionize the atom, which may be a considerable part of the total energy. Additional energy is required to excite bound electrons to higher states. Since positive ions, by the nature of the coulomb interactions, will generally be surrounded by negative charges, the energy density in the plasma increases when an ion-electron pair is produced by ionization. In addition, the electrons are subject to Fermi statistics when the density is very high. As the density of the plasma decreases, this deviation of the electrons from classical particles becomes less important. At low densities and high temperatures, another quantum phenomena becomes important; i.e. the radiation energy content of the plasma. Finally, the plasma oscillation energy must be considered. Since the plasma experiences considerable motion during expansion, it is assumed that oscillations exist throughout the expansion.

From the preceeding, the total internal energy density is presumed to be composed of seven components:

$$E_{TOT} = E_{KD} + E_{ION} + E_{EXC} + E_{FN} + E_{DEG} + E_{RAD} + E_{OSC} \qquad (3.5)$$

where

E_{TOT} = Total energy density

E_{IO} = Ideal gas translation or kinetic energy density

E_{ION} = Ionization energy density

E_{EXC} = Electron excitation energy density

E_{IN} = Particle interaction energy density

E_{DEG} = Degeneracy energy density correction (Fermi correction)

E_{RAD} = Radiation energy density

E_{OSCL} = Plasma oscillation energy density

Each of the above energy components are defined below. All symbols are defined in Chapter IV. For reference see Appendix IV.

b. Ideal Energy -E_{ID}

The term which accounts for the classical kinetic energy of the particles is directly derivable from the partition function, 2.14. This is the ideal gas translational energy term:

$$E_{ID} = \frac{3}{2} C k T \tag{3.6}$$

where C is the total particle number density.

c. Ionization Energy -E_{ION}

The ionization energy is the total energy that is required to ionize each species:

$$E_{ION} = \sum_{i=2}^{14} C_i \left(\sum_{j=1}^{i-1} I_j \right) = C_2 I_1 + C_3 (I_1 + I_2) + \cdots \tag{3.7}$$

where I_j is the uncorrected ionization potential. The effect of the reduction in ionization potential, ΔI_j, is accounted for in the interaction energy.

d. Electron Excitation Energy - E_{EXC}

The total energy involved in exciting electrons to energy levels above the ground state can be given by

$$E_{EXC} = \sum_{i=1}^{13} C_i \sum_{j=2}^{j_{max}} P_{ij} E_{ij} \tag{3.8}$$

where P_{ij} is the probability of the i^{th} species being excited to the j^{th} energy level, E_{ij} is the energy between the levels i and j. The second sum is over all bound states. The highest bound energy level, j_{max}, is the highest remaining energy level in the atom. It is lower than the highest bound level in an isolated atom by the amount of the reduced ionization potential, ΔI_i. In terms of the electronic partition function Z_i (E), an equivalent statement is

$$E_{EXC} = \sum_{i=1}^{13} C_i \left(\frac{kT^2}{Z_i(E)} \frac{\partial Z_i(E)}{\partial T} \right) \tag{3.9}$$

Both of the preceeding expressions become, assuming Boltzman statistics,

$$E_{EXC} = \sum_{i=1}^{13} \frac{C_i}{Z_i(E)} \left(\sum_{j=1}^{j_{max}} E_{ij} g_{ij} \exp\{-E_{ij}/kT\} \right), \tag{3.10}$$

where g_{ij} is the degeneracy state. The electronic partition function is defined as follows:

$$Z_i(E) = \sum_{j=1}^{j_{max}} g_{ij} \exp\{-E_{ij}/kT\}. \qquad (3.11)$$

e. Interaction Energy - E_{IN}

The interaction energy is obtained from the excess Helmholtz interaction free energy, F_{IN}, using the Gibbs-Helmholtz relation

$$E_{IN} = -T^2 \left(\frac{\partial}{\partial T} (F_{IN}/T) \right)_{V, C_i} \qquad (3.12)$$

where F_{IN} is obtained by one of the methods given in the preceeding.

f. Degeneracy Correction - E_{DEG}

Electrons satisfy Boltzman statistics only in the high temperature, lower density regions. In high density regions, corrections must be made to account for the fact that electrons are Fermi particles. Basic considerations for electron gases were made and equations given by Stoner (1939). Define **W** as the Fermi energy

$$W = \frac{h^2}{2 m_e} \left(\frac{3 C_e}{4\pi g_e} \right) \qquad (3.13)$$

where g_e is the statistical weight for free electrons (equal to 2). The degeneracy correction, in the high temperature limit,

$$kT > W,$$

is given by

$$E_{DEG} = \frac{3}{2} C_e kT \sum_{y=1}^{\infty} C_y (W/kT)^{3y/2}, \qquad (3.14)$$

where the C_y are coefficients evaluated by Stoner. Using the first three terms, 3.14, becomes

$$E_{DEG} = \frac{3}{2} C_e kT \left[1.32\times10^{-1}\left(\frac{W}{kT}\right)^{3/2} - 1.867\times10^{-3}\left(\frac{W}{kT}\right)^{3} + 4.7\times10^{-5}\left(\frac{W}{kT}\right)^{9/2} \right]. \quad (3.15)$$

In the low temperature limit,

$$kT < W$$

the following expression that was developed by Stoner (ibid) is valid:

$$E_{DEG} = -\frac{3}{2} C_e kT + \frac{3}{5} C_e W \left[1 + \frac{5\pi^2}{12}\left(\frac{kT}{W}\right)^2 - \frac{\pi^4}{16}\left(\frac{kT}{W}\right)^4 + \cdots \right]. \quad (3.16)$$

The regions of validity of the two series do not quite meet. The first equation, 3.15, may be used for

$$\frac{kT}{W} > 0.5,$$

and the last equation, 3.16, is valid for

$$\frac{kT}{W} < 0.2$$

For accurate energies in the intermediate region, the tables of Fermi integrals that were compiled by McDougall and Stoner (1939), should be used.

The above expression omits all correlation effects. To be correct, a quantum correlation energy for the electrons must be included. Several expressions for this energy correction are available in the literature, but, unfortunately, all of the equations that were investigated gave a

negative value for the total degeneracy energy. In addition, the various expressions differed to a considerable extent. For this reason, quantum correlation energies were not included. Instead, the correlation energy in E_{IN} was retained. This introduces some error; however, one feels that the uncertainty would be the same, if not greater, provided quantum correlation expressions were employed.

g. Radiation Energy Density - E_{RAD}

The Stefan-Boltzman law is assumed for the radiation term in the equilibrium equation of state:

$$E_{RAD} = \frac{4\sigma}{c} T^4 \tag{3.17}$$

where c is the velocity of light and σ is the Stefan-Boltzman constant.

h. Plasma Oscillation Energy - E_{OSCL}

Dittmer (1926) first proposed the possibility of strong internal oscillations in an ionized gas as a possible explanation of the anamalous electron energies observed in arcs. Tonks and Langmuir (1929) showed that the electrons in an uniform, zero temperature plasma oscillated with a frequency, ω_p, given by

$$\omega_p = \left(4\pi \epsilon_e \varepsilon^2 / m_e\right)^{1/2}, \tag{3.18}$$

where m_e is the electron mass and ω_p is called the plasma frequency. Subsequently, Landeau (1946), Bohn and Gross (1949) showed that a damped frequency spectrum existed. Gabor (1952), using Bohm and Gross' dispersion relation, calculated an average energy associated with the oscillations. Drummond (1961) used a somewhat different method to obtain oscillation energy:

$$E^{c}_{osc} = \frac{.182}{4\pi}\,\varepsilon^{3} C_e^{3/2}/(kT)^{1/2}. \tag{3.19}$$

Neither Drummond's equation, nor Gabor's expression, which differ by a numerical factor, is applicable in the high density region.

As a first approximation for the high density region, it is assumed that electrons are excited to oscillation states for which the probability of the excited state is proportional to the energy of the state,

$$\text{probability} \approx e^{-\hbar\omega_p/kT}. \tag{3.20}$$

Considering a zero energy ground state and only one excited state, the oscillation energy is approximated by

$$E^{q}_{osc} = \frac{C_e \hbar\omega_p e^{-\hbar\omega_p/kT}}{1+e^{-\hbar\omega_p/kT}}, \tag{3.21}$$

which is

$$E^{q}_{osc} = C_e \hbar\omega_p / \left(1+e^{\hbar\omega_p/kT}\right) \tag{3.22}$$

This expression leads to the same electron density dependence, $C_e^{3/2}$, but a different temperature dependence when compared to 3.19. In addition, Equation 3.22 is presumed valid in the quantum region. The Drummond equation is valid in the classical region. In the intermediate region, a linear combination of the two expressions is assumed:

$$E_{osc} = Y E^{q}_{osc} + (1-Y) E^{c}_{osc}. \tag{3.23}$$

The quantity Y is made dependent upon the ratio of the electron density to the same-classical limiting electron density,

$$C_{e_{LIM}} = \left(2\pi m_e kT/h^2\right)^{3/2}. \tag{3.24}$$

By introducing a variable, R, which is defined by the following relation

$$R = C_e / \left(2\pi m_e kT/h^2\right)^{3/2}, \tag{3.25}$$

Y may be defined by

$Y = 1$ for $R \geq 1$;

$Y = R$ for $.02 < R < 1$;

$Y = 0$ for $R \leq .02$.

2. Plasma Pressure

The plasma pressure is considered to be the sum of four terms:

$$P_{TOT} = P_{PERF} + P_{IN} + P_{RAD} + P_{DEG}; \tag{3.26}$$

where

P_{TOT} = Total Pressure,

P_{PERF} = Ideal Gas Pressure,

P_{IN} = Interaction Pressure Correction,

P_{RAD} = Radiation Pressure, and

P_{DEG} = Degeneracy Pressure.

Each of the above terms is defined below.

a. Ideal Gas Pressure - P_{PERF}

This term is simply

$$P_{PERF} = kT\left(C_e + \sum_i C_i\right), \tag{3.27}$$

the kinetic energy of the gas particles.

b. Interaction Pressure Correction - P_{IN}

Pressure is related to the Helmholtz free energy of the system by the relation

$$P = -\left(\frac{\partial A}{\partial V}\right)_T ; \tag{3.28}$$

and since the free energy components are addative,

$$P_{IN} = -\left(\frac{\partial A_{IN}}{\partial V}\right)_T , \tag{3.29}$$

where V is volume and A_{IN} is the interaction free energy of the system.

Considering that the cluster integrals are defined in terms of the limit as $V \to \infty$, it is more convenient to express 3.29 in terms of the free energy per unit volume, F_{IN}, and the number densities. In analytical form,

$$P_{IN} = -\left(\frac{\partial (F_{IN}/C)}{\partial 1/C}\right)_{T, x_i} \tag{3.30}$$

in which X_i are the mole fractions, $X_i = C_i/C$. In terms of the cluster expansion,

$$F_{IN} = -kT\mathfrak{S} , \tag{3.31}$$

where

$$\mathfrak{S} = \frac{x^3}{12\pi} + \sum_{\underline{u}} \underline{c}^{\underline{u}} B_{\underline{u}}(x) , \tag{3.32}$$

Eq. 3.30 becomes

$$P_{IN} = kT \frac{\partial(\mathfrak{S}/c)}{\partial(1/c)}. \tag{3.33}$$

Through two body terms, u = 2, the preceeding equation is

$$P_{IN} = kT\left[\frac{1}{12\pi}\frac{\partial(\chi^3/c)}{\partial(1/c)} + \frac{\partial}{\partial(1/c)}\left(\frac{1}{c}\sum_{i=1}^{15}\sum_{j=1}^{15} c_i c_j B_{ij}(\chi)\right)\right], \tag{3.34}$$

where B_{ij} is defined by

$$B_{ij}(\chi) = \left[V(1+\delta_{ij})\right]^{-1}\int_V \left\{\left[1+k_{ij}\right]e^{g_{ij}} - 1 - g_{ij} - g_{ij}^2/2\right\} d\vec{r}_i\, d\vec{r}_j, \tag{3.35}$$

in which

$$k_{ij} = e^{-u_{ij}^{+}/kT} - 1, \tag{3.36}$$

$$g_{ij} = -\left(\lambda z_i z_j e^{-\chi r}\right)/4\pi r \tag{3.37}$$

and

$$\lambda = (4\pi\varepsilon^2/kT) \tag{3.38}$$

for which z_i is the core charge parameter, u_{ij}^{+}, short range potential, δ_{ij} is the Kronocker delta and C_{15} indicates electron density. If i, j or both i and j are neutral particles, 3.35 reverts to the non-coulomb integral:

$$B_{ij} = \left[V(1+\delta_{ij})\right]^{-1}\int_V \left(e^{-u^{+}/kT} - 1\right) d\vec{r}_i\, d\vec{r}_j. \tag{3.39}$$

In terms of mole fractions, 3.34 simplifies to

$$P_{IN} = kT\left[\frac{1}{12\pi}\frac{\partial(\chi^3/c)}{\partial(1/c)} + \frac{\partial c}{\partial(1/c)}\left(\sum_{i=1}^{15}\sum_{j=i}^{15} x_i x_j B_{ij}\right) + c\sum_{i=1}^{15}\sum_{j=i}^{15} x_i x_j \frac{\partial B_{ij}}{\partial(1/c)}\right] \tag{3.40}$$

The first term of 3.40 is evaluated as follows:

$$\frac{\partial(\chi^3/c)}{\partial(1/c)} = \chi^3 + \frac{1}{c}\frac{\partial\chi^3}{\partial(1/c)}\,; \tag{3.41}$$

or by the chain rule

$$\frac{\partial(\chi^3/c)}{\partial(1/c)} = \chi^3 + \frac{1}{c}\frac{\partial\chi^3}{\partial\chi}\frac{\partial\chi}{\partial(1/c)}, \tag{3.42}$$

Since

$$\frac{\partial\chi}{\partial(1/c)} = \frac{\partial}{\partial(1/c)}\left[\frac{4\pi\varepsilon^2 c\sum_i x_i z_i^2}{kT}\right]^{1/2} = \frac{1}{2\chi}\left(4\pi\varepsilon^2\sum_i x_i z_i^2\right)\frac{\partial c}{\partial(1/c)}$$

one obtains

$$\frac{\partial\chi^3}{\partial(1/c)} = -\frac{\chi^3}{2}, \tag{3.43}$$

The second term in 3.40 is elementary. The third term is converted, by the chain rule, to

$$\frac{\partial B_{ij}}{\partial(1/c)} = \frac{\partial B_{ij}}{\partial\chi}\frac{d\chi}{d(1/c)} = -\frac{c\chi}{2}\frac{\partial B_{ij}}{\partial\chi}, \tag{3.44}$$

because the B_{ij}'s depend upon the concentration through $\varkappa$ (the neutral atom interaction have no such dependence). Using 3.43 and 3.44,

$$P_{IN} = -kT\left[\frac{\varkappa^3}{24\pi} + C^2\sum_{i=1}^{15}\sum_{j=i}^{15} x_i x_j B_{ij} + C^2\varkappa\sum_{i=1}^{15}\sum_{j=i}^{15} x_i x_j \frac{dB_{ij}}{d\varkappa}\right] \qquad (3.45)$$

or more simply,

$$P_{IN} = F_{IN} + \frac{kT\varkappa^3}{24\pi} - \frac{kTC^2\varkappa}{2}\sum_{i=1}^{15}\sum_{j=i}^{15} x_i x_j \frac{dB_{ij}}{d\varkappa} . \qquad (3.46)$$

It is interesting to note that, in the first approximation (the 1st two terms of 3.46), the pressure correction is given by the Helmholtz free energy minus the Debye-Huckel-limiting-law pressure term. If the Mayer rigid-sphere approximation is used, the pressure correction term from Duclos and Cambel (1962) is:

$$P_{IN} = -\frac{kT\varkappa^3}{24\pi} - \frac{kT}{2\sum_i c_i z_i^2}\sum_{i=1}^{5}\sum_{j=1}^{5}\sum_{\nu=1}^{16} c_i c_j z_i z_j (-1)^{\nu}\alpha_{ij}^{1-\nu}\left[b_\nu(\phi_{ij}) - g_\nu(\phi_{ij})\right]_j \qquad (3.47)$$

where symbols have the same meaning as given in Chapter II--see 2.34.

c. Radiation Pressure - P_{RAD}

This term is simply

$$P_{RAD} = \frac{4\sigma}{3c} T^4 . \qquad (3.48)$$

d. Degeneracy Pressure - P_{DEG}

The pressure of an ideal, Fermi-Dirac gas is related to its energy in the same manner that the pressure and energy are related for an ideal gas (Stoner, 1939)

$$P = \frac{2}{3} E. \tag{3.49}$$

Thus, in both the high and low temperature limit

$$P_{DEG} = \frac{2}{3} E_{DEG}. \tag{3.50}$$

3. Summary - Equations of State - Current Models

The complexity of the equation of state is now apparent. No simple closed expression can be used to give any of the thermodynamics of ionization properties except in the ideal gas approximation and then only for a hydrogen plasma. In general, equations must be specified for each of the following:

A. Ionization Properties

a. Effective Ionization Potential

1. Chemical Potentials

B. Internal Energy

a. Energy Components

1. Excess Helmholtz Free Energy and Related Equations

C. Pressure

a. Pressure Components

1. Interaction Pressure Terms

There are four different equations of state for which the above systems of equations will be specified. The systems differ, basically, in the approximations to calculate the interaction, Helmholtz free energy. The net result of these different approximations is very pronounced since the effective ionization potential is dependent upon F_{IN}.

The four equations of state are:

1. Ideal gas approximation,

2. Debye-Huckel approximation,

3. Mayer-Ecker and Kroll rigid sphere model,

4. Arbitrary potential model.

The arbitrary potential model is treated in Sections 5 and 6. Equations specifying the other models are specified below.

a. Ideal Gas Model

The interaction is completely neglected; thus, the ionization is obtained from the uncorrected Saha system of equations

$$\frac{c_{i+1}}{c_i} = \frac{2(2\pi m_e kT)^{3/2}}{c_e\, h^3} \frac{z_{i+1}(E)}{z_i(E)} e^{-I_i/kT} \; ; \; i = 1, \cdots, 13 ; \tag{3.51}$$

$$c_e = \sum_{i=2}^{14} (i-1)\, c_i \; ; \tag{3.52}$$

$$\sum_{i=1}^{14} c_i = \rho / m_{al} \; ; \tag{3.53}$$

where ρ is the mass density and m_{al} is the mass of the aluminum ion. In the last equation, the mass of the electrons is neglected.

The internal energy density is specified by

$$E_{TOT} = E_{ID} + E_{ION} + E_{EXC} + E_{DEG} + E_{RAD} + E_{OSCL} \; , \tag{3.54}$$

where

$$E_{ID} = \tfrac{3}{2} C kT \; ; \tag{3.6}$$

$$E_{ION} = \sum_{i=2}^{14} c_i \left(\sum_{j=1}^{i-1} I_j \right) ; \tag{3.7}$$

$$E_{EXC} = \sum_{i=1}^{13} \frac{C_i}{Z_i(E)} \left[\sum_{j=2}^{j_{max}} E_{ij}\, g_{ij}\, \exp(-E_{ij}/kT) \right], \tag{3.10}$$

in which

$$Z_i(E) = \sum_{j=2}^{j_{max}} g_{ij} \exp(-E_{ij}/kT); \tag{3.11}$$

$$E_{DEG} = \frac{3}{2} C_e kT \left[1.32\times10^{-1} \left(\frac{W}{kT}\right)^{-3/2} - 1.867\times10^{-3} \left(\frac{W}{kT}\right)^{3} + 4.7\times10^{-5} \left(\frac{W}{kT}\right)^{9/2} \right] \tag{3.15}$$

for

$$kT > .5,$$

and

$$E_{DEG} = -\frac{3}{2} C_e kT + \frac{3}{5} C_e W \left[1 + \frac{5\pi^2}{12} \left(\frac{kT}{W}\right)^2 - \frac{\pi^4}{16} \left(\frac{kT}{W}\right)^4 \right] \tag{3.16}$$

for

$$kT < .2,$$

where

$$W = \frac{h^2}{2m_e} \left(\frac{3C_e}{4\pi g_e} \right)^{2/3}; \tag{3.13}$$

$$E_{RAD} = \frac{4\sigma T}{c}; \tag{3.17}$$

and

$$E_{osc} = Y E^{q}_{osc} + (1-Y) E^{c}_{osc} , \tag{3.23}$$

where

$$E^{q}_{osc} = C_e \hbar \omega_p / (1 + e^{\hbar\omega_p/kT}) , \tag{3.22}$$

$$E^{c}_{osc} = .182\, \varepsilon^2 C_e^{3/2} / (4\pi (kT)^{1/2}) , \tag{3.19}$$

$$\omega_p = (4\pi \varepsilon^2 C_e / m_e)^{1/2} \tag{3.18}$$

and

Y = 1 for R ≥ 1

Y = R for .02 ≤ R ≤ 1

Y = 0 for R < .02

for which

$$R = C_e / (2\pi m_e kT/h^2)^{3/2} . \tag{3.25}$$

The total pressure is given by

$$P_{TOT} = P_{PER} + P_{DEG} + P_{RAD} \tag{3.55}$$

where

$$P_{PER} = \frac{2}{3} E_{ID} , \tag{3.56}$$

$$P_{DEG} = \frac{2}{3} E_{DEG} , \tag{3.50}$$

and

$$P_{RAD} = \frac{4\sigma}{3c} T^4 . \tag{3.48}$$

For the ideal gas formalism, the j_{MAX} in 3.10 and 3.11 is entirely arbitrary. In theory, the partition function diverges to an infinity of states as the $E_{ij} \rightarrow I_i$. In practice, the sum is cut when the individual terms become negligible. The inclusion of the degeneracy correction is somewhat academic; in the model's validity region E_{DEG} and P_{DEG} are negligible. This comment could also be applied to the Debye Model.

b. Debye-Hückel Approximation

The Debye-Hückel theory requires corrections to the basic equations in the preceeding section. Modifications are necessary to the ionization equations and additions are needed to the energy and pressure expressions.

The Saha system of Equations, 3.51, are modified by replacing the ionization potentials, I_i, by the effective ionization potentials, I_i^*, where

$$I_i^* = I_i - \Delta I_i \tag{3.57}$$

and

$$\Delta I = \frac{\chi}{2D}\left[\epsilon_{i+1}^2 - \epsilon_i^2 + \varepsilon^2\right], \tag{3.58}$$

To the energy equation, an expression for E_{IN} must be added:

$$E_{IN} = -\frac{kT\chi^3}{8\pi}. \tag{3.59}$$

The pressure equations are modified by the additional term

$$P_{IN} = -\frac{kT\chi^3}{24\pi}, \tag{3.60}$$

No great increase in complexity is created in this approximation, however the region of validity is only slightly increased.

c. Mayer-Ecker and Kröll Rigid Sphere Model

The modifications for the Mayer-Ecker and Kröll model are more complicated, but the validity region is considerably extended. Ionization equations are modified with an effective ionization potential

$$I_i^* = I_i - \Delta I_i \,. \tag{3.57}$$

In this equation, ΔI_i is specified by the following:

for $C \leq C_{CR}$,

$$\Delta I_i = \frac{\mathcal{H}}{2D}\left[\epsilon_{i+1}^2 - \epsilon_i^2 + \varepsilon^2\right], \tag{3.58}$$

and for

$C \geq C_{CR}$,

$$\Delta I_i = \left(\mathcal{C}/2Dr_0\right)\left[\epsilon_{i+1}^2 - \epsilon_i^2 + \varepsilon^2\right], \tag{3.61}$$

where

$$\mathcal{C} = Z^2\left[\sum_\beta C_{\beta_{CR}} \epsilon_\beta^2 / kT\right]^{1/2} C_{CR}^{1/3}, \tag{3.62}$$

$$r_0 = \left(3/4\pi C\right)^{1/3}, \tag{3.63}$$

and

$$C_{CR} = \left(\frac{3}{4\pi}\right)\left[\frac{kT}{\epsilon_{i\,max}^2}\right]^3. \tag{3.64}$$

The energy correction is obtained from the excess Helmholtz free energy by the relation

$$E_{IN} = -T^2 \left(\frac{\partial (F_{IN}/T)}{\partial T} \right)_{V, C_i} , \tag{3.12}$$

where

$$F_{IN} = -\frac{kT\kappa^3}{12\pi} - \frac{kT}{2\sum_i c_i z_i^2} \sum_i \sum_j \sum_\nu c_i c_j z_i^\nu z_j^\nu (-1)^\nu \alpha_{ij}^{1-\nu} \left[b_\nu(\phi_{ij}) + q_\nu(\phi_{ij}) \right] , \tag{3.65}$$

for which

$$\alpha_{ij} = a_{ij}\, kT/\varepsilon^2 , \tag{3.66}$$

$$\phi_{ij} = a_{ij}\, \kappa , \tag{3.67}$$

$$a_{ij} = C_a \left[-\lambda_D/2 + \left(\frac{\lambda_D^2}{4} + A_{ij}\lambda_D \right)^{1/2} \right] \tag{3.68}$$

and

$$A_{ij} = |z_i z_j| \varepsilon^2/kT . \tag{3.69}$$

C_a is an arbitrary constant used to adjust the value of F_{IN}. The pressure correction is given by

$$P_{IN} = -\frac{kT\kappa^3}{24\pi} - \frac{kT}{2\sum_i c_i z_i^2} \sum_i \sum_j \sum_\nu c_i c_j z_i^\nu z_j^\nu (-1)^\nu \alpha_{ij}^{1-\nu} \left[b_\nu(\phi_{ij}) - q_\nu(\phi_{ij}) \right] \tag{3.47}$$

where the symbols are defined by 3.66 thru 3.69.

It is noted that the first term in both the pressure correction and the energy correction corresponds to the Debye corrections. Since the critical density, C_{CR}, defines the validity limit of the Debye theory, the Debye correction is included in the first approximation for the entire

equation of state. The unsatisfactory features of this model are the uncertainty in the distance of closest approach, a_{ij} and the failure to consider reasonable, short range potentials. This can cause some uncertainty in the high density region.

5. Arbitrary Potential Model - Short Range Potential Specification

The final form of the equations for the arbitrary potential model are dependent upon the short range potentials, U^{+}_{ij}. Levine and Wrigley (1957) found that U^{+}_{ij} does not decrease more slowly than r^{-4}. In general, the short range potential may be expressed as a series,

$$u^{+} = Ar^{-4} + Br^{-5} + Cr^{-6} + \cdots , \tag{3.70}$$

where there the values of the constants in u^{+} should be determined for each different pair interaction. This generalized form would be very difficult to calculate and would introduce an impossible number of parameters. In the next subsection, it will be shown that the short range potentials may be simplified in order to express the equation of state in terms of three parameters: two potential depths and one potential range. In the final subsection, the specifying equations will be given.

a. Interaction Potentials

The short range potentials are taken to be of the form

$$u^{+}_{ij} = uo_{ij}\left[\left(\frac{r_o}{r}\right)^{M} - 2\left(\frac{r_o}{r}\right)^{N}\right] , \tag{3.71}$$

where uo_{ij} is the depth of the potential well and r_o is its range. To reduce the number of parameters, the repulsive components, except for

electron-electron interactions, are all assumed to be $\left(\frac{r_o}{r}\right)^{12}$: M = 12. For neutral-neutral species interactions it is assumed that N = 6. For all others, except electron-electron interactions, N = 4 is assumed. This latter assumption is based upon an induced dipole interaction. The electron-electron interaction is assumed to be a rigid sphere potential. To further simplify the number of parameters, the same r_o is assumed for all short range potentials except electron-ion interactions. To account for the increased penetratability of the electrons, r_{oe}, the range of the electron interactions is assumed to be related to r_o:

$$r_{oe} = r_o Z^{-1/3} . \tag{3.72}$$

Further simplification is obtained by assuming that all species, other than electrons, have the same polarizability. This allows the well depths for all pair interactions, except neutral-neutral and electron-electron interactions, to be given in terms of the same parameter; therefore, the well depths are defined in the following manner:

1. UNNO = well depth for neutral-neutral interactions; independent parameter.

2. $UNIO_i$ = well depth for neutral-ion interactions where i is the ion species. If Z_i is the core charge of the ion, then

$$UNIO_i = UIO \cdot Z_i \; ; \; UIO = \text{independent parameter.} \tag{3.73}$$

3. $UIIO_{ij}$ = well depth for ion-ion interactions where i and j identify ion species. The well depth is defined

$$UIIO_{ij} = UIO \cdot (Z_i + Z_j) . \tag{3.74}$$

4. UENO = electron-neutral interaction well depth. It is defined

$$UENO = UIO. \tag{3.75}$$

5. $UEIO_i$ = electron-ion interaction well depth - similarly defined

$$UEIO_i = UIO \cdot (z_i). \tag{3.76}$$

6. U_{EE} = The electron-electron interaction is assumed to be a sphere interaction for which the distance of closest approach is determined by the thermal energy in classic ranges and by the Fermi energy in high density regions.

The respective short-range potentials are

1. Neutral-neutral $\longrightarrow u^{+}_{NN} = UNNO\left[\left(\frac{r_o}{r}\right)^{12} - 2\left(\frac{r_o}{r}\right)^{6}\right]$; (3.77)

2. Neutral-ion $\longrightarrow u^{+}_{NI;i} = UIO \cdot z_i\left[\left(\frac{r_o}{r}\right)^{12} - 2\left(\frac{r_o}{r}\right)^{4}\right]$; (3.78)

3. Neutral-electron $\longrightarrow u^{+}_{NE} = UIO\left[\left(\frac{r_{oe}}{r}\right)^{12} - 2\left(\frac{r_{oe}}{r}\right)^{4}\right]$; (3.79)

4. Ion-ion $\longrightarrow u^{+}_{II;ij} = UIO \cdot (z_i + z_j)\left[\left(\frac{r_o}{r}\right)^{12} - 2\left(\frac{r_o}{r}\right)^{4}\right]$; (3.80)

5. Electron-ion $\longrightarrow u^{+}_{EI;i} = UIO \cdot z_i\left[\left(\frac{r_{oe}}{r}\right)^{12} - 2\left(\frac{r_{oe}}{r}\right)^{4}\right]$; (3.81)

6. Electron-electron $\longrightarrow u^{+}_{EE} = \infty \; ; \; r \le a_{EE}$

$$u^{+}_{EE} = 0 \; ; \; r > a_{EE}$$

The distance of closest approach, a_{ee} is obtained by equating electrostatic energy to thermal energy in classical regions,

$$a_{EE} = \varepsilon^2/kT \, . \tag{3.82}$$

In quantum regions, Fermi energy is equated to electrostatic energy:

$$a_{EE} = \varepsilon^2 / w \,, \tag{3.83}$$

where

$$w = \frac{h^2}{2m_e}\left(\frac{3C_e}{4\pi g_e}\right)^{2/3}. \tag{3.84}$$

By using the preceeding approximations, the entire short range potential system is governed by three parameters: UNO, UIO and r_o. A fourth parameter can enter by varying the closest approach distance for electron-electron interactions. This is a manageable number and will allow some insight into the physical nature of the plasma. The potentials assumed are believed to be physically reasonable.

6. Specifying Equations - Arbitrary Potential Model

With the above short range potential functions, the individual B_{ij} are grouped in the following manner

$$\begin{aligned} F_{IN} = -kT\Bigg[& \frac{C_1^2}{2} 4\pi \int_0^\infty \left[e^{-u^+_{NN}/kT} - 1\right] r^2 dr + C_1 \sum_{j=2}^{14} C_j \, 4\pi \int_0^\infty \left[e^{-u^+_{NI}/kT} - 1\right] r^2 dr \\ & + C_1 C_e \, 4\pi \int_0^\infty \left[e^{-u^+_{NE}/kT} - 1\right] r^2 dr \\ & + \frac{\chi^3}{12\pi} + \sum_{i=2}^{14} C_i \sum_{j=i}^{14} C_j \left\{ \sum_{k=2}^{n} f_{k;ij} \left[\rho_{ij}^{r_k - \frac{\Delta r}{2}} - \rho_{ij}^{r_k + \frac{\Delta r}{2}} \right] + \rho_{ij}^{r_n + \frac{\Delta r}{2}} \right\} \\ & + C_e \rho_{ee}^{a_{ee}} + C_e \sum_{j=2}^{14} C_j \left\{ \sum_{k_e=2}^{n} f_{k_e;ej} \left[\rho_{ej}^{r_{k_e} - \frac{\Delta r}{2}} - \rho_{ej}^{r_{k_e} + \frac{\Delta r}{2}} \right] + \rho_{ej}^{r_{n_e} + \frac{\Delta r}{2}} \right\} \Bigg], \end{aligned} \tag{3.85}$$

where

$$f_{k;ij} = \left(e^{-u^{+}_{II;ij}/kT} \right)_{r=r_k} , \tag{3.86}$$

and

$$f_{k;ef} = \left(e^{-u^{+}_{EI;i}/kT} \right)_{r=r_{ke}} , \tag{3.87}$$

$$Q_{ij}^{r_k \pm \frac{\Delta r}{2}} = \frac{4\pi}{1+\delta_{ij}} \left[\int_{r_k \pm \frac{\Delta r}{2}}^{\infty} (e^{q_{ij}} - Q_{ij}) r^2 dr - \int_{0}^{r_k \pm \frac{\Delta r}{2}} Q_{ij} r^2 dr \right] \tag{3.88}$$

for which

$$Q_{ij} = 1 + q_{ij} + q_{ij}^2/2 , \tag{3.89}$$

and

$$q_{ij} = (4\pi\varepsilon^2/DkT) z_i z_j e^{-\varkappa r}/(4\pi r) . \tag{3.90}$$

The basic ionization equations for the ideal gas model are modified, as before, by employing a reduced ionization potential

$$I_i^* = I_i - \Delta I_i \tag{3.57}$$

where

$$\Delta I_i = -\mu_{i+1} + \mu_i - \mu_e \tag{3.91}$$

and

$$\mu_i = \frac{\partial F_{IN}}{\partial c_i} = \frac{-\varkappa \epsilon_i^2}{2D} - kT \sum_j (1+\delta_{ij}) c_j B_{ij}(\varkappa) - \frac{2\pi z_i^2}{\varkappa D} \sum_{j=2}^{15} \sum_{k=j}^{15} c_j c_k \frac{\partial B_{jk}(\varkappa)}{\partial \varkappa} , \tag{3.92}$$

in which the B_{jk} are the terms given in the expansion of F_{IN}. Since the interactions involving neutral atoms are not functions of $\varkappa$, the last term is summed from $j = 2$ through $j = 15$ where $C_{15} = C_e$. For ion and electron interactions, the $\varkappa$ dependence enters in the P_{ij}. Thus, the last term of 3.92 may be written in terms of the derivatives of P_{ij}.

The energy expressions may be corrected by the addition of E_{IN} where

$$E_{IN} = -T^2 \left(\frac{\partial (F_{IN}/T)}{\partial T} \right)_{V, C_i} . \tag{3.93}$$

The pressure correction term is

$$P_{IN} = F_{IN} + \frac{kT\varkappa^3}{24\pi} - \frac{kT\varkappa}{2} \sum_{i=2}^{15} \sum_{j=i}^{15} C_i C_j \frac{\partial B_{ij}}{\partial \varkappa} . \tag{3.94}$$

The arbitrary potential model is valid to the semiclassical limit. The model does not contain the disadvantages of the rigid sphere model: 1) the effect of short range potentials is considered, 2) the validity criteria is not limited by a closest approach parameter and 3) ionization is consistent with thermodynamic calculations. The inclusion of the degeneracy correction term probably extends the validity region slightly beyond the semiclassical limit.

Of the four models for the equation of state, only the last two are of interest in this thesis. Calculations have been made for the Mayer-Ecker and Kröll Model and for the Arbitrary Potential Model. The analysis method for these calculations is described in the next chapter. Analysis of the predictions by the various models is given in Chapter VII.

CHAPTER IV

NUMERICAL METHODS: EQUATION OF STATE

Digital computer programs for the IBM 7094 Mod 2 facility were designed to compute the tabular equation of state. Two related programs were constructed. One calculated pressures, energies, etc. for various temperatures and densities. This program is called the "Isotherm Program". The other more complex program, called the "Constant Energy" Program, calculated the properties of the plasma as functions of energy density and mass density. Temperature is used in the Constant Energy Program as an independent parameter to converge the calculated energy density on the given value. The essential scheme of calculation is given in Section 1. A more complete, yet simplified, flow diagram is given in Section 4.

In Section 2, the modifications of the basic equations for the Mayer-Ecker-Kröll Rigid Sphere model, which are needed to facilitate calculations, are given. Difficulties and estimated errors are also given in Section 2. Alterations of the basic program in order to convert to the arbitrary potential model are given in Section 3.

Comparisons of the equations of state from the different models and their region of validity are given in Chapter VII.

1. Basic Scheme of Calculation

The density of ionization of the plasma must be calculated first. With ionization determined, the other properties of the plasma easily follow. The basic calculation scheme for the Isotherm Program is given in Figure 4-1. The temperature and the mass density are independent variables. The temperature may be held constant and the density varied in order to obtain an isotherm.

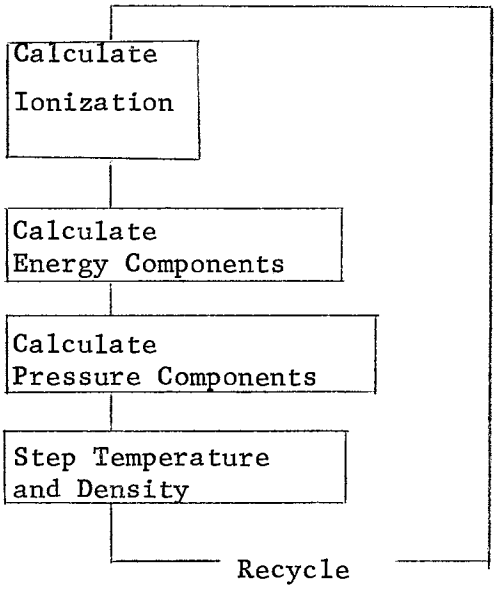

Figure 4.1. Basic Flow Diagram for the Isotherm Program

If constant energy density surfaces are calculated (energy density mass density are independent variables), the basic cycle outlined above must be modified so that convergence on a given energy density is gotten with the temperature used as the parameter. Figure 4-2 shows the basic flow diagram. This is the basic cycle for the Constant Energy program.

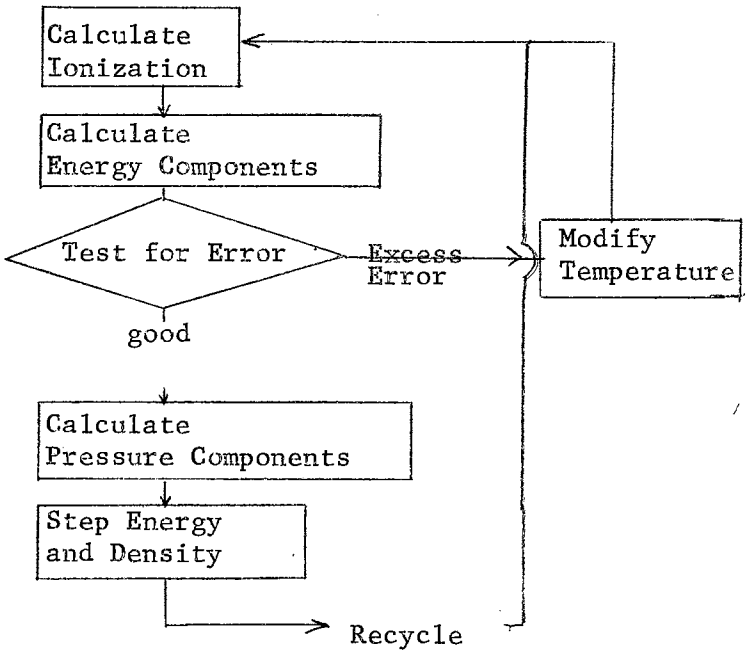

Figure 4.2. Basic Flow Diagram for the Constant Energy Program

---

The only essential difference between the two programs is the routine to converge on the energy and the modifications in stepping the program.

The same basic programs may be employed to calculate the equations of state for any model. Only two models, however, were calculated with any degree of completeness. They are:

1. Mayer-Ecker and Kröll Rigid Sphere Model
2. Arbitrary Potential Model

When the basic computer programs are changed from one model to the other, modifications are required in only three areas:

1. Ionization calculation
2. Excess free energy calculation
3. Interaction pressure correction

The interaction energy code is not changed, since it is obtained by numerically differentiating the excess Helmholtz free energy.

2. Mayer-Ecker and Kröll Model

a. Ionization

The method for calculating the ionization is based on a suggestion by Rouse (1961). The method is derived from the fact that the number density of any species may be expressed in terms of the number density of neutral particles, the Saha ratio , SK_i, and the electron density. The Saha ratios are defined by the following equations

$$SK_i = 2\left[\frac{2\pi m_e kT}{h^2}\right]^{3/2} \frac{Z_{i+1}(E)}{Z_i(E)}\, e^{-I_i^*/kT} . \qquad (4.1)$$

Thus

$$C_{i+1} = \frac{C_i}{C_e} SK_i = \frac{SK_{i-1}}{C_e} \cdot C_{i-1}\frac{SK_i}{C_e} = C_1 \frac{\prod_{j=1}^{i} SK_j}{C_e^i} . \qquad (4.2)$$

Using Equation 4.2, the total density of heavy particles is

$$C_H = \sum_{i=1}^{14} C_i = C_1\left(1 + \sum_{i=1}^{13} \frac{\prod_{j=1}^{i} SK_j}{C_e^i}\right) = C_1 S_H , \qquad (4.3)$$

and the calculated electron density is

$$C_e^* = C_1\left(\sum_{i=1}^{13} i \frac{\prod_{j=1}^{13} SK_i}{C_e^i}\right) = C_1 S_H . \qquad (4.4)$$

The calculated electron density is indicated by C_e^*. In Equation 4.3 and Equation 4.4, C_e refers to the trial electron density. Equations 4.3 and

4.4 serve as definitions for S_H and S_E. When S_H and S_E are determined, C_1 is calculated by combining the relation,

$$C_H = \rho / m_{al} \, , \tag{4.5}$$

with Equation 4.3 to obtain

$$C_1 = C_H / S_H \, ; \tag{4.6}$$

and C_e^* is determined from Equation 4.4.

The trial and calculated electron density are averaged and the cycle is repeated. The chief computation difficulty with this method is the calculation of the ΔI_i in the high density limit where $C > C_{CR}$. For this case

$$\Delta I_i = (C / 2Dr_0)(\epsilon_{i+1}^2 - \epsilon_i^2 + \varepsilon^2) \, , \tag{4.7}$$

for which

$$C = 2.2 \left[\sum_\beta C_{\beta CR} \epsilon_\beta^2 / kT \right] C_{CR}^{1/3} \, . \tag{4.8}$$

Obviously, difficulty is encountered in Equation 4.8 with the distribution of particles at the critical density, $C_{\beta CR}$. Before the ΔI_i may be calculated, which are needed for S_H and S_E, the distribution of species at the critical density must be determined. This may be accomplished since the ΔI_i can be calculated by the Debye approximation:

$$\Delta I_i = (\chi / 2D) \left[\epsilon_{i+1}^2 - \epsilon_i^2 + \varepsilon^2 \right] , \tag{4.9}$$

where χ is defined in the earlier discussion of the Debye equation in Chapter III. The same format that was given through Equation 4.6 is used

for this calculation. Since C_{CR} is the total particle density, it was necessary to step the heavy particle density at the critical density, $C_{H_{CR}}$, until the total particle density agreed with the required critical density. The basic method consisted of:

1. Choosing a value for $C_{H_{CR}}$;
2. Calculating a $C_{e_{CR}}$ by iterative convergence;
3. Compare the calculated C_{CR} to the specified value;
4. Step the $C_{H_{CR}}$ to converge on the specified critical density;
5. Repeat the cycle until convergence was obtained.

When the $C_{\beta_{CR}}$'s are calculated, the ΔI_i are evaluated and the ionization determined. Unfortunately, the situation is complicated by the fact that C_{CR} is based upon the highest degree of ionization present in the plasma:

$$C_{CR} = \left(\frac{3}{4\pi}\right)\left[\frac{kT}{\epsilon_{i_{max}}^2}\right]^3, \tag{4.10}$$

As expected, $\epsilon_{i_{max}}$ changes as the calculation progresses. Consequently, new $C_{\beta_{CR}}$'s must be calculated. The entire process becomes quite laborious and convergence borders on being intolerably slow. The basic flow chart for the ionization calculation is shown in Figure 4-3.

In order to assure convergence, a weighted average of C_e and C_e^* must be used. The weights used have to be modified as the number of iterative cycles increase to assure that the calculations do not oscillate about the true value. In order to assure correct $C_{\beta_{CE}}$, a new critical density calculation is desirable for every fifth iteration.

b. Partition Functions and Excitation Energy

For the summation over electron excitation levels which appear in the electronic partition functions and the excitation energy equations, experimentally determined energy levels and degeneracies are used. For energies higher than those which have been determined experimentally, hydrogen-like term values may be used. The hydrogen-like term is varied by the degeneracy of the next higher ground state in order to account for the increase in degeneracy over hydrogen levels (Griem, 1964). The upper limit on the summation is determined by the condition

$$E_{ij} < I_i^* \tag{4.11}$$

where E_{ij} is the experimentally determined energy of the j^{th} level, or the equivalent energy of the hydrogen-like term. Since the upper limit of the summation is based upon ΔI_i and noting that $Z_i(E)$ must be included in the Saha ratios, SK_i, new electronic partition functions were computed approximately every fifth iteration during the ionization calculation.

c. Interaction Energy

The interaction energy was numerically evaluated by the following approximations:

$$E_{IN} = \frac{-T^2}{2\Delta T}\left[\frac{F_{IN}(T+\Delta T)}{T+\Delta T} - \frac{F_{IN}(T-\Delta T)}{T-\Delta T}\right], \tag{4.12}$$

In order to assure reasonable accuracy, the derivative was recalculated with successively smaller ΔT until successive calculations were within 5% of each other.

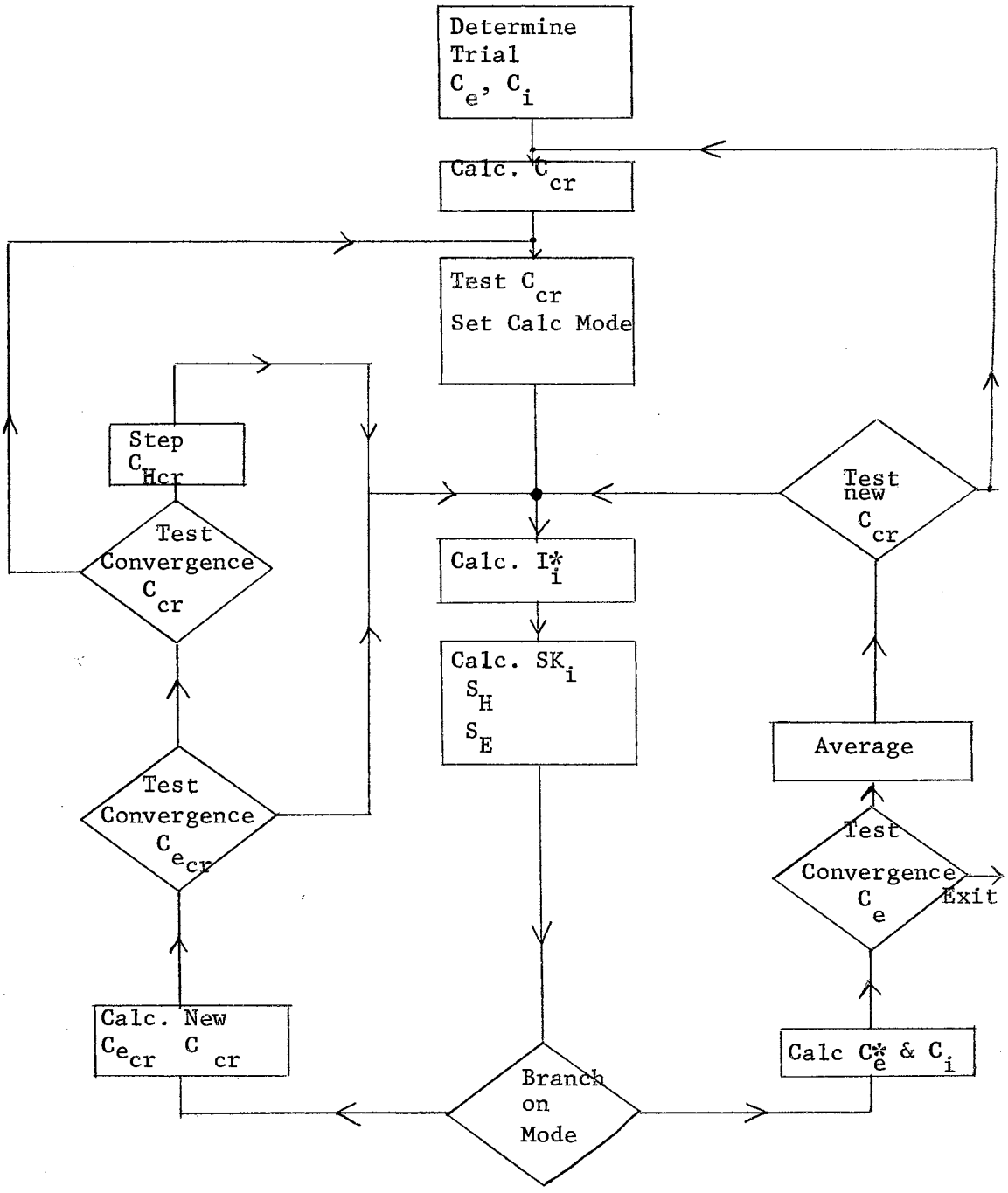

Figure 4.3. Simplified Flow Chart for Calculating Ionization by the Ecker and Kroll Method

d. Excess Free Energy

Poirier's tabulated values for $L_{ij}(\phi)$ and $S_{ij}(\phi)$ were used to compute the excess free energy. Simple two point interpolation was used to determine the value of the individual integrals for different values of the argument, ϕ. The one major uncertainty in the F_{IN} calculation was the value of a_{ij}, the closest approach parameter. Duclos and Cambel (1962) suggested that the following relation be used:

$$a_{ij} = C_a \left[-\frac{1}{2\kappa} + \left(\frac{1}{4\kappa^2} + \frac{A_{ij}}{\kappa} \right)^{1/2} \right], \tag{4.13}$$

where

$$A_{ij} = |\epsilon_i \epsilon_j| / DkT . \tag{4.14}$$

This relation is employed to make the distance of closest approach somewhat temperature dependent. In order to merge to the Thomas-Fermi model, the best value of C_a was found to be 1.95. Comparisons of different a's for a hydrogen plasma were reported by Bruce and Todd (1964) and are reviewed in the next chapter.

3. Arbitrary Potential Model

It was previously indicated (Section 1) that only limited modifications are needed to convert the basic computer program to the new model. The basic difference in the models is the free energy calculation. In order to calculate F_{IN}, it was necessary to compile tables of cluster integrals. Tables were assembled for integrals of the following type:

$$I = \int_{r=0}^{\infty} \left[\exp\left\{ -u\left(\frac{1}{x^{12}} - \frac{2}{x^{N}} \right) \right\} - 1 \right] x^2 dx , \tag{4.15}$$

where N = 6 and N = 4. These are approximations to the Leonard-Jones potential. To simplify the calculations, the exponential term was presumed to be 0 for $x \leq 2^{-1/2}$. The remainder of the integral was evaluated by Simpson's rule between $x=2^{-1/2}$ and x = 3. The integrals were evaluated for different arguments of u from u = 0.01 to u = 20. Simple interpolation was used to obtain the value of a given integral in terms of its table argument: $u = u_{ij}/kT$. (u_{ij} is the corresponding well depth). Two tables were compiled, one for N = 4 and the other for N = 6.

Tables for the integrals $P_{ij}^{a_{ij}}$ were also calculated. The following substitutions were used to convert the integrals to dimensionless form.

$$L_{ij} = -\lambda z_i z_j / 4\pi a_{ij} , \tag{4.16}$$

$$K_{ij} = \varkappa a_{ij} , \tag{4.17}$$

and

$$x_{ij} = r/a_{ij} . \tag{4.18}$$

Then

$$P_{ij}^{a_{ij}} = \frac{-\lambda z_i z_j}{(1+\delta_{ij})\varkappa^2} \frac{K_{ij}^2}{L_{ij}} \left[\int_1^\infty [e^{q_{ij}} - Q_{ij}] x^2 dx - \int_0^1 Q_{ij} x^2 dx \right], \tag{4.19}$$

where

$$q_{ij} = \frac{L_{ij} e^{-K_{ij}x}}{x} , \tag{4.20}$$

and

$$Q_{ij} = 1 + q_{ij} + (q_{ij}^2/2) . \tag{4.21}$$

Defining

$$I(K,L) = \frac{K^2}{L}\left[\int_1^{\infty}(e^{g}-g)x^2dx - \int_0^{1} g\,x^2dx\right], \qquad (4.22)$$

then

$$\rho_{ij}^{a_{ij}} = \frac{-z_i z_j \lambda}{(1+\delta_{ij})\chi^2} I(K_{ij}, L_{ij}) . \qquad (4.23)$$

Tables of the integral, I(K, L), were calculated by Simpson's rule for various arguments of K and L. Approximately 3,000 values were needed to cover the estimated ranges of K and L.

For the calculation of the chemical potentials, μ_i, a table of $\frac{\partial \rho_{ij}}{\partial \chi}$ was calculated. No difficulty is encountered since K is a function of χ. The original tables for I(K, L) were used to build a set of tables DI(K,L) where

$$DI(K,L) = \frac{\partial I(K,L)}{\partial K} . \qquad (4.24)$$

Therefore

$$\frac{\partial \rho_{ij}^{a_{ij}}}{\partial \chi} = \frac{2 z_i z_j}{(1+\delta_{ij})\chi^3} I(K,L) - \frac{z_i z_j \lambda}{(1+\delta_{ij})\chi^2} a_{ij} \frac{\partial I(K,L)}{\partial K} , \qquad (4.25)$$

or

$$\frac{\partial \rho_{ij}^{a_{ij}}}{\partial \chi} = -\frac{2\rho_{ij}^{a_{ij}}}{\chi} - \frac{z_i z_j \lambda a_{ij}}{(1+\delta_{ij})\chi^2} DI(K,L) . \qquad (4.26)$$

With these tables the new equation of state is reduced in complexity.

a. Ionization Modification

All of the complications caused by the $C_{\rho_{CR}}$ computation and the difficulties in convergence are removed with this model. In place of the Ecker and Kröll equations for ΔI_i, the various chemical potentials, μ_i, are calculated on every iteration of the ionization cycle by referring to the tables noted in the preceeding section. One only sums over the integral values that are extracted from the various tables. The ΔI_i's are then computed using the values of μ_i. The time for each cycle is certainly increased, but the repeated iterations for the $C_{\rho_{CR}}$ calculations are removed.

b. Excess Free Energy Modification

The excess Helmholtz free energy, F_{IN}, specified by Equation 3.85, is readily calculated using the table of integrals I(K, L). The problem is reduced to summing over all integral contributions. Linear interpolation was used to determine the cluster integral values for the arguments K and L.

c. Pressure Modification

No difficulty was encountered in writing a program to evaluate Equation 3.94. A subroutine was used to evaluate the excess Helmholtz free energy, F_{IN}, and a new code was used to calculate the values of μ_i which are all that is required to modify the program for the Rigid Sphere Model. As before, only linear interpolation was used for all of the tables.

4. Summary

Although a program to compute constant energy density surface was constructed, it was found more practical to calculate isotherms and then

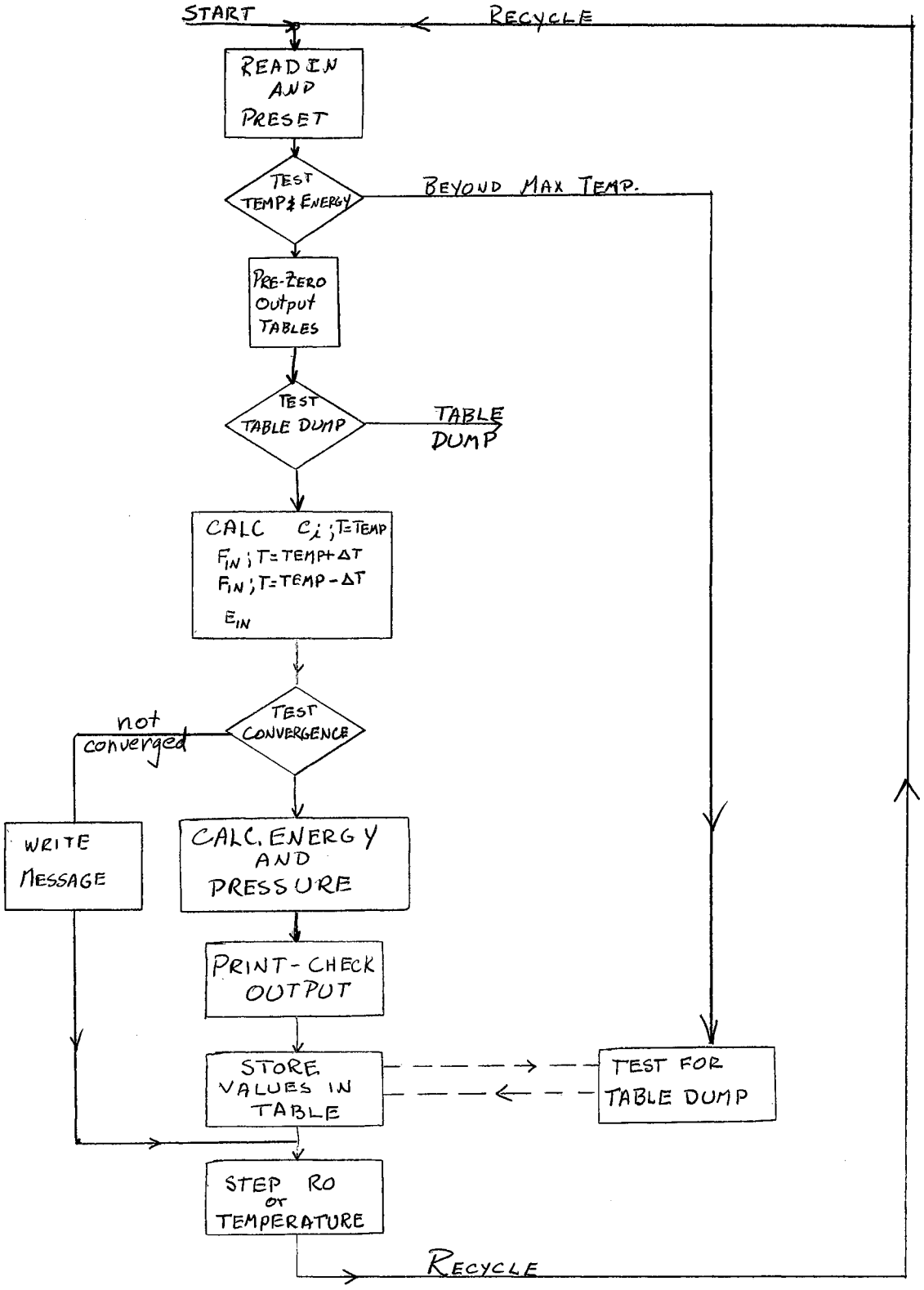

Figure 4.4. Simplified Flow Diagram for the Tabular Equation of State

use the isotherm data to determine the constant energy surface. The IBM 7094 computer time was consequently reduced by a factor of approximately 70%. A separate program was compiled to convert the isotherm data to constant energy data. Standard, three point interpolation was used to convert the data.

The isotherm data was calculated, stored internally and printed at the end of all computation in tabular form. The flow diagram for the final program is given in somewhat simplified form in Figure 4.4. Evaluation of the numerical results is given in Chapter VII.

CHAPTER V

PLASMA FLOW - FUNDAMENTAL DESCRIPTION

1. Introduction

In plasma dynamics problems called magnetegasdynamics, the quantities of interest are the macroscopic properties: temperature, pressure, flow-velocity, charge distribution, etc. The determination of these quantities requires that a theoretical method be decided upon and then a model be chosen that is compatible with the method.

Basically, there are two methods that may be considered for finding these quantities. One is the microscopic approach of kinetic theory and the other is the macroscopic approach of fluid dynamic continuum theory. Of the two, the latter is the most practical method (Shih-I-Pai, 1962). In this approach, the conservation laws of mass, momentum, energy and charge, etc. are postulated. To these are added Maxwell's equations and the required thermodynamic relations to obtain a definitive mathematical model that describes the plasma flow. The resulting equations are far more manageable than the kinetic heirarchy of non-linear, partial differentio-integral equations.

Generally speaking, two methods are available for the description of the continuum equation:

a. The Eulerian method, which describes the phenomena at a given point in space

b. The Lagrangian method, which describes the phenomena which occur to a given, elementary mass of fluid.

The Eulerian reference system is the ordinary, fixed laboratory frame of reference in which intuition can operate more freely. This is an important advantage in manipulating the numerical methods which, of necessity, must be used for the complex system of equations. Consequently, the Eulerian method is chosen even though the Lagrangian reference frame produces to some extent, simpler equations for a one-dimensional problem.

In order to specify the required set of equations for the flow, a suitable model must be chosen for the plasma. The model choice is based upon the minimum number of microscopic quantities which are of interest. To illustrate, consider the following two cases:

a. A fifteen component aluminum plasma model could yield temperature, partial pressure, density and flow velocity for each component species, plus the electric field. This model could require a system of up to 61 coupled equations.

b. The one component plasma model could be specified with five equations; however, no information would be obtained on the behavior of the individual species.

The predictions of a one component model are highly suspect because of the disregard of the vastly different properties of the component species. Kunth (1959) has indicated that a successful grouping of the plasma components is attained only when the properties of the groups are nearly the same such as the masses, the transport properties, etc. Based on this consideration, the two component model is the simplest plasma model which should be considered. The plasma will be considered as composed of

electrons and heavy particles. The latter group is called the ionic component; each particle is assumed to have the average ionization charge. The electrons are called the electronic component.

In the remainder of this chapter, the equations specifying the plasma flow properties are given. The relations define the gross quantities of the plasma. Diffusion velocities are employed to differentiate between motion of the two components.

2. Basic Equations Defining Gross Flow Properties

Derivations of the basic conservation equations are presented in practically all fluid dynamics texts, such as that of Landau and Lifshitz (1959), and in several of the plasma dynamics texts (Samaras, 1962). The form of the equations immediately below are those from Richtmyer (1957).

a. Conservation of Mass-Continuity Equation

$$\frac{\partial \rho}{\partial t} + \vec{u} \cdot \nabla \rho = -\rho \nabla \cdot \vec{u} \tag{5.1a}$$

b. Conservation of Momentum-Equation of Motion

$$\rho \frac{d\vec{u}}{dt} + \rho (\vec{u} \cdot \nabla) \vec{u} = -\nabla p \tag{5.1b}$$

c. Conservation of Energy-Energy Equation

$$\rho \frac{d \varepsilon_{in}}{dt} + \rho \vec{u} \cdot \nabla \varepsilon_{in} = -p \nabla \cdot \vec{u} \tag{5.1c}$$

In the preceding equations,

ρ = mass density

$\vec{u}$ = flow density

P = total gas pressure

$\mathcal{E}_{in}$ = internal energy

t = time

$\nabla = \sum_i \vec{e}_i \frac{\partial}{\partial x_i}$

$\vec{e}_i$ = unit vector

x_i = space coordinate

By defining the total energy per unit mass as

$$\mathcal{E}_T = \mathcal{E}_{in} + \frac{1}{2}(\vec{u}\cdot\vec{u}), \tag{5.2}$$

the conservation of energy equation may be written as

$$\frac{\partial(\rho\mathcal{E}_T)}{\partial t} + \nabla\cdot(\rho\mathcal{E}_T\vec{u}) = -\nabla\cdot(p\vec{u}). \tag{5.3}$$

The preceding equations involve five dependent variables: $\rho, \vec{u}, \mathcal{E}_{in}$ p and $\mathcal{E}_T$. One additional relation is needed for the description of the gross microscopic properties of the expansion. This relation is an equation of state in the form

$$p = p(\rho, \mathcal{E}_{in}). \tag{5.4}$$

In like manner, the temperature may be specified through the equation of state

$$T = T(\rho, \mathcal{E}_{in}) \tag{5.5}$$

Usual practice in plasma dynamics of assuming the ideal gas theory has

been found to be inadequate; the theory is not valid for the initial conditions of the problem when the density is high and the temperature is low. A more adequate equation of state has been developed and is given in Chapters II, III, IV and VII.

3. Modifications of Basic Flow Equations

The preceeding equations define the flow properties of a inviscid fluid. The basic motion and energy equations are modified for a plasma by adding terms of the electric body forces, viscosity forces, conduction and radiation transfer. Corrections for each equation are considered separately.

a. Equation of Motion

The equation of motion contains the term ∇p. Pressure in this case should be

$$p = p_G + p_R \tag{5.6}$$

where P_G is the kinetic gas pressure and P_R is the radiation pressure. Radiation pressure is assumed to be composed of two parts; 1) thermal radiation arrising at the given point in space and, 2) radiation from other regions. Thus

$$p_R = p_{RL} + p_{RT} \tag{5.7}$$

The local radiation, P_{RL}, is approximated by blackbody radiation and is included in the equation of state pressure, 5.4. With this inclusion, the pressure gradient term becomes

$$\nabla p \Rightarrow \nabla p + \nabla p_{RT} \tag{5.8}$$

In addition to the pressure gradient term, body force terms must be specified. The most important body forces (excluding gravitational) are the electric and viscous forces. The electric body force is simply

$$\vec{F}_E = q\vec{E}, \tag{5.9}$$

where q is the electric charge per unit volume and E is the electric field vector.

The usual correction for the viscous force is given by Samaras (1962) as

$$F_v = \mu \nabla^2 \vec{u} + \frac{\mu}{3} \nabla(\nabla \cdot u). \tag{5.10}$$

With these modifications the momentum equation may be rewritten as

$$\rho \frac{d\vec{u}}{dt} + \rho (\vec{u} \cdot \nabla)\vec{u} = -\nabla p - \nabla p_{RT} + \mu\left(\nabla^2 \vec{u} + \frac{\nabla}{3}(\nabla \cdot \vec{u})\right) + qE, \tag{5.11}$$

b. Conservation of Energy

The correction attributable to radiation conduction is somewhat similar in nature to a heat conduction term. If Q_R is the radiation flux, then the corrective term is of the form Q_R. The radiation flux can be approximated (Shih-I-Pai, 1962) by

$$\vec{Q}_R = D_R \nabla E_R, \tag{5.12}$$

where E_R is the radiation energy per unit volume and D_R is known as the diffusion coefficient for radiation. It may be written as

$$D_R = \frac{c}{3} l_R, \tag{5.13}$$

where C is the velocity of light and

$$L_R = 1/K_R \rho . \tag{5.14}$$

K_R is the Roseland mean absorption coefficient and is defined by

$$\frac{1}{K_R} = \left[\int_0^\infty \frac{1}{k_\nu (1 - e^{-h\nu/kT})} \frac{dB_\nu(T)}{dT} d\nu \right] \Big/ \left[\int_0^\infty \frac{dB_\nu(T)}{dT} d\nu \right] \tag{5.15}$$

where $B_\nu(T)$ is the Planck function, k_ν is the monochromatic absorption coefficient and is frequency. A more complete discussion of the radiation phenomena is included in Chapter IX.

Somewhat similarly, the heat conduction corrective term is added. Defining $\vec{Q}_H$ as the heat conduction flux, the corrective term is $\nabla \cdot \vec{Q}_H$. As a first approximation

$$\vec{Q}_H = \mathcal{H} \nabla T , \tag{5.16}$$

$\mathcal{H}$ is the coefficient of heat conductivity. This term is defined by Equation 5.36 farther along in this thesis.

The energy source term, from the electric fields, is $\vec{E} \cdot (q \vec{v})$ and the viscosity term is approximated by $\vec{u} \cdot \vec{F}_\nu$. With these corrections the energy equation is written as

$$\frac{\partial (\rho \mathcal{E}_T)}{\partial t} + \nabla \cdot (\rho \vec{u} \mathcal{E}_T) = -\nabla (p \vec{u}) + \nabla \cdot \bar{q} + \vec{u} \cdot \vec{F}_\nu + E \cdot (q \vec{v}), \tag{5.17}$$

where

$$Q = Q_R + Q_H \tag{5.18}$$

4. Conservation of Charge

The charge distribution is determined from the equation for the conservation of charge. Excluding external sources, the total charge of the plasma must be conserved during the plasma state. This conservation principle requires that the rate of charge increase within an arbitrary volume V, must equal the rate of inward flow across the boundary of the volume,

$$\int_V \frac{\partial q}{\partial \tau} \, dV = -\int_S q \vec{v} \cdot d\vec{S} \tag{5.19}$$

In Equation 5.19, is the charge velocity, q is charge per unit volume, t is time and is the vector differential surface element with outward normal. Application of the divergence theorem leads to

$$\frac{\partial q}{\partial t} + \nabla \cdot (q \vec{v}) = 0 \tag{5.20}$$

If charge sources are present, Equation 5.20 takes the form

$$\frac{\partial q}{\partial t} + \nabla \cdot (q \vec{v}) = \sigma_q \tag{5.21}$$

where σ_q is the charge source per unit volume.

5. Further Relations Required

a. Diffusion Equation

Thus far, the equations adequately describe the gross properties of the plasma but no information is provided concerning the composition of the flowing matter. In order to delineate mass migration of the components, the diffusion of the ionic and electronic components relative to the gross mass flow velocity (average mass flow velocity), $\vec{u}$, will be

considered. The diffusion equation that follows is based upon a treatment by F. A. Williams (1958) and adapted to the two component plasma model by Ables (1963). In developing the equation, pressure gradients and electric body forces are included but thermal gradients and non-isotropic terms are omitted. If

X_j = the mole fraction of the j^{th} component

D_{ie} = the electron diffusion coefficient

$\vec{W}_j$ = the diffusion velocity of the j^{th} component

Y_j = the mass fraction of the j^{th} component

then the diffusion equation becomes

$$\nabla X_e = \frac{X_e X_i}{D_{ie}} (\vec{W}_i - \vec{W}_e) + (Y_e - X_e) \frac{\nabla p}{p} + \frac{\rho}{p} Y_e Y_i (\vec{F}_e - \vec{F}_i) \qquad (5.22)$$

In Equation 5.22 the subscripts "i" and "e" stand for ionic and electronic components, respectively, p is pressure, ρ is mass density and F_e and F_i represent the electric body forces on the two components (Equation 5.9).

b. Diffusion Constant

Transport coefficients for a plasma were evaluated by R. L. Liboff (1959). The values reported by Liboff for the shielded coulomb potential, to the first order, are

$$D_{ie} = \frac{3kT}{16 m_e \Omega_1' n} = [D_{ie}]_1 \; ; \qquad (5.23)$$

and to the second order

$$D_{ie} = \frac{[D_{ie}]}{1 - \delta} \qquad (5.24)$$

where

$$\delta = \frac{[2\Omega_2^1 - 5\Omega_1^1]}{[2\Omega_2^1 - 5\Omega_1^1] - 4[\Omega_2^1]^2 + 4\Omega_3^1\Omega_1^1} \quad . \tag{5.25}$$

The Ω_m^ℓ are given as

$$\Omega_1^1 = \nu_0 \Delta^2 [\ln(1/x) - 0.961]/2; \tag{5.26}$$

$$\Omega_2^1 = \nu_0 \Delta^2 [\ln(1/x) + 0.039]/2; \tag{5.27}$$

$$\Omega_3^1 = \nu_0 \Delta^2 [\ln(1/x) + 1.039]; \tag{5.28}$$

$$\Omega_1^2 = \nu_0 \Delta^2 [\ln(1/x) - 1.461]; \tag{5.29}$$

and

$$\Omega_2^2 = \nu_0 \Delta^2 [\ln(1/x) - 0.461]; \tag{5.30}$$

where

$$\nu_0 = \left(\frac{\pi kT}{2m_e}\right)^{1/2} \tag{5.31}$$

$$\Delta = Z\epsilon^2/kT \tag{5.32}$$

$$x = \Delta/2\lambda_D \tag{5.33}$$

$$\lambda_D = \left[\frac{4\pi\epsilon^2}{kT}\left(C_e + \sum_i z_i^2 C_i\right)\right]^{1/2} \tag{5.34}$$

and z_i is the dimensionless charge parameter for the ionic species i whose concentration is given by C_i. Z is the average ionization.

c. Coefficient of Viscosity and Coefficient of Thermal Conductivity

Liboff's (1959) approximations for the coefficient of viscosity and thermal conductivity were used:

$$\mu = 5kT/8\Omega_{22}^{2}, \tag{5.35}$$

and

$$\lambda = 2.7\mu C_v. \tag{5.36}$$

In the preceeding equation, C_v is the specific heat at constant volume of the plasma and may be derived from the equation of state.

d. Charge Velocity

The charge velocity, $\vec{w}$, used in the charge conversation equation is not the gross flow velocity, $\vec{u}$. Ables (1963) has shown that the charge velocity can be related to $\vec{u}$ through the electron diffusion velocity, W_e, the average ionization, Z_A^*, and the total charge q by the relation

$$\vec{w}q = (\vec{u} + \vec{w}_e)q - \vec{w}_e \rho \frac{Z_A^*}{m_i}, \tag{5.37}$$

where m_i is the mass of aluminum ions.

6. Electric Field Equations

The equations for the electrostatic fields are simply

$$\vec{E} = -\nabla\phi \tag{5.38}$$

and

$$\nabla^2\phi = -4\pi q, \tag{5.39}$$

where $\vec{E}$ is the electric field vector and ϕ is the electric potential.

7. Initial and Boundary Conditions

The flow field boundary conditions are

$$\left.\begin{aligned} \vec{u} &= 0 \\ \vec{\nabla}\cdot\vec{u} &= 0 \end{aligned}\right\} \; r = 0 \; ; \tag{5.40}$$

no velocity flow through the center of the exploding sphere is allowed.

The initial conditions are

$$\left.\begin{aligned} \rho &= \rho_0 \\ p &= p_0 \\ \varepsilon_{in} &= \varepsilon_{in_0} \\ \vec{u} &= 0 \\ v &= 0 \end{aligned}\right\} \; 0 \le r \le r_0 \; ; \; t = 0 \quad , \tag{5.41}$$

and

$$\left.\begin{aligned} \rho &= 0 \\ p &= 0 \\ \varepsilon_{in} &= 0 \end{aligned}\right\} \; r > r_0 \; ; \; t = 0 \quad . \tag{5.42}$$

The above initial conditions specify a hot, stationary plasma sphere of radius r_0 in a vacuum.

The electric field equations are subject to the boundary conditions

$$\begin{aligned} \phi &= 0 \; ; \; r = \delta \\ \phi &= \phi_0 \; ; \; r = R_E \end{aligned} \tag{5.43}$$

where R_E and ϕ_o are the radius and potential of the outer electrode. δ is chosen to be small enough so that it will not effect the accuracy of the solution but large enough to avoid the singularity difficulties at the origin.

8. Summary

The preceeding equations, boundary conditions and initial conditions define the macroscopic flow properties of the exploding plasma. This complex system of equations does not lend itself to an analytic solution; therefore, numerical methods are required. Since the emphasis for this thesis is concerned the development of the method and the solution technique, many of the approximations in the preceeding formulations were not refined to obtain a higher order of accuracy. Fortunately, approximations in the corrective terms have not been found to be of importance.

The modifications required to convert the equations to different form and the general numerical method are outlined in the next chapter.

CHAPTER VI

NUMERICAL METHOD - FLOW PROBLEM

Before the solution of the partial differential equation system may be started, a suitable coordinate system for the problem is required. For this problem, the initial and boundary conditions have spherical symmetry and furthermore there exists no inherent property of the problem which would serve to differentiate between any two radial directions from the center of the initial sphere. From these considerations, one can see that a basic spherical symmetry exists with no angular dependence. All equations may be written in spherical coordinates and the angularly dependent terms deleted, leaving only a radial dependence.

1. The Equations in Spherical Coordinates

The fundamental equations given in Chapter V may be expressed in spherical coordinates with radial dependence only, by using the following vector relations:

$$\nabla G = \frac{dG}{dr} \; ; \tag{6.1}$$

$$\nabla \cdot \vec{G} = \frac{1}{r^2} \frac{\partial}{\partial r} (r^2 G) \; ; \tag{6.2}$$

$$(\vec{G} \cdot \nabla) \vec{G} = \frac{1}{2} \nabla (\vec{G})^2 + (\nabla \times \vec{G}) \cdot \vec{G} \; . \tag{6.3}$$

The last of the above expressions for spherical symmetry (lamular flow) becomes

$$(\vec{G}\cdot\vec{\nabla})\vec{G} = \frac{1}{2}\nabla G^2 \tag{6.4}$$

With these substitutions, the fundamental equations become

$$\rho\frac{\partial\rho}{\partial t} + \frac{1}{r^2}\frac{\partial}{\partial r}(r^2\rho u) = 0 \; ; \tag{6.5}$$

$$\frac{\partial q}{\partial t} + \frac{1}{r^2}\frac{\partial}{\partial r}(r^2 q_N) = 0 \; ; \tag{6.6}$$

$$\rho\frac{\partial u}{\partial t} + \frac{\rho}{2}\frac{\partial}{\partial r}(u^2) = -\frac{\partial p}{\partial r} - \frac{\partial p_e}{\partial r} + F_N + qE \; ; \tag{6.7}$$

$$\frac{\partial(\rho\mathcal{E}_T)}{\partial t} + \frac{1}{r^2}\frac{\partial(\rho u\mathcal{E}_T r^2)}{\partial r} = -\frac{1}{r^2}\frac{\partial(pur^2)}{\partial r} + \frac{1}{r^2}\frac{\partial(Qr^2)}{\partial r} + uF_N + Eq_N \; ; \tag{6.8}$$

$$F_N = \frac{\mu}{r^2}\frac{\partial}{\partial r}\left(r^2\frac{\partial u}{\partial r}\right) + \frac{\mu}{3}\frac{\partial}{\partial r}\left(\frac{1}{r^2}\frac{\partial(ur^2)}{\partial r}\right) \; ; \tag{6.9}$$

$$Q = \mathcal{H}\frac{\partial T}{\partial r} + D_R\frac{\partial E_{RAD}}{\partial r} \; ; \tag{6.10}$$

$$\frac{\partial X_e}{\partial r} = \frac{X_e X_i}{D_{ie}}(W_i - W_e) + (Y_e - X_e)\frac{1}{p}\frac{\partial p}{\partial r} + \frac{\rho}{p}Y_e Y_i(E_e - E_i) \; ; \tag{6.11}$$

$$\frac{\partial\phi}{\partial r} = -E_r \; ; \tag{6.12}$$

and

$$\frac{\partial^2\phi}{\partial r^2} = -4\pi q \; . \tag{6.13}$$

Examination of the conservation equations, 6.5 thru 6.8, shows that all but Eqn. 6.7 are in conservative form. If Equation 6.5 is multiplied by u and then added to Equation 6.7, the latter is converted to conservative form:

$$\frac{\partial(\rho u)}{\partial t} + \frac{1}{r^2}\frac{\partial(\rho u^2 r^2)}{\partial r} = -\frac{\partial p}{\partial r} - \frac{\partial p_k}{\partial r} + F_r + q_f E . \qquad (6.14)$$

The boundary and the initial conditions are, of course, identical with those in Chapter II. These equations, the equation of state and all necessary boundary conditions form a complete mathematical model for the problem.

2. The Method of Finite Differences

A problem, identical in nature but with a simpler mathematical model was solved by Ables (1963). The method for solving this problem is very similar to the one that was employed by Ables and it is given below.

The solution to this mathematical model may be obtained through the use of numerical methods with the aid of a large scale digital computer. The selected method of solution was the well known method of finite differences (Richtmyer 1957) (Milne, 1953) (Scarborough, 1950). A brief description of the method will be given here.

The r, t plane is subdivided by a uniform rectangular mesh with the edges parallel to the r and t axes. The cell dimensions are Δr and Δt in the r and t directions, respectively. The coordinates of the mode of a general mesh are designated by (r_n, t_m) where

$$r_n = r_o + n\Delta r , \qquad (6.15)$$

$$t_m = t_o + m\Delta t , \qquad (6.16)$$

and r_o, t_o are constants. The value of any function f(r,t), at the node (r_n, t_m), is designated by $f^{(n,m)}$. If $\mathbf{X}_1$, $\mathbf{X}_2$, $\mathbf{X}_3$ are successive modal

values of either coordinate and $f^{(1)}$, $f^{(2)}$, $f^{(3)}$ are the related values of $f(r,t)$, the following approximations may be written:

$$\left.\frac{\partial f}{\partial x}\right|_{X_1} = \frac{1}{2\Delta X}\left(-3f^1 + 4f^2 - f^3\right), \tag{6.17}$$

$$\left.\frac{\partial f}{\partial x}\right|_{X_2} = \frac{1}{2\Delta X}\left(-f^1 + f^3\right), \tag{6.18}$$

$$\left.\frac{\partial f}{\partial x}\right|_{X_3} = \frac{1}{2\Delta X}\left(f^1 - 4f^2 + 3f^3\right) \tag{6.19}$$

These are often known as back difference, central difference, and forward difference derivative formulas, respectively. Discussions of the accuracy of these formulas may be found in the cited references. By using these formulas, the approximate value of the partial derivative is known. These formulas provide approximate values at the neighboring mesh points about any nodal point for which the value of $f(r,t)$ is known.

In terms of these mesh points, an initial condition on a variable is specified by giving the values of the variable at the nodes related to the intersections of the $t = 0$ and $r_n = r_o + n\Delta r$, $n = 0, 1, 2 \ldots$ mesh lines. On the other hand, a boundary condition at $r = r_o$, as an example, could be specified by giving the values of the variable in question on the intersections of the line $r = r_o$ and $t = n\Delta t$, $n = 0, 1, 2 \ldots$. When a functional relationship exists which specifies the partial derivative of $f(r_n,t_o)$ in terms of the values of other variables at $t = t_o$; then, by use of the differential, difference formulas, one computes approximate value for $f(r_n, t_o + \Delta t)$. The values $f(r_n, t_o)$ and $f(r_n, t_o + \Delta t)$, $n = o, 1, 2 \ldots$ are commonly called the old and the new radial profiles of the function $f(r,t)$.

After new profiles have been computed for all of the variables in a problem, the same procedure may be repeated again and again. In each repetition, the new profile of the previous computation are the old profiles of the present computation. In this manner, the solution may be advanced step-wise in the time direction from the initial condition profiles; provided that an expression for the time derivative of each variable is known implicitly or explicitly, in terms of the nodal values of the variables on the old profiles.

For this problem, the necessary relationships are available for density, charge density, material flow velocity, and energy density in the forms of Equations 6.5, 6.6, 6.14 and 6.8, respectively. Profiles may be computed for the time $(t + \Delta t)$ directly from the time, t, profiles. Through the equation of state, the pressure and temperature is obtained. Only the electric field, the diffusion velocity and various coefficients are left to be determined at time $(t + \Delta t)$.

The electric field problem is easily solved by using Gauss' integral for the electric field and the known radial symmetry. If Gauss' integral is applied to a spherically symmetric charge distribution, one may write as a consequence

$$E_r\Big|_{r_n} = \int_0^{r_n} 4\pi q r^2 dr, \qquad (6.20)$$

where E_r has units of statvolts/cm. Since $q(r_n, t = \Delta t)$, $n = 0, 1, 2 \ldots$, is known by virtue of Equation 6.6, one may employ a step-wise numerical integration technique such as Simpson's method to evaluate the integral in Equation 6.20 and to find $E_r(r_n, t = \Delta t)$, $n = 0, 1, 2 \ldots$. For the

diffusion velocity, one may employ Equation 6.11. The various transport coefficients are easily determined without difficulty. This completes one cycle of computation, the continuous reiteration of which will steadily advance the solution of all of the problem variables in the time direction from the initial condition profiles.

Any attempt to employ the outlined method will bring up a number of difficulties. The first problem is the exact form of the differencing that is required. Generally speaking, there is no assurance that a given differencing system may be used successfully. For flow problems, central differencing schemes are unstable (Richtmyer, 1957). The differencing scheme found successful in the problem combines central differencing for all pressure terms and a simplified back differencing for all of the other terms.

A second problem concerns the precise form used for the equation of state. The most desirable form would be closed expressions for each of the state variables in terms of the density and energy; but, no such closed forms are known from theory. The best equation of state data available, Chapter VII, is given only in tabular form. All attempts to fit various analytical forms to the tabulated data were unsuccessful. For this reason, the closed algebraic form was abandoned in favor of a purely numerical method. This method employs the tabulated data with suitable interpolation and extrapolation methods to extend the values into interstitial and boundary regions which are not specifically enumerated in the available tables. The standard logrithmic interpolation and extrapolation scheme was employed which Ables (1963) developed for this thesis.

A choice must be made of the values for Δr and Δt. The choice for Δr is dictated by the physical dimensions of the initial boundaries of the

problem and by the degree of fineness which is desired in the solution. The fineness is determined, to a great extent, by the size of the digital computer, both as to storage capacity and as to speed of computation. The choice of a value for Δt is a much more annoying problem. A relatively large Δt is desired in order for the solution to be obtained as rapidly as possible; however, a small Δt is desirable from the standpoint of accuracy. In addition to these considerations, it was found that the convergence of this type of numerical solution is dependent on the relative size of Δr and Δt (Richtmyer, 1957; Scarborough, 1950). The precise relationship between Δr and Δt for convergence is known only for certain simple systems. An exact analysis of the system of equations under consideration is not possible in the present state of the art. Courant, et al, (1948) have given a simple convergence and stability criteria for compressible fluid flow problems which appears to have validity in many areas which are not covered by the assumptions to obtain this relationship. This, known as the Courant Condition, states that $\Delta r/\Delta t$ may not be larger than the maximum velocity of propagation, V_{max}, of a disturbance in the fluid. In the present application, V_{max} may be taken as the sum of the flow velocity and of the velocity of sound in the plasma. If

$$\frac{\Delta r}{\Delta t} = C V_{max}, \quad C \leq 1$$

then the solution is said to have been developed at C x Courant.

Since the memory of a computer is limited, only a finite number of mesh points may be considered. As a consequence, there will exist a limit to the radial distance which may be separated into meshes and kept in the computer at any given time. As the plasma expands, this maximum radius will

eventually is overrun. At this point in the solution, it is necessary to increase the length of the meshes, Δr, so as to increase the radius while the number of mesh points remain constant. Of course, it is also necessary to increase Δt by the same proportion to keep the Courant value, C, constant throughout the solution. To minimize the number of such adjustments, Δr and Δt should be doubled each time it becomes necessary. The process will, hereafter, be called a machine condensation.

3. The Machine Code

A machine code embodying the above concepts was developed in FORTRAN (FORmula TRANslator) computer language by the author. Able's program was employed as a basis. FORTRAN is a high order computer language which, in slight modifications, is acceptable to a wide assortment of large scale digital computers. The relative ease with which scientific programs may be encoded in the FORTRAN language leads to a drastic reduction in labor for encoding a large scientific program. On the other hand, the time to debug a program may be extended on account of the quite involved translation process which separates the program-as-believed-to-be-encoded from program-as-run.

The final version of the FORTRAN program was prepared especially for use on an IBM 7094 digital computer. It was a few more than 1200 FORTRAN statements in length which were divided into a main program and 13 subroutines. This was translated into approximately 14000 machine language instructions for the 7094 computer. A simplified flow chart for the program is shown in Figure 6.1. Results of the expansion program are in Chapter VIII.

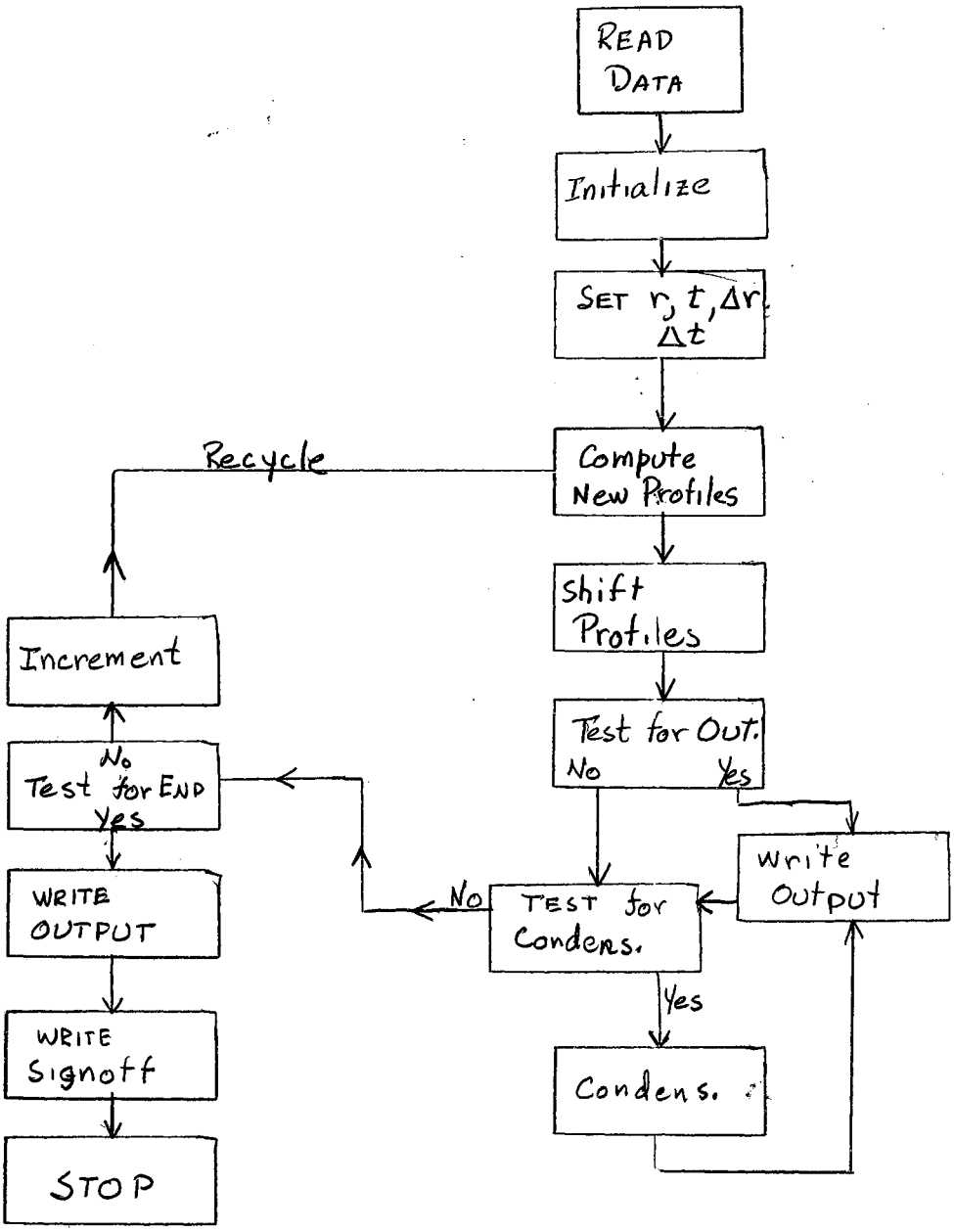

Figure 6.1. Simplified Flow Diagram

CHAPTER VII

SOLUTION AND REDUCTION OF DATA - EQUATION OF STATE

Two preliminary studies of the Mayer-Ecker and Kroll model were made. The computer programs for these studies were run on the IBM 1410 computer facility at Oklahoma State University. A summary of the reported results is given in Section 1. Upon completion of the preliminary studies, a computer code for the complete equation of state according to the Mayer-Ecker and Kroll model was written. Initial debugging was accomplished with the IBM 7090 which was available at Continental Oil Company, Ponca City, Oklahoma. Finally, the code was brought to Goddard Space Flight Center, Greenbelt, Maryland. The final check-out and production run utilized the IBM 7094, Mod II, at NASA. Results of the production run are given in Section 2.

A code for the arbitrary potential model equation of state was tested at the Goddard Space Flight facility during July of 1965. Results of this test are reviewed in Section 3.

1. Preliminary Studies

The initial study of the equation of state was concerned with methods for calculating the reduction in ionization potential and the regions of validity (Bruce and Todd, 1965) of these methods. The Debye theory was compared to Ecker and Kroll's method. For a singly ionized gas, limiting values of the temperature dependent electron densities by each theory were

determined and are shown in Figure 7.1. It is apparent that the Ecker and Kröll approximation is, in theory, valid further in the low temperature high density region. Comparisons of the ionization produced in aluminum plasma are shown in Figures 7.2 and 7.3. Substantially higher degrees of ionization are indicated by the Ecker and Kröll approximation. The comparison values used in this study were obtained from data reported by C. Ronse (1961 and 1962b).

The second study was directed at evaluation of the closest approach parameter in Mayer's theory (Bruce and Todd, 1964). Hydrogen was chosen the plasma for study. At this time, it was deemed desirable to make a further check on the Ecker and Kröll method. For this last comparison, binding energies for the hydrogen atom were calculated from Schroedinger's equation by using the Yukawa potential as the potential function. The results were reduced so that the effective ionization potential could be expressed as a function of the Debye length as is shown in Figure 4.1.

In order to determine the effect of the closest approach parameter pressure isotherms were calculated. The total pressure was determined by

$$P_{TOT} = P_{PERF} + P_{DEB} + P_{MA} + P_{DEG} \,, \tag{7.1}$$

where

$$P_{MA} = P_{IN} - P_{DEB} \,, \tag{7.2}$$

for which

$$P_{DEB} = -\frac{kT\varkappa^3}{24\pi} \,, \tag{7.3}$$

and P_{IN} was given by equation 5.47. P_{DEG} was obtained by multiplying

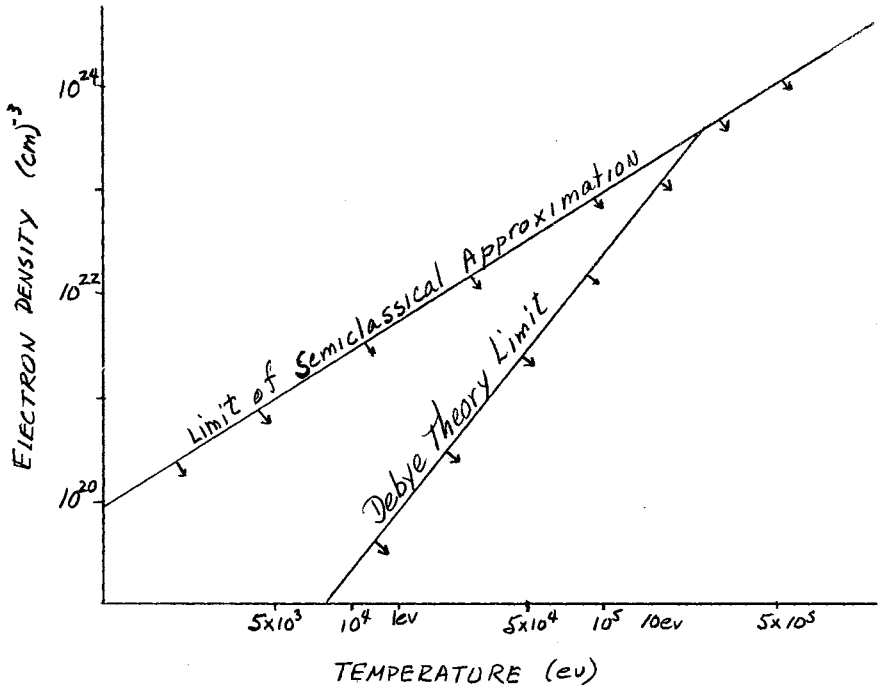

Figure 7.1. Regions in which Debye Theory and Ecker and Kröll Methods Are Valid (Singly Ionized Plasma).

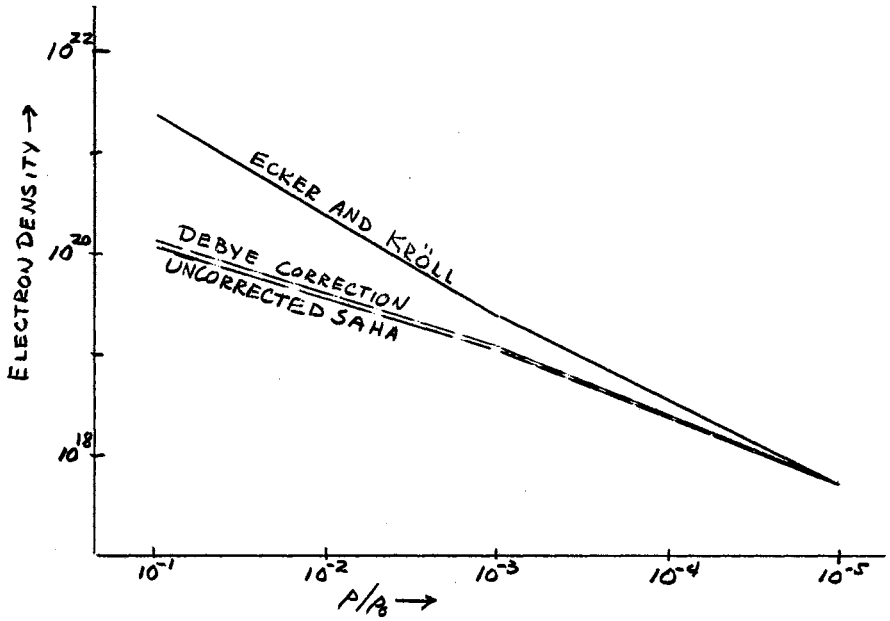

Figure 7.2. Comparison of Aluminum Ionization Electron Density Calculated for T = 1 ev.

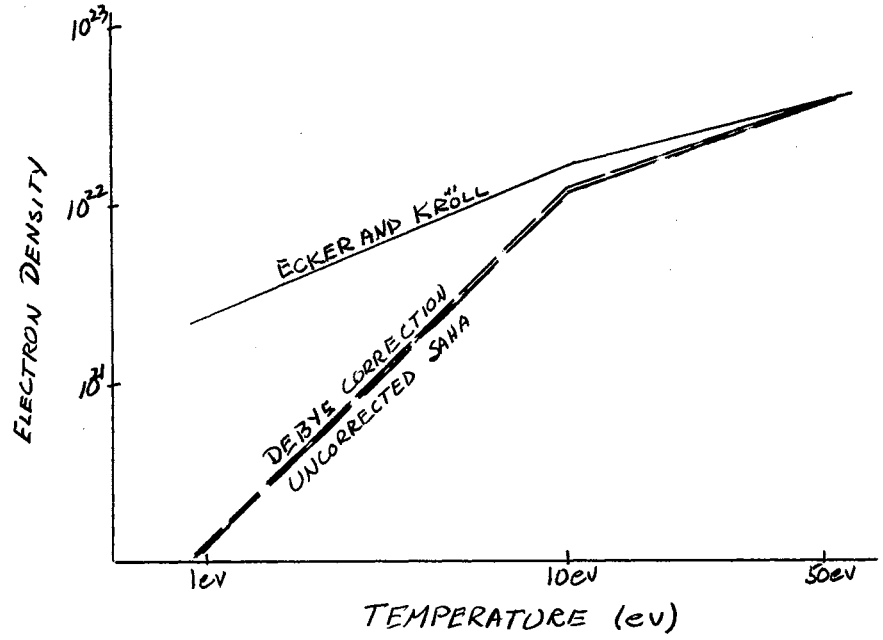

Figure 7.3. Comparison of Aluminum Ionization Electron Density Calculated for C=6.02 x 10^{21}.

equation 5.15 by 2/3, i.e., equation 5.50. The typical variation with density of each pressure component is shown in Figure 7.4. Specifically this figure shows the 5_{ev} isotherm components for an a_{ij} ten times larger than that indicated by equation 4.35 for which the ionization calculation was by the Yukawa method. The effect of variation of the a_{ij} parameter on this isotherm is shown in Figure 7.5. The same variation of a_{ij} on the 5en isotherm by the Ecker and Kröll approximation is given in Figure 7.6. Two ev and 5ev isotherms are compared on the basis of the ionization in Figures 7.7 and 7.8. In these figures, the graphs in the upper right hand corner compare the calculated ionizations. Ideal gas ionizations were also calculated by the unmodified Saha equation. The ideal pressure contained no modifications, i.e. designated, P_{PER}.

The very close comparison of the Yukawa and Ecker and Kröll methods gave increased confidence in the Ecker and Kroll approximation. The studies demonstrated both the accuracy and practicality of the Mayer-Ecker and Kröll model and served as valuable guides against which to check the results of the more complete equation of state.

2. Tabular Equation of State

The fullscale isotherm program was written, debugged and brought to Goddard Space Flight Center. Before final production runs could be completed, a suitable value for the closest approach parameter was needed. The value for the constant C_a, in equation 4.35, was obtained by merging the tabular equation of state into the Thomas-Fermi model at a relative density of P/Po = .1. For this purpose, the total energy did not include oscillation energy. The best value for C_a was found to be 1.95.

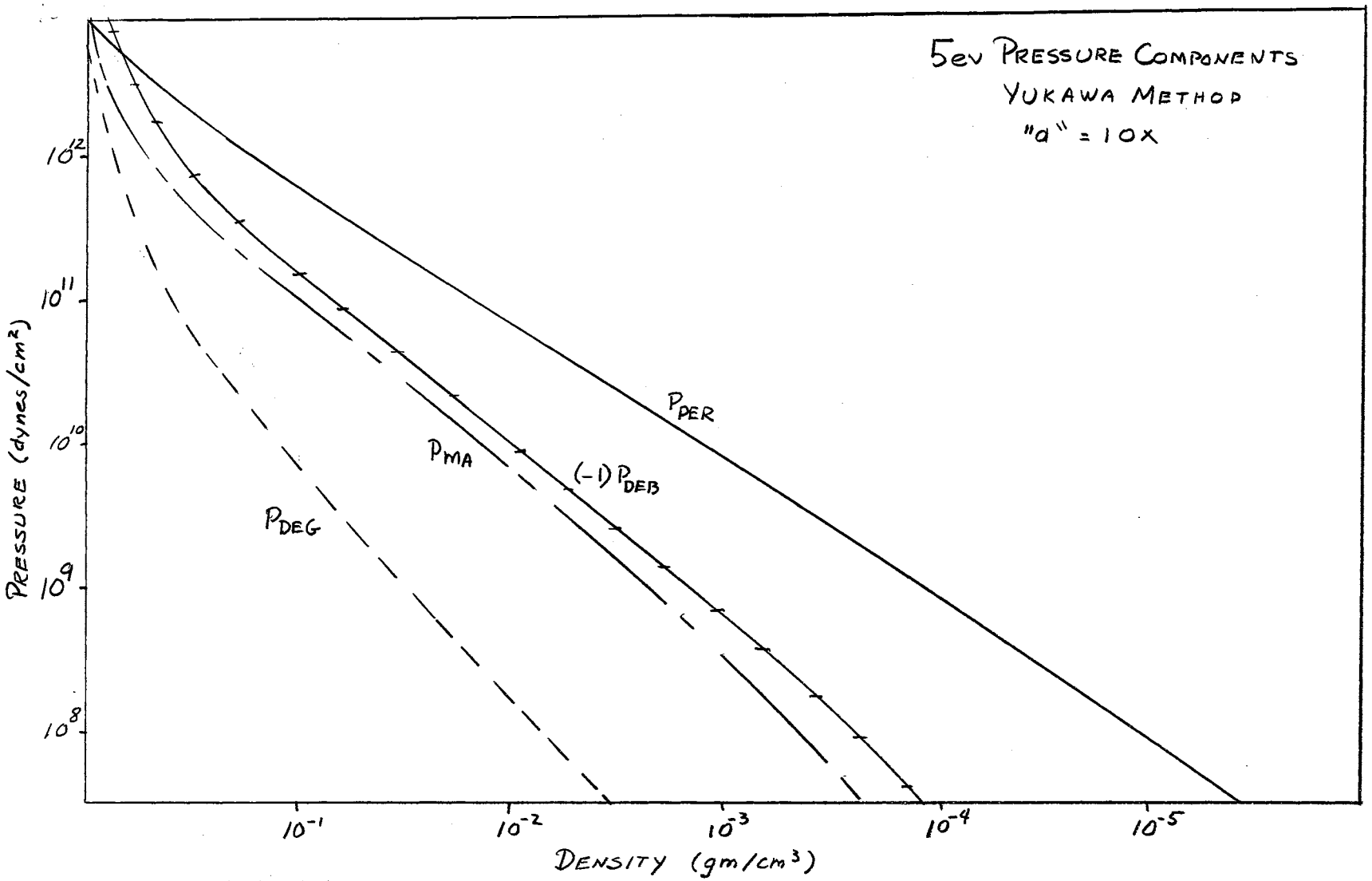

Figure 7.4. Components of Pressure for 5 Electron-volt Isotherm by Yukawa Method.

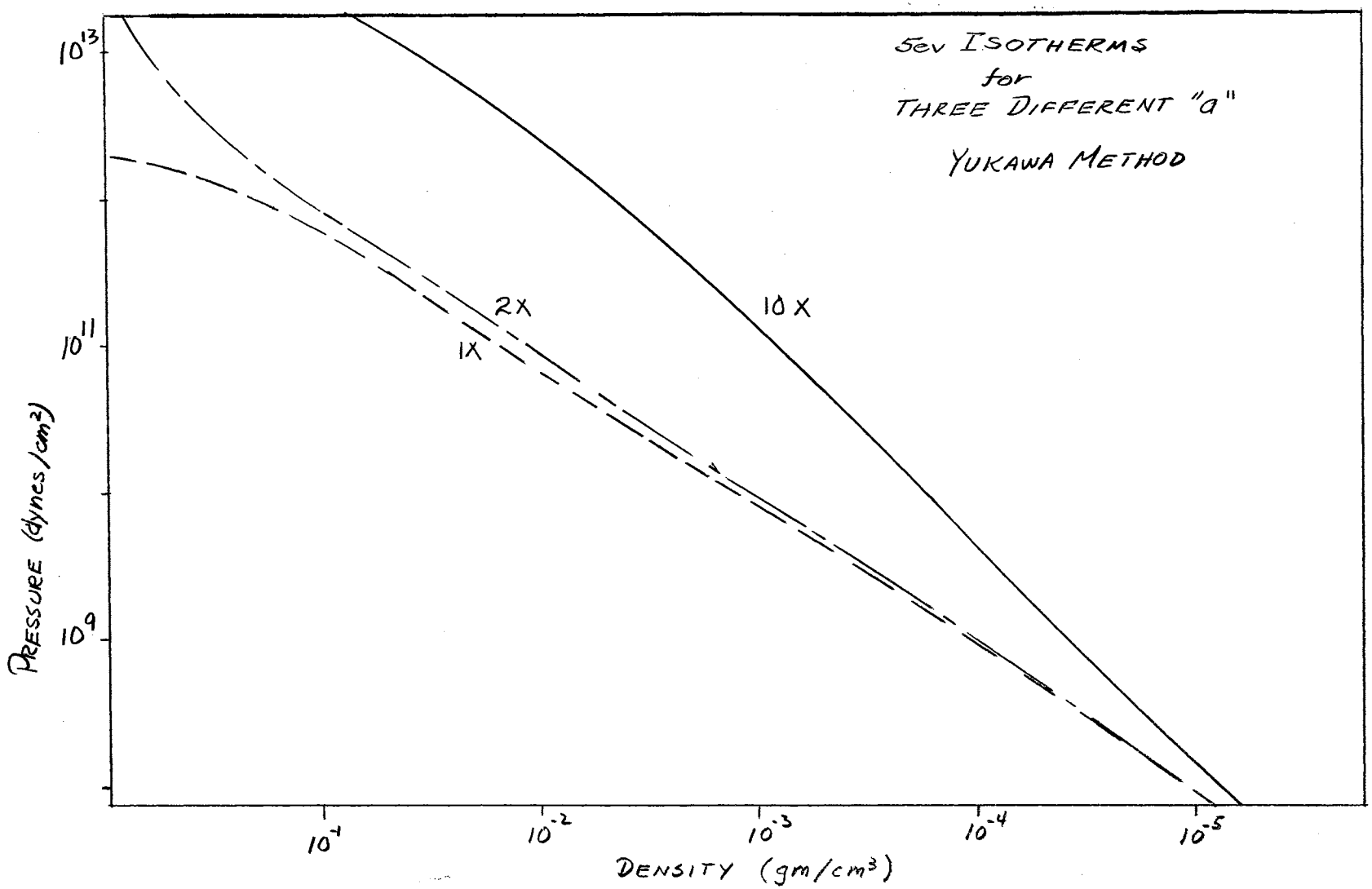

Figure 7.5. Isotherms for 5 Electron-volts Using Three Different Closest Approach Values.

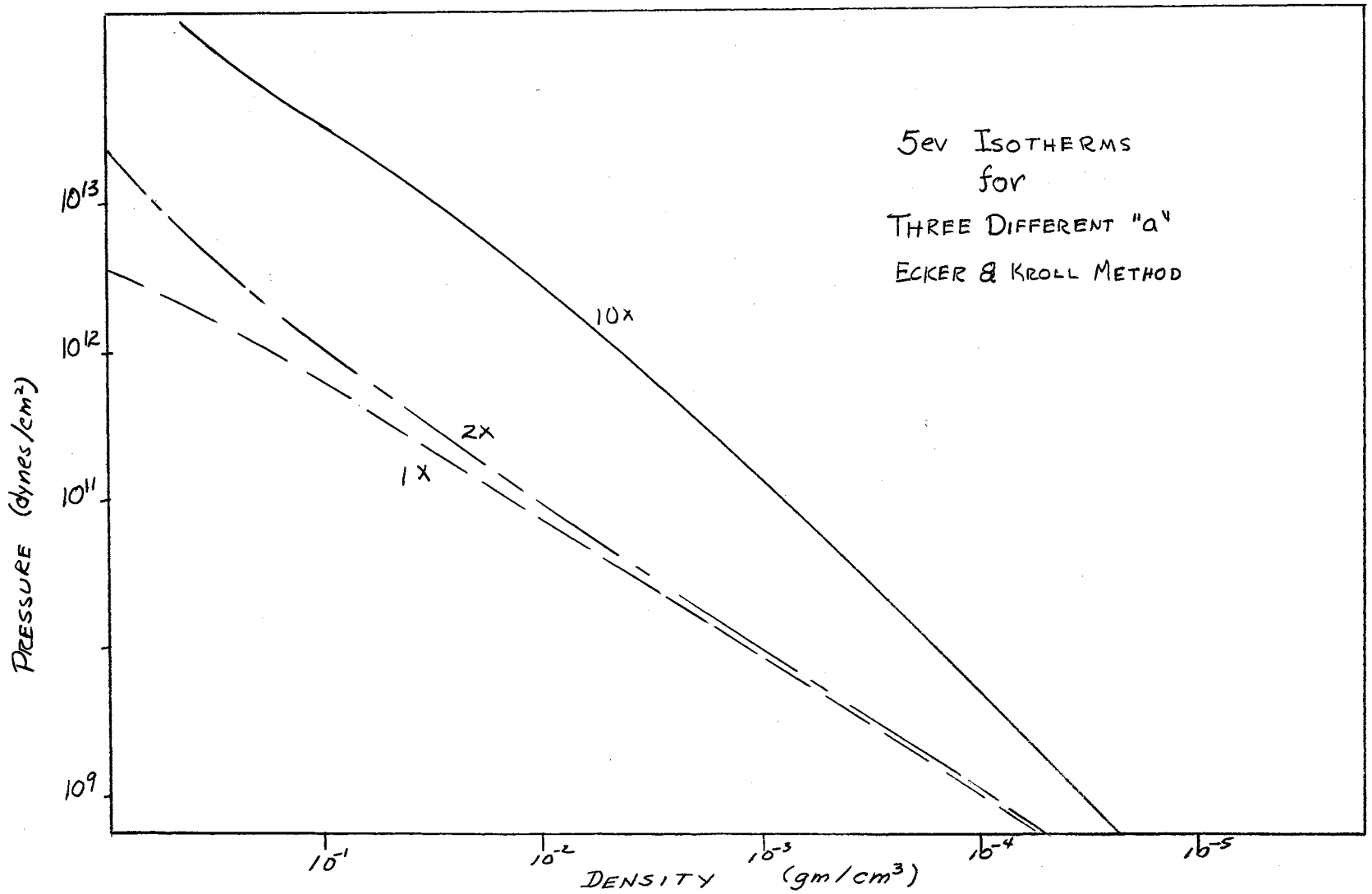

Figure 7.6. Five Electron-volt Isotherms Using Three Different Closest Approach Values.

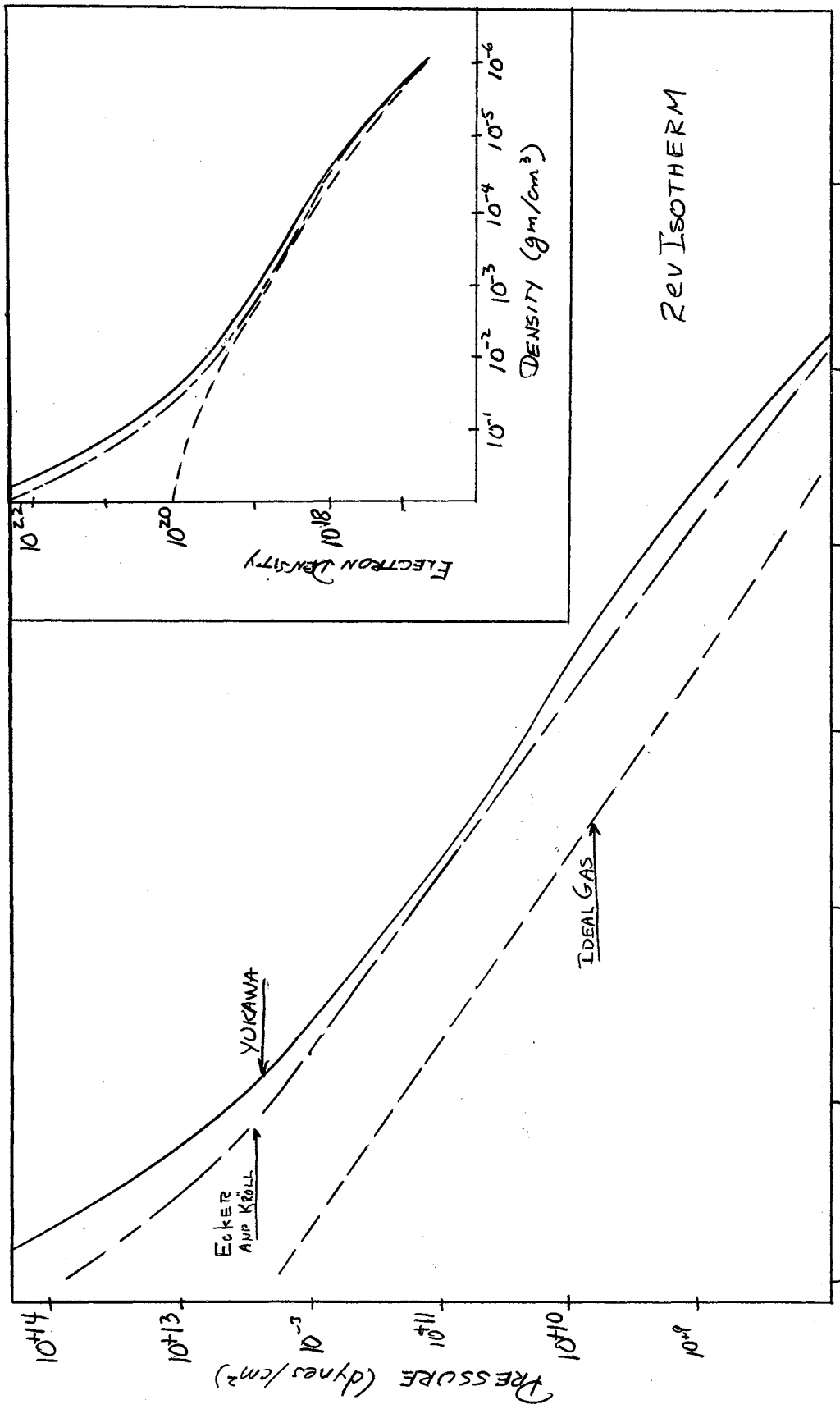

Figure 7.7. Comparison of 2 Electron-volt Isotherms.

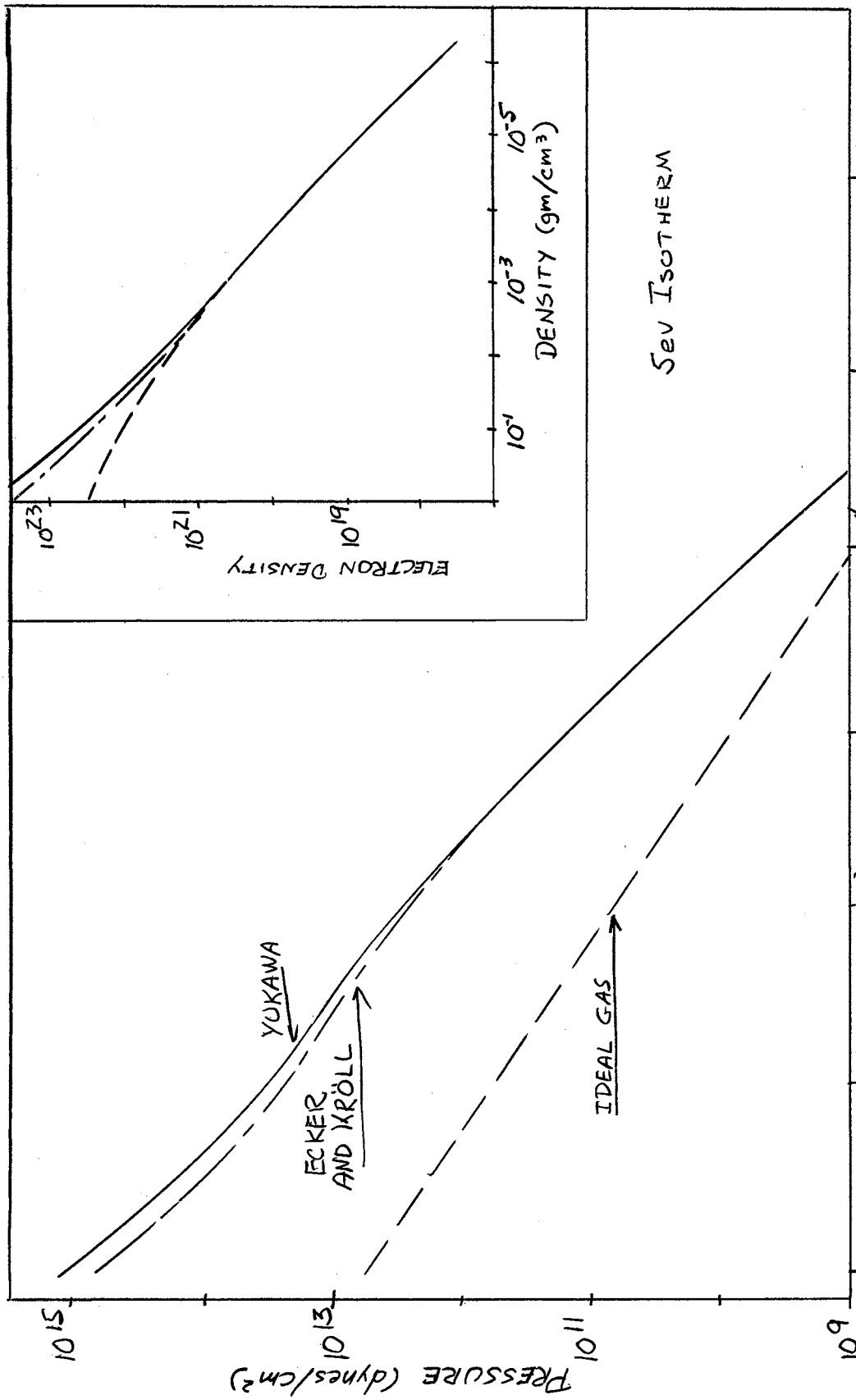

Figure 7.8. Comparison of 5 Electron-volt Isotherms

Subsequent production runs showed that the extreme high density-low temperature region of the tabular output was outside the validity range of the method. The results in this region are, therefore, suspect. An extrapolation program was written to modify the data in this region. This gave only limited improvement. Finally it was necessary to hand extrapolate the energy and pressure isotherms to obtain input data for the flow program.

3. Reduction of Output Data

Numerical output is arranged in the following form:

A. Figures 7.9 and 7.10 show the final energy-density and pressure-density isotherms that were employed as input for the flow part.

B. Table I through Table VIII are the results of the extrapolation program.

1. Table I - Extrapolated Energy Isotherm
2. Table II - Extrapolated Pressure Isotherm
3. Table III - Extrapolated Energy Per Atom
4. Table IV - Extrapolated Average Ionization
5. Table V - Temperature-Constant Energy Per Atom
6. Table VI - Energy Per Cubic Centimeter for Constant Energy Per Atom. This served as a check on the extrapolation program.
7. Table VII - Pressure for Constant Energy Per Atom
8. Table VIII- Energy Per Particle-Constant Energy Per Atom.

C. Table XI through XXIII are unmodified tabulation of the various parameters calculated by the equation of state program.

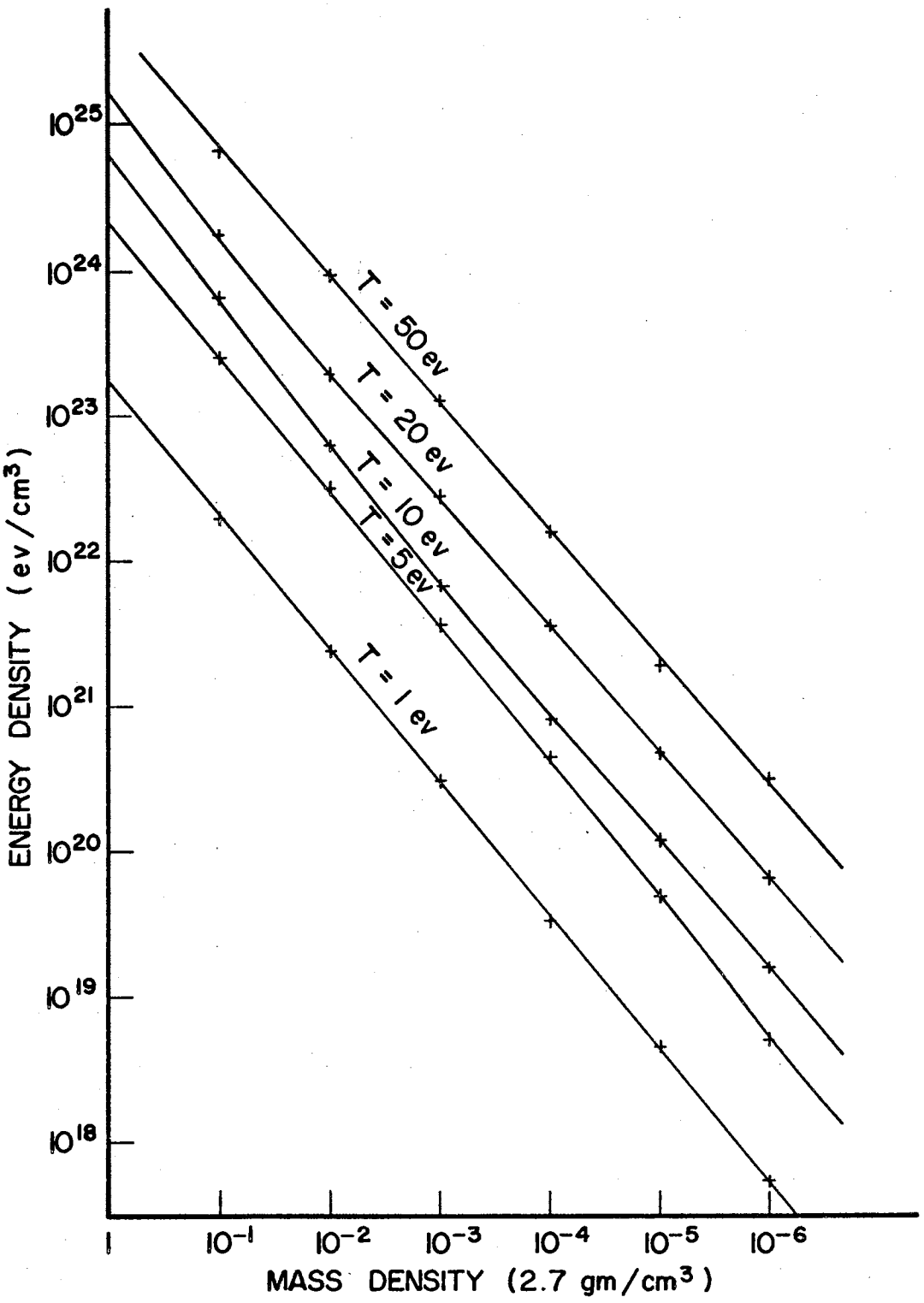

FIGURE 7.9 E-ρ ISOTHERMS – ALUMINUM ENERGY DENSITY AS A FUNCTION OF MASS DENSITY PLOTTED FOR VARIOUS TEMPERATURES, T, EXTRAPOLATED INPUT FOR FLOW PROBLEM.

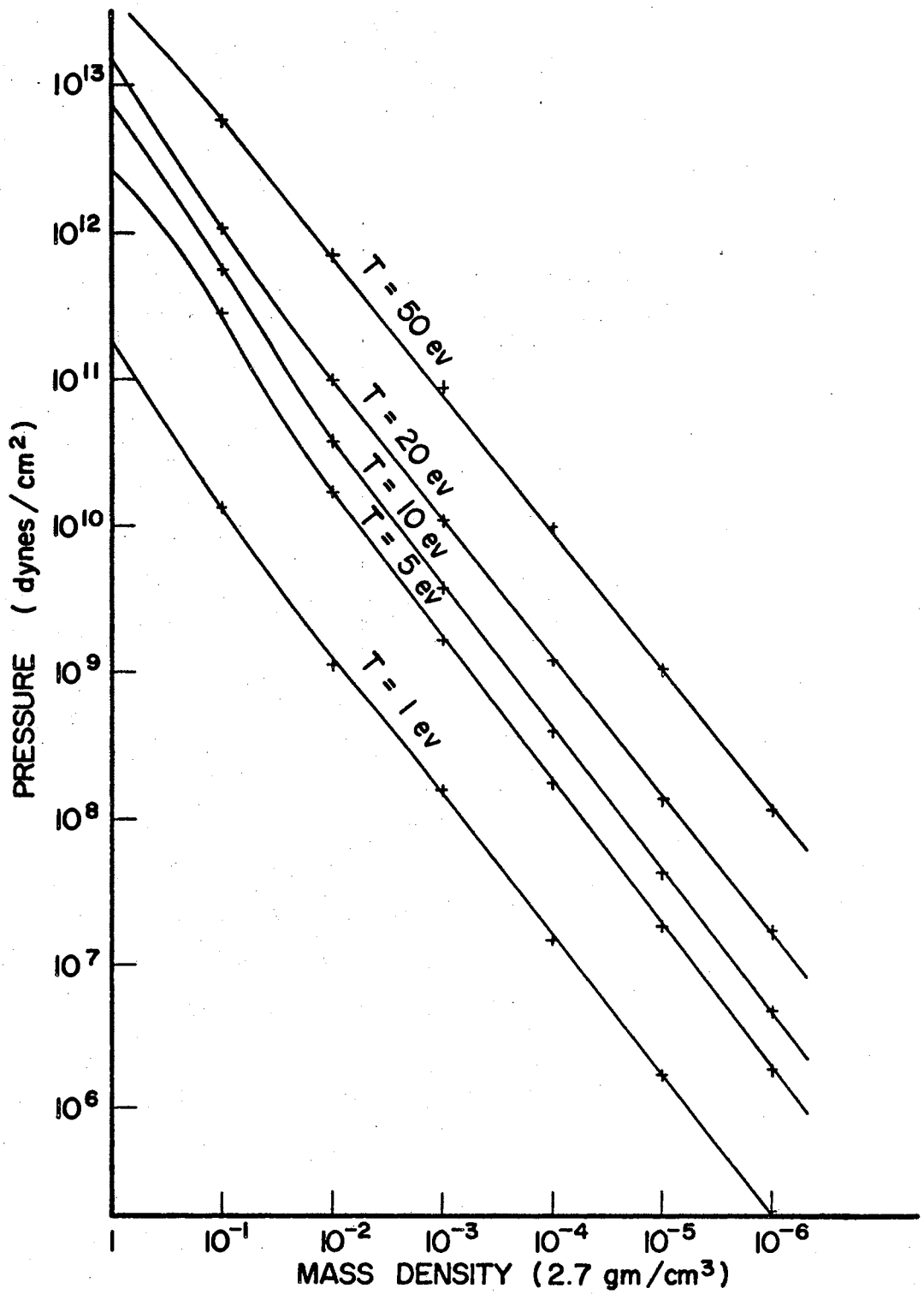

FIGURE 7.10 P-ρ ISOTHERMS—ALUMINUM PRESSURE AS A FUNCTION OF MASS DENSITY FOR 5 TEMPERATURES. EXTRAPOLATED INPUT FOR FLOW PROBLEM

TABLE I

ENERGY ISOTHERMS - EXTRAPOLATION

Density Ratio - - Tempera-Ture	1.0	1.0E-1	2.0E-2	1.0E-3	1.0E-4	1.0E-5	1.0E-6
0.1000E 01	0.7351E 24	0.1542E 23	0.2346E 22	0.3009E 21	0.3329E 20	0.4581E 19	0.5413E 18
0.2000E 01	0.9586E 24	0.1124E 24	0.1082E 23	0.9026E 21	0.1076E 21	0.1471E 20	0.1945E 19
0.5000E 01	0.8328E 24	0.3645E 24	0.3106E 23	0.3665E 22	0.4440E 21	0.4870E 20	0.4972E 19
0.1000E 02	0.5874E 25	0.6752E 24	0.6229E 23	0.6848E 22	0.8143E 21	0.1179E 21	0.1579E 20
0.2000E 02	0.1621E 26	0.1651E 25	0.1898E 24	0.2652E 23	0.3577E 22	0.4866E 21	0.6474E 20
0.5000E 02	0.5234E 26	0.6865E 25	0.9424E 24	0.1275E 24	0.1589E 23	0.1901E 22	0.3185E 21

TABLE II

PRESSURE ISOTHERMS - EXTRAPOLATION

Density Ratio - - Tempera-ture	1.0	1.0E-1	2.0E-2	1.0E-3	1.0E-4	1.0E-5	1.0E-6
0.1000E 01	0.5682E 12	0.1359E 11	0.1140E 10	0.1527E 09	0.1455E 08	0.1690E 07	0.1861E 06
0.2000E 01	0.3628E 12	0.1026E 12	0.5751E 10	0.4007E 09	0.4143E 08	0.4770E 07	0.5522E 06
0.5000E 01	0.2111E 13	0.3260E 12	0.1742E 11	0.1680E 10	0.1800E 09	0.1874E 08	0.1905E 07
0.1000E 02	0.6997E 13	0.5583E 12	0.3949E 11	0.3852E 10	0.3965E 09	0.4408E 08	0.4950E 07
0.2000E 02	0.1427E 14	0.1106E 13	0.9927E 11	0.1106E 11	0.1230E 10	0.1407E 09	0.1722E 08
0.5000E 02	0.3994E 14	0.3995E 13	0.4389E 12	0.4921E 11	0.5424E 10	0.6331E 09	0.1288E 09

TABLE III

ENERGY PER ATOM - EXTRAPOLATION

Density Ratio - - Temperature	1.0	1.0E-1	2.0E-2	1.0E-3	1.0E-4	1.0E-5	1.0E-6
0.1000E 01	0.2451E 02	0.1269E 02	0.5946E 01	0.4999E 01	0.5528E 01	0.7610E 01	0.8991E 01
0.2000E 01	0.3104E 02	0.2848E 02	0.1796E 02	0.1500E 02	0.1789E 02	0.2443E 02	0.3231E 02
0.5000E 01	0.4608E 02	0.6055E 02	0.5160E 02	0.6088E 02	0.7376E 02	0.8091E 02	0.8259E 02
0.1000E 02	0.9757E 02	0.1122E 03	0.1035E 03	0.1138E 03	0.1353E 03	0.1959E 03	0.2624E 03
0.2000E 02	0.2692E 03	0.2742E 03	0.3154E 03	0.4405E 03	0.5941E 03	0.8082E 03	0.1075E 04
0.5000E 02	0.8695E 03	0.1140E 04	0.1565E 04	0.2118E 04	0.2640E 04	0.3157E 04	0.5290E 04

TABLE IV

AVERAGE IONIZATION - EXTRAPOLATION

Density Ratio - - Temperature	1.0	1.0E-1	2.0E-2	1.0E-3	1.0E-4	1.0E-5	1.0E-6
0.1000E 01	0.3306E 01	0.1503E 01	0.6681E 00	0.4188E-00	p.4715E 00	0.7534E 00	0.9396E 00
0.2000E 01	0.3890E 01	0.2193E 01	0.1115E 01	0.9026E 00	0.1105E 01	0.1471E 01	0.1875E 01
0.5000E 01	0.3606E 01	0.2878E 01	0.1852E 01	0.2153E 01	0.2611E 01	0.2874E 01	0.2952E 01
0.1000E 02	0.3011E 01	0.2962E 01	0.2530E 01	0.2811E 01	0.3080E 01	0.3567E 01	0.4029E 01
0.2000E 02	0.3722E 01	0.3516E 01	0.3652E 01	0.4495E 01	0.5276E 01	0.6174E 01	0.6992E 01
0.5000E 02	0.5301E 01	0.6073E 01	0.7359E 01	0.8789E 01	0.9939E 01	0.1062E 02	0.1091E 02

TABLE V

TEMPERATURE - CONSTANT ENERGY PER ATOM

Density Ratio - - Energy Per Atom	1.0	1.0E-1	2.0E-2	1.0E-3	1.0E-4	1.0E-5	1.0E-6
0.1000E 01	0.1409E 01	0.3462E-00	0.5916E 00	0.5901E 00	0.6254E 00	0.6033E 00	0.6719E 00
0.1000E 02	0.7677E 00	0.8344E 00	0.1295E 01	0.1681E 01	0.1591E 01	0.1222E 01	0.5995E 00
0.5000E 02	0.7204E 01	0.3960E 01	0.4846E 01	0.3951E 01	0.3004E 01	0.3620E 01	0.4077E 01
0.1000E 03	0.1014E 02	0.9245E 01	0.9836E 01	0.9578E 01	0.9227E 01	0.8423E 01	0.7975E 01
0.5000E 03	0.3171E 02	0.2998E 02	0.2622E 02	0.2087E 02	0.1757E 02	0.1486E 02	0.1287E 02

TABLE VI

ENERGY PER CUBIC CENTIMETER - CONSTANT ENERGY/ATOM

Density Ratio - - Energy Per Atom	1.0	1.0E-1	2.0E-2	1.0E-3	1.0E-4	1.0E-5	1.0E-6
0.1000E 01	0.3996E 25	0.5140E 23	0.1195E 22	0.6025E 20	0.6042E 19	0.6008E 18	0.6018E 17
0.1000E 02	0.1257E 25	0.8134E 21	0.6023E 22	0.6017E 21	0.6016E 20	0.6025E 19	0.6022E 18
0.5000E 02	0.3010E 25	0.3011E 24	0.3010E 23	0.3010E 22	0.3010E 21	0.3010E 20	0.3010E 19
0.1000E 03	0.6020E 25	0.6019E 24	0.6020E 23	0.6020E 22	0.6018E 21	0.6019E 20	0.6016E 19
0.5000E 03	0.3010E 26	0.3011E 25	0.3010E 24	0.3009E 23	0.3010E 22	0.3010E 21	0.3010E 20

TABLE VII

PRESSURE - CONSTANT ENERGY/ATOM

Density Ratio - - Energy Per Atom	1.0	1.0E-1	2.0E-2	1.0E-3	1.0E-4	1.0E-5	1.0E-6
0.1000E 01	0.2100E 13	0.4848E 11	0.7773E 09	0.5438E 08	0.4791E 07	0.5180E 06	0.7038E 05
0.1000E 02	0.2735E 12	0.1351E 10	0.3047E 10	0.2647E 09	0.2242E 08	0.1168E 07	0.6982E 05
0.5000E 02	0.4982E 13	0.2779E 12	0.1674E 11	0.1227E 10	0.9453E 08	0.1185E 08	0.1351E 07
0.1000E 03	0.7100E 13	0.5172E 12	0.3851E 11	0.3549E 10	0.3325E 09	0.2911E 08	0.2558E 07
0.5000E 03	0.2413E 14	0.1863E 13	0.1502E 12	0.1242E 11	0.1071E 10	0.9368E 08	0.8665E 07

TABLE VIII

ENERGY PER PARTICLE - CONSTANT ENERGY/ATOM

Density Ratio - - Energy Per Atom	1.0	1.0E-1	2.0E-2	1.0E-3	1.0E-4	1.0E-5	1.0E-6
0.1000E 01	0.2105E 02	0.4298E 01	0.2567E 01	0.1727E 01	0.1970E 01	0.2080E 01	0.2294E 01
0.1000E 02	0.1291E 02	0.5814E 01	0.6171E 01	0.6623E 01	0.6806E 01	0.7072E 01	0.6910E 01
0.5000E 02	0.1510E 02	0.1300E 02	0.1775E 02	0.1713E 02	0.1543E 02	0.1487E 02	0.1515E 02
0.1000E 03	0.2479E 02	0.2586E 02	0.2868E 02	0.2772E 02	0.2839E 02	0.3182E 02	0.3559E 02
0.5000E 03	0.8930E 02	0.9361E 02	0.9209E 02	0.8391E 02	0.7874E 02	0.7610E 02	0.7594E 02

TABLE IX

TOTAL ENERGY LESS OSCILLATION ENERGY VERS TEMPERATURE AND ALUMINUM MASS DENSITY RATIO

RO Temperature	1.00E 00	1.00E-01	1.00E-02	1.00E-03	1.00E-04	1.00E-05	1.00E-06
0.10000E 01	-0.29473E 25	-0.19693E 25	0.14445E 23	0.29624E 21	0.33106E 20	0.45696E 19	0.54080E 18
0.20000E 01	-0.99157E 24	-0.54562E 22	0.10168E 23	0.88766E 21	0.10701E 21	0.14676E 20	0.19441E 19
0.50000E 01	-0.28055E 26	0.27987E 24	0.29679E 23	0.36103E 22	0.44173E 21	0.48624E 20	0.49691E 19
0.10000E 02	0.30086E 25	0.58684E 24	0.60082E 23	0.67663E 22	0.81132E 21	0.11781E 21	0.15793E 20
0.20000E 02	0.12270E 26	0.15366E 25	0.18604E 24	0.26355E 23	0.35701E 22	0.48630E 21	0.64732E 20
0.50000E 02	0.45649E 26	0.66055E 25	0.93153E 24	0.12703E 24	0.15874E 23	0.19001E 22	0.31848E 21

TABLE X

PLASMA OSCILLATION ENERGY = c_e hw_o VERS TEMPERATURE AND ALUMINUM MASS DENSITY RATIO

RO Temperature	1.00E 00	1.00E-01	1.00E-02	1.00E-03	1.00E-04	1.00E-05	1.00E-06
0.10000E 01	0.39283E 24	0.11876E 24	0.26575E 22	0.43912E 19	0.17758E 18	0.11346E 17	0.50006E 15
0.20000E 01	0.54894E 24	0.70156E 23	0.82364E 21	0.15830E 20	0.63988E 18	0.30933E 17	0.14075E 16
0.50000E 01	0.44512E 25	0.84598E 23	0.13640E 22	0.54929E 20	0.23110E 19	0.84516E 17	0.27805E 16
0.10000E 02	0.25144E 25	0.88404E 23	0.22200E 22	0.81795E 20	0.29618E 19	0.11677E 18	0.44318E 16
0.20000E 02	0.38842E 25	0.10506E 24	0.38590E 22	0.16553E 21	0.66526E 19	0.26615E 18	0.10133E 17
0.50000E 02	0.64599E 25	0.25176E 24	0.10856E 23	0.44967E 21	0.17145E 20	0.60023E 18	0.19753E 17

TABLE XI

PLASMA OSCILLATION ENERGY VERS TEMPERATURE AND ALUMINUM MASS DENSITY RATIO

RO Temperature	1.00E 00	1.00E-01	1.00E-02	1.00E-03	1.00E-04	1.00E-05	1.00E-06
0.10000E 01	0.12454E 21	0.38034E 21	0.29687E 21	0.99877E 17	0.37730E 16	0.24099E 15	0.10615E 14
0.20000E 01	0.57226E 22	0.64319E 22	0.28677E 20	0.22346E 18	0.95777E 16	0.46486E 15	0.21163E 14
0.50000E 01	0.10710E 24	0.12506E 23	0.13134E 20	0.52077E 18	0.21989E 17	0.80303E 15	0.26429E 14
0.10000E 02	0.48954E 24	0.68573E 22	0.14833E 20	0.54917E 18	0.19924E 17	0.78510E 15	0.29799E 14
0.20000E 02	0.98100E 24	0.44559E 22	0.18184E 20	0.78528E 18	0.31583E 17	0.12641E 16	0.48182E 14
0.50000E 02	0.82358E 24	0.77991E 21	0.32901E 20	0.13580E 19	0.51641E 17	0.18043E 16	0.59388E 14

TABLE XII

TOTAL PRESSURE VERS TEMPERATURE AND ALUMINUM MASS DENSITY RATIO

RO Temperature	1.00E 00	1.00E-01	1.00E-02	1.00E-03	1.00E-04	1.00E-05	1.00E-06
0.10000E 01	-0.11017E 13	-0.14725E 13	0.66317E 10	0.15274E 09	0.14552E 08	0.16904E 07	0.18605E 06
0.20000E 01	0.64700E 12	0.12877E 12	0.57511E 10	0.40072E 09	0.41431E 08	0.47702E 07	0.55215E 06
0.50000E 01	-0.77337E 13	0.32604E 12	0.17418E 11	0.16795E 10	0.18000E 09	0.18741E 08	0.19054E 07
0.10000E 02	0.69973E 13	0.55828E 12	0.39486E 11	0.38517E 10	0.39651E 09	0.44079E 08	0.49502E 07
0.20000E 02	0.14270E 14	0.11064E 13	0.99267E 11	0.11062E 11	0.12299E 10	0.14065E 09	0.17223E 08
0.50000E 02	0.39939E 14	0.39954E 13	0.43893E 12	0.49209E 11	0.54236E 10	0.63314E 09	0.12883E 09

TABLE XIII

IDEAL GAS PRESSURE VERS TEMPERATURE AND ALUMINUM MASS DENSITY RATIO

RO Tempera- ture	1.00E 00	1.00E-01	1.00E-02	1.00E-03	1.00E-04	1.00E-05	1.00E-06
0.10000E 01	0.17101E 12	0.52149E 11	0.37254E 10	0.13686E 09	0.14194E 08	0.16915E 07	0.18711E 06
0.20000E 01	0.38586E 12	0.68229E 11	0.40767E 10	0.36710E 09	0.40598E 08	0.47632E 07	0.55438E 06
0.50000E 01	0.26871E 13	0.18688E 12	0.13755E 11	0.15214E 10	0.17419E 09	0.18692E 08	0.19043E 07
0.10000E 02	0.38704E 13	0.38188E 12	0.34059E 11	0.36724E 10	0.39336E 09	0.44011E 08	0.48466E 07
0.20000E 02	0.91124E 13	0.87051E 12	0.89753E 11	0.10592E 11	0.12114E 10	0.13847E 09	0.15406E 08
0.50000E 02	0.30369E 14	0.34121E 13	0.40288E 12	0.47176E 11	0.52714E 10	0.55994E 09	0.57384E 08

TABLE XIV

PLASMA FREQUENCY VERS TEMPERATURE AND ALUMINUM MASS DENSITY RATIO

RO Tempera- ture	1.00E 00	1.00E-01	1.00E-02	1.00E-03	1.00E-04	1.00E-05	1.00E-06
0.10000E 01	0.19370E 16	0.14621E 16	0.37286E 15	0.45083E 14	0.15127E 14	0.60467E 13	0.21355E 13
0.20000E 01	0.22039E 16	0.11101E 16	0.23257E 15	0.66185E 14	0.23162E 14	0.84489E 13	0.30168E 13
0.50000E 01	0.47112E 16	0.11818E 16	0.29979E 15	0.10223E 15	0.35597E 14	0.11810E 14	0.37848E 13
0.10000E 02	0.38227E 16	0.11990E 16	0.35042E 15	0.11679E 15	0.38664E 14	0.13157E 14	0.44217E 13
0.20000E 02	0.42499E 16	0.13062E 16	0.42098E 15	0.14769E 15	0.50603E 14	0.17310E 14	0.58253E 13
0.50000E 02	0.50721E 16	0.17167E 16	0.59761E 15	0.20653E 15	0.69451E 14	0.22705E 14	0.72763E 13

TABLE XV

AVERAGE IONIZATION VERS TEMPERATURE AND ALUMINUM MASS DENSITY RATIO

RO Temperature	1.00E 00	1.00E-01	1.00E-02	1.00E-03	1.00E-04	1.00E-05	1.00E-06
0.10000E 01	0.77312E 00	0.44049E 01	0.28646E 01	0.41879E-00	0.47150E-00	0.75339E 00	0.93964E 00
0.20000E 01	0.10008E 01	0.25394E 01	0.11145E 01	0.90260E 00	0.11054E 01	0.14709E 01	0.18754E 01
0.50000E 01	0.45734E 01	0.28777E 01	0.18519E 01	0.21533E 01	0.26111E 01	0.28741E 01	0.29516E 01
0.10000E 02	0.30111E 01	0.29621E 01	0.25302E 01	0.28108E 01	0.30804E 01	0.35670E 01	0.40286E 01
0.20000E 02	0.37216E 01	0.35156E 01	0.36517E 01	0.44948E 01	0.52763E 01	0.61738E 01	0.69923E 01
0.50000E 02	0.53009E 01	0.60725E 01	0.73590E 01	0.87892E 01	0.99388E 01	0.10622E 02	0.10910E 02

TABLE XVI

ELECTRON DENSITY VERS TEMPERATURE AND ALUMINUM MASS DENSITY RATIO

RO Temperature	1.00E 00	1.00E-01	1.00E-02	1.00E-03	1.00E-04	1.00E-05	1.00E-06
0.10000E 01	0.46542E 23	0.26518E 23	0.17245E 22	0.25211E 20	0.28384E 19	0.45354E 18	0.56567E 17
0.20000E 01	0.60251E 23	0.15287E 23	0.67093E 21	0.54337E 20	0.66548E 19	0.88547E 18	0.11290E 18
0.50000E 01	0.27532E 24	0.17324E 23	0.11148E 22	0.12963E 21	0.15719E 20	0.17302E 19	0.17769E 18
0.10000E 02	0.18127E 24	0.17832E 23	0.15232E 22	0.16921E 21	0.18544E 20	0.21473E 19	0.24252E 18
0.20000E 02	0.22404E 24	0.21164E 23	0.21983E 22	0.27059E 21	0.31764E 20	0.37166E 19	0.42093E 18
0.50000E 02	0.31911E 24	0.36557E 23	0.44301E 22	0.52911E 21	0.59832E 20	0.63945E 19	0.65675E 18

TABLE XVII

DEBYE RADIUS VERS TEMPERATURE AND ALUMINUM MASS DENSITY RATIO

RO Temperature	1.00E 00	1.00E-01	1.00E-02	1.00E-03	1.00E-04	1.00E-05	1.00E-06
0.10000E 01	0.15918E-08	0.17120E-08	0.90602E-08	0.10465E-06	0.31192E-06	0.78021E-06	0.22089E-05
0.20000E 01	0.23488E-08	0.43954E-08	0.27070E-07	0.98019E-07	0.27005E-06	0.68639E-06	0.18216E-05
0.50000E 01	0.12024E-08	0.63870E-08	0.28426E-07	0.80046E-07	0.21736E-06	0.63803E-06	0.19828E-05
0.10000E 02	0.26504E-08	0.88363E-08	0.31498E-07	0.91852E-07	0.26815E-06	0.74564E-06	0.21225E-05
0.20000E 02	0.31640E-08	0.10653E-07	0.32308E-07	0.85623E-07	0.23315E-06	0.63813E-06	0.18131E-05
0.50000E 02	0.36625E-08	0.10271E-07	0.27226E-07	0.73092E-07	0.20631E-06	0.61435E-06	0.18935E-05

TABLE XVIII

TRANSLATION ENERGY VERS TEMPERATURE AND ALUMINUM MASS DENSITY RATIO

RO Temperature	1.00E 00	1.00E-01	1.00E-02	1.00E-03	1.00E-04	1.00E-05	1.00E-06
0.10000E 01	0.16013E 24	0.48828E 23	0.34882E 22	0.12814E 21	0.13290E 20	0.15838E 19	0.17520E 18
0.20000E 01	0.36129E 24	0.63885E 23	0.38171E 22	0.34372E 21	0.38013E 20	0.44599E 19	0.51908E 18
0.50000E 01	0.25160E 25	0.17498E 24	0.12879E 23	0.14245E 22	0.16310E 21	0.17502E 20	0.17830E 19
0.10000E 02	0.36240E 25	0.35757E 24	0.31890E 23	0.34386E 22	0.36831E 21	0.41209E 20	0.45380E 19
0.20000E 02	0.85322E 25	0.81508E 24	0.84039E 23	0.99180E 22	0.11342E 22	0.12965E 21	0.14425E 20
0.50000E 02	0.28435E 26	0.31948E 25	0.37723E 24	0.44172E 23	0.49358E 22	0.52428E 21	0.53731E 20

TABLE XIX

IONIZATION ENERGY VERS TEMPERATURE AND ALUMINUM MASS DENSITY RATIO

RO Temperature	1.00E 00	1.00E-01	1.00E-02	1.00E-03	1.00E-04	1.00E-05	1.00E-06
0.10000E 01	0.18929E 25	0.24062E 25	0.29769E 23	0.15089E 21	0.16987E 20	0.27147E 19	0.33898E 18
0.20000E 01	0.84314E 24	0.25077E 24	0.50925E 22	0.36546E 21	0.51736E 20	0.90078E 19	0.13629E 19
0.50000E 01	0.22858E 26	0.29975E 24	0.14044E 23	0.18230E 22	0.25503E 21	0.29930E 20	0.31191E 19
0.10000E 02	0.52407E 25	0.31819E 24	0.24409E 23	0.30208E 22	0.41954E 21	0.74059E 20	0.10870E 20
0.20000E 02	0.91738E 25	0.70650E 24	0.84362E 23	0.15226E 23	0.23200E 22	0.34244E 21	0.45911E 20
0.50000E 02	0.24056E 26	0.33613E 25	0.52547E 24	0.79350E 23	0.10519E 23	0.12235E 22	0.12999E 21

TABLE XX

EXCITATION ENERGY VERS TEMPERATURE AND ALUMINUM MASS DENSITY RATIO

RO Temperature	1.00E 00	1.00E-01	1.00E-02	1.00E-03	1.00E-04	1.00E-05	1.00E-06
0.10000E 01	0.71840E 19	0.73013E 14	0.	0.11432E 20	0.26300E 19	0.28518E 18	0.28743E 17
0.20000E 01	0.10135E 09	0.67416E 02	0.12675E 22	0.16148E 21	0.16980E 20	0.12393E 19	0.67102E 17
0.50000E 01	0.24790E 19	0.28953E 14	0.23783E 22	0.30649E 21	0.21424E 20	0.12594E 19	0.65796E 17
0.10000E 02	0.26678E 22	0.24650E 22	0.25845E 22	0.23388E 21	0.23587E 20	0.25506E 19	0.19196E 18
0.20000E 02	0.57341E 23	0.63933E 23	0.15752E 23	0.10779E 22	0.10784E 21	0.10939E 20	0.10055E 19
0.50000E 02	0.94406E 24	0.29520E 24	0.32960E 23	0.31638E 22	0.26606E 21	0.18271E 20	0.10183E 19

TABLE XXI

DEGENERACY ENERGY VERS TEMPERATURE AND ALUMINUM MASS DENSITY RATIO

RO Temperature	1.00E 00	1.00E-01	1.00E-02	1.00E-03	1.00E-04	1.00E-05	1.00E-06
0.10000E 01	0.77817E 23	0.26399E 23	0.12008E 21	0.25810E 17	0.32718E 15	0.83536E 13	0.12995E 12
0.20000E 01	0.97701E 23	0.65936E 22	0.12916E 20	0.84778E 17	0.12717E 16	0.22515E 14	0.36601E 12
0.50000E 01	0.12789E 25	0.54228E 22	0.22565E 20	0.30518E 18	0.44873E 16	0.54368E 14	0.57343E 12
0.10000E 02	0.41414E 24	0.40759E 22	0.29791E 20	0.36769E 18	0.44161E 16	0.59216E 14	0.75534E 12
0.20000E 02	0.45205E 24	0.40643E 22	0.43881E 20	0.66487E 18	0.91619E 16	0.12544E 15	0.16090E 13
0.50000E 02	0.58310E 24	0.76726E 22	0.11271E 21	0.16079E 19	0.20560E 17	0.23484E 15	0.24772E 13

TABLE XXII

MAYER CORRECTION ENERGY VERS TEMPERATURE AND ALUMINUM MASS DENSITY RATIO

RO Temperature	1.00E 00	1.00E-01	1.00E-02	1.00E-03	1.00E-04	1.00E-05	1.00E-06
0.10000E 01	-0.50768E 25	-0.44507E 25	-0.18932E 23	0.57558E 19	0.19895E 18	-0.14057E 17	-0.21336E 16
0.20000E 01	-0.22927E 25	-0.32670E 24	-0.22505E 20	0.16911E 20	0.28377E 18	-0.31555E 17	-0.53877E 16
0.50000E 01	-0.54708E 26	-0.20029E 24	0.35469E 21	0.55980E 20	0.21566E 19	-0.80808E 17	-0.12264E 17
0.10000E 02	-0.62729E 25	-0.95449E 23	0.11690E 22	0.72453E 20	-0.33843E 18	-0.22355E 18	-0.21107E 17
0.20000E 02	-0.59450E 25	-0.53027E 23	0.18428E 22	0.12909E 21	0.45173E 19	-0.15311E 18	-0.36200E 17
0.50000E 02	-0.83702E 25	-0.25359E 24	-0.43705E 22	0.20962E 21	0.19547E 20	0.28877E 18	-0.84025E 17

TABLE XXIII

RADIATION ENERGY VERS TEMPERATURE AND ALUMINUM MASS DENSITY RATIO

RO Temperature	1.00E 00	1.00E-01	1.00E-02	1.00E-03	1.00E-04	1.00E-05	1.00E-06
0.10000E 01	0.21413E 14	0.21413E 14	0.21413E 14	0.21413E 14	0.21413E 14	0.21413E 14	0.21413E 14
0.20000E 01	0.34261E 15	0.34261E 15	0.34261E 15	0.34261E 15	0.34261E 15	0.34261E 15	0.34261E 15
0.50000E 01	0.13383E 17	0.13383E 17	0.13383E 17	0.13383E 17	0.13383E 17	0.13383E 17	0.13383E 17
0.10000E 02	0.21413E 18	0.21413E 18	0.21413E 18	0.21413E 18	0.21413E 18	0.21413E 18	0.21413E 18
0.20000E 02	0.34261E 19	0.34261E 19	0.34261E 19	0.34261E 19	0.34261E 19	0.34261E 19	0.34261E 19
0.50000E 02	0.13383E 21	0.13383E 21	0.13383E 21	0.13383E 21	0.13383E 21	0.13383E 21	0.13383E 21

3. Arbitrary Potential Model

Computer code for the IBM 7094 was written and tested at the Goddard facility. It was demonstrated that the arbitrary model is feasable. provided sufficient time is available to determine the best choice of potential parameters. Unfortunately, sufficient time was unavailable at the time that the program was tested. It is felt that the preliminary tests show that the model may be successfully calculated.

CHAPTER VIII

SOLUTION AND REDUCTION OF DATA - FLOW PROBLEM

1. Machine Computations

As a preliminary to the calculations in this thesis, a simplified version of the problem was solved. This version employed a one fluid model of the plasma and a much simplified equation of state. Successful runs of this problem served to establish a stable differencing scheme and demonstrated the feasibility of the proposed method of solution.

The full scale program was debugged by using the IBM 7094 computer at the Continental Oil Company, Ponca City, Oklahoma. When the validity of the program was established, the code was carried to Goddard Space Flight Center, Greenbelt, Maryland for subsequent check out and production runs.

2. Initial Conditions

The problem was run for four sets of initial conditions. These conditions differed only in the initial energy density of the sample. These energy densities were chosen to give initial temperatures of approximately 3.5 ev, 10 ev, 20 ev and 45 ev. Figure 8.1 corrolates the original energy input values to original energy per atom. All runs started from the same initial boundary, a sphere of aluminum with a radius of 4.25×10^{-3} cm and a density of 2.7 gn/cm^3. The Courant value for all runs was 0.1. In all cases the external electric field was set to start at 1 cm radius.

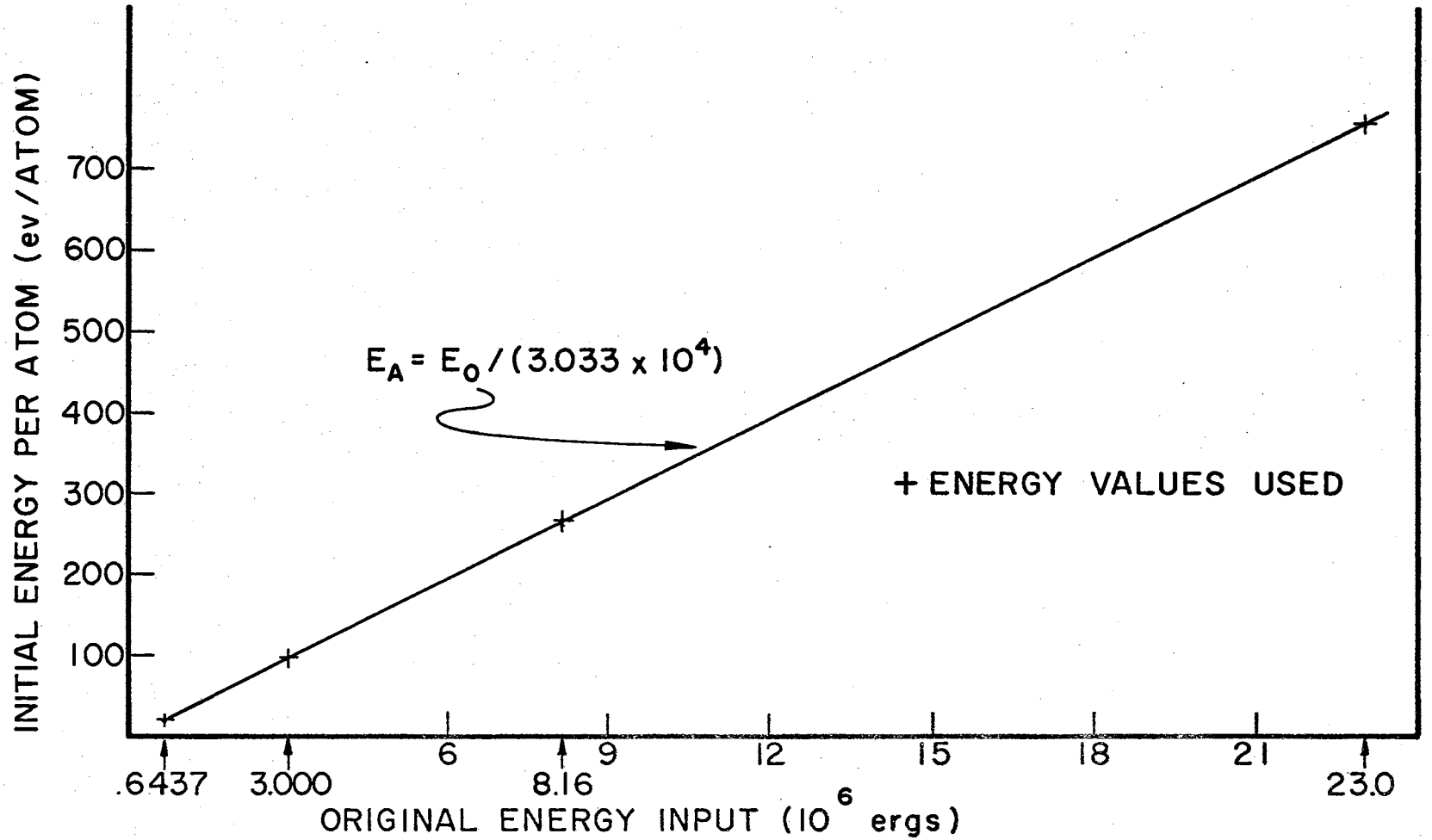

FIGURE 8.1 CONVERSION OF INITIAL ENERGY INPUT TO INITIAL ENERGY PER ATOM

The initial Δr for all runs was taken as 1.41×10^{-3} cm which spread the initial sphere over the first 25 cells of the mesh. A total of 201 radial mesh spaces were maintained throughout the solution by means of periodic machine condensations. All runs were terminated at 2500 cycles and the output was taken every 100 cycles, except when a condensation occurred. Outputs were also taken immediately before each condensation. Each output yields radial profiles of the density, pressure, charge, temperature, flow velocity, election diffusion velocity, internal energy density, total energy density, average ionization and electric field strength.

3. Reduction of Output Data

The numerical output produced in these four runs is of such a large extent that only a small portion of it can be given here. In order to give as much of the truly meaningful data as space permits, a graphical representation was chosen. Profiles generated after 300, 500, 1000, 2000 and 2500 cycles are presented here. This allows one to follow the time development of the plasma expansion. The profiles of the principal variables are plotted against radial distance. In all cases the indications on the radial distances are for 10 mesh numbers. The mesh number are related to the radial distance through Δr by the formula

$$r = r_0 + n\Delta r \quad . \tag{8.1}$$

4. Organization of Results

The graphical results are grouped according to initial conditions; each being further subdivided according to the time elapsed. For easy

reference, a list of the graphs is given below. In each time group the first figure shows the density and pressure profile; the second shows the temperature and ionization profile and the third shows the distribution of excess charges.

I. $E_o = 6.437 \times 10^5$ ergs

A. Time = 2.744 n sec

1. Figure 8.2
2. Figure 8.3
3. Figure 8.4

B. Time = 5.028 n sec

1. Figure 8.5
2. Figure 8.6
3. Figure 8.7

C. Time = 10.74 n sec

1. Figure 8.8
2. Figure 8.9
3. Figure 8.10

D. Time = 28.6 n sec

1. Figure 8.11
2. Figure 8.12
3. Figure 8.13

E. Time = 44.47 n sec

1. Figure 8.14
2. Figure 8.15
3. Figure 8.16

F. Figure 8.17 - Flow Velocity for All Profile Times

II. $E_o = 3.000 \times 10^6$ erg

A. Time = 1.192 n sec

1. Figure 8.18

2. Figure 8.19

3. Figure 8.20

B. Time = 2.25 n sec

1. Figure 8.21

2. Figure 8.22

3. Figure 8.23

C. Time = 4.895 n sec

1. Figure 8.24

2. Figure 8.25

3. Figure 8.26

D. Time = 13.08 n sec

1. Figure 8.27

2. Figure 8.28

3. Figure 8.29

E. Time = 20.26 n sec

1. Figure 8.30

2. Figure 8.31

3. Figure 8.32

F. Figure 8.33 Flow Velocity for All Profile Times

III. $E_o = 8.16 \times 10^6$ erg

A. Time = .7091 n sec

1. Figure 8.34

2. Figure 8.35

3. Figure 8.36

B. Time =

1. Figure 8.37

2. Figure 8.38

3. Figure 8.39

C. Time = 2.954 n sec

1. Figure 8.40

2. Figure 8.41

3. Figure 8.42

D. Time = 7.884 n sec

1. Figure 8.43

2. Figure 8.44

3. Figure 8.45

E. Time = 12.14 n sec

1. Figure 8.46

2. Figure 8.47

3. Figure 8.48

F. Figure 8.49 Flow Velocity for All Profile Times

IV. $E_o = 2.3 \times 10^7$ erg

A. Time = .343 n sec

1. Figure 8.50

2. Figure 8.51

3. Figure 8.52

B. Time = .7252 n sec

1. Figure 8.53
2. Figure 8.54
3. Figure 8.55

C. Time = 1.68 n sec

1. Figure 8.56
2. Figure 8.57
3. Figure 8.58

D. Time = 4.527 n sec

1. Figure 8.59
2. Figure 8.60
3. Figure 8.61

E. Time = 6.873 n sec

1. Figure 8.62
2. Figure 8.63
3. Figure 8.64

F. Figure 8.65 Flow Velocity for All Profile Times

5. Validity of the Numerical Solution

Two checks on the numerical solution are possible:

1. The maximum terminal velocity may not exceed that which internal energy allows;
2. The density maximum and leading edge of the expanding plasma must expand with approximately the terminal velocity.

Figure 8.66 shows the maximum allowed terminal velocity which is given by the formula

$$V_{max} = (2E_0/\rho)^{1/2}. \qquad (8.2)$$

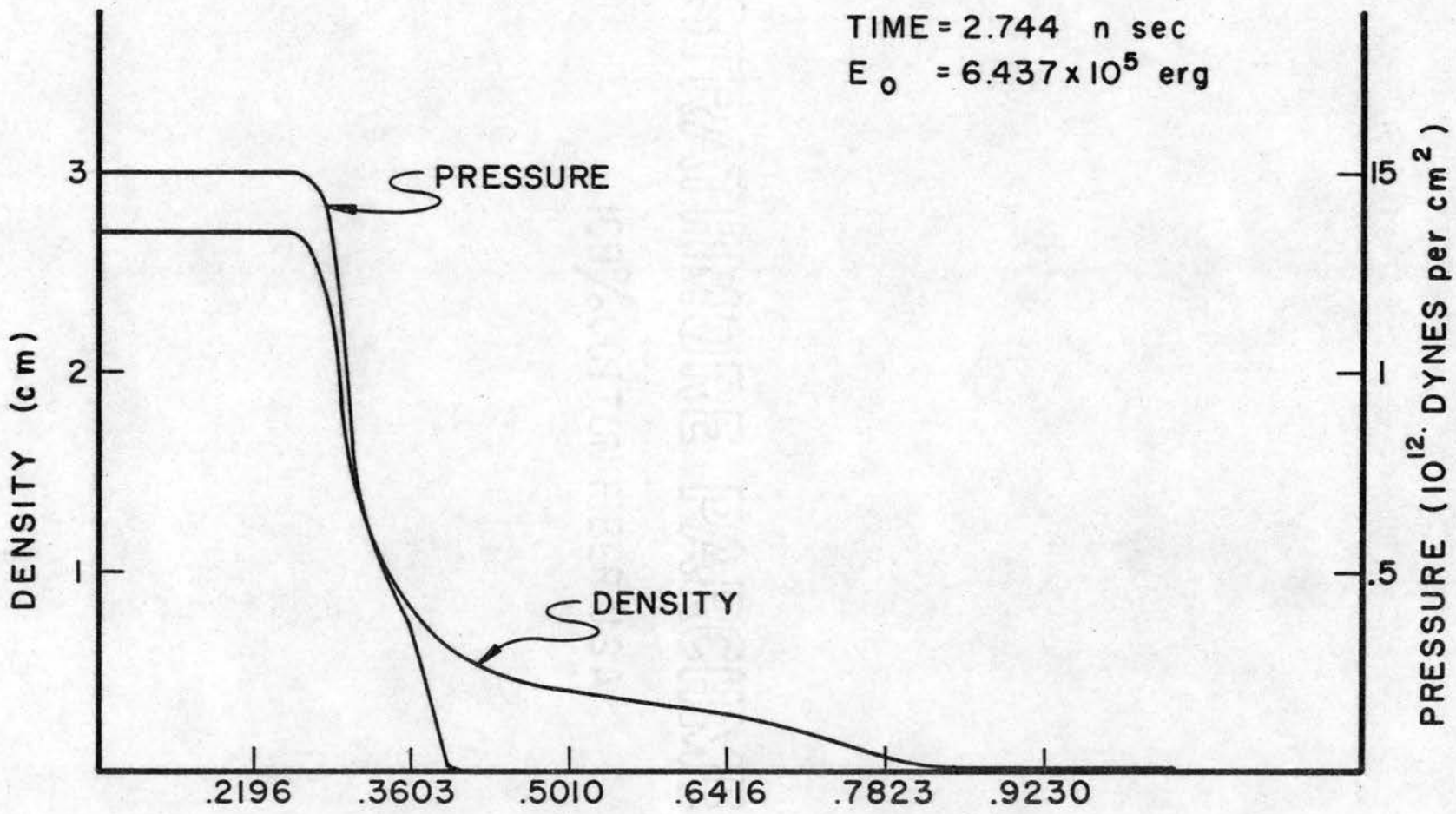

FIGURE 8.2 DENSITY AND PRESSURE VERS RADIUS

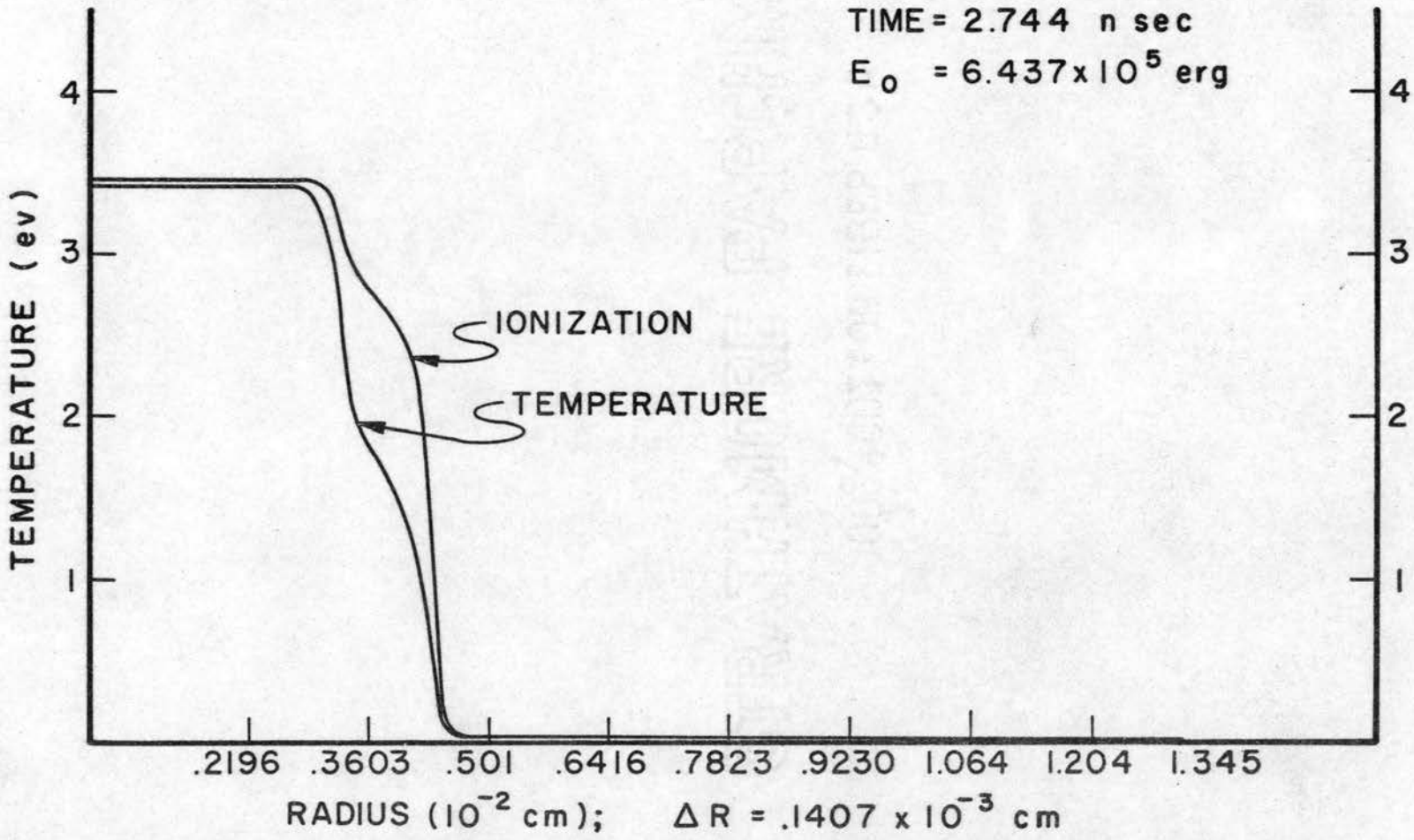

FIGURE 8.3 TEMPERATURE AND AVERAGE IONIZATION VERS RADIUS

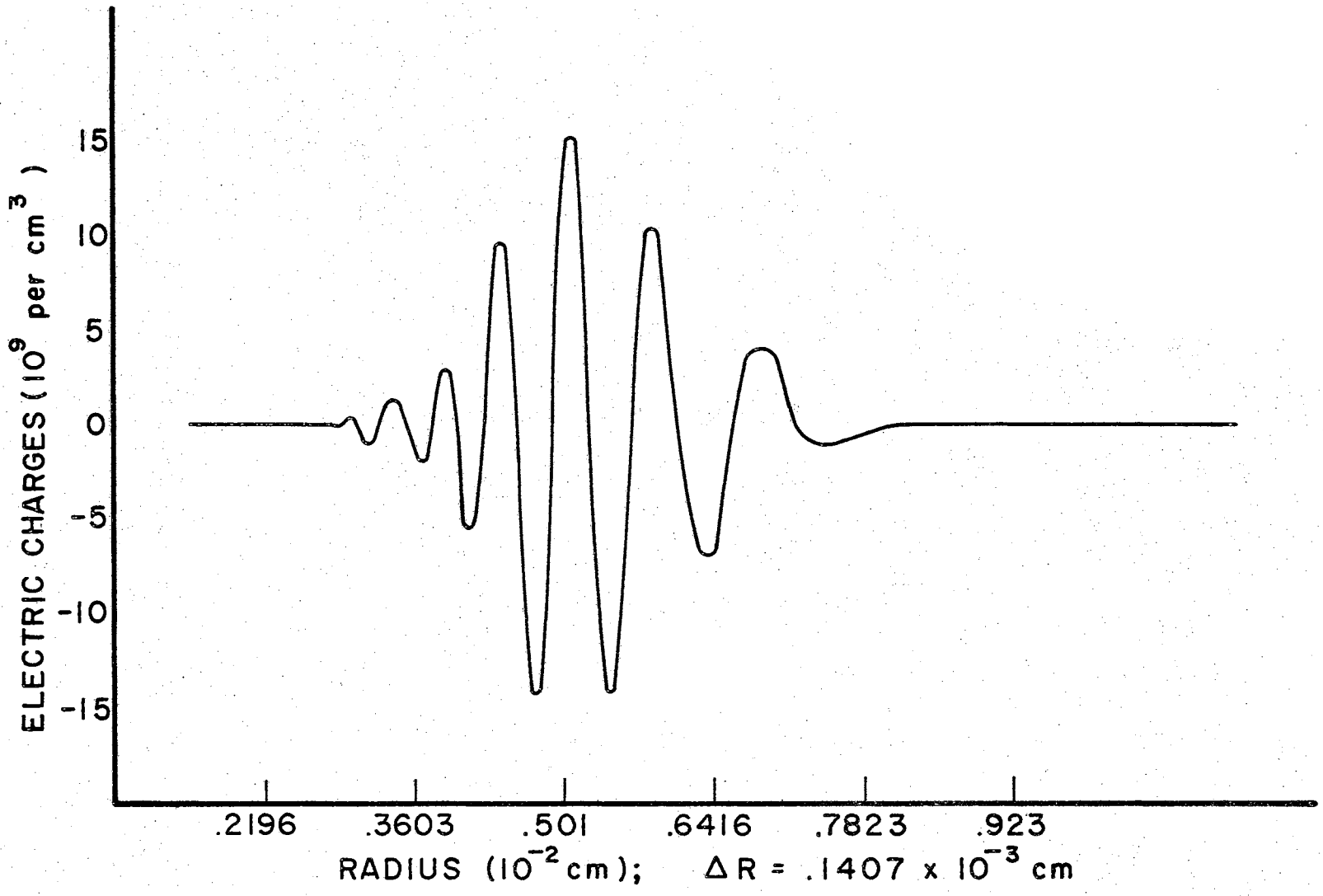

FIGURE 8.4 NUMBER OF EXCESS ELECTRONIC CHARGES VERS RADIUS

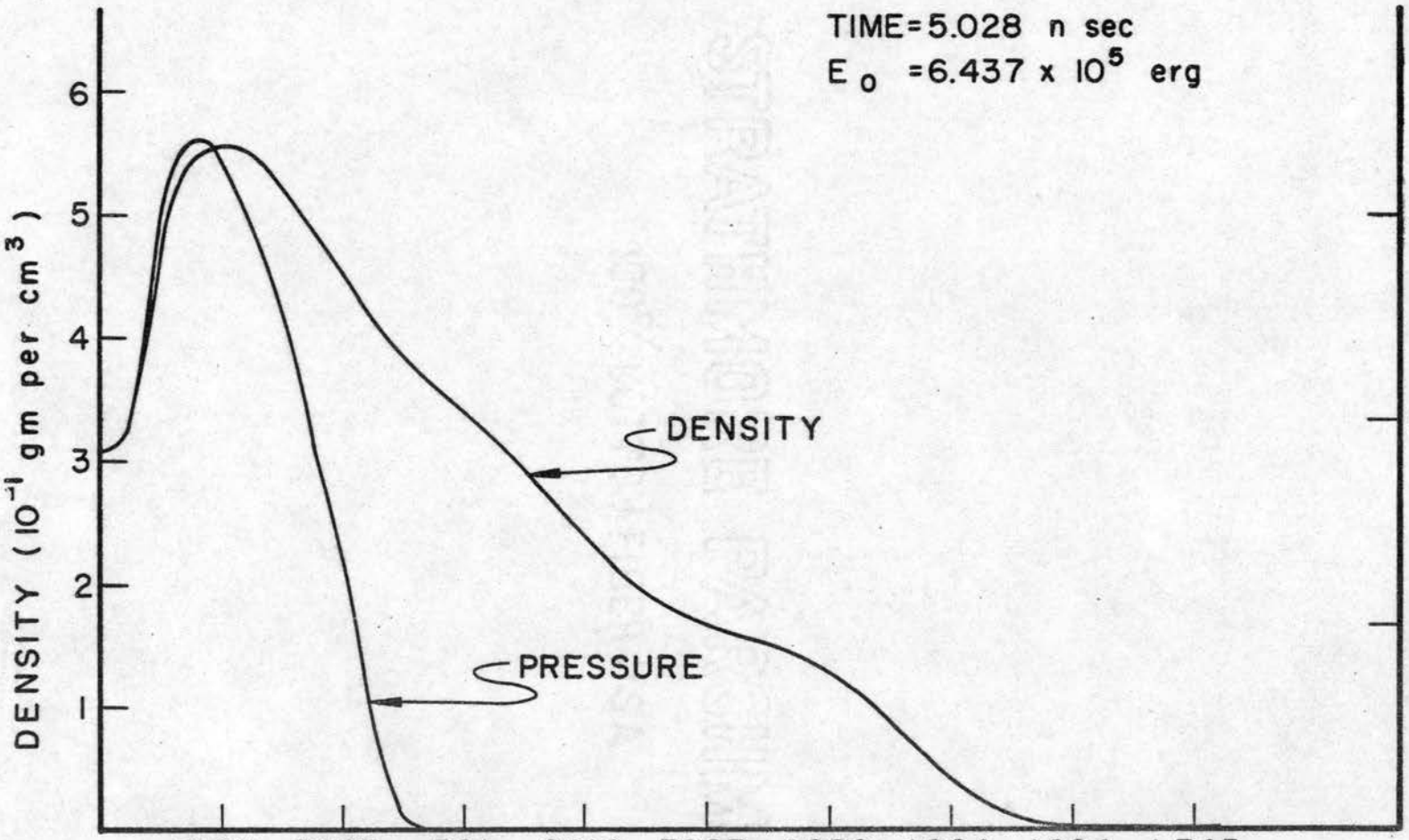

FIGURE 8.5 DENSITY AND PRESSURE VERS RADIUS

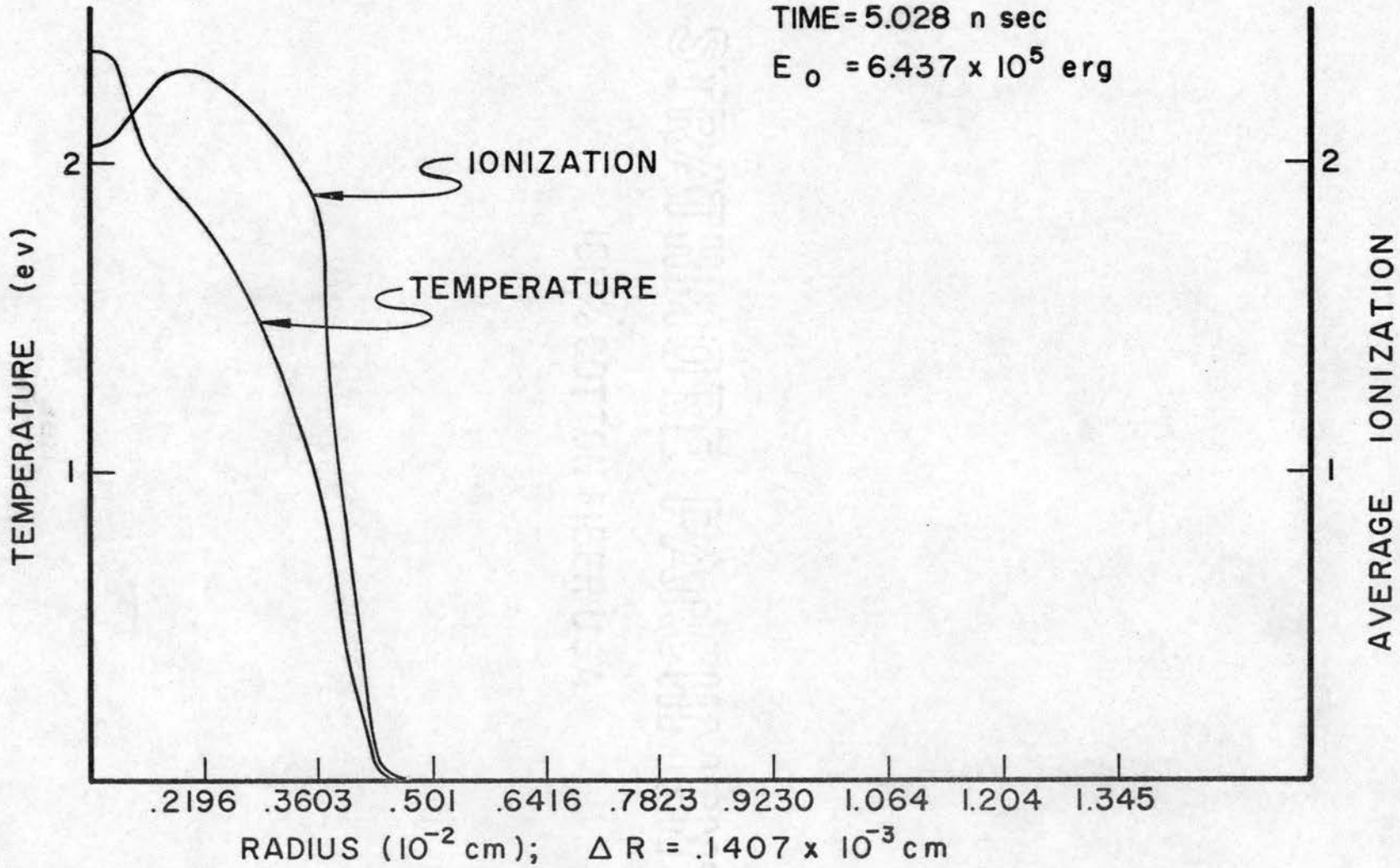

FIGURE 8.6 TEMPERATURE AND AVERAGE IONIZATION VERS RADIUS

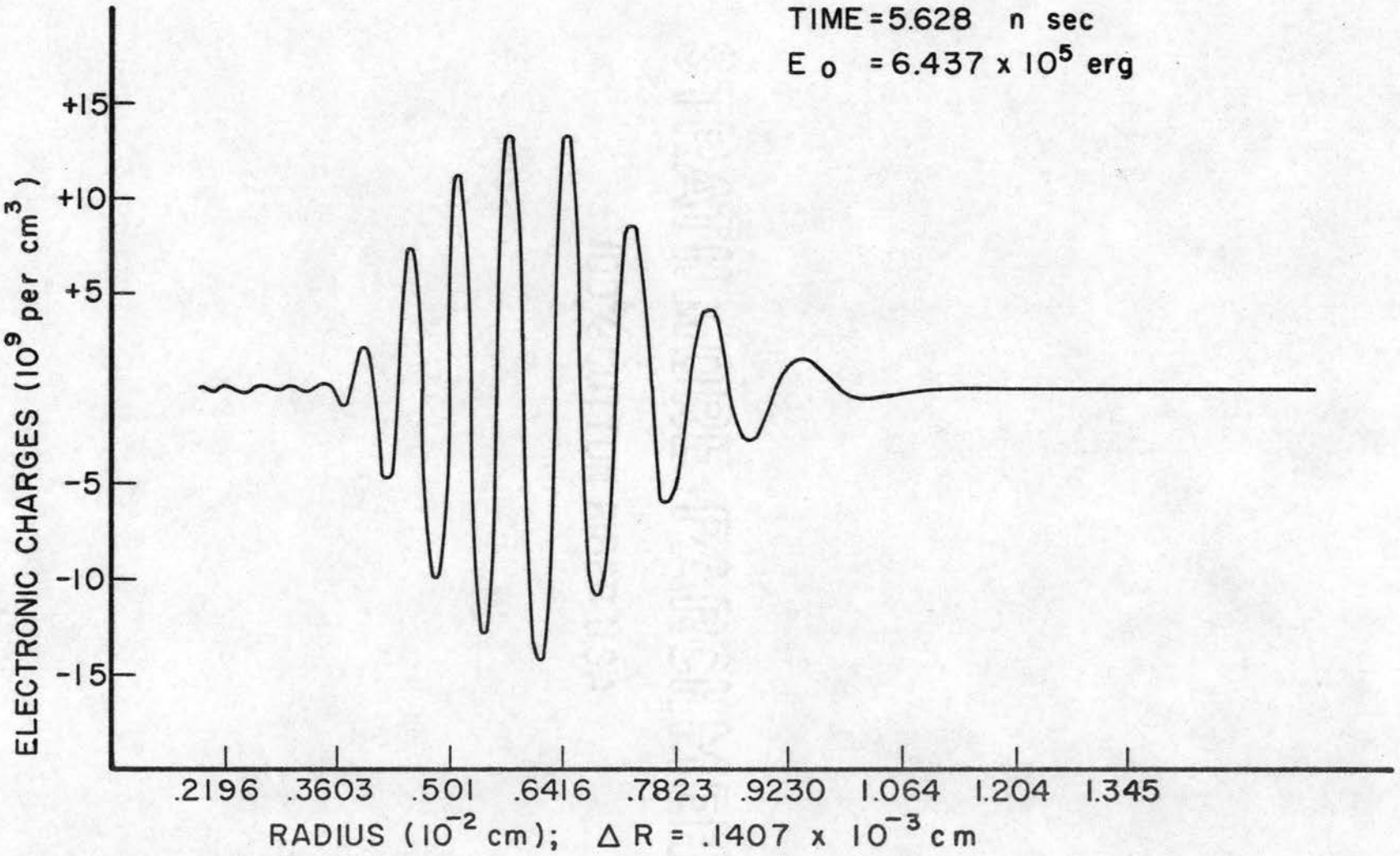

FIGURE 8.7 NUMBER OF EXCESS ELECTRONIC CHARGES VERS RADIUS

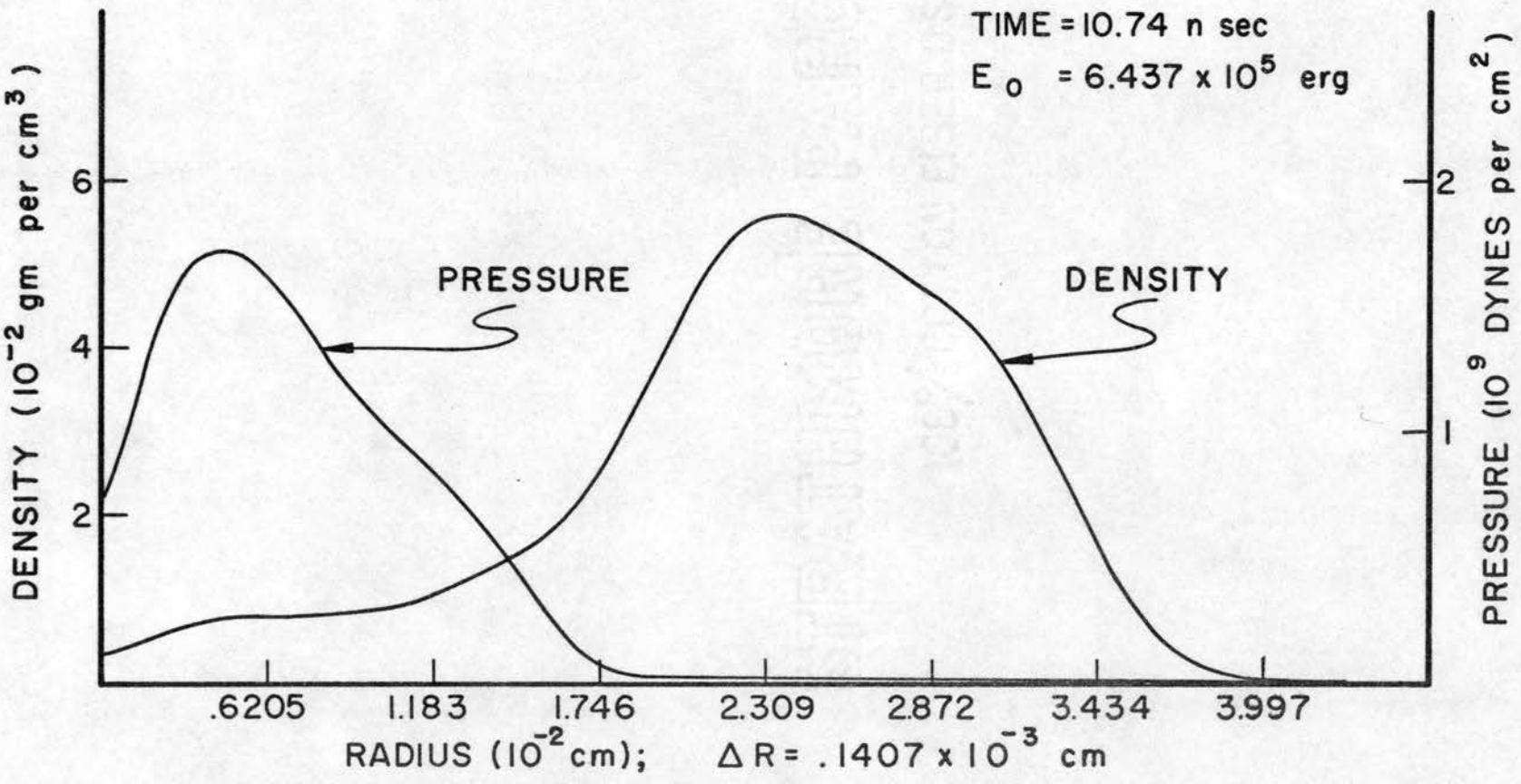

FIGURE 8.8 DENSITY AND PRESSURE VERS RADIUS

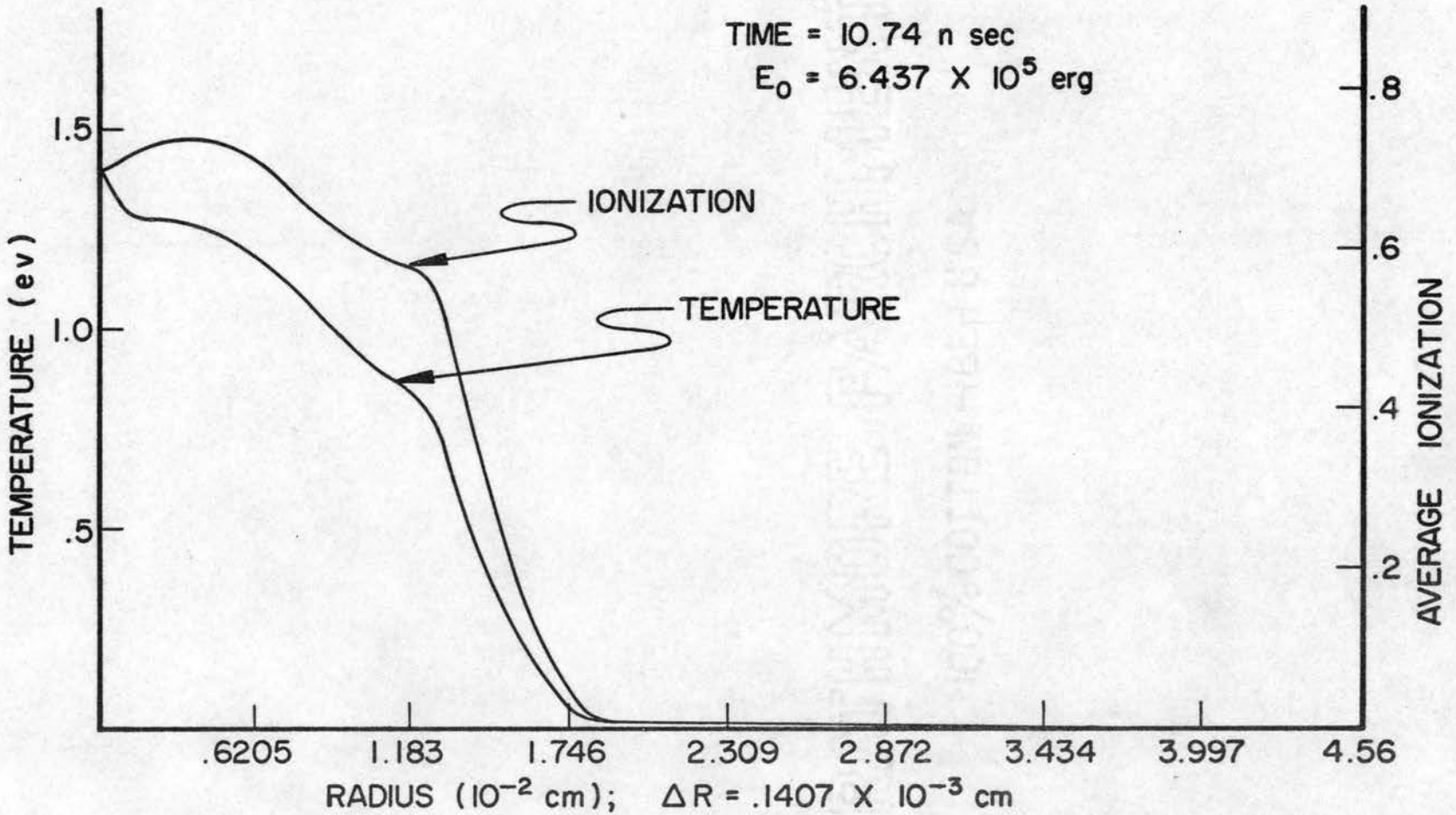

FIGURE 8.9 TEMPERATURE AND AVERAGE IONIZATION VERS RADIUS

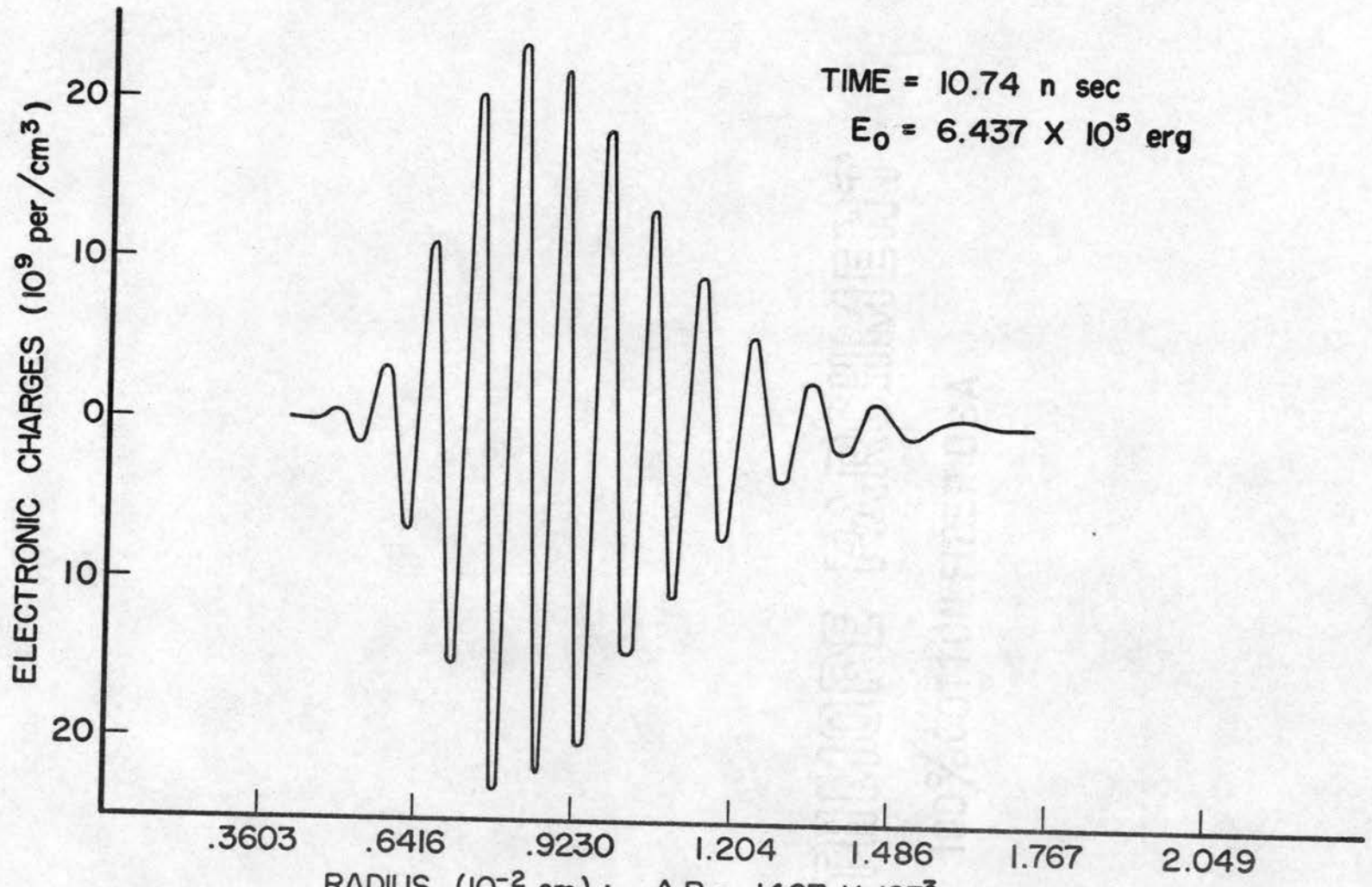

FIGURE 8.10 NUMBER OF EXCESS ELECTRONIC CHARGES VERS RADIUS

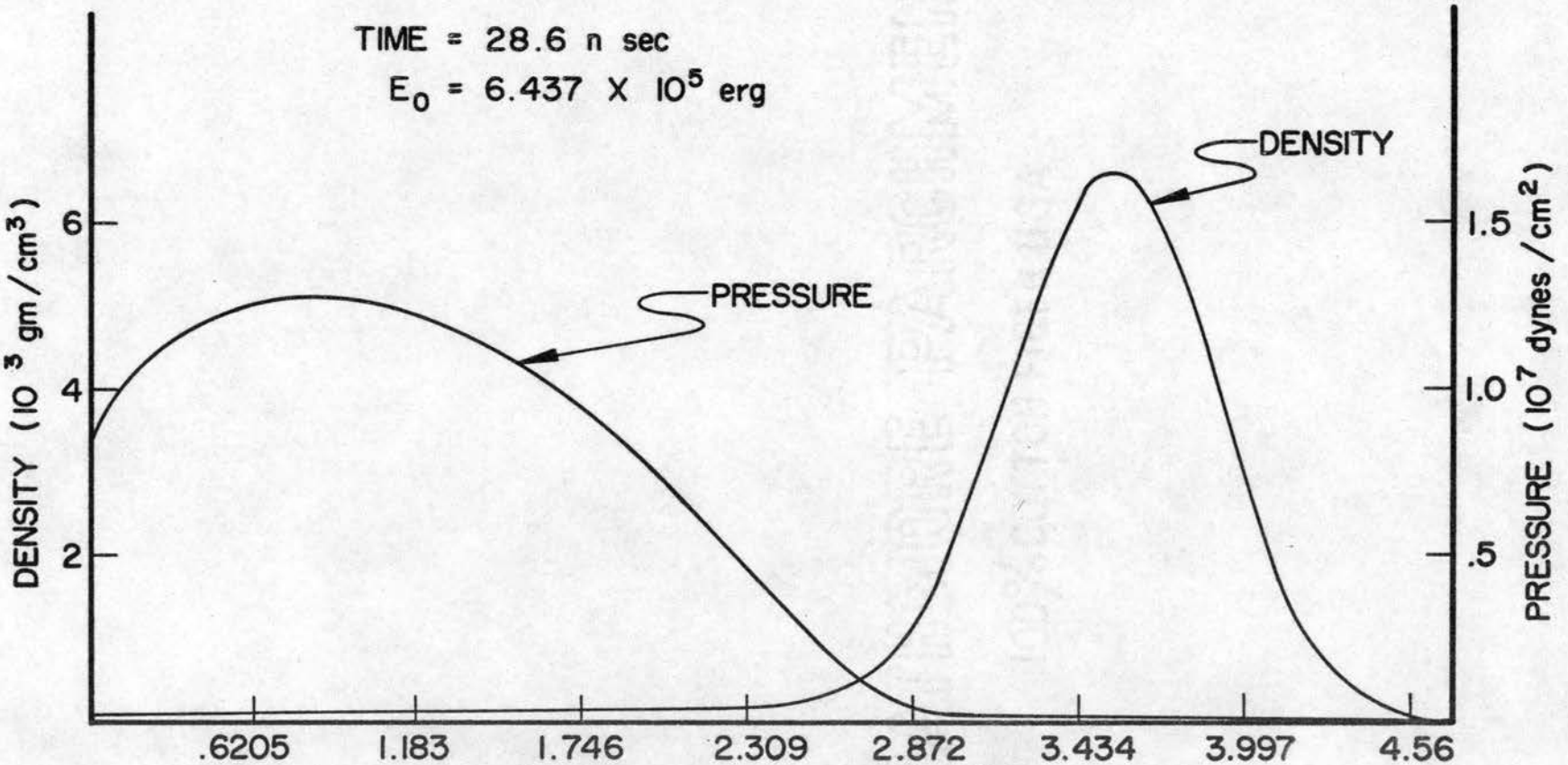

FIGURE 8.11 DENSITY AND PRESSURE VERS RADIUS

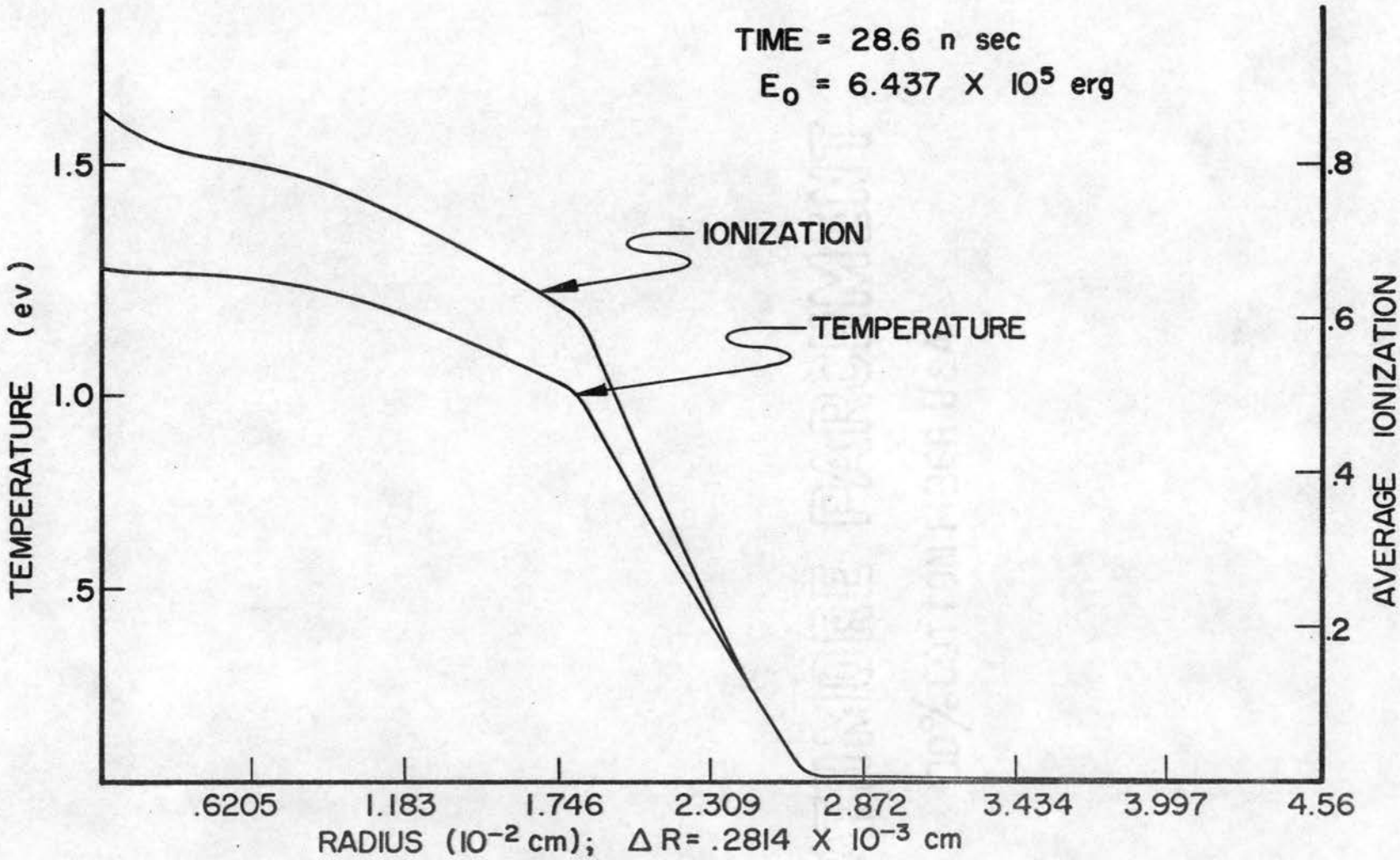

FIGURE 8.12 TEMPERATURE AND AVERAGE IONIZATION VERS RADIUS

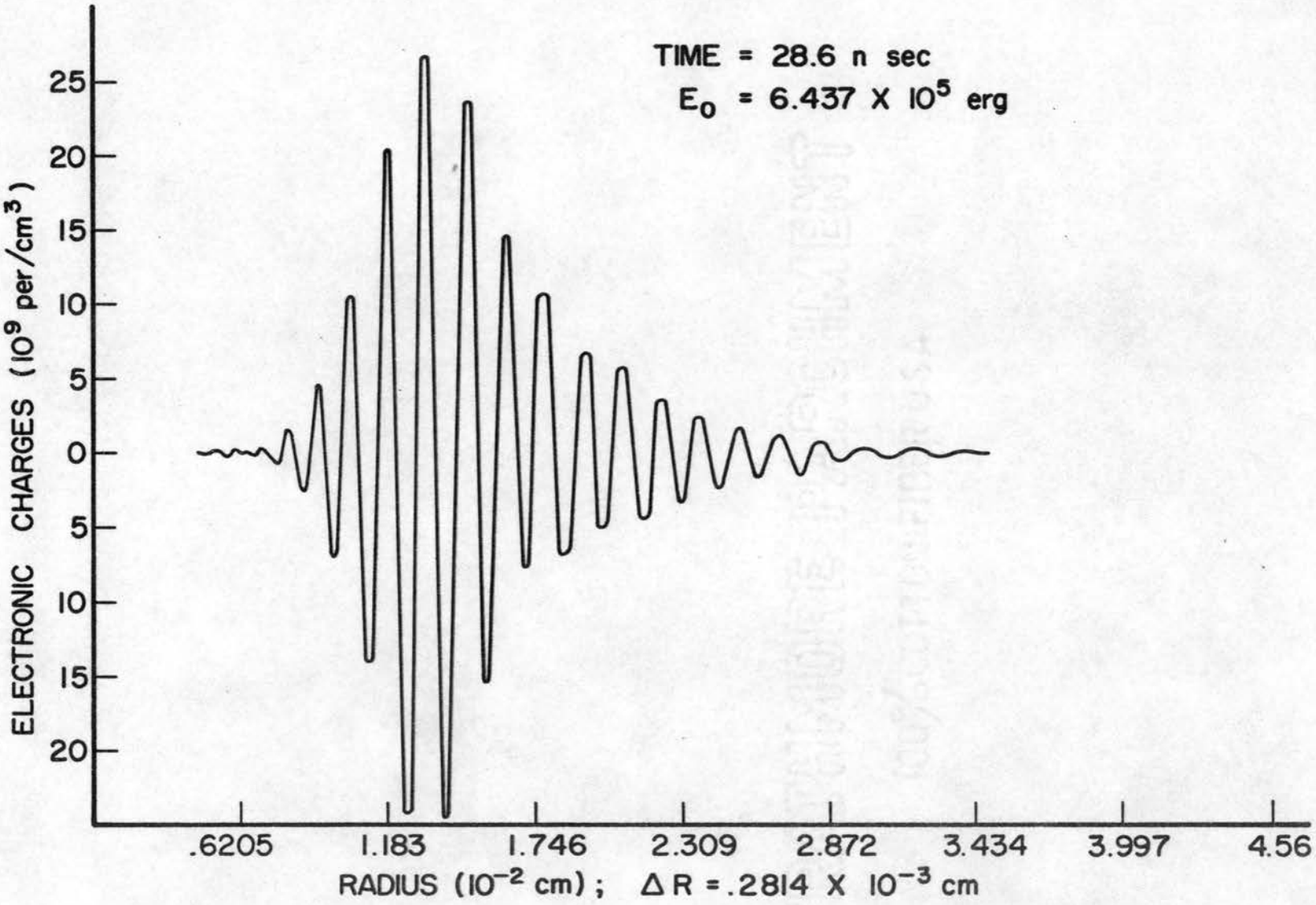

FIGURE 8.13 NUMBER OF EXCESS ELECTRONIC CHARGES VERS RADIUS

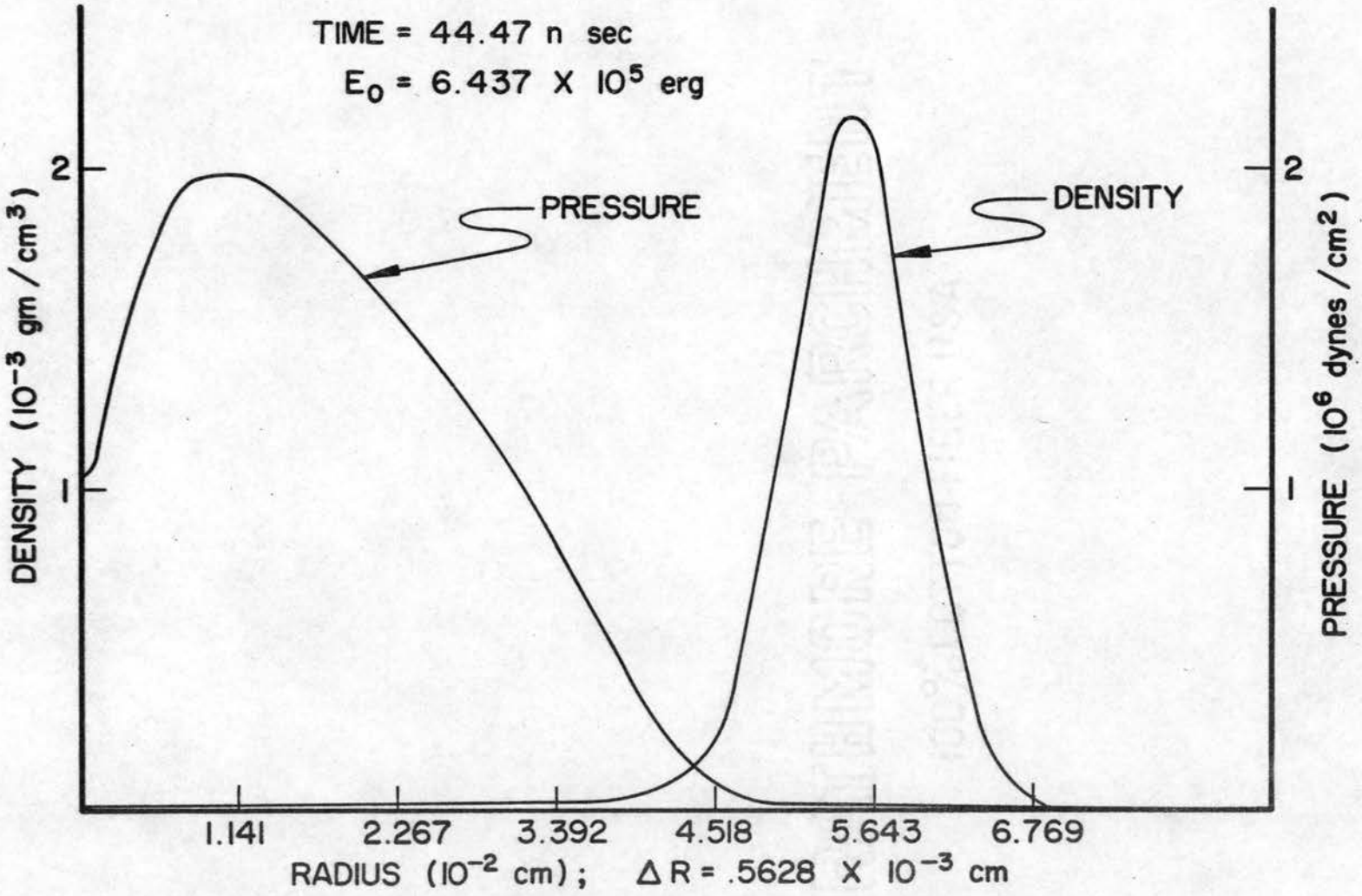

FIGURE 8.14 DENSITY AND PRESSURE VERS RADIUS

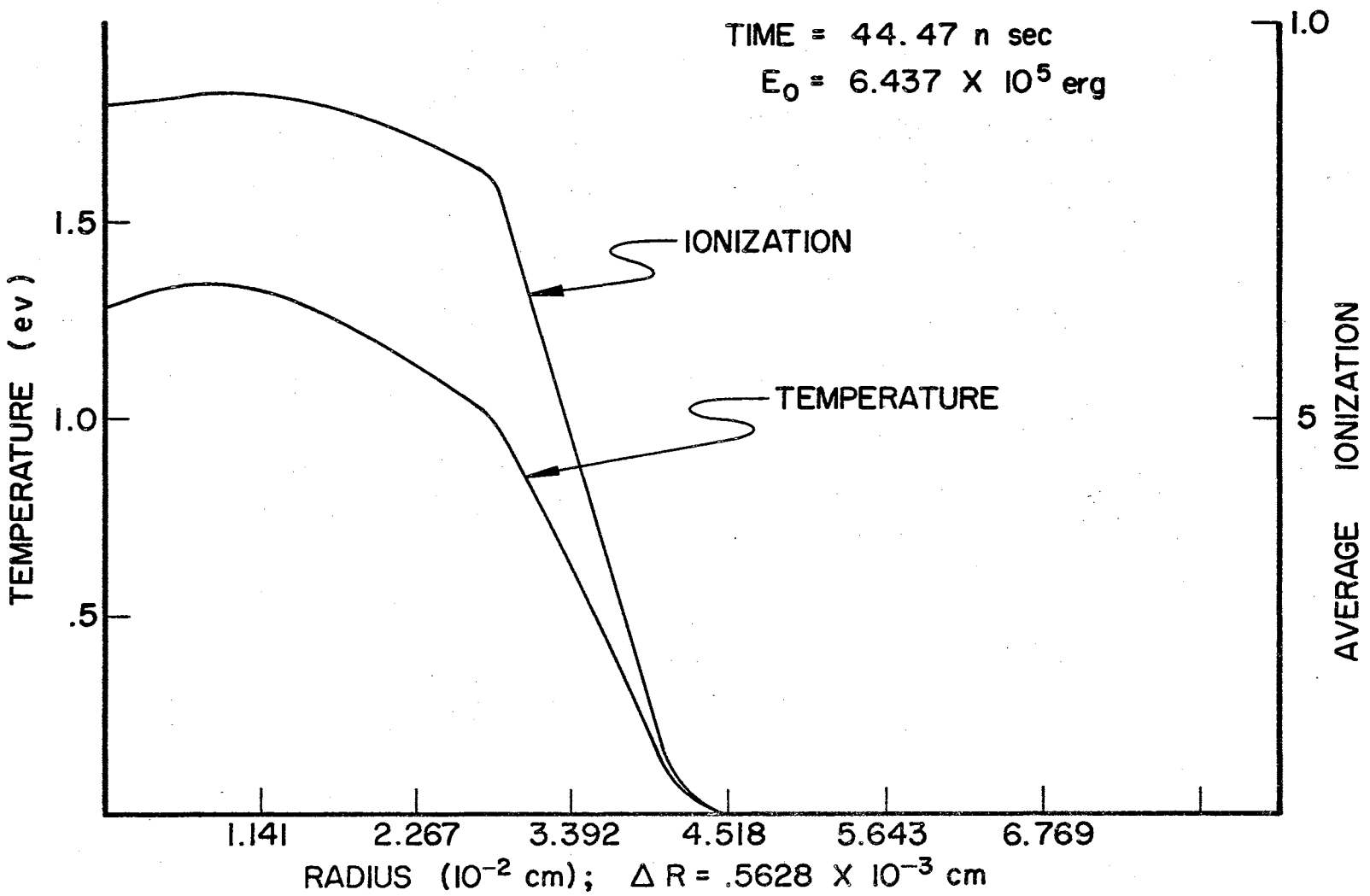

FIGURE 8.15 TEMPERATURE AND AVERAGE IONIZATION VERS RADIUS

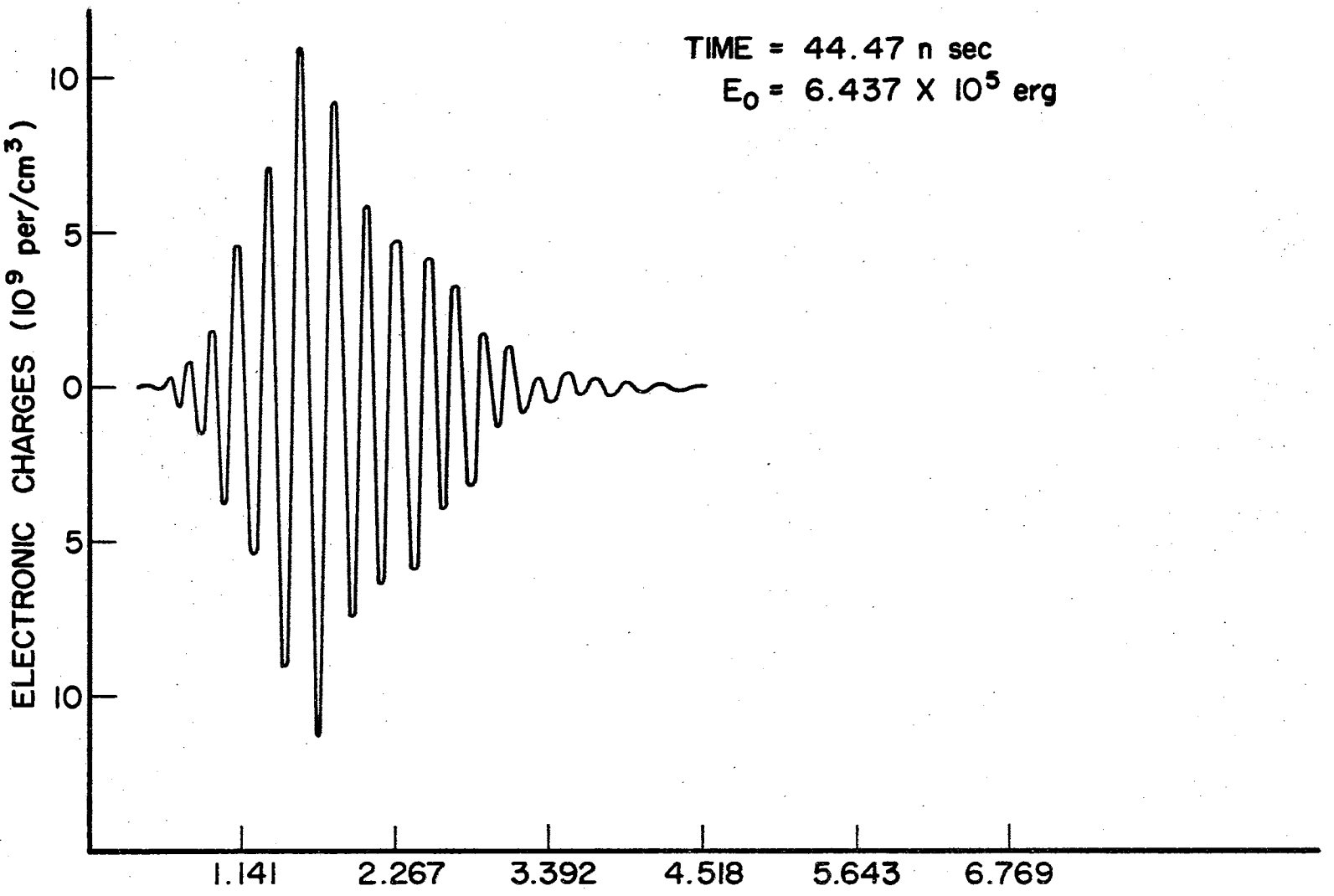

FIGURE 8.16 NUMBER OF EXCESS ELECTRONIC CHARGES VERS RADIUS

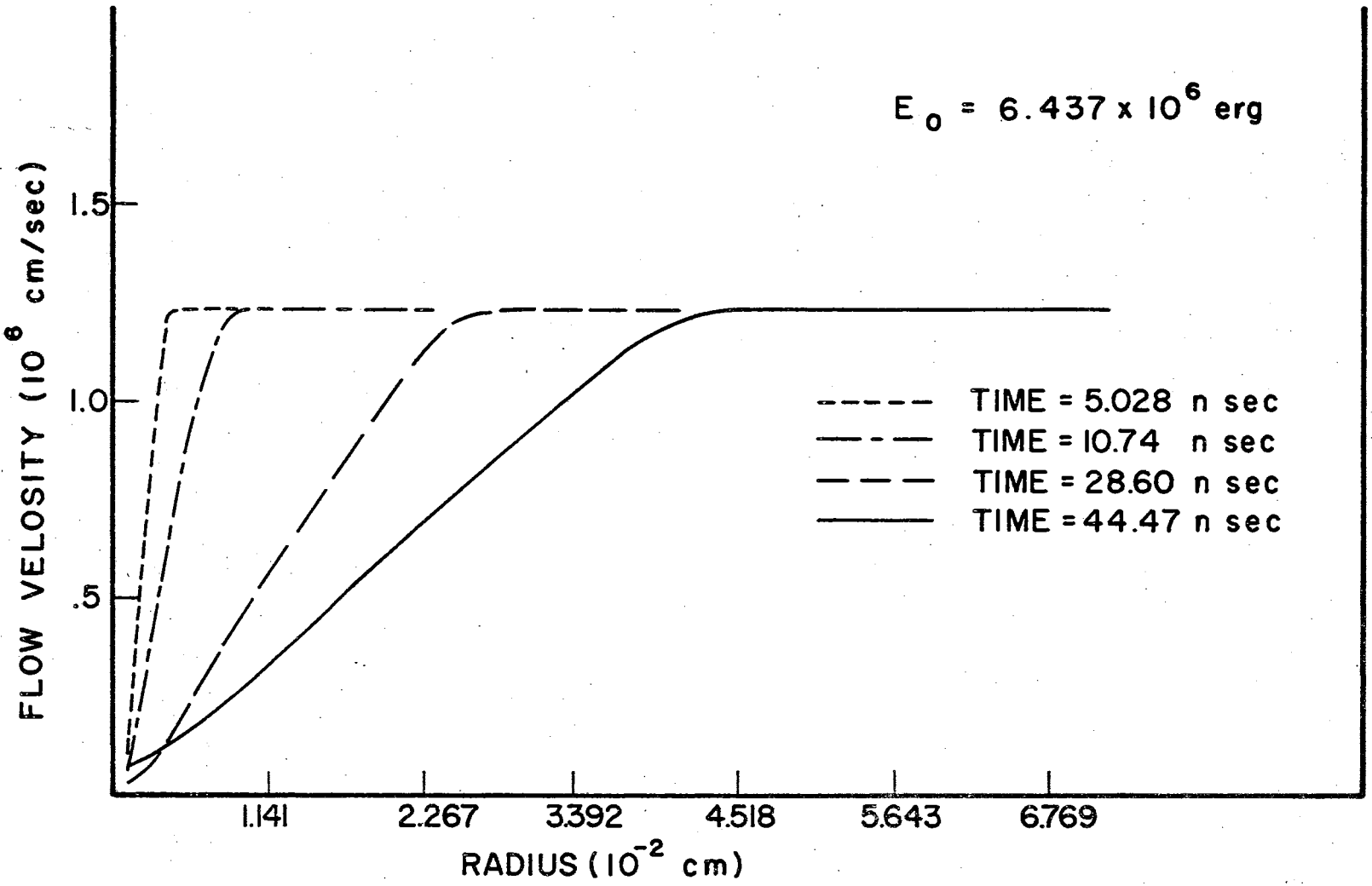

FIGURE 8.17 FLOW VELOCITIES VERS RADIUS

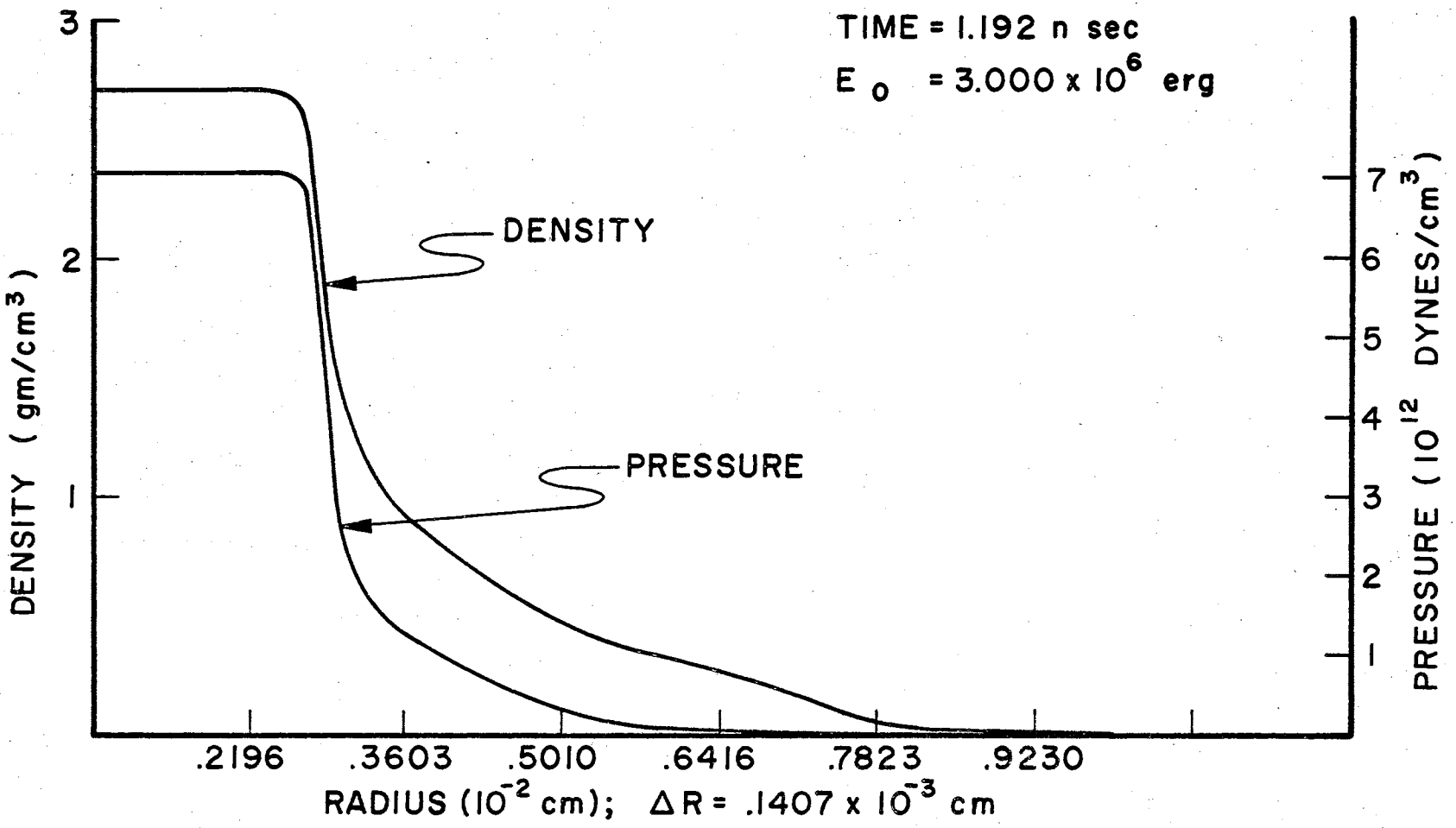

FIGURE 8.18 DENSITY AND PRESSURE VERS RADIUS

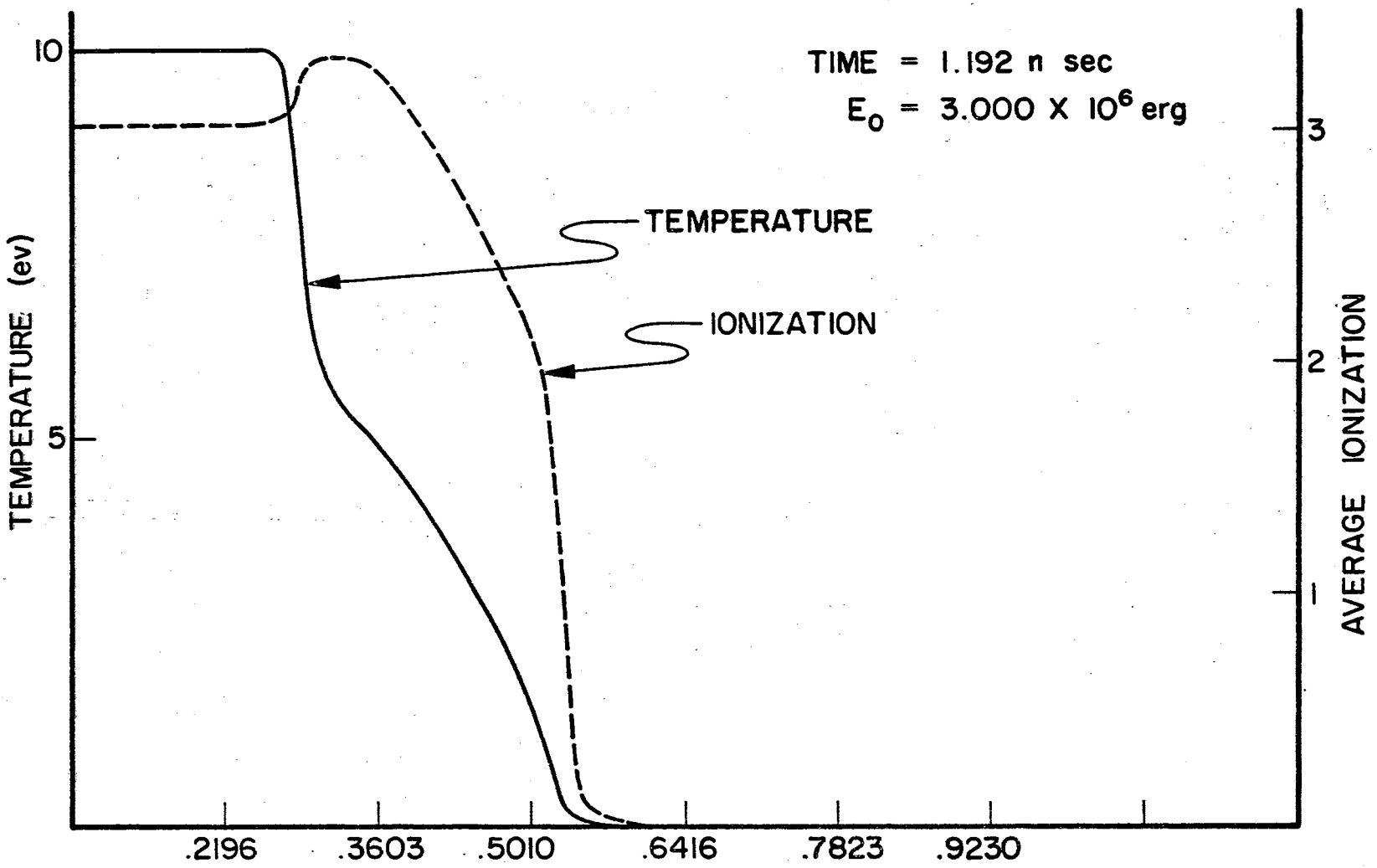

FIGURE 8.19 TEMPERATURE AND AVERAGE IONIZATION VERS RADIUS

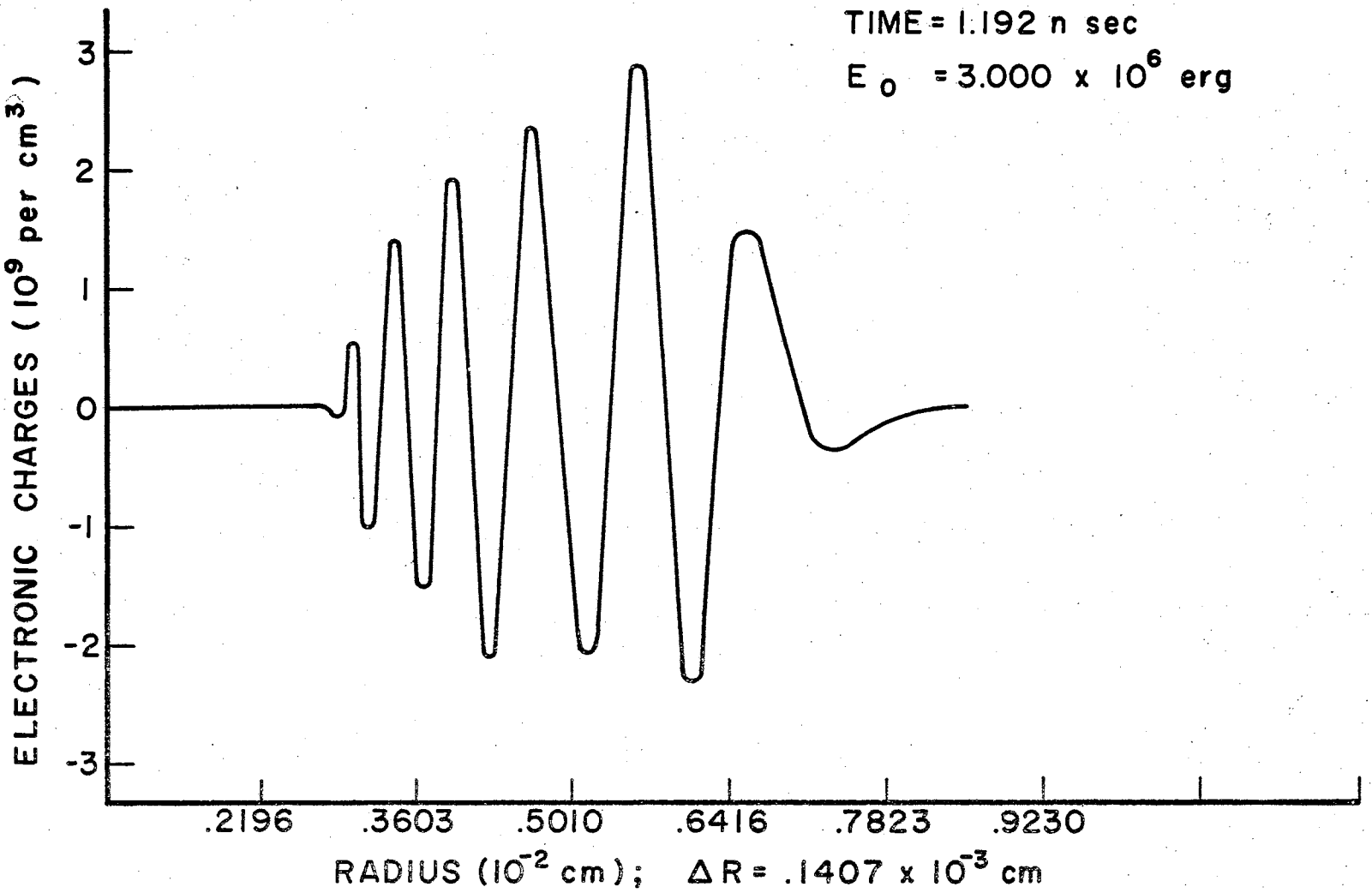

FIGURE 8.20 NUMBER OF EXCESS ELECTRONIC CHARGES VERS RADIUS

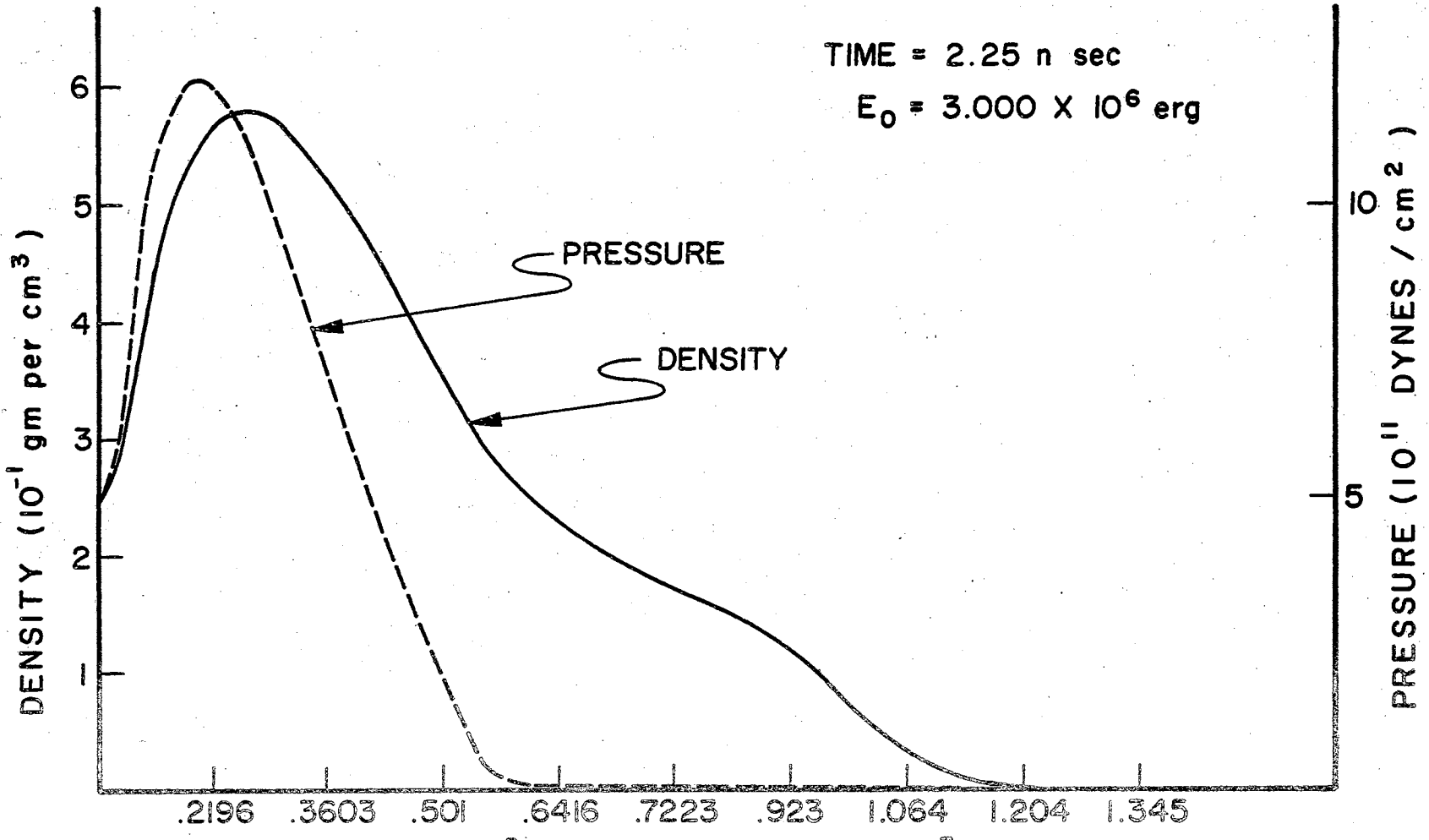

FIGURE 8.21 DENSITY AND PRESSURE VERS RADIUS

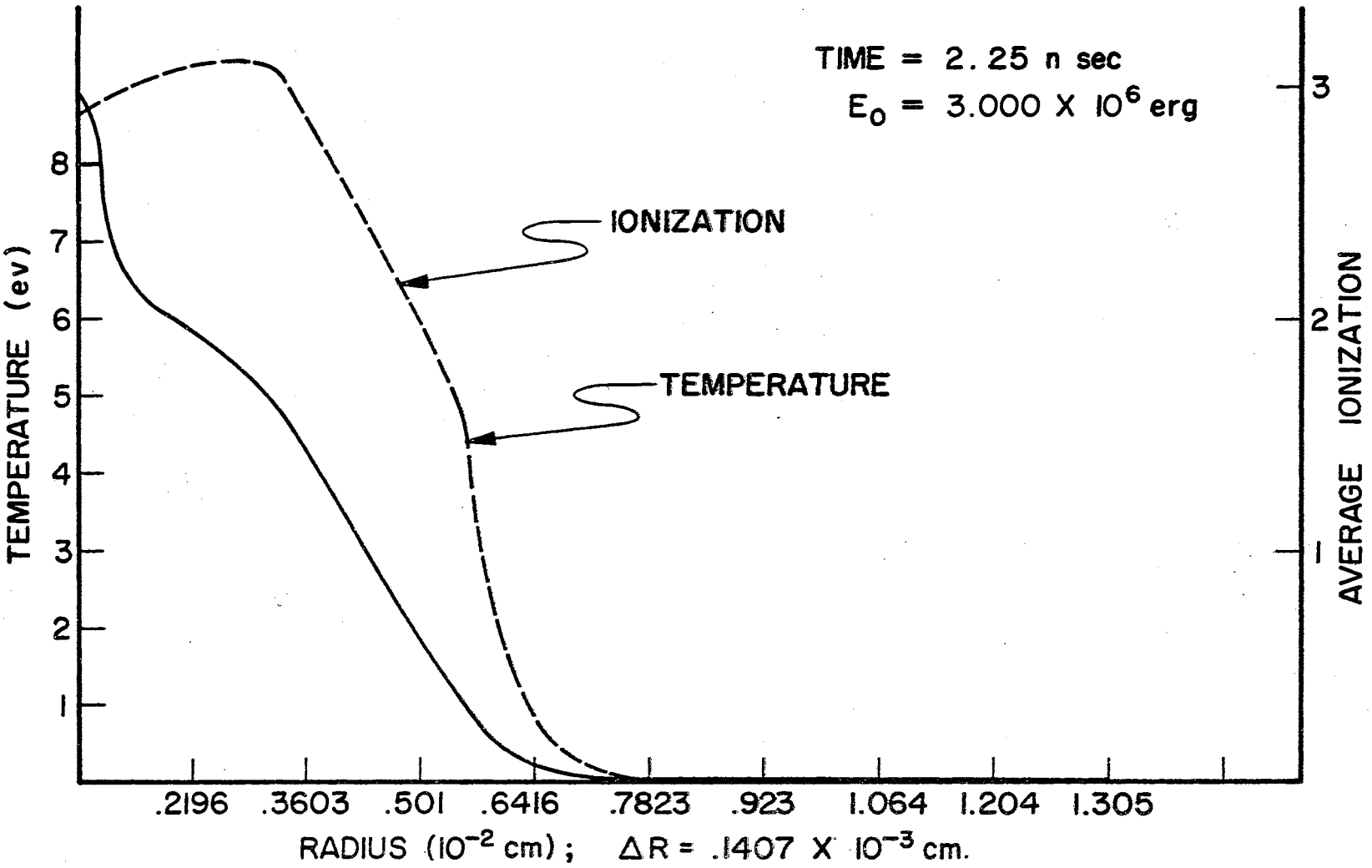

FIGURE 8.22 TEMPERATURE AND AVERAGE IONIZATION VERS RADIUS

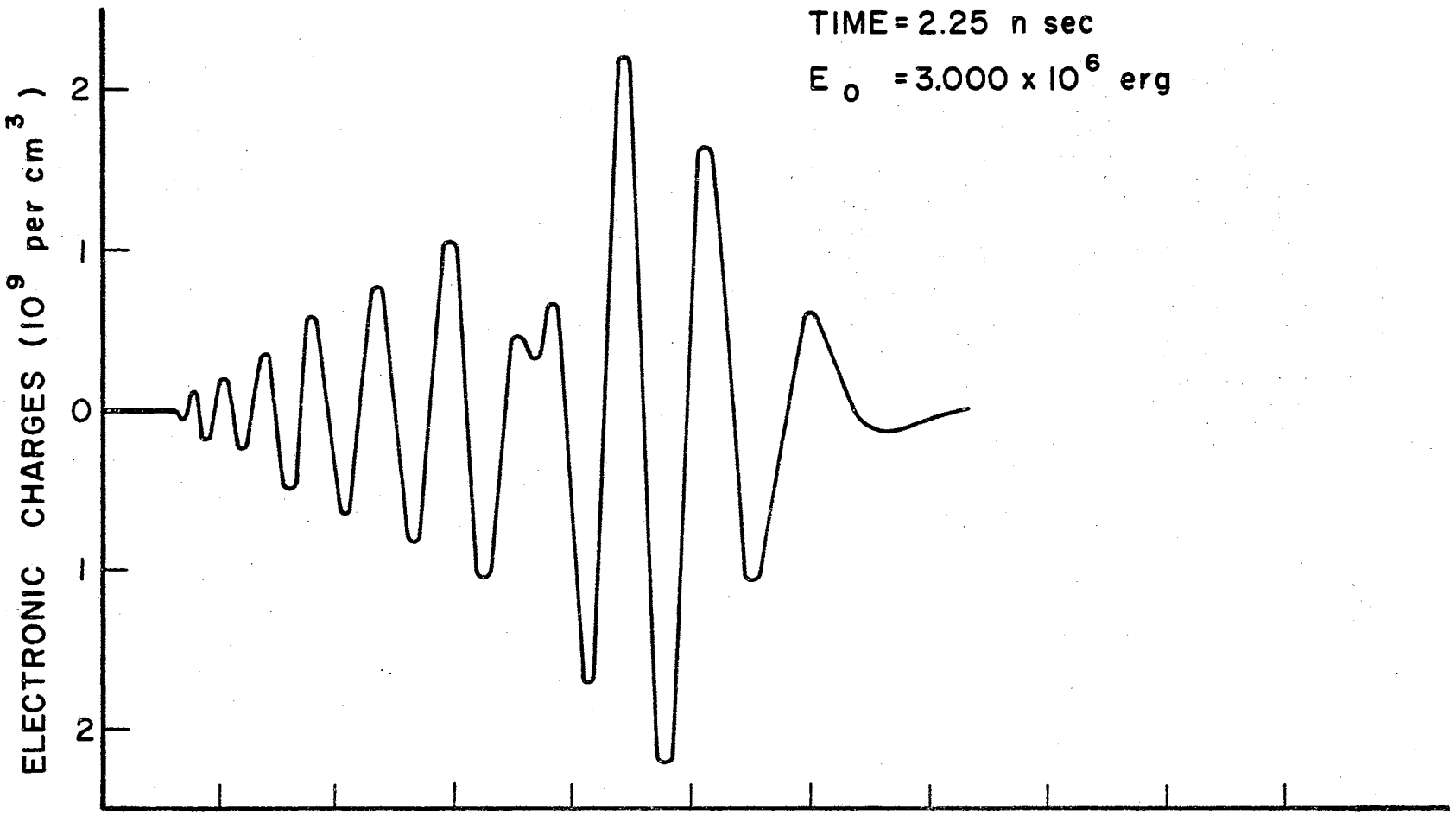

FIGURE 8.23 NUMBER OF EXCESS ELECTRONIC CHARGES VERS RADIUS

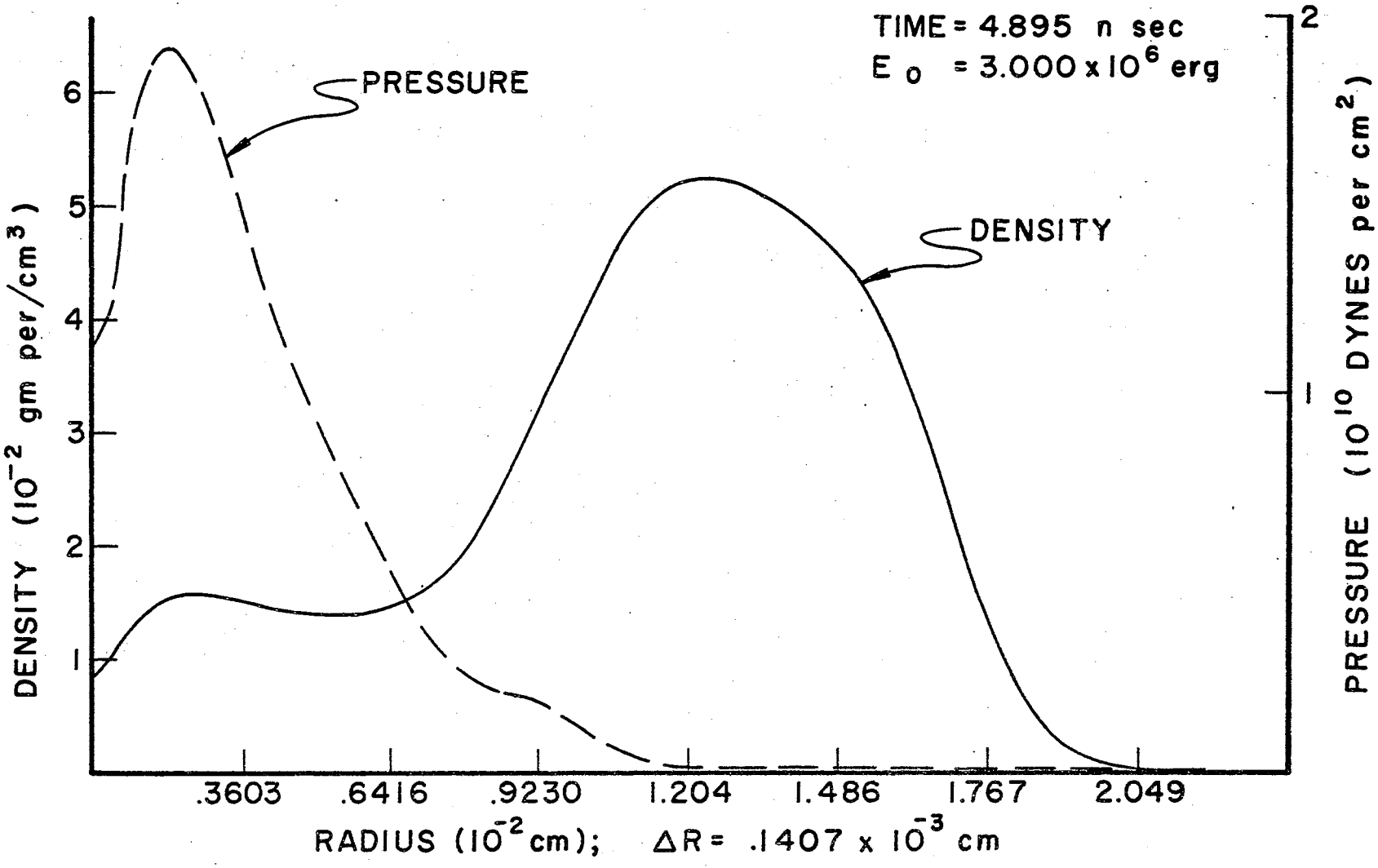

FIGURE 8.24 DENSITY AND PRESSURE VERS RADIUS

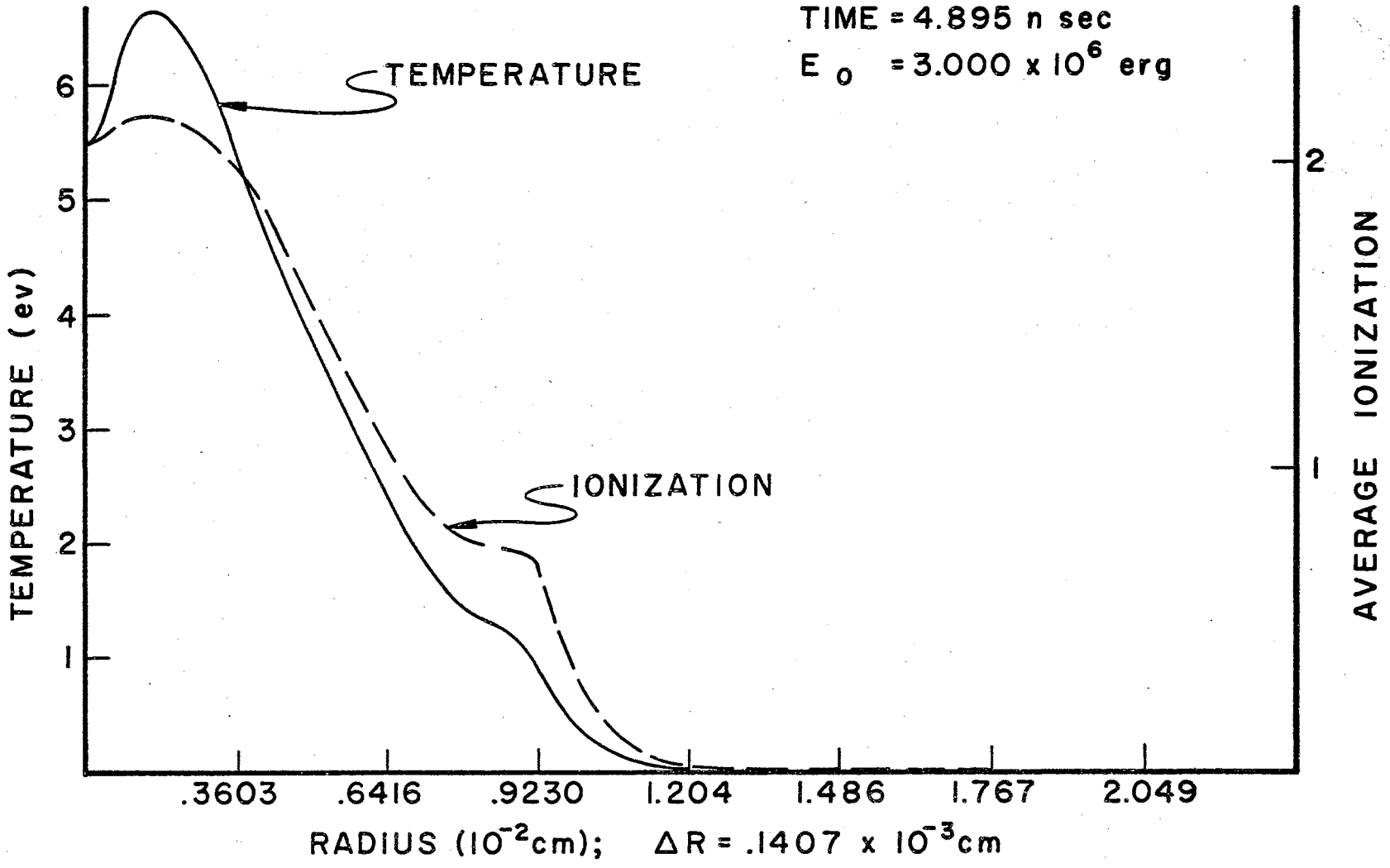

FIGURE 8.25 TEMPERATURE AND AVERAGE IONIZATION VERS RADIUS

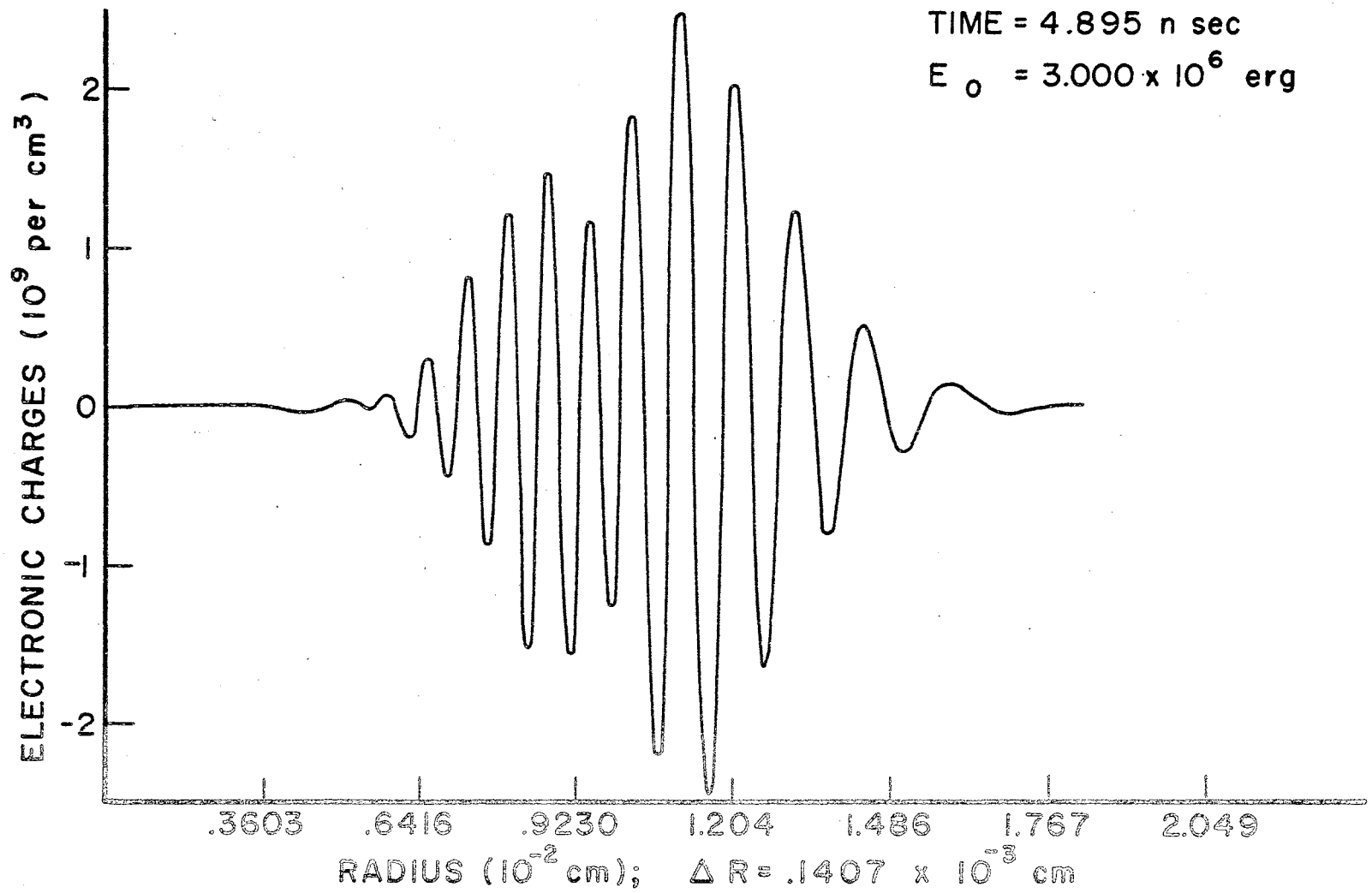

FIGURE 8.26 NUMBER OF EXCESS ELECTRONIC CHARGES VERS RADIUS

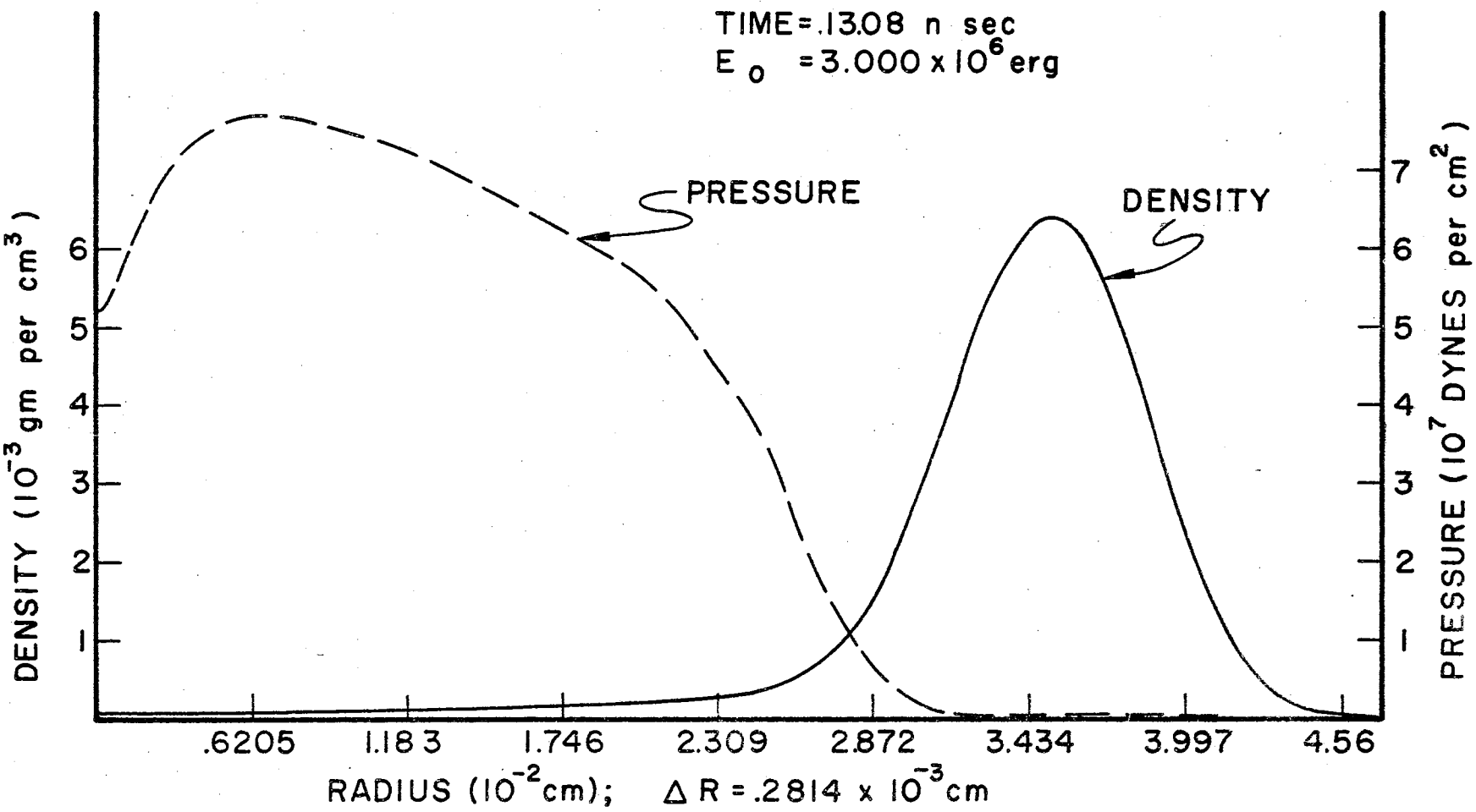

FIGURE 8.27 DENSITY AND PRESSURE VERS RADIUS

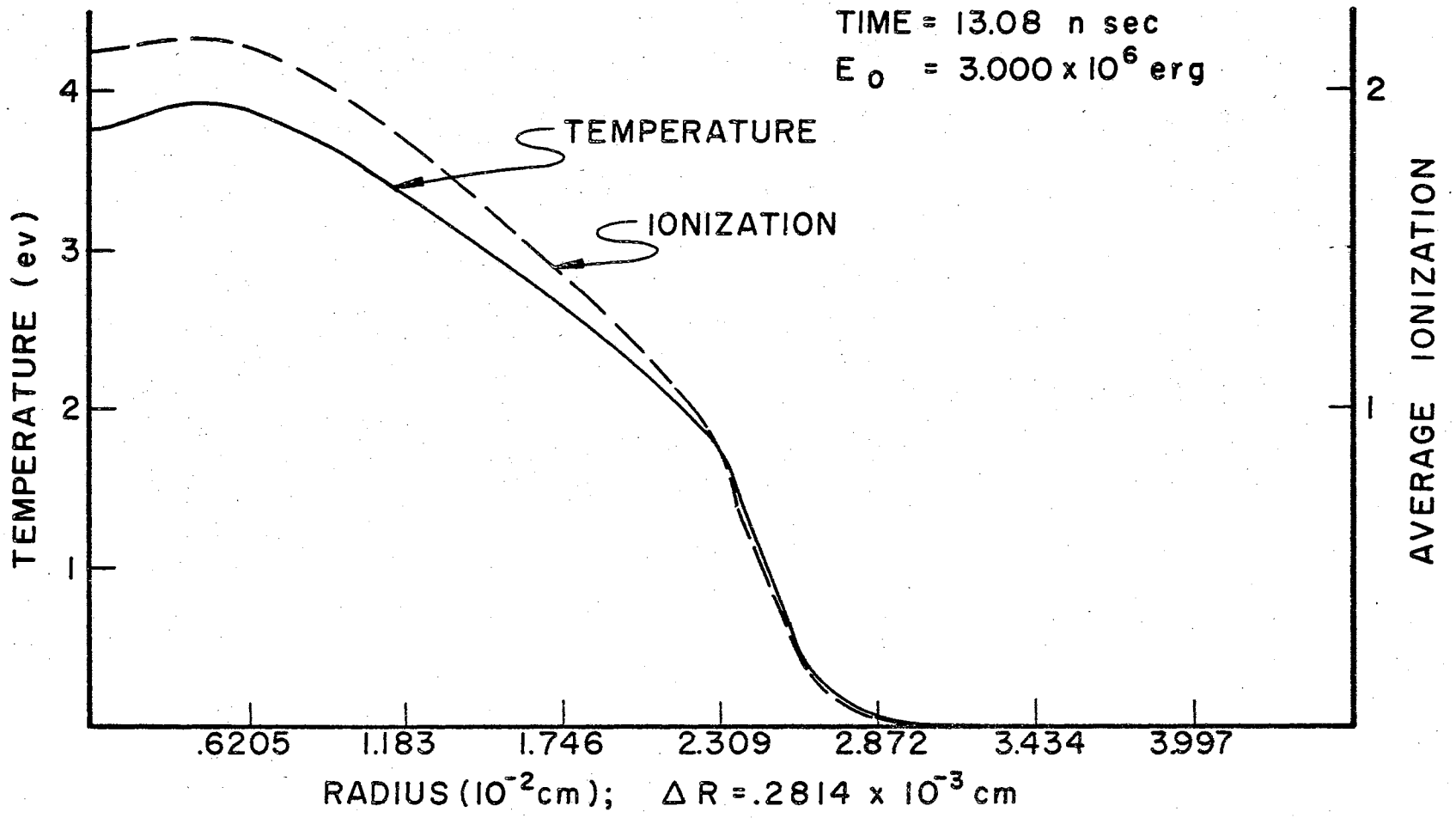

FIGURE 8.28 TEMPERATURE AND AVERAGE IONIZATION VERS RADIUS

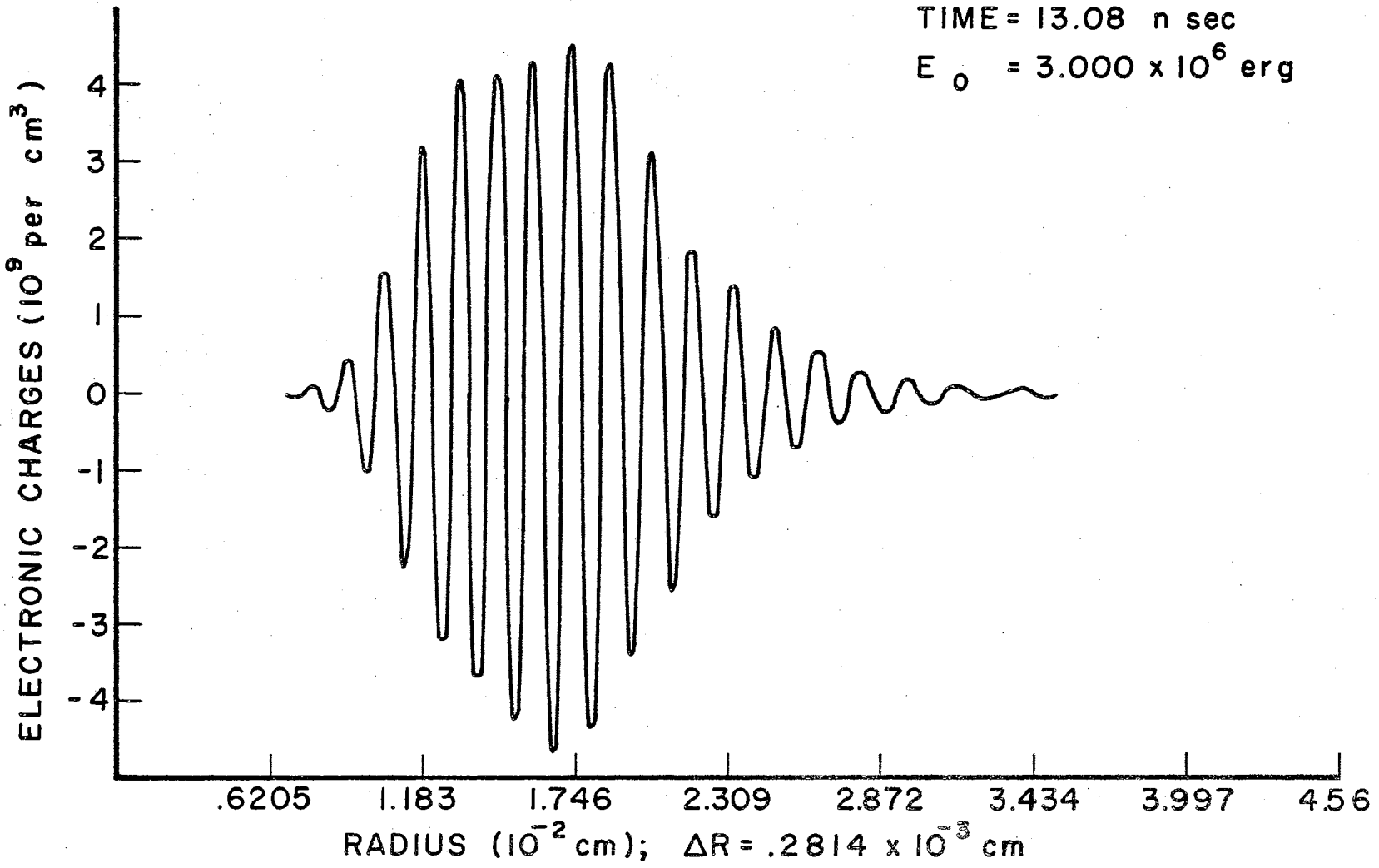

FIGURE 8.29 NUMBER OF EXCESS ELECTRONIC CHARGES VERS RADIUS

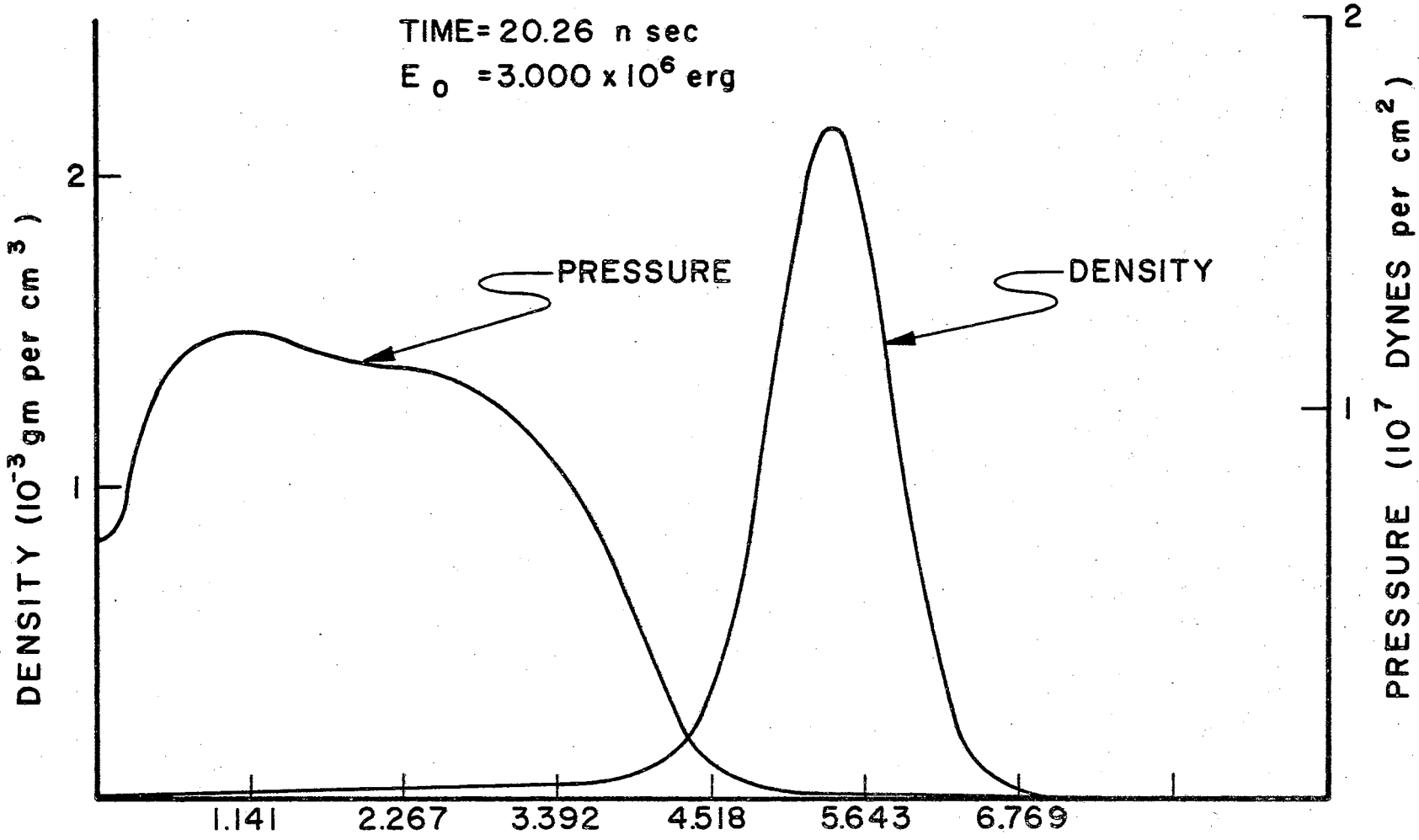

FIGURE 8.30 DENSITY AND PRESSURE VERS RADIUS

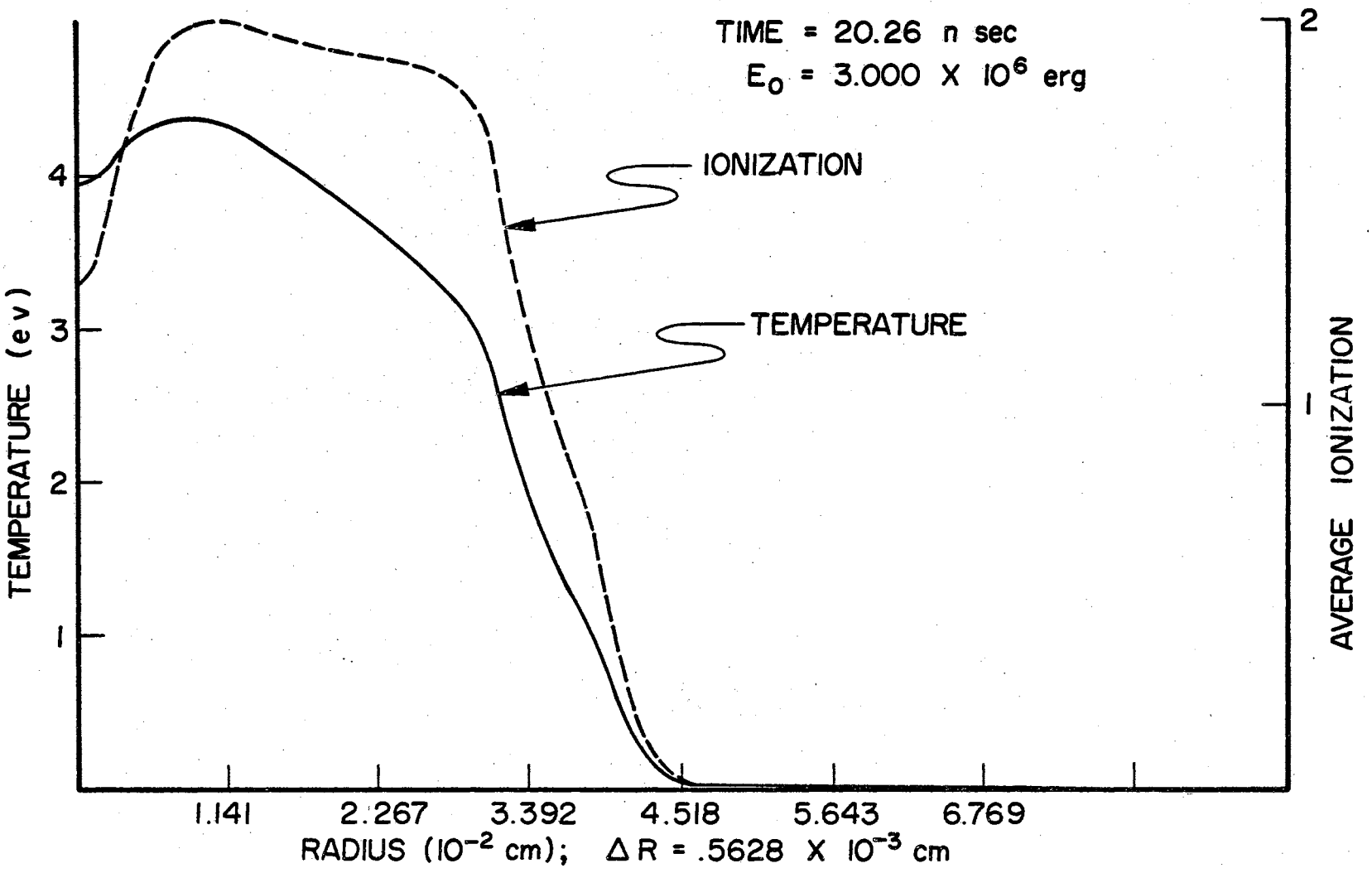

FIGURE 8.31 TEMPERATURE AND AVERAGE IONIZATION VERS RADIUS

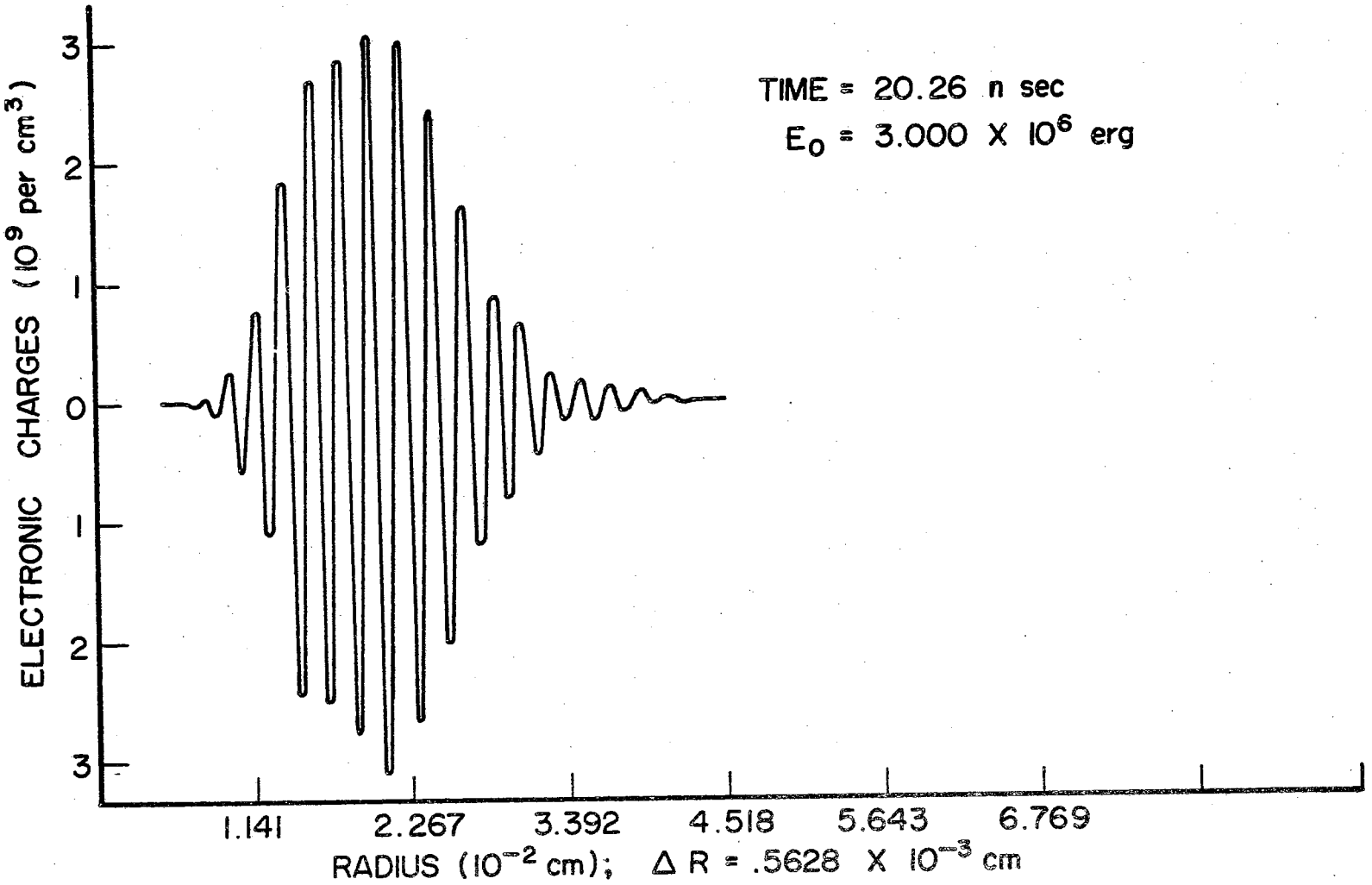

FIGURE 8.32 NUMBER OF EXCESS ELECTRONIC CHARGES VERS RADIUS

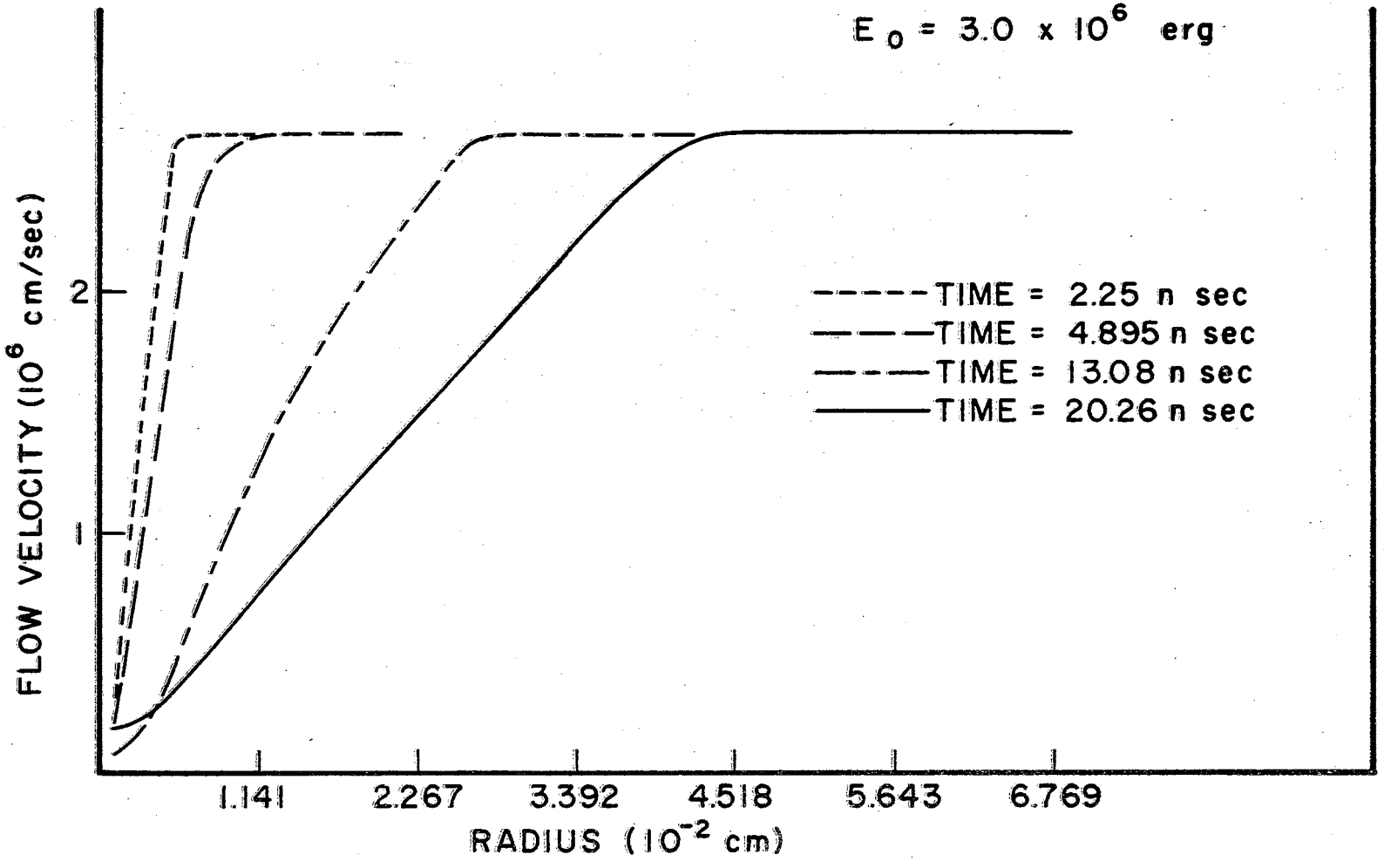

FIGURE 8.33 FLOW VELOCITIES VERS RADIUS

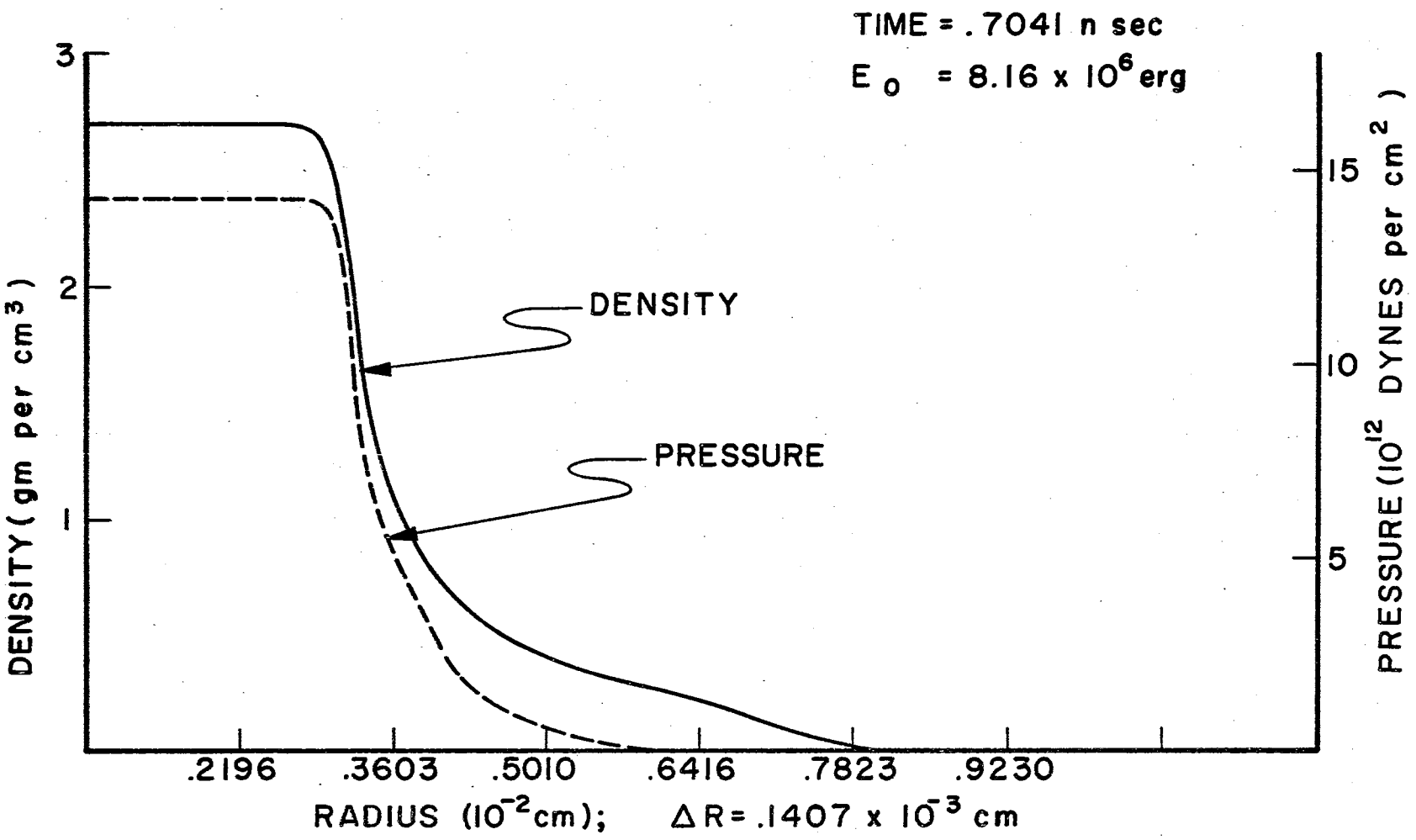

FIGURE 8.34 DENSITY AND PRESSURE VERS RADIUS

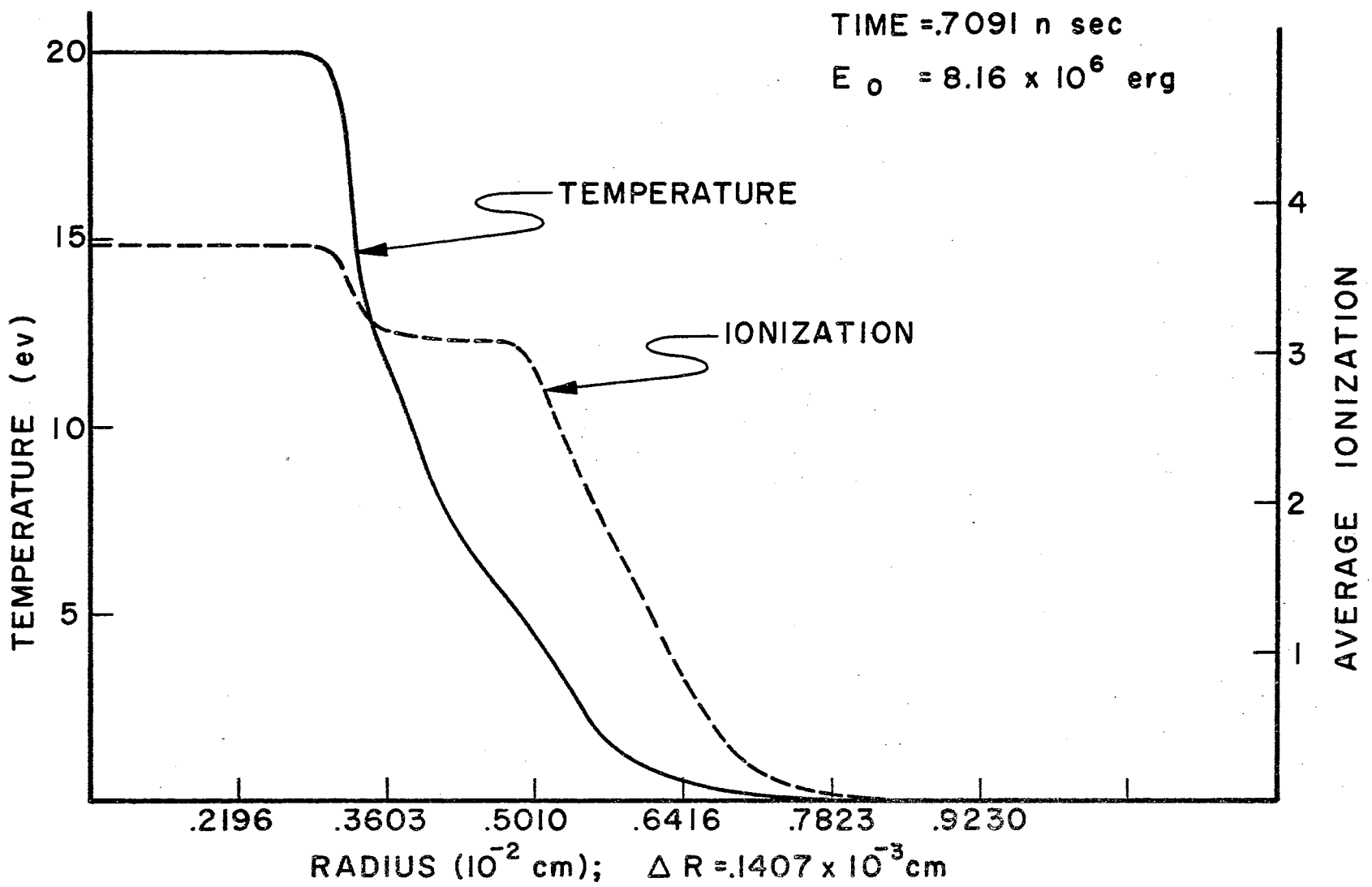

FIGURE 8.35 TEMPERATURE AND AVERAGE IONIZATION VERS RADIUS

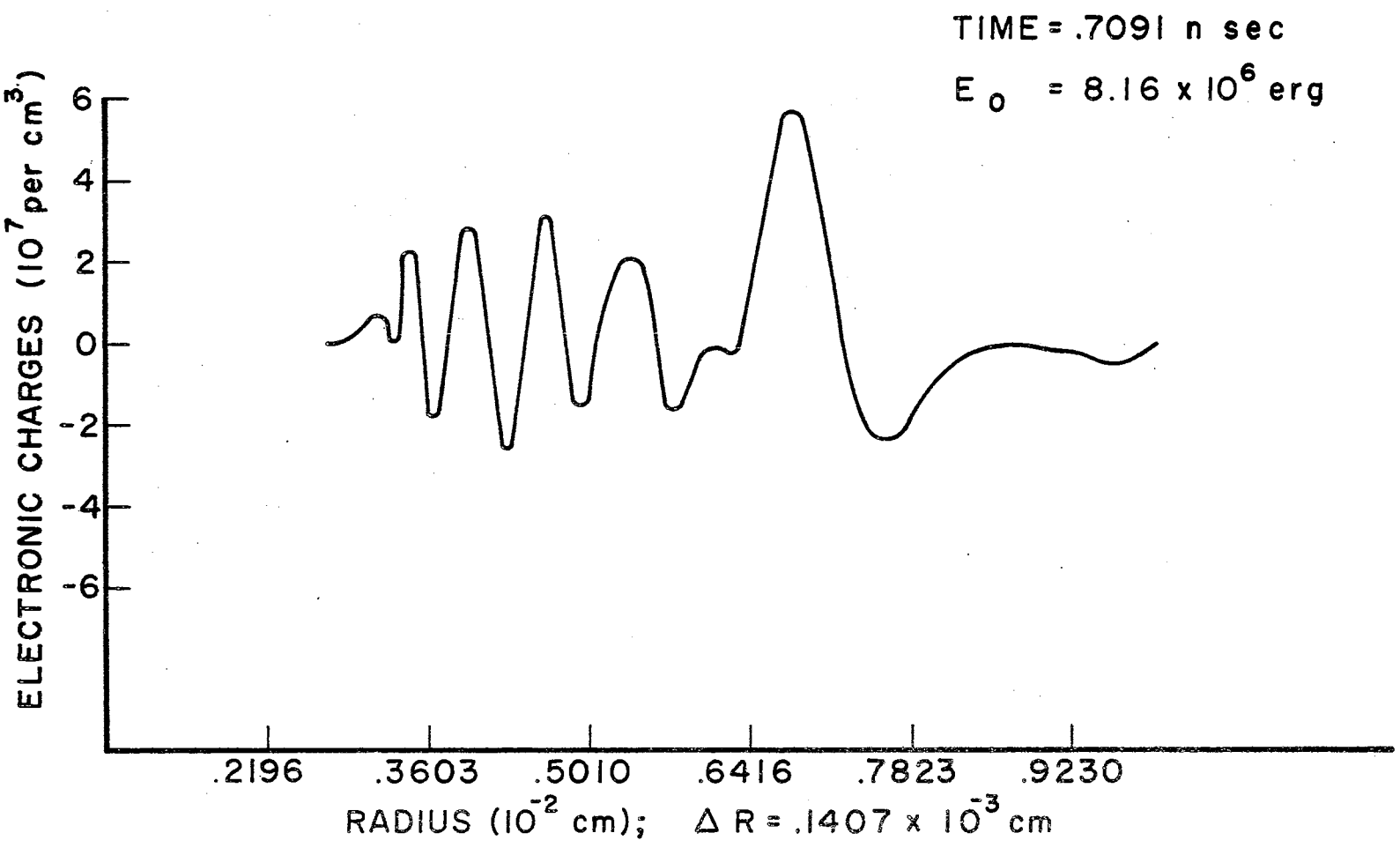

FIGURE 8.36 NUMBER OF EXCESS ELECTRONIC CHARGES VERS RADIUS

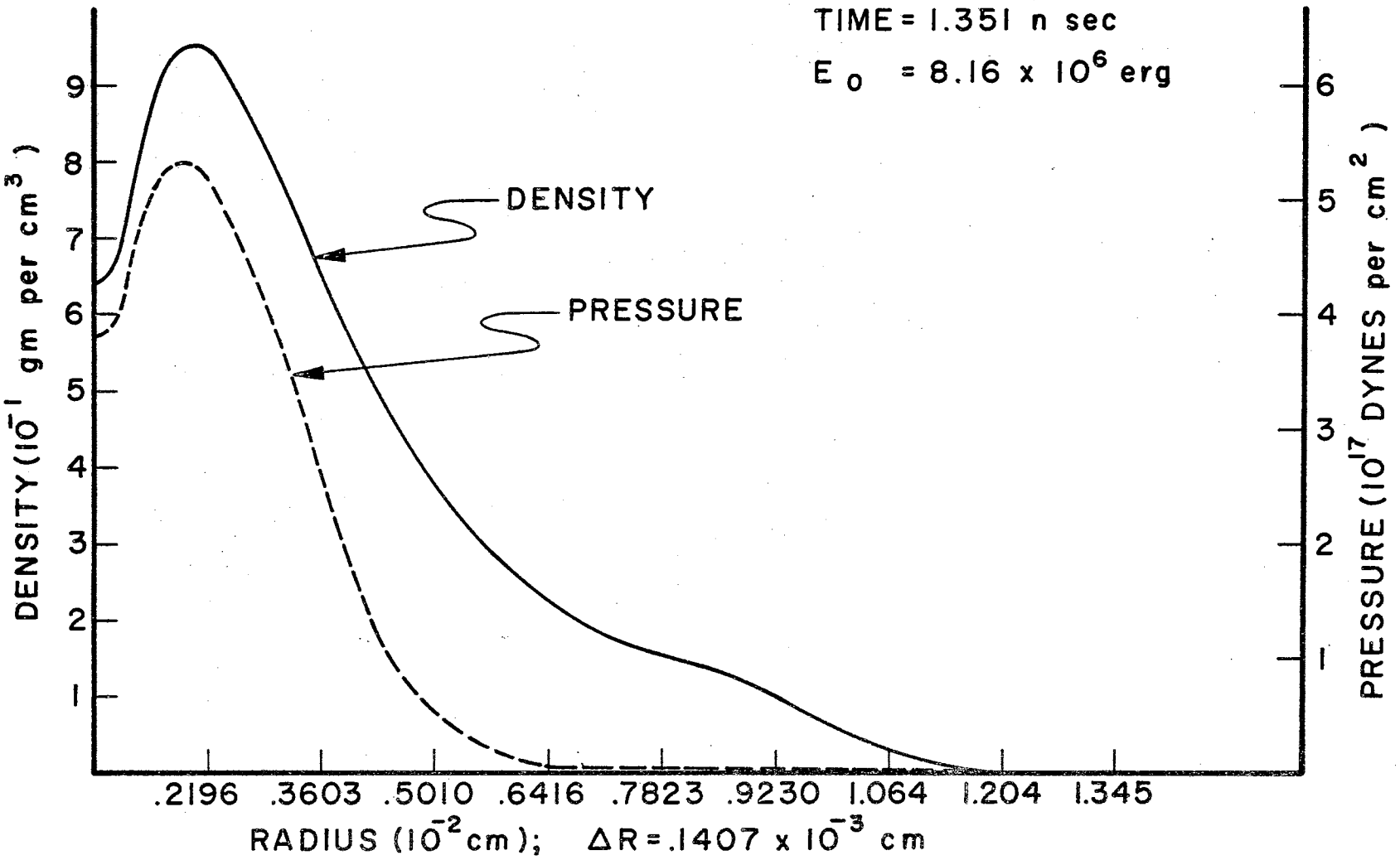

FIGURE 8.37 DENSITY AND PRESSURE VERS RADIUS

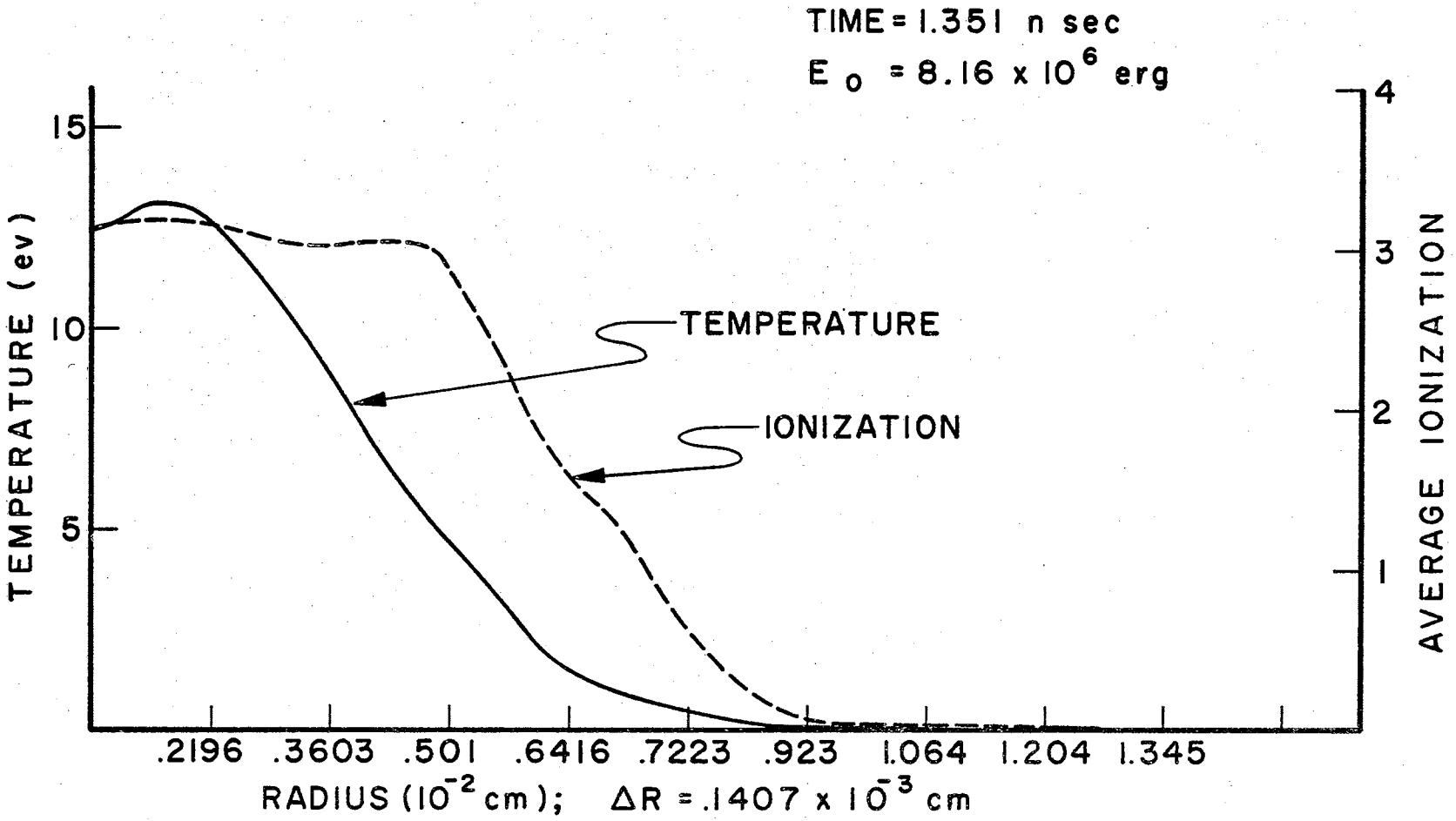

FIGURE 8.38 TEMPERATURE AND AVERAGE IONIZATION VERS RADIUS

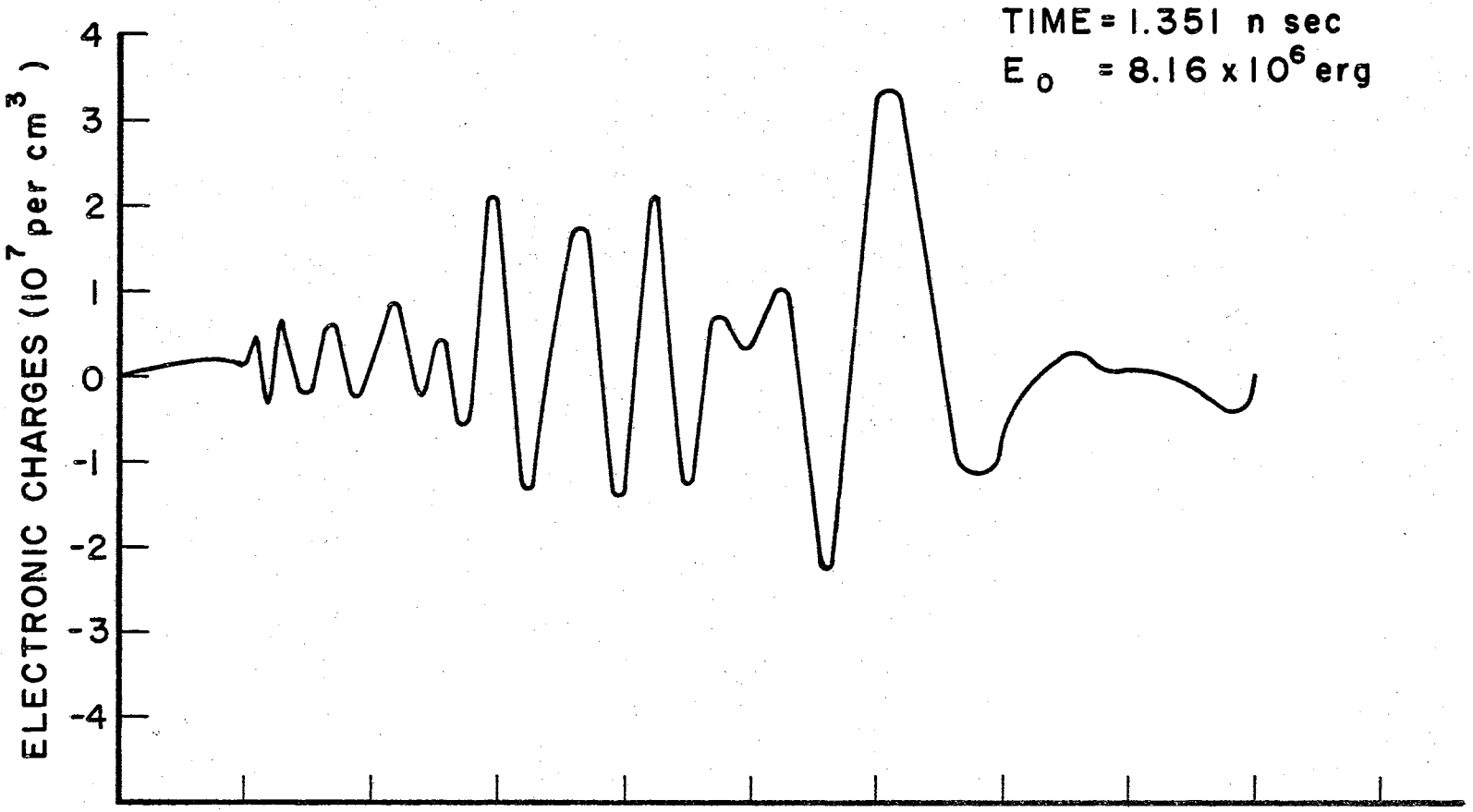

FIGURE 8.39 NUMBER OF EXCESS ELECTRONIC CHARGES VERS RADIUS

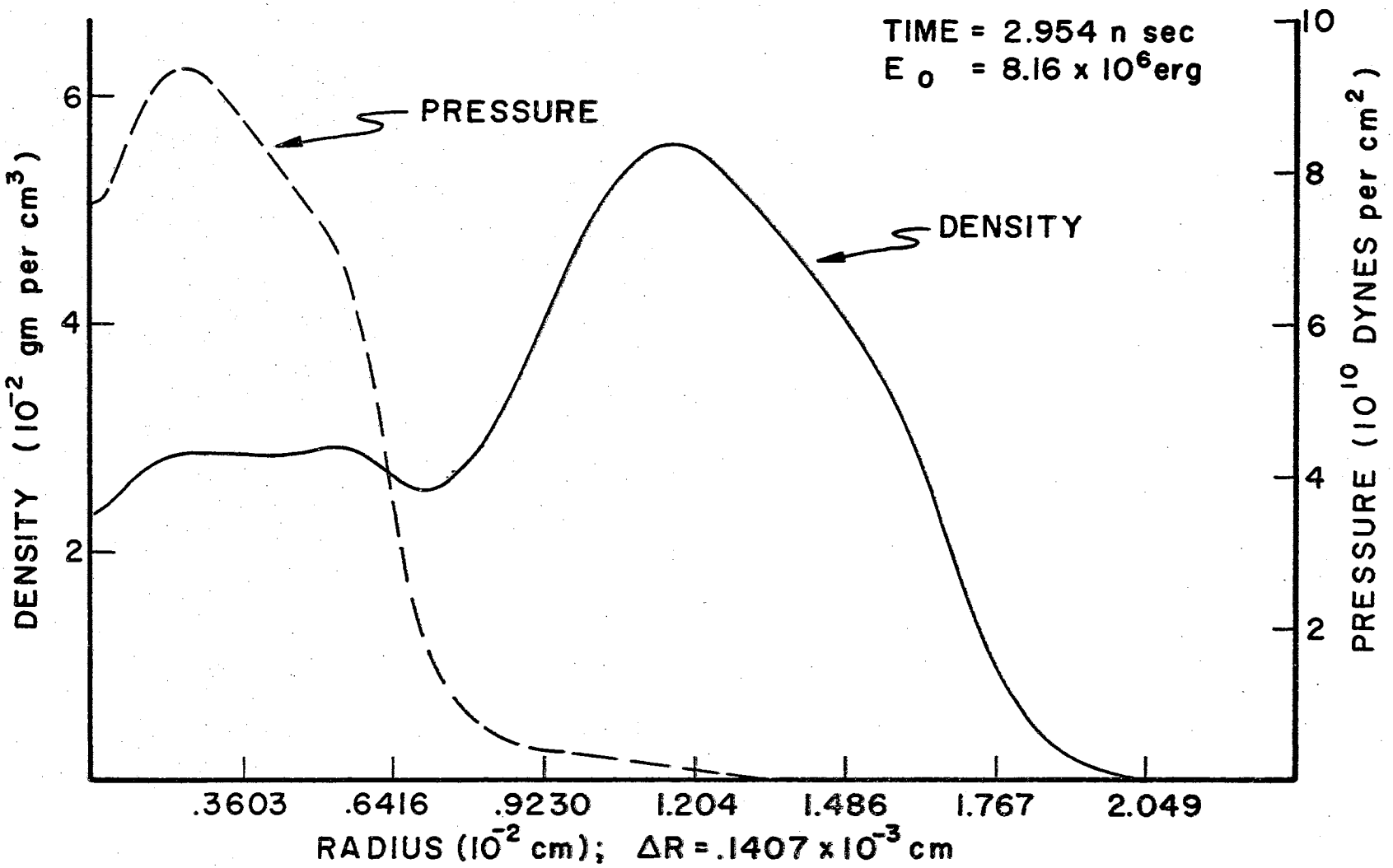

FIGURE 8.40 DENSITY AND PRESSURE VERS RADIUS

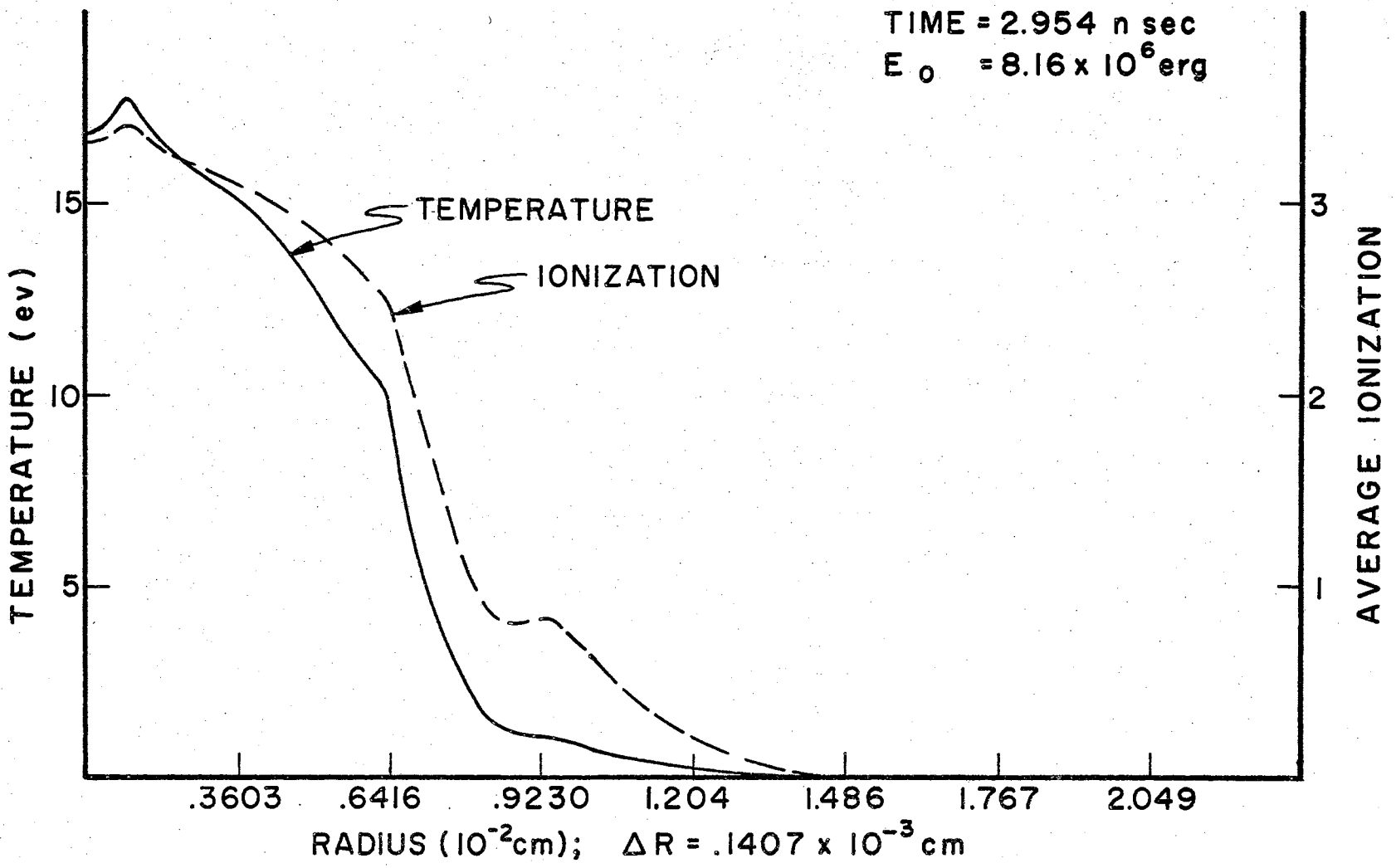

FIGURE 8.41 TEMPERATURE AND AVERAGE IONIZATION VERS RADIUS

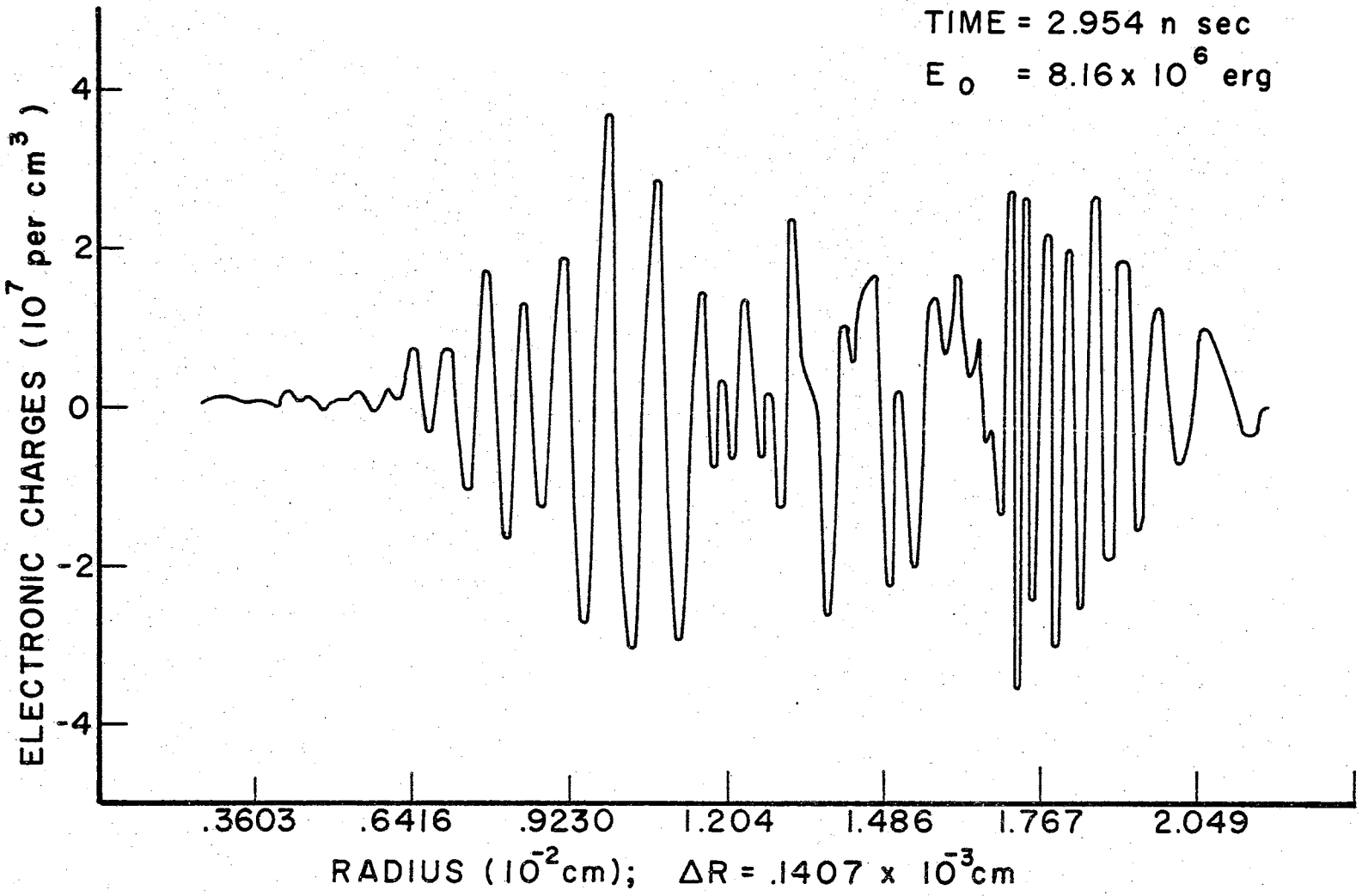

FIGURE 8.42 EXCESS NUMBER OF ELECTRONIC CHARGES VERS RADIUS

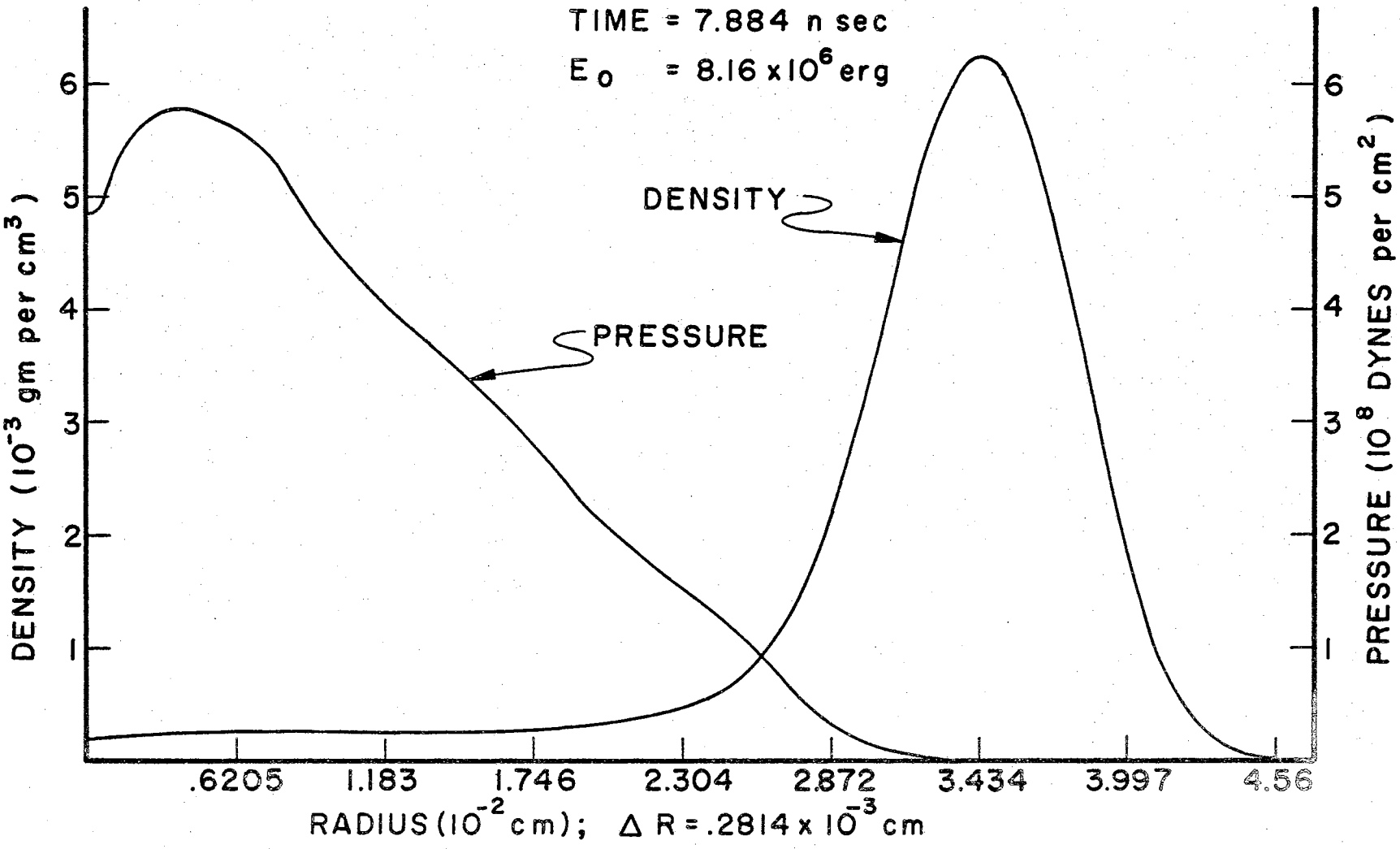

FIGURE 8.43 DENSITY AND PRESSURE VERS RADIUS

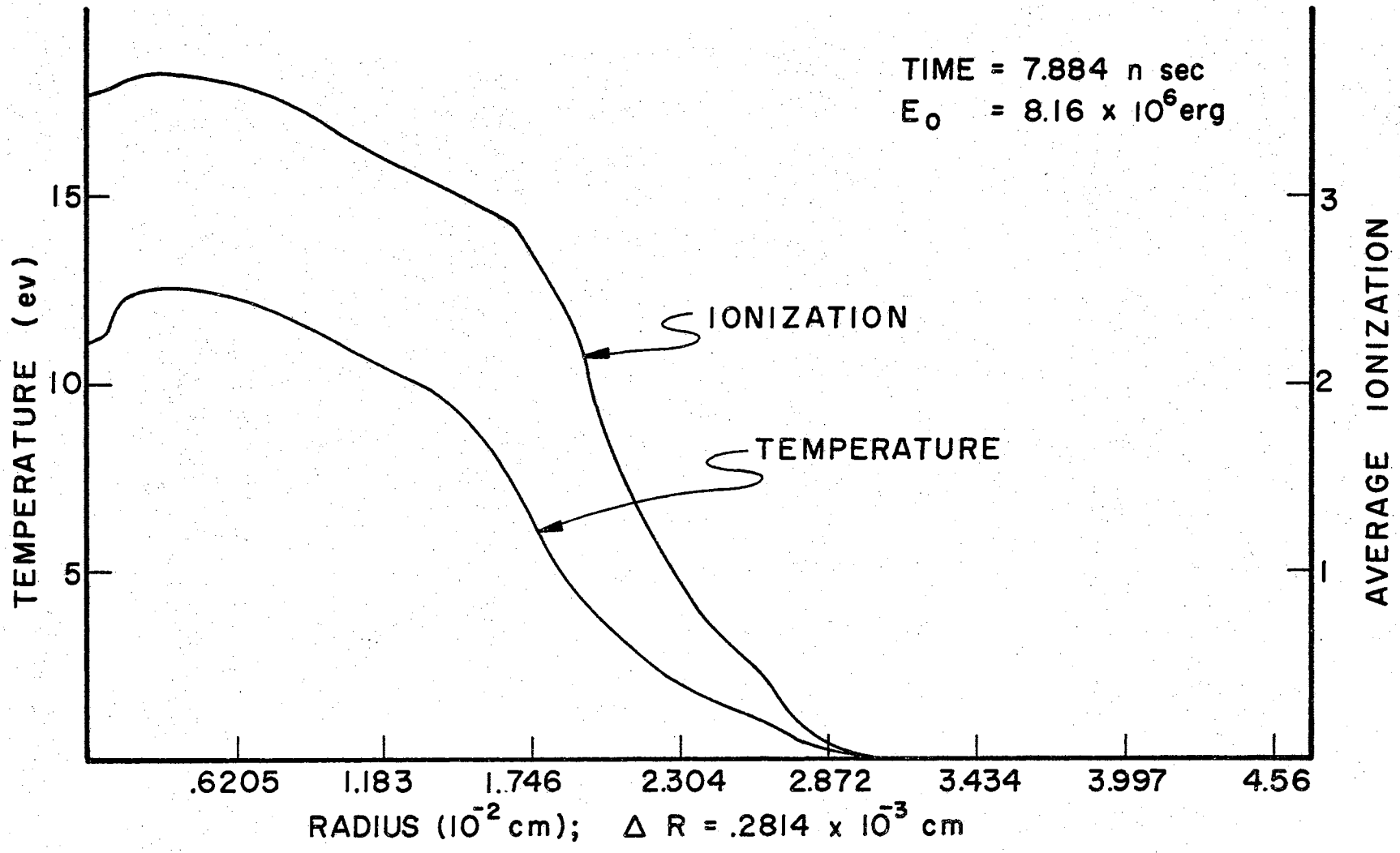

FIGURE 8.44 TEMPERATURE AND AVERAGE IONIZATION VERS

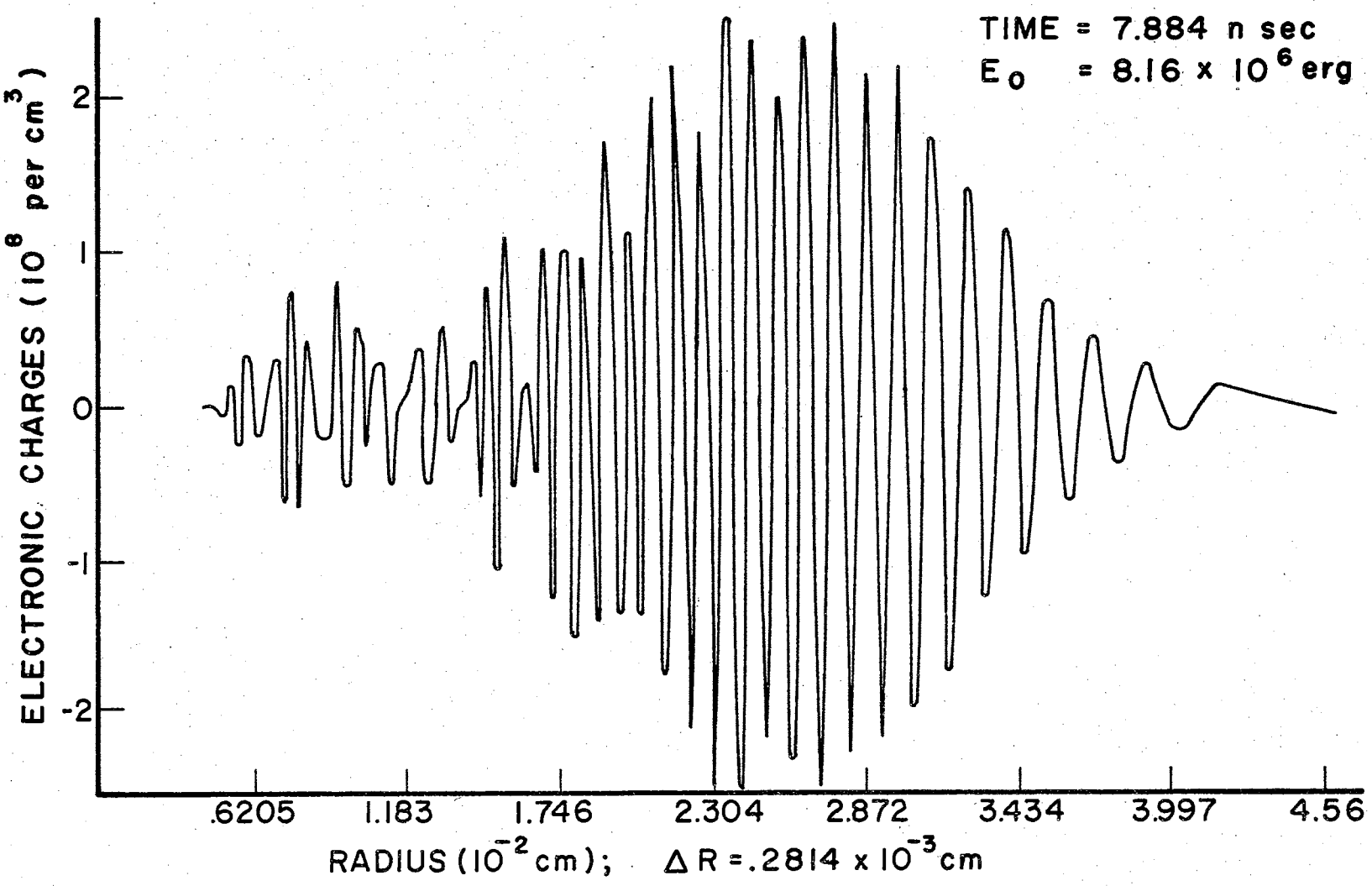

FIGURE 8.45 NUMBER OF EXCESS ELECTRONIC CHARGES VERS RADIUS

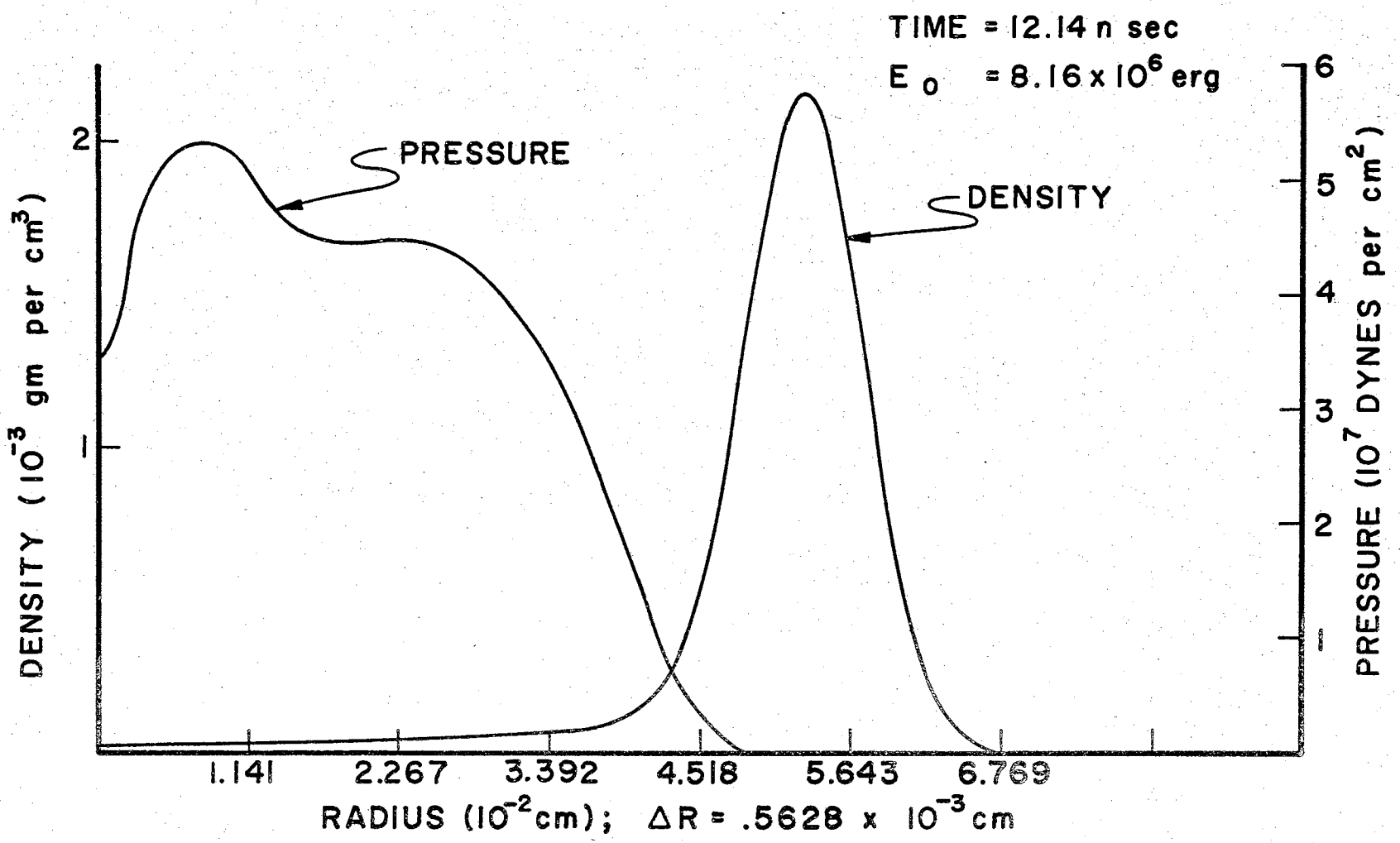

FIGURE 8.46 DENSITY AND PRESSURE VERS RADIUS

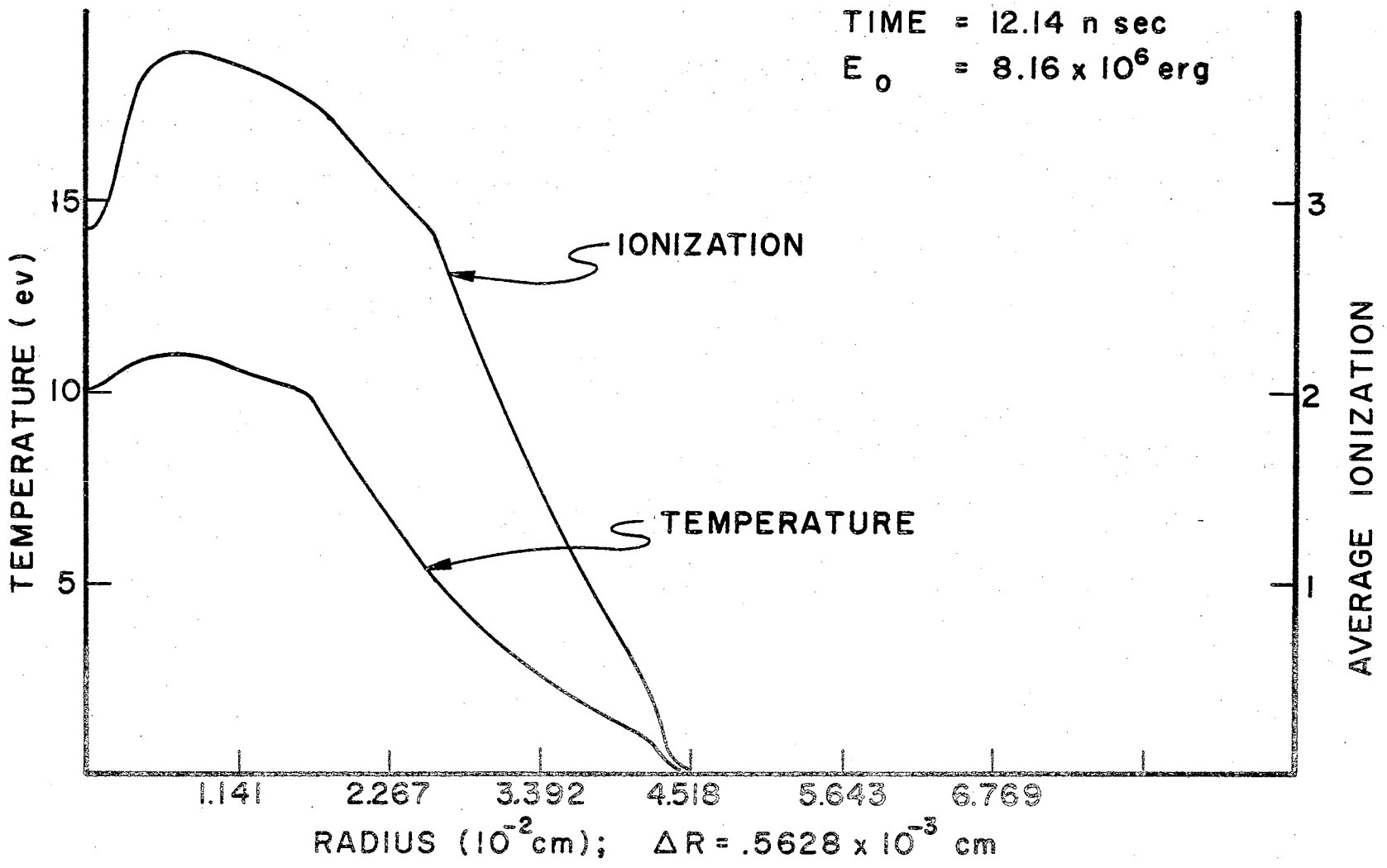

FIGURE 8.47 TEMPERATURE AND AVERAGE IONIZATION VERS RADIUS

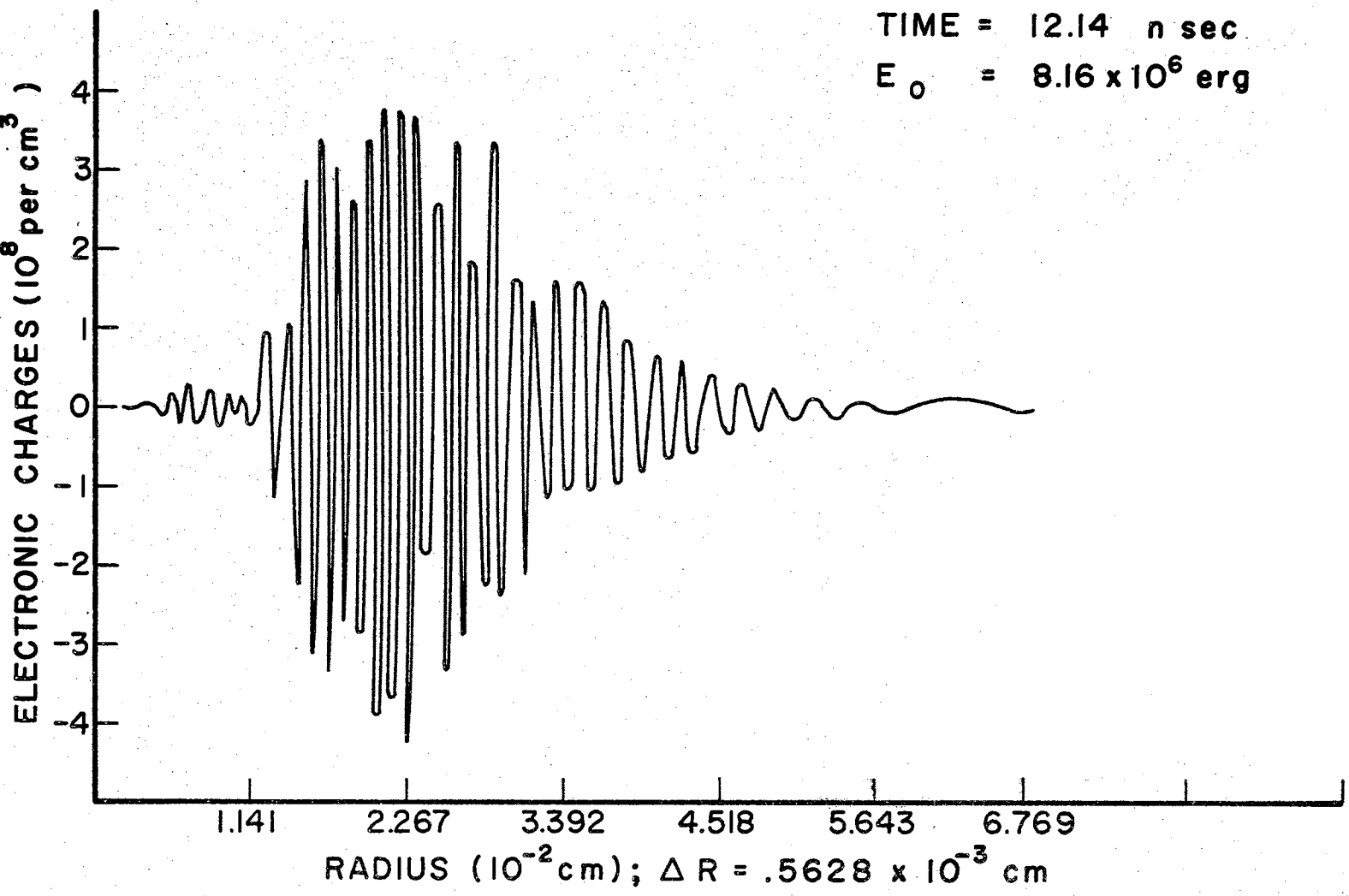

FIGURE 8.48 NUMBER OF EXCESS ELECTRONIC CHARGES VERS RADIUS

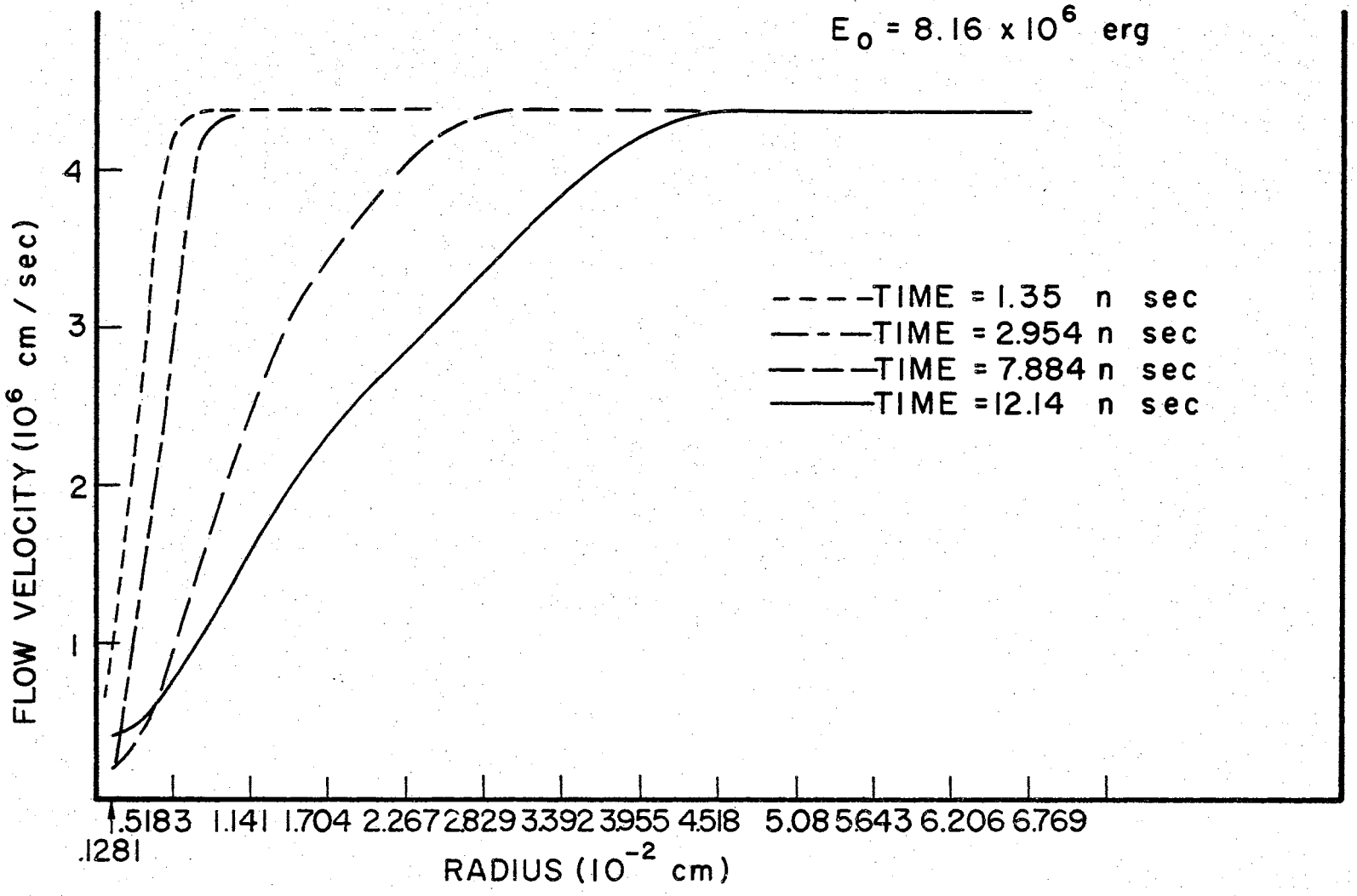

FIGURE 8.49 FLOW VELOCITIES VERS RADIUS

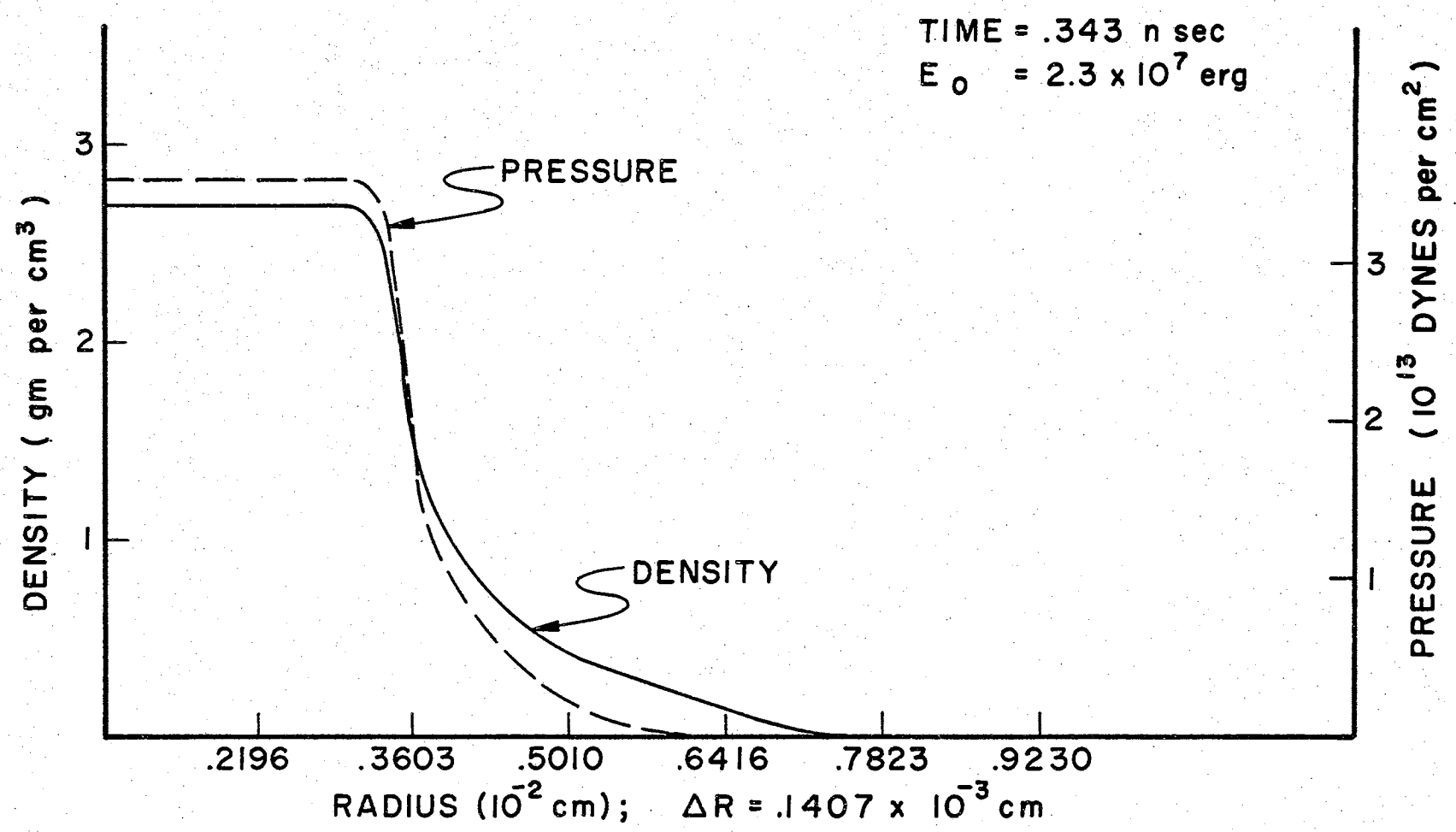

FIGURE 8.50 DENSITY AND PRESSURE VERS RADIUS

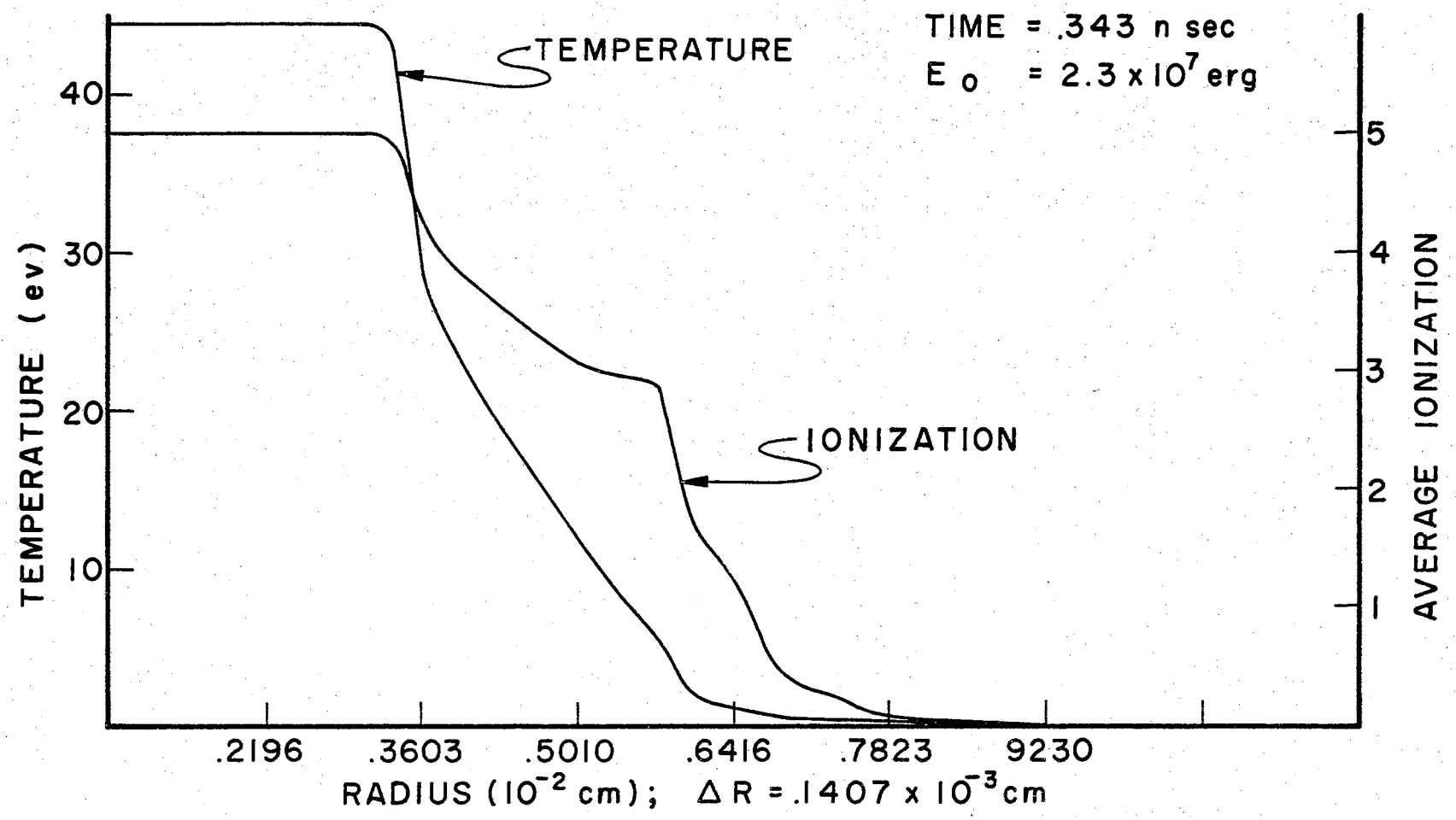

FIGURE 8.51 TEMPERATURE AND AVERAGE IONIZATION VERS RADIUS

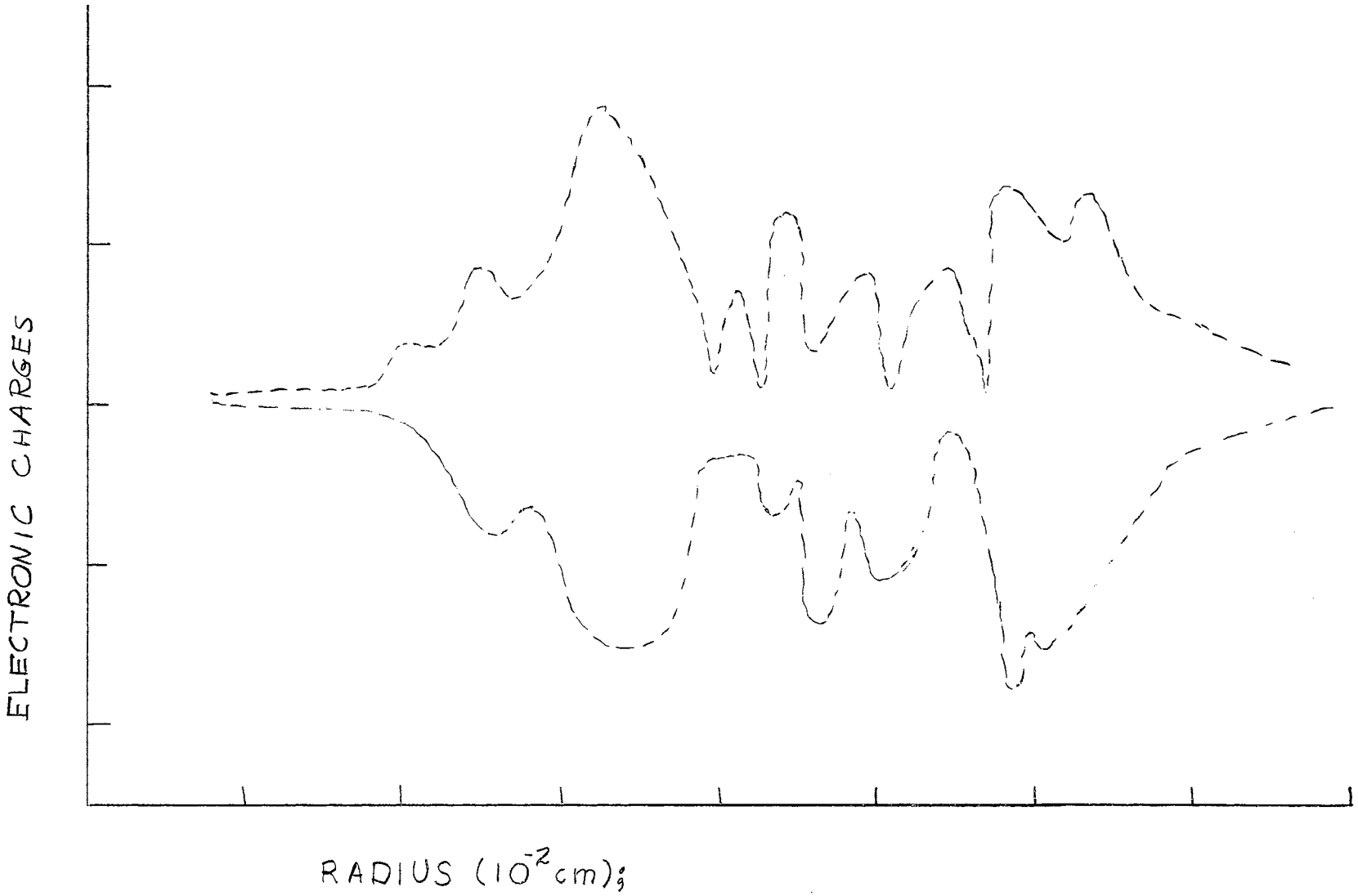

Figure 8.52. Number of Excess Electronic Charges vers Radius (Envelope)

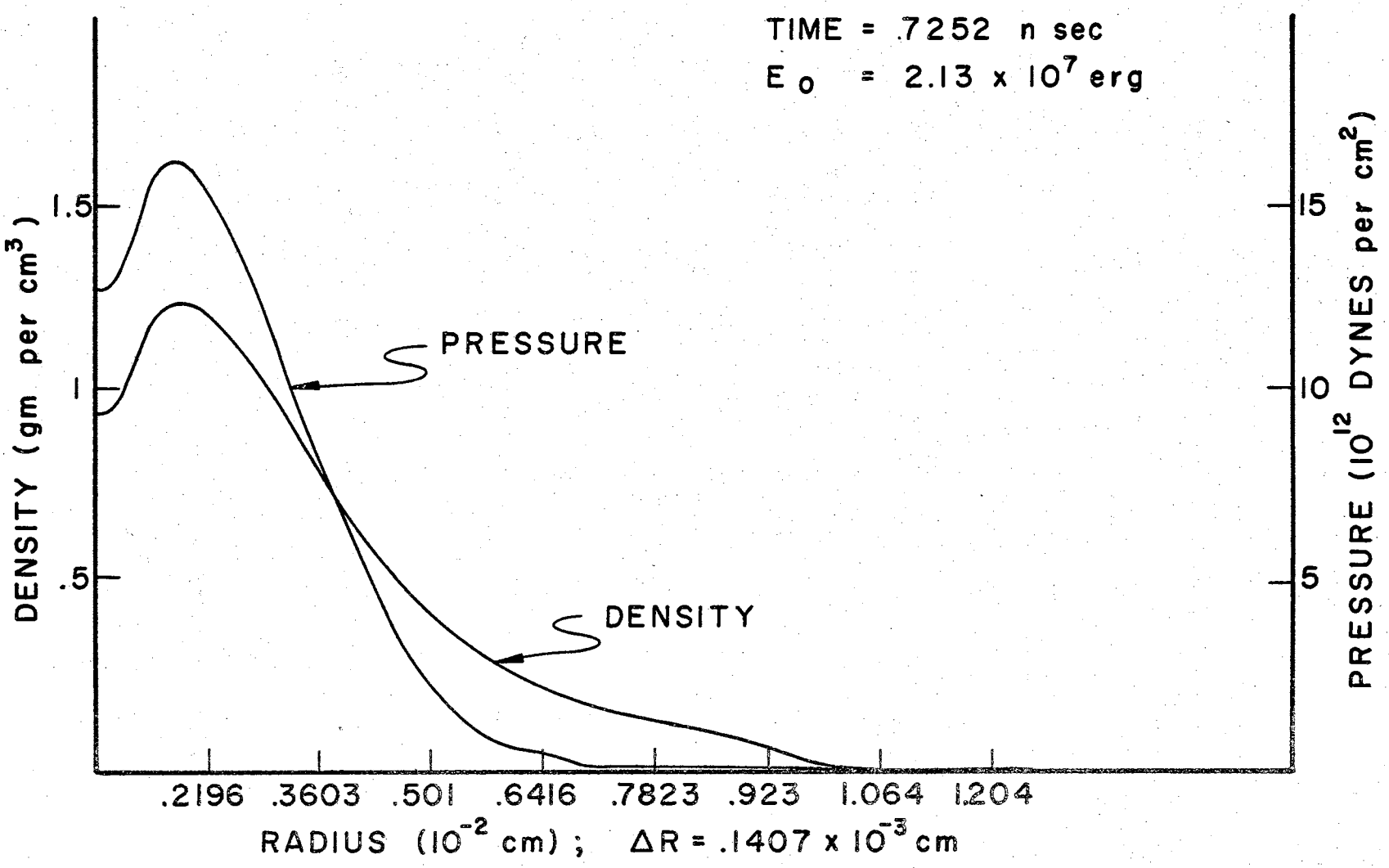

FIGURE 8.53 DENSITY AND PRESSURE VERS RADIUS

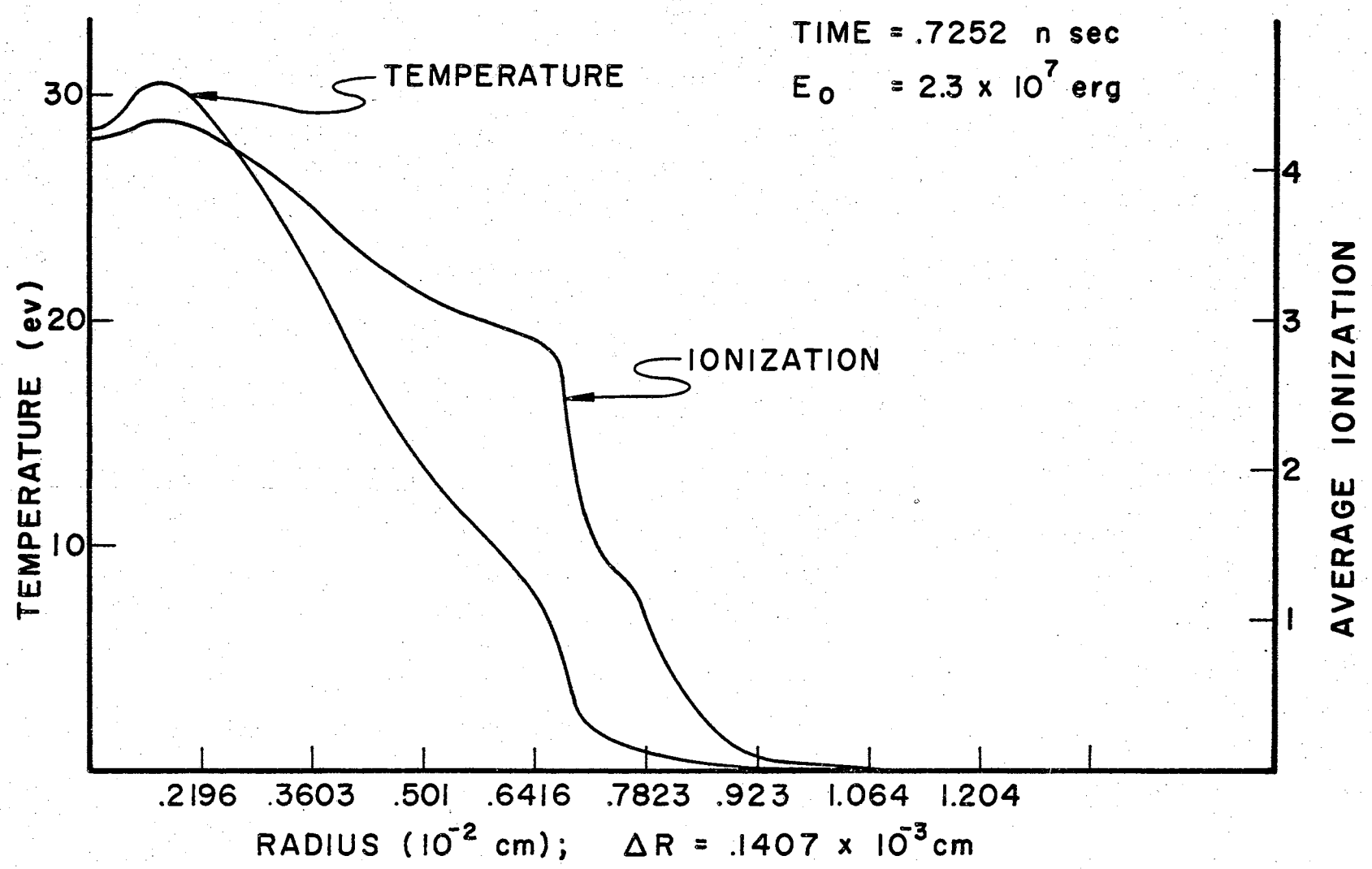

FIGURE 8.54 TEMPERATURE AND AVERAGE IONIZATION VERS RADIUS

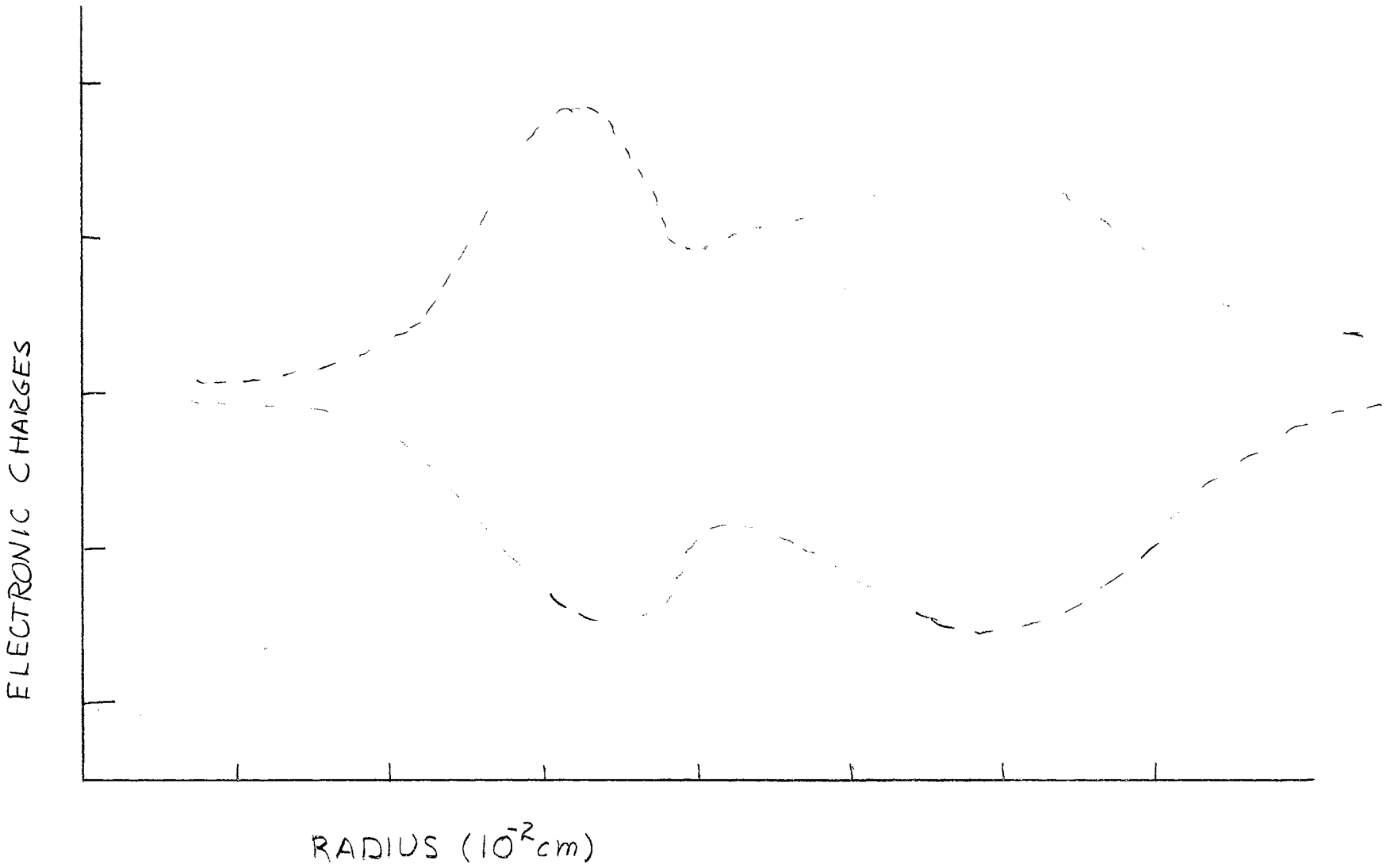

Figure 8.55. Number of Excess Electronic Charges vers Radius (Envelope)

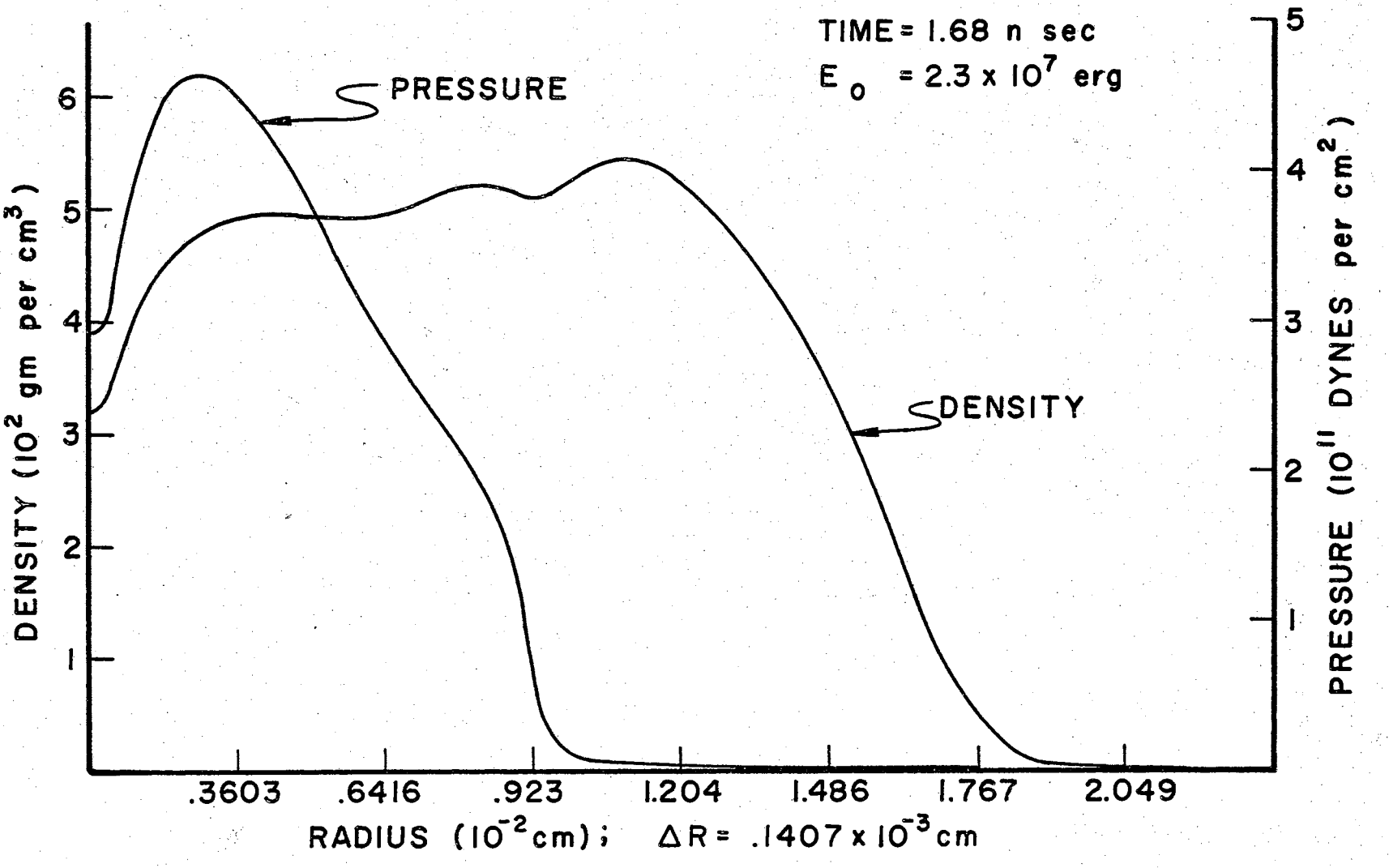

FIGURE 8.56 DENSITY AND PRESSURE VERS RADIUS

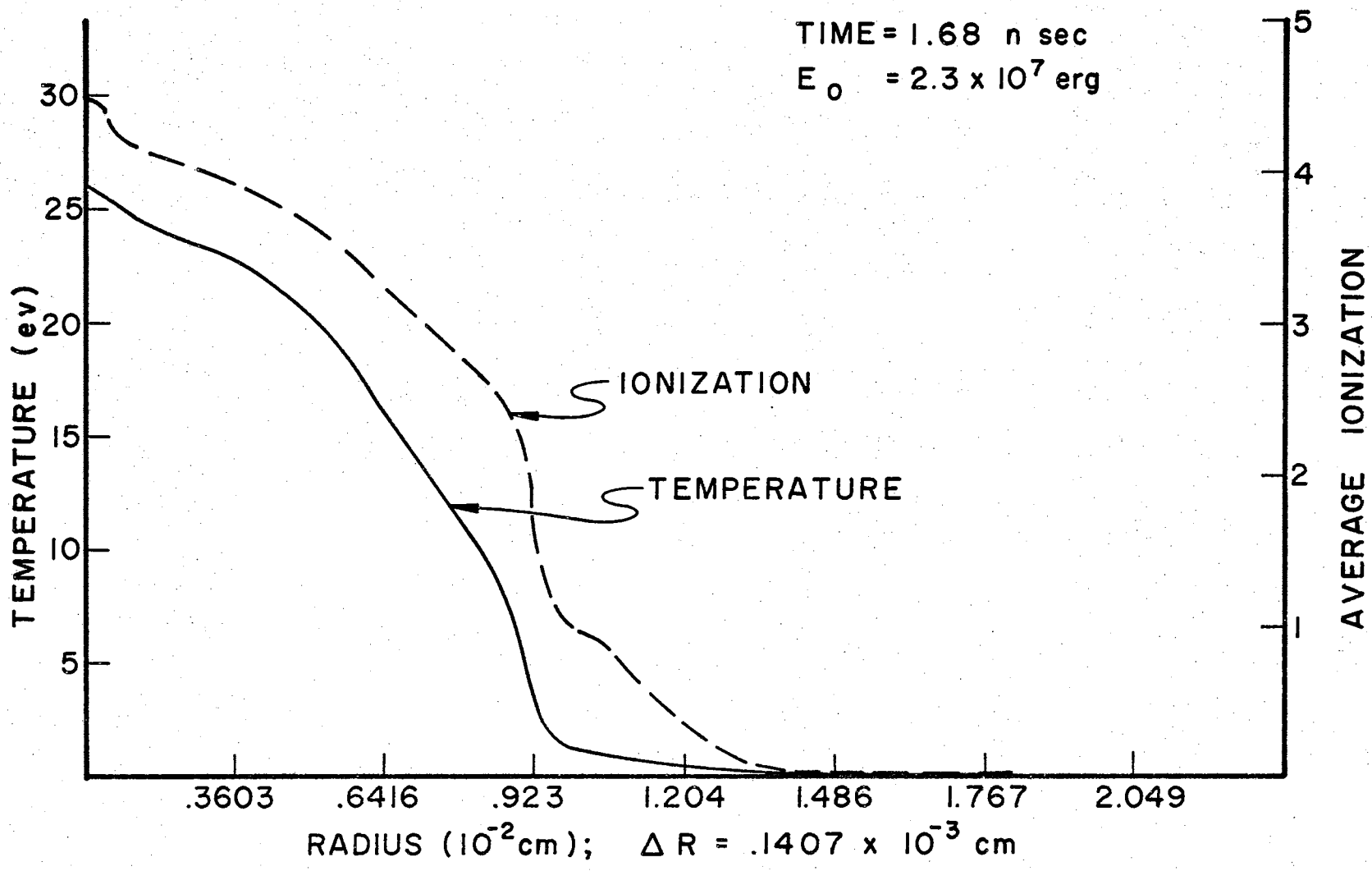

FIGURE 8.57 TEMPERATURE AND AVERAGE IONIZATION VERS RADIUS

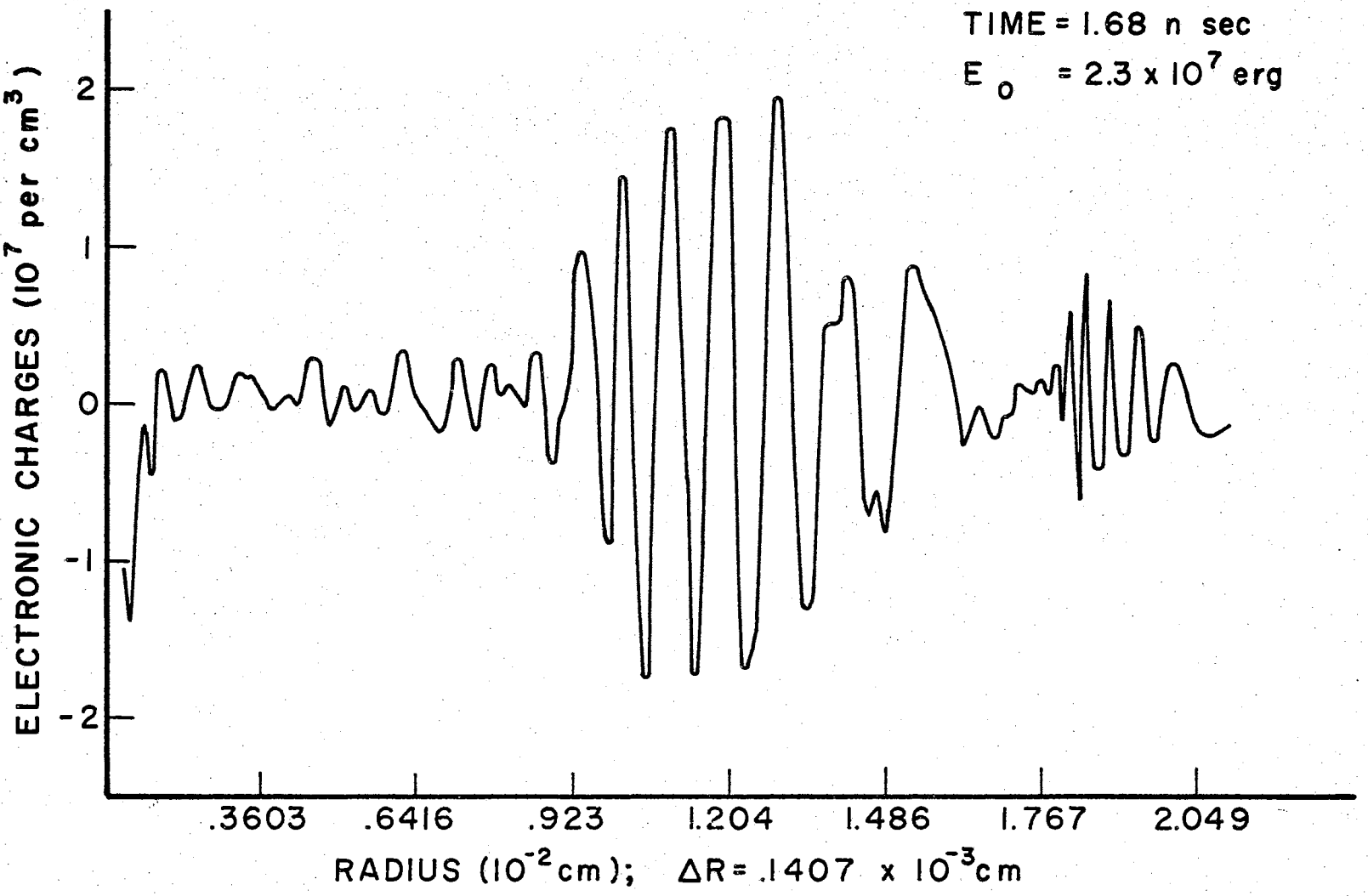

FIGURE 8.58 NUMBER OF EXCESS ELECTRONIC CHARGES VERS RADIUS

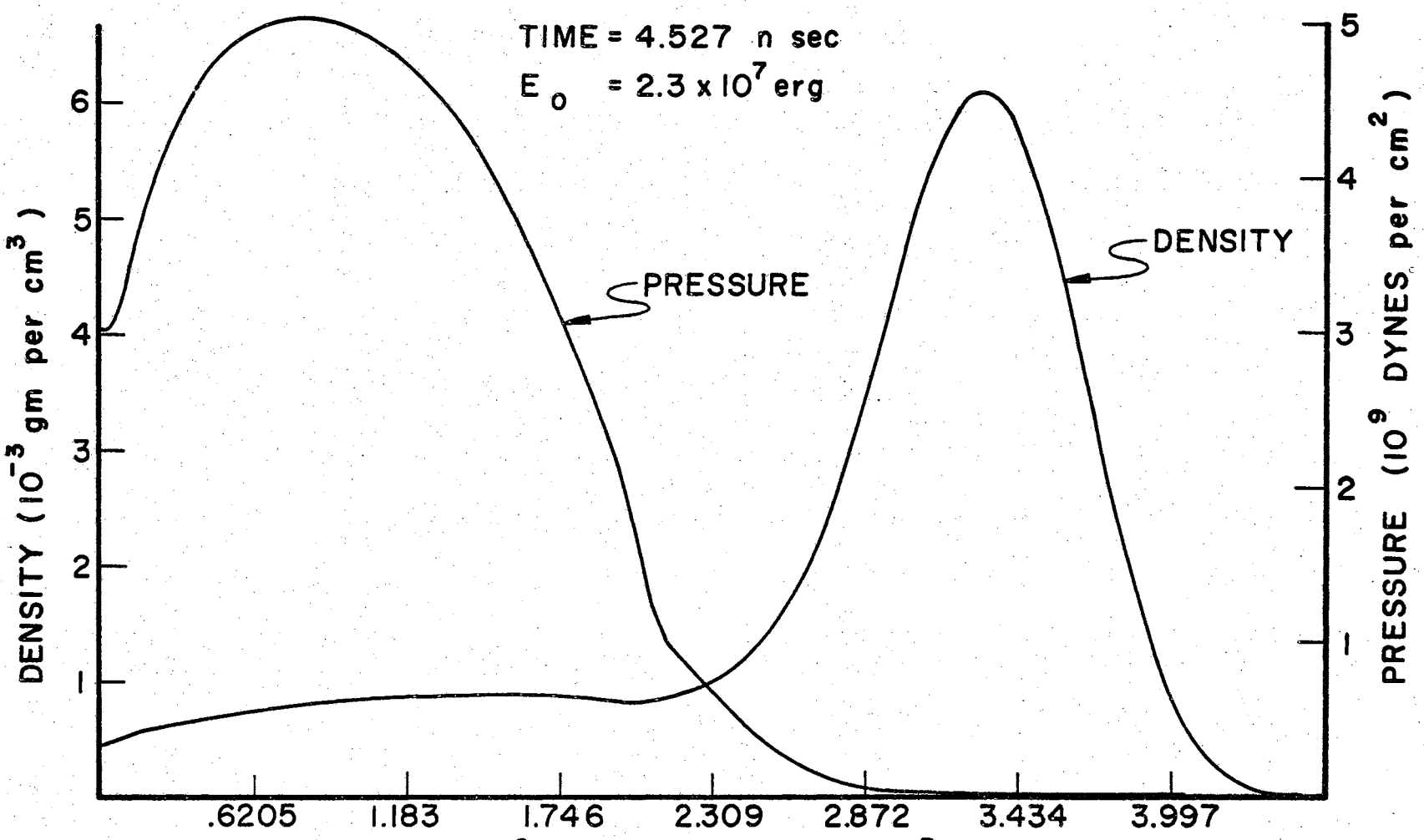

FIGURE 8.59 DENSITY AND PRESSURE VERS RADIUS

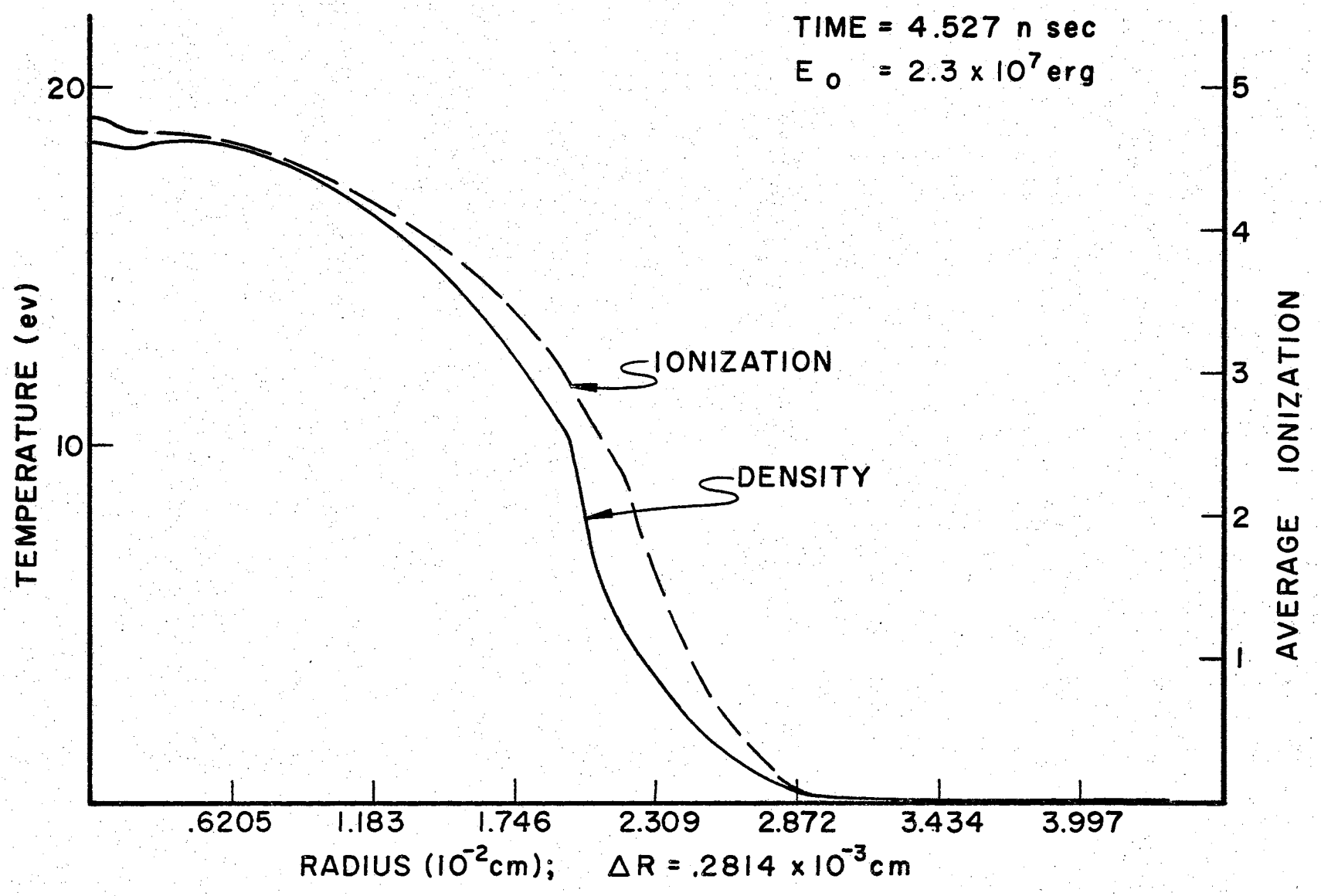

FIGURE 8.60 TEMPERATURE AND AVERAGE IONIZATION VERS RADIUS

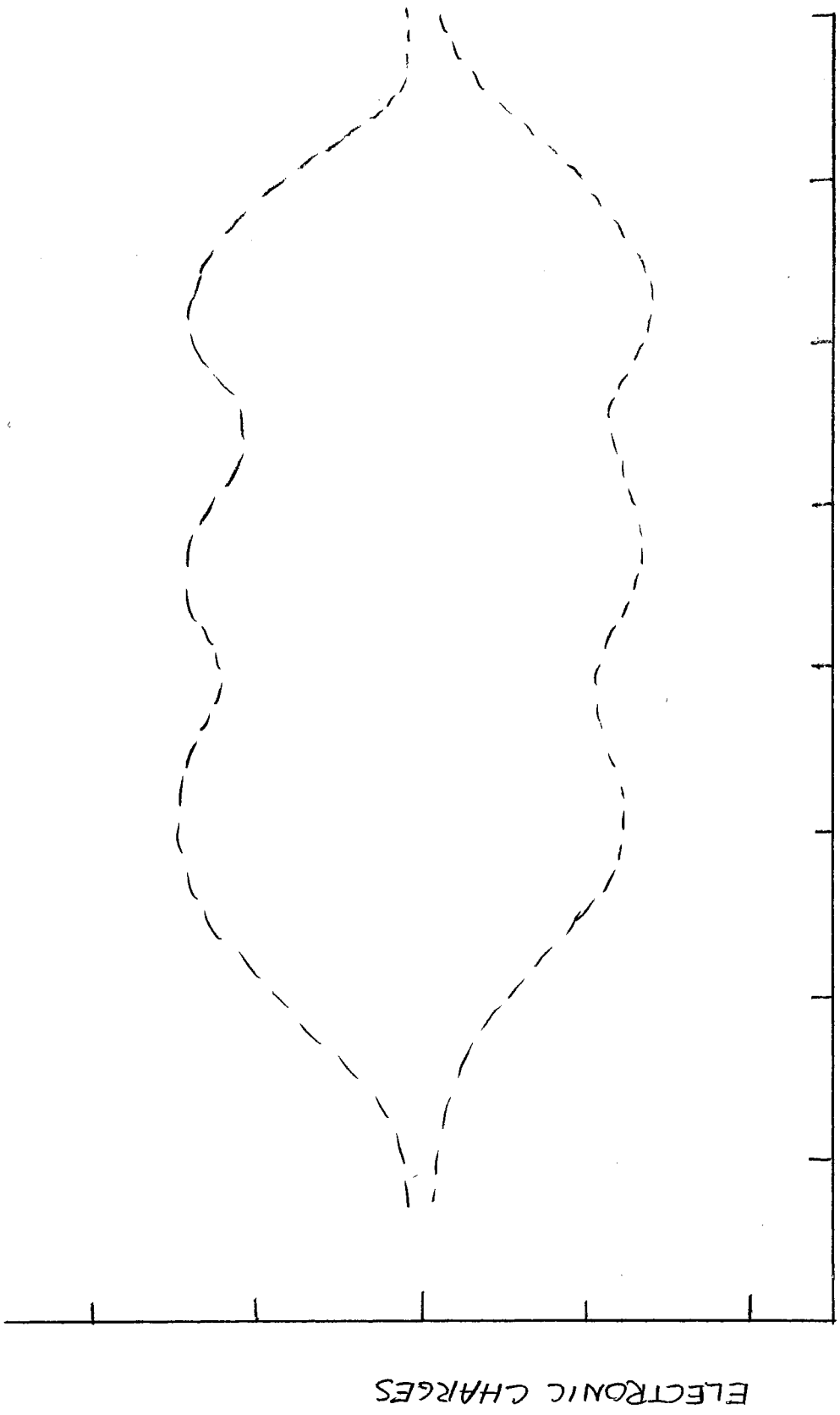

Figure 8.61. Number of Excess Electronic Charges vers Radius (Envelope).

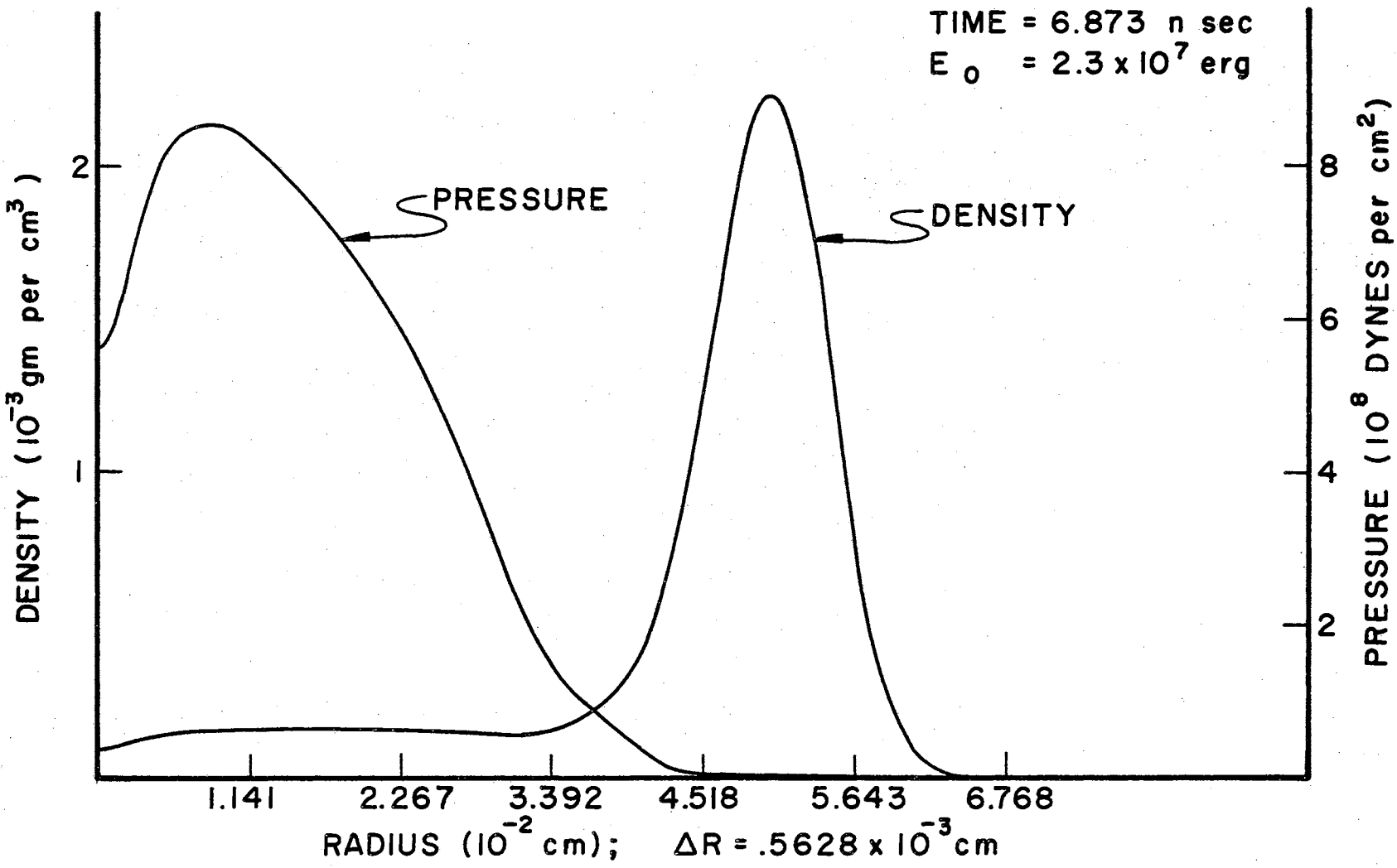

FIGURE 8.62 DENSITY AND PRESSURE VERS RADIUS

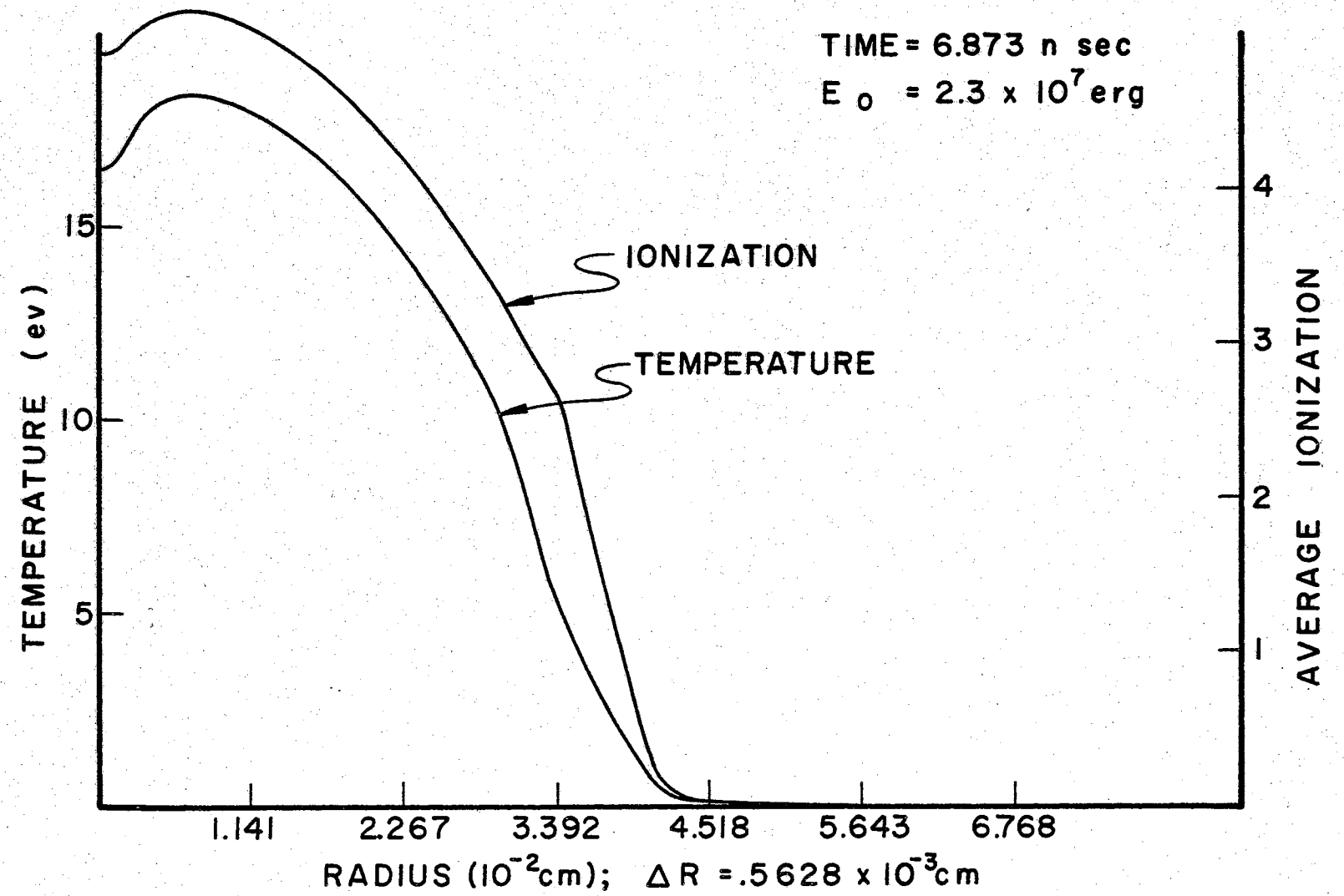

FIGURE 8.63 TEMPERATURE AND AVERAGE IONIZATION VERS RADIUS

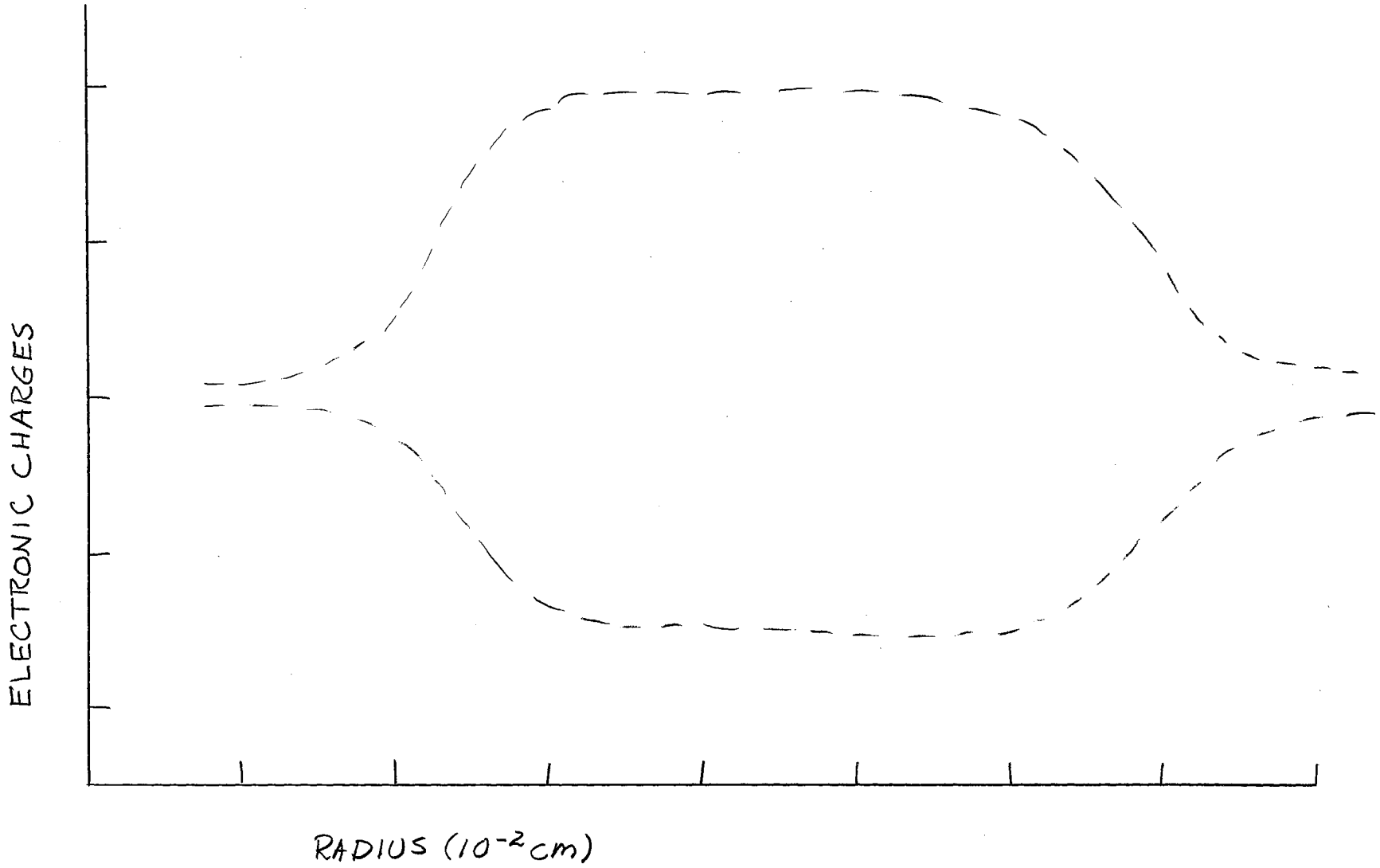

Figure 8.64. Number of Excess Electronic Charges vers Radius (Envelope)

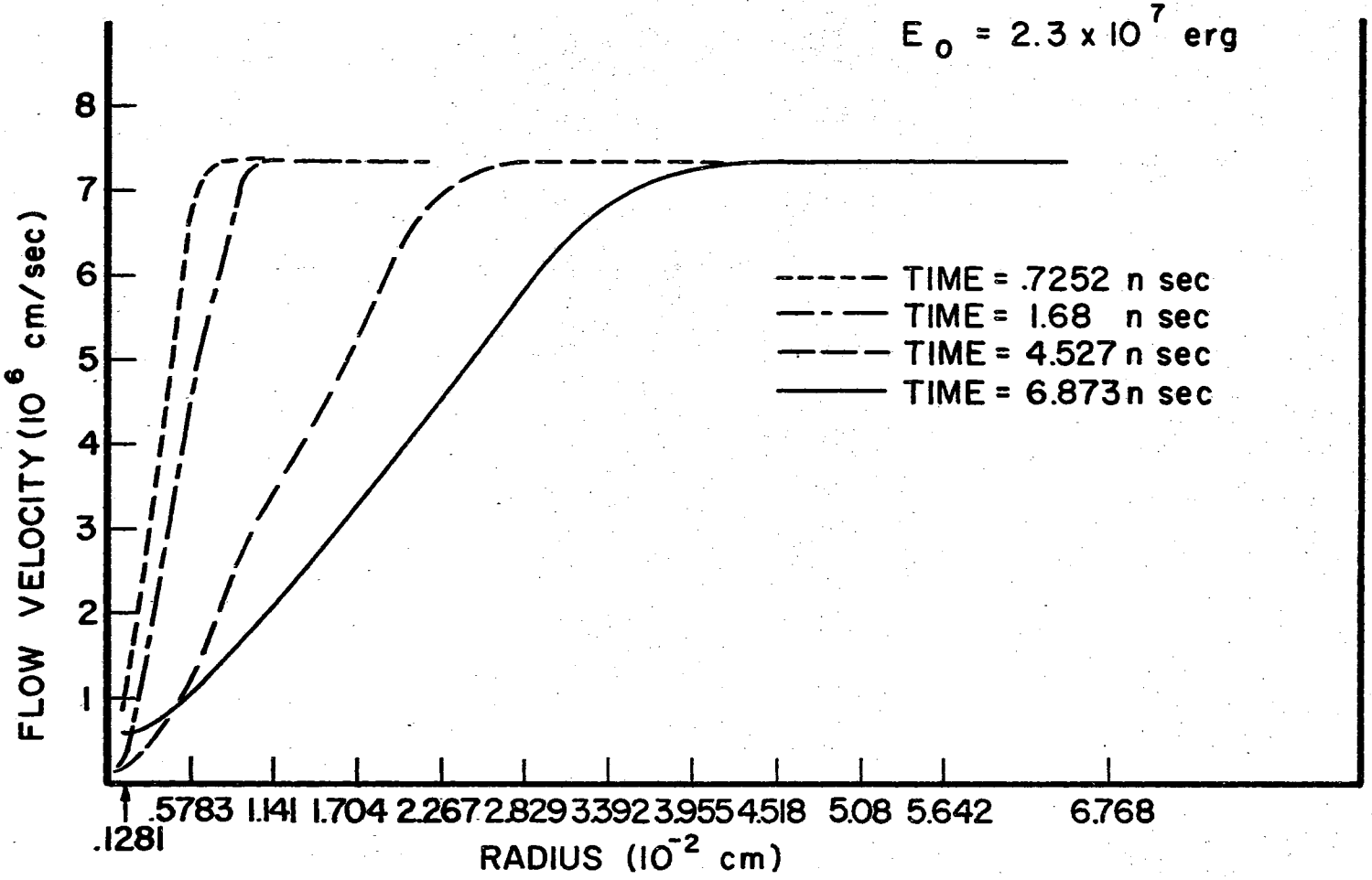

FIGURE 8.65 FLOW VELOCITIES VERS RADIUS

The cross marks on Figure 8.66 are the generated terminal velocities. Examination of this figure shows that no error exists in this respect.

Table XXIV shows that the density maximum propagates almost 2% fast. Table XXV shows that the leading edge of the plasma is being propagated about 12.5% fast. From these calculations one can conclude that the density maximums should be more peaked and slightly steeper on the leading edge. Generally speaking, the results are well within allowable limits.

6. Difficulties Encountered During Production Runs

The most trying difficulty was encountered when diffissional effects were included in the problem. In this case the solution is oscillatory with the oscillations building until the solution became unstable. No value of the Courant condition seemed to alleviate this instability. Close inspection revealed that this instability resulted from excessively large diffusion velocities. This difficulty was overcome by introducing an artificial density dependent damping coefficient. The coefficient was such that the theoretical diffusion coefficient was reduced by a density factor whenever the density was greater than 2.7×10^{-6} gm/cm^3. This more closely followed the observed phenomenon of ambipolar diffusion.

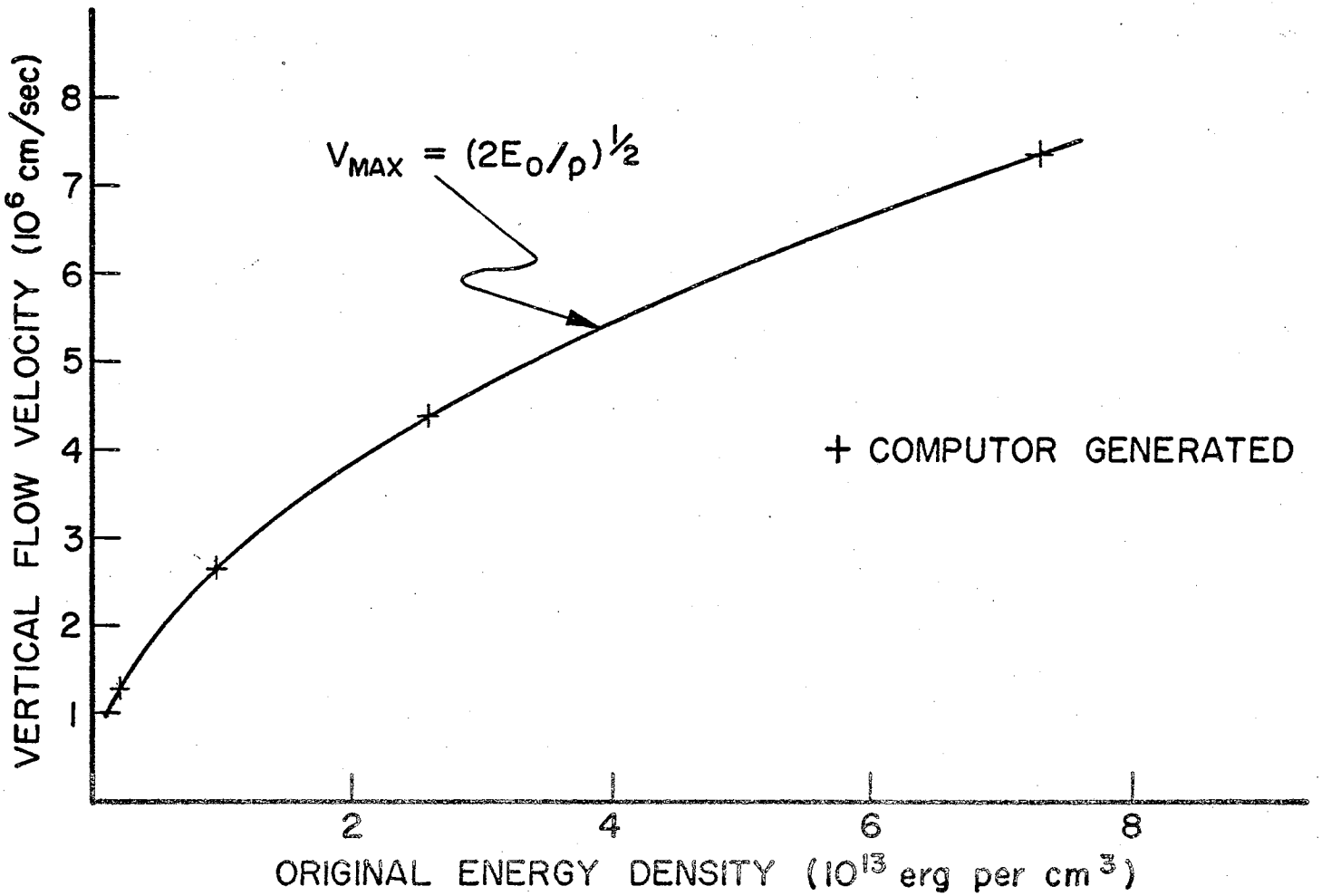

FIGURE 8.66 COMPARISON OF COMPUTER GENERATED TERMINAL VELOCITIES TO THEORETICAL MAXIMUMS

TABLE XXIV

PROPAGATION OF DENSITY MAXIMUM

1000 to 2500 cycles

$Temp_o$	t_o	R_o	t_t	R_t	Δt	V_f	ΔR_c	R_{f_c}	Error
3.416ev	$.1074 \times 10^{-7}$	$.1233 \times 10^{-1}$	$.4474 \times 10^{-7}$	$.5474 \times 10^{-1}$	$.34 \times 10^{-7}$	$.1232 \times 10^{7}$	$.4189 \times 10^{-1}$	$.5422 \times 10^{-1}$	1.0096
10.08ev	$.4895 \times 10^{-8}$	$.1241 \times 10^{-1}$	$.2026 \times 10^{-7}$	$.5418 \times 10^{-1}$	$.1536 \times 10^{-7}$	$.266 \times 10^{7}$	$.4086 \times 10^{-1}$	$.5327 \times 10^{-1}$	1.0171
20.00ev	$.2954 \times 10^{-8}$	$.1162 \times 10^{-1}$	$.1214 \times 10^{-7}$	$.5305 \times 10^{-1}$	$.09186 \times 10^{-7}$	$.4386 \times 10^{7}$	$.4029 \times 10^{-1}$	$.5191 \times 10^{-1}$	1.0220
44.49ev	$.168 \times 10^{-8}$	$.1099 \times 10^{-1}$	$.6873 \times 10^{-8}$	$.5024 \times 10^{-1}$	$.05193 \times 10^{-7}$	$.7361 \times 10^{7}$	$.3823 \times 10^{-1}$	$.9922 \times 10^{-1}$	1.0207

TABLE XXV

PROPAGATION OF LEADING EDGE

300 to 2500 cycles

$Temp_o$	t_o	R_o	t_f	R_f	Δt	V_f	ΔR_c	R_{f_c}	Error
3.416ev	$.2744 \times 10^{-8}$	$.1022 \times 10^{-1}$	$.4447 \times 10^{-7}$	$.6937 \times 10^{-1}$	$.4173 \times 10^{-7}$	$.1232 \times 10^{7}$	$.5141 \times 10^{-1}$	$.6163 \times 10^{-1}$	1.1256
10.08ev	$.1192 \times 10^{-8}$	$.9934 \times 10^{-2}$	$.2026 \times 10^{-7}$	$.6825 \times 10^{-1}$	$.1907 \times 10^{-7}$	$.266 \times 10^{7}$	$.5073 \times 10^{-1}$	$.6066 \times 10^{-1}$	1.1251
20.00ev	$.7091 \times 10^{-9}$	$.9793 \times 10^{-2}$	$.1214 \times 10^{-7}$	$.6769 \times 10^{-1}$	$..114 \times 10^{-7}$	$.4386 \times 10^{7}$	$.5000 \times 10^{-1}$	$.5979 \times 10^{-1}$	1.1321
44.49ev	$.343 \times 10^{-9}$	$.8949 \times 10^{-2}$	$.6873 \times 10^{-8}$	$.6431 \times 10^{-1}$	$.0653 \times 10^{-7}$	$.7361 \times 10^{7}$	$.4807 \times 10^{-1}$	$.5702 \times 10^{-1}$	1.1278

CHAPTER IX

SPECTRA

1. Introduction

One of the objectives of this research is the formulation of a method for calculating the spectra emitted during the expansion of the plasma sphere. In this chapter the basic equations, which define the emitted continuous spectra, are developed and shown to be functions of the density and temperature profiles. The continuous spectra is considered to be the best indicator of the gross plasma properties in consideration of the extreme densities that occur. In addition, based upon astrophysical models, over 90% of the emitted radiation should be continuous.

The fundamental assumptions that are required for this solution are:

1. Local thermodynamic equilibrium exists,
2. no magnetic fields exist in the plasma (thus no synchrotron radiation is generated), and
3. plasma oscillation emission is negligible.

In Section 2, the basic classical transfer equation is developed. The form of the solution of the equation of transfer is in Section 3. Some simplifications are reviewed in Section 4. The evaluation of the monochromatic absorption coefficient, k_ν, is discussed in Section 5.

The numerical methods and results of the evaluation are given in the remainder of the chapter.

2. Equation of Transfer

Consider an elementary cylinder of thickness, ds, and surface area dS, upon which radiation in the frequency range from ν to $\nu + d\nu$ strikes normal to dS, as shown in Figure 9.1. If the energy that is incident on the surface per second is E_i and is entirely within the solid angle, $d\omega$, then,

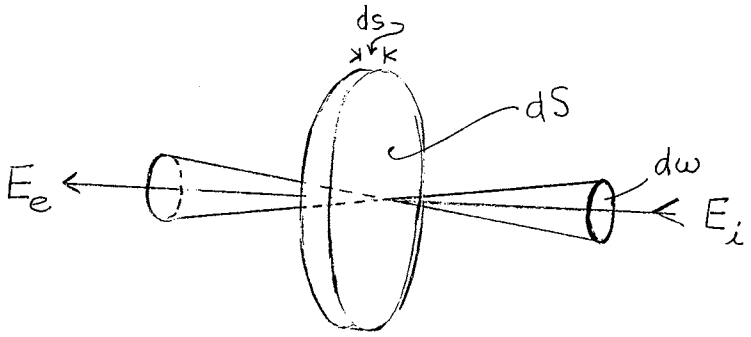

Figure 9.1. Geometry of Absorption.

$$E_i = I_\nu \, d\omega \, dt \, d\nu \, dS. \tag{9.1}$$

Equation 9.1 also serves as a definition of the specific monochromatic intensity, I_ν. The energy emerging at the second surface of the cylinder E_e, will be

$$E_e = (I_\nu + dI_\nu) \, d\omega \, d\nu \, ds \, dt. \tag{9.2}$$

Neglecting scattering (the scattering coefficient is negligible compared to the absorption coefficient), the energy absorbed within the cylinder is given by

$$\Delta E_{ab} = -E_i k_\nu \rho \, ds \tag{9.3}$$

and the energy emitted within the cylinder in the same frequency range is

$$\Delta E_e = \frac{j_\nu \rho}{4\pi} \, dS \, ds \, d\omega \, dt \, d\nu, \tag{9.4}$$

where k_ν is the monochromatic absorption coefficient, j_ν is the monochromatic coefficient of emission and ρ is the density of the material. It is evident that

$$E_e = E_i + \Delta E_e + \Delta E_{ab} . \tag{9.5}$$

Using Equations 9.1, 9.3 and 9.2 in 9.5 and simplifying, one obtains an equation of transfer:

$$dI_\nu/ds = -I_\nu k_\nu \rho + \frac{j_\nu \rho}{4\pi} . \tag{9.6}$$

This equation relates the intensity of the radiation to the properties of the medium through which it passes. The local thermodynamic equilibrium assumption allows the use of Kirchoff's law,

$$\frac{j_\nu}{k_\nu} = 4\pi B_\nu(T), \tag{9.7}$$

where $B_\nu(T)$ is the Planck function:

$$B_\nu(T) = \frac{2h\nu^3}{c^2} \left[\exp(h\nu/kT) - 1 \right]^{-1} . \tag{9.8}$$

Thus, Equation 9.6 may be written

$$\frac{d I_\nu(\theta,r)}{ds} = -k_\nu \rho \left[I_\nu(\theta,r) - B_\nu(T) \right]. \qquad (9.9)$$

The notation $I_\nu(\theta,r)$ indicates that in general the specific monochromatic intensity is a function of the direction of propagation and the position in the gas.

3. Geometry and Form of the Solution

Assuming that k_ν, ρ and T are known functions of the position, Equation 9.9 can be solved. For a specified direction of radiation, the equation of transfer is of the form

$$\frac{dy}{dx} + P(x)y + Q(x) = 0, \qquad (9.10)$$

which has a general solution of the form

$$y(x) = D_\nu \exp\left(-\int P(r)dr\right) + \exp\left(-\int P(r)dr\right)\left[\int Q(r) e^{\int P(r')dr'} dr\right]. \qquad (9.11)$$

where D_ν is a constant to be determined. Converting to the form of measuring distances inward, opposite to the direction of radiation, 9.11 converts to the form

$$I_\nu(x) = D_\nu \exp\left(+\int_{x_o}^{x} \rho k_\nu dr\right) + \exp\left(+\int_{x_o}^{x} \rho k_\nu dr\right) \int_{x}^{\infty} \rho k_\nu B_\nu(T) \exp\left(-\int_{x_o}^{r} k_\nu \rho dr'\right) dr. \qquad (9.12)$$

D_ν is noted to be zero since otherwise $I_\nu(\infty)$ would have to be infinite of the same order as $\exp\left(\int_{x_o}^{\infty} \rho k_\nu dr\right)$. The emergent radiation, in the specified direction, that reaches the surface, x_o, becomes

$$I_\nu(x_0) = \int_{x_0} \rho\, k_\nu\, B_\nu(T) \exp\left(-\int_{x_0}^{r} k_\nu \rho\, dx\right) dr \qquad (9.13)$$

The solution may now be specialized for determining the emergent light (in a given direction) from the spherical plasma model of radius, R.

Consider a plasma sphere of radius, R, with the line of sight, AB, in Figure 9.2. To calculate the intensity of emitted light along this

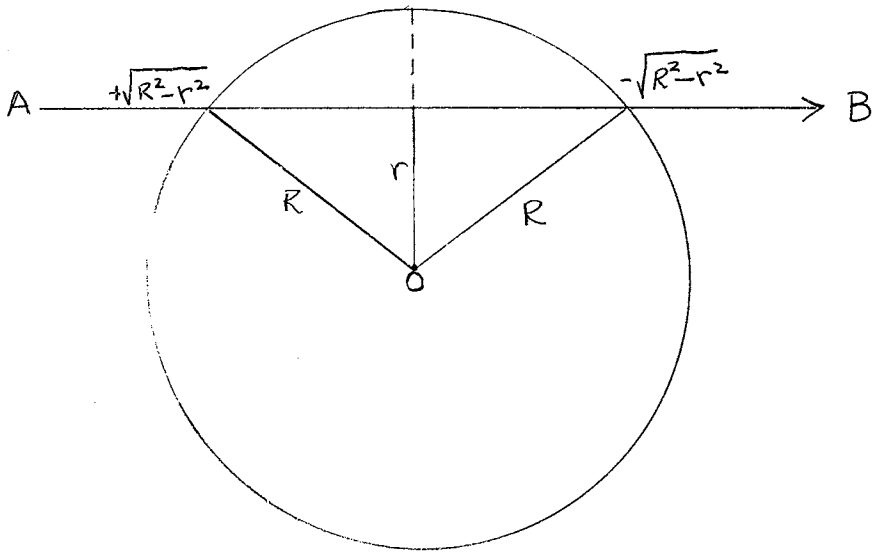

Figure 9.2. Geometry of Radiation Problem

line, AB, the integral must be completed along the line BA. The total radiation in the direction B is then the evaluation of the integral as r varies from 0 to R. The integration limits are from - to +. Equation 9.13 (for the emitted monochromatic specific intensity) becomes

$$I_\nu(r) = \int_{-\sqrt{R^2-r^2}}^{+\sqrt{R^2-r^2}} k_\nu \rho\, B_\nu(T)\; e^{-\int_{-\sqrt{R^2-r^2}}^{x} k_\nu \rho\, dh}\, dx\,. \qquad (9.14)$$

The flux in the direction B is simply the integral over the total disc

$$F_{\nu_B} = 2\pi \int_0^R dr \int_{-\sqrt{R^2-r^2}}^{+\sqrt{R^2-r^2}} k_\nu \rho B_\nu(T)\, e^{-\int_{-\sqrt{R^2-r^2}}^{\hat{x}} k_\nu \rho\, dh}\, dx \quad . \tag{9.15}$$

To evaluate this integral, the variables, ρ and T, must be known functions of the radius. It will be shown later that $k_\nu = k_\nu(\rho, T)$. If the directional flux is known for a particular sphere of radius, R, it is possible, knowing how ρ varies with depth, to determine a reasonable estimate of the temperature profile.

4. Simplified Uniform Plasma Sphere

For simplicity, consider that the plasma sphere has uniform density and temperature. (This is not nearly as bad an approximation as it first appears.)

For the uniform sphere, Equation 9.15 is readily evaluated since k_ν, ρ and T are known constants.

$$F_{\nu_B} = 2\pi \int_0^R dr\, B_\nu(T) \left[1 - e^{-2k_\nu \rho \sqrt{R^2-r^2}}\right] \tag{9.16}$$

since

$$e^{-\int_{-\sqrt{R^2-r^2}}^{S} k_\nu \rho\, dh} = \frac{1}{k_\nu \rho}\, e^{-k_\nu \rho \left[\sqrt{R^2-r^2} - S\right]} \quad . \tag{9.17}$$

Completing the second integral yields

$$F_{\nu_B} = \frac{\pi}{2} R^2 B_\nu(T) \left[1 + \frac{e^{-2k_\nu \rho R}}{k_\nu \rho R} - \frac{\left(1 - e^{-2k_\nu \rho R}\right)}{2(k_\nu \rho R)^2}\right] . \tag{9.18}$$

If the product, $k_{\nu}\rho R$, is defined in terms of optical depth of the sphere,

$$\tau_{\nu} = k_{\nu} \rho R, \tag{9.19}$$

Equation 9.18 becomes

$$F_{\nu B} = \frac{\pi}{2} R^2 B_{\nu}(T) \left[1 + \frac{e^{-2\tau_{\nu}}}{\tau_{\nu}} - \frac{(1 - e^{2\tau_{\nu}})}{2\tau_{\nu}^2} \right]. \tag{9.20}$$

The general relation in Equation 9.16 and the above limited relation in Equation 9.20, show that the continuous radiation may be evaluated except for the numberical value of k_{ν}.

5. Absorption Coefficient, k_{ν}

There are, in general, five processes responsible for continuous absorption (L. H. Aller, 1953):

1. Photoionization from discrete atomic levels to the continuum,
2. Free-Free transitions,
3. Electron scattering,
4. Photodissociation of negative ions, and
5. Molecular dissociation.

For the plasma under consideration, each of the last three processes is either not applicable, or is negligible. Only photoionization and free-free transitions are considered.

a. Photoionization

Start with an atomic system in an initial state, i, with the energy, E_i. Consider the process by which the system absorbs a photon and makes a transition to another state, f, in which the electron is free. The set of all states in which one electron is free and the residual system is in

a state of stable energy is called a continuum of the system. Light of frequency, ν, can cause transitions to those continuum states whose energies are equal to, or less than $h\nu + E_i$.

The cross section for the absorption of a light quantum of frequency ν, accompanied by such a transition, is given by Ditchburn and Öpik (1962) as

$$\alpha(\nu) = \frac{\pi^3}{c} \frac{\nu}{\omega_i} \sum_i \sum_f \left| \int \psi_f^* \sum_\mu e_\mu \vec{r}_\mu \psi_i \, d\tau \right|^2, \qquad (9.21)$$

where the ψ_i are wavefunctions of the ω_i-fold degenerate initial state, ψ_f are continuum eigenfunctions belonging to the eigenvalue, $h\nu + E_i$. e_μ is the charge and $\vec{r}_\mu$ is the position vector of the μth particle in the system. The summations are over all particles, μ, over all ω_i initial states and over all f final states. Solution of 9.21 is formidable. The most frequently used approximation is the central field approximation. This procedure is not very reliable according to R. V. Ditchburn and U. Öpik (1962), who state: "general formula based upon approximate wave functions do not always give even the correct order of magnitude". In view of the difficulty of the problem, the usual practice is to use the hydrogen cross-section:

$$\alpha(\nu, n) = g\,(32\pi^2 e^6 R_e Z^4)/(3^{3/2} h^3 \nu^3 n^5), \qquad (9.22)$$

with Z replaced by an effective Z_{eff} (Schwartzchild, 1961). In equation 9.22, $\alpha(\nu, n)$ is the cross section for photoionization from the n^{th} level by a photon of frequency, ν, provided $h\nu + E_i$ is a continuum eigenvalue, e is electronic charge, R_e is the Rydberg constant, Z is the core charge,

h is Planck's constant and n is the principle quantum number. The effective Z value for a given level is related to the n value and the term value, T_n, for the level through

$$Z_{eff} = n\sqrt{\frac{T_n}{R_\infty}}\ , \tag{9.23}$$

where R_∞ is the Rydberg constant and T_n is in wave numbers. The total photoionization cross section, α_ν, may be obtained from the expression

$$\alpha_\nu C = \sum_{n_0}^{n_{max}} \alpha(\nu, n)\, C_n\ , \tag{9.24}$$

where C is the total number density and C_n is the number of atoms, or ions, in each level, n. The mass photoionization coefficient, k^*_ν, is related to α_ν through

$$\alpha_\nu C = \rho\, k^*_\nu\ . \tag{9.25}$$

If several different species are present

$$\rho\, \overline{k^*_\nu} = \sum_i \rho_i\, k^*_{\nu_i} = \sum_i \alpha_{\nu_i} C_i\ , \tag{9.26}$$

or, using 9.24,

$$\rho\, \overline{k^*_\nu} = \sum_{i=1}^{\sigma} \sum_{n=n_0}^{n_{max}} \alpha_i(\nu, n)\, C_{in}\ , \tag{9.27}$$

where the summation is over all allowed energy levels, n, of each species then over the σ species. The lower limit on the sum over n is determined by the condition

$$h\nu \geq |I_{eff}| - |E_n|\ , \tag{9.28}$$

where I_{eff} is the effective ionization potential and E_n is the energy of level, n. The upper limit, n_{max}, is determined from the condition that the highest discrete level be

$$|E_n| \leq |I_{eff}| . \tag{9.29}$$

The state must be a bound state.

The value thus obtained for $\overline{k_\nu^*}$ must be corrected for stimulated emission. This correction is made by multiplying by a factor $(1-e^{-h\nu/kT})$. The derivation of this term appears in an appendix to this thesis. The final, monochromatic photoionization coefficient is approximated by

$$\overline{k_\nu^*} = \left(\sum_{i=1}^{\sigma} \sum_{n=n_0}^{n_{max}} \alpha_i(\nu, n) C_{i,n} \right) \left(1 - e^{-h\nu/kT} \right) / \rho . \tag{9.30}$$

To be more precise, each $\alpha_i(\nu, n)$ should be evaluated in a slightly different manner. The term values for aluminum energy levels are known experimentally; n values for each of these levels are also known. The degeneracy of the hydrogen function, $2n^2$, should be replaced in Equation 9.22. The cross section from each experimentally determined level, l, with quantum number n becomes

$$\alpha(\nu, n)_l = g \left(64 \pi^2 e^2 R_e Z_{eff_l}^4 \right) / \left(3^{3/2} h^3 \nu^3 n^3 g_l \right) \tag{9.31}$$

where g_l is the degeneracy of the level and Z_{eff_l} is the effective Z for that g_l degenerate level. The cross section $\alpha(\nu, n)$ is then obtained by summing over all l levels having the same n

$$\alpha(\nu, n) = \frac{g(64 \pi^2 e^2 R_e)}{(3^{3/2} h^3 \nu^3 n^3)} \sum_l \left(Z_{eff}^4 / g_l \right) . \tag{9.32}$$

For further details of the hydrogen photoionization coefficient, reference is made to the appendix.

6. Free-Free Absorption

E. R. Mustel's (1956) approximation for the free-free absorption coefficient was used

$$k_{ff} = \frac{C_o (z_i^*)^2 C_e (kT)}{T^{3/2} \nu^3} \left(1 - e^{-h\nu/kT}\right) g'' , \tag{9.33}$$

where

$$C_o = \frac{2^4 \pi \varepsilon^6}{3^{3/2} c h} \cdot \frac{1}{(2\pi m k)^{3/2}} = 2.67 \times 10^{24} , \tag{9.34}$$

$$g'' = 1 + .1728 \left(\frac{\nu}{R(z^*)^2}\right)\left(1 - \frac{2kT}{h\nu}\right) , \tag{9.35}$$

and C_e is the electron density, k is the Boltzman's constant and c is the speed of light and Z* is the average core charge. The mass absorption coefficient, k_ν, is obtained by adding both components

$$k_\nu = \overline{k_\nu^*} + k_{ff} , \tag{9.36}$$

where $\overline{k^*}$ is defined by 9.30 and k_{ff} by 9.33.

7. Numerical Method and Results of Calculation

Prior to obtaining the solution of the flow problem, fortran was written to calculate the emitted continuous spectra. The programs are designed to evaluate the radiation in the range from 50 Å to 8000 Å was accomplished by calculating the emitted radiation intensity at 50Å

and at 100 Å intervals over the entire range of wavelengths. The total integrated emitted radiation is obtained by using Simpson's rule over the entire frequency interval. Increments in the integral evaluations were 50 Å and 100 Å.

The method, as outlined, required that monochromatic absorption coefficients be determined for each wavelength over the entire density and temperature range. Using the table of experimentally determined energy levels (including the level degeneracies, n values and term values) and the tabular equation of state, monochromatic absorption coefficients were calculated. The number of atoms, or ions, in each energy level, C_{i_n}, was assumed to be given by a Boltzman distribution

$$C_{i_n} = \frac{C_i \, g_{i_n} \, e^{-E_{i_n}/(kT)}}{Z_i^{el}} \tag{9.37}$$

where g_{i_n} is the degeneracy of the level, C_i is the total number density of that species, Z_i^{el} is the electronic partition (corresponding to a particular I_{eff}) and E_{i_n} is the energy of the particular level. For each given ρ and T, the k_ν were evaluated by the method outlined in the previous section. All output values from the computer program for the equation of state were used in building the k_ν table.

Fortran code was written to evaluate Equation 9.15 by Simpson's rule, using the generated profiles of ρ and T and the table of k_ν values. The program was tested by the use of the profiles generated by Ables (1963).

When the spectra routines were incorporated into the main flow program, the machine core storage was exceeded. The choice, at this point

was either to reduce the k_ν table to average $\bar{k}$ values or to write a separate program to use the flow profiles as input. Insufficient machine time was available to run separate programs. The use of average absorption coefficients proved entirely unsatisfactory since density and temperature effects were lost. When the uncertainties in the absorption coefficient and the character of the flow solution were evaluated, it was decided to suspend the spectra calculation for a simpler method.

Examination of the density and temperature profiles make it apparent that the simplified spectra solution equation, Equation 9.18, is a reasonable approximation for the emitted radiation from the core since the inner core is of almost uniform density and temperature. The absorption of the outer layers about the central core is governed by

$$\frac{dI}{dx} = -k_\nu \rho \,, \tag{9.38}$$

or the observed spectra along any line is given by

$$I_r = I_{o_r} e^{-\int_0^{x_o} k_\nu \rho \, dx} \,, \tag{9.39}$$

where I_{o_r} is the emitted intensity of the core at the distance r from the center of the disc, Figure 9.2, and the internal 0 to X_o is the thickness of the cold density front along the observation line, i.e. along line AB in Figure 9.2. This approximation appears to be as reliable for an indication of the spectra as the more rigorous evaluation.

8. Summary

The uncertainty in the thermodynamic properties of the outer density shell make a rigorous spectra calculation unjustified at this time.

Until these properties are determined with greater accuracy, the approximation suggested in the preceeding section appears best. A discussion of the qualitative results is given in the next chapter. Suggestions for improvement in the method also appear in Chapter X.

CHAPTER X

SUMMARY, CONCLUSIONS AND RECOMMENDATIONS

This thesis presents, in considerable detail, advances and improvements in the theory and application of plasmas that may be grouped under three headings. (1) An improved equation of state is obtained for aluminum over a wide range of densities, pressures and temperatures. Numerical values for the Equation are tabulated. (2) Under the assumption of thermodynamic equilibrium, density and temperature profiles were obtained in order to follow the spherical expansion of a highly compressed plasma into a vacuum. (3) A technique and equations for calculating the continuum emission spectrum during the expansion of the plasma have been assembled and derived. Experience on an I. B. M. 7094 has indicated approximations which are necessary in order to make the numerical calculations without the lapping of programs on the I. B. M. 7094. Qualitative evaluation of the calculations are awaiting completion of programmed experiments by other members of the group who are working on this program.

Comparison of the results of the computations with the reported phenomena for exploding wires gives a reasonably good qualitative agreement. W. Müller (1957) obtained photographs which show that exploding wires expand as hollow-cylinders. G. L. Clark et al (1962) confirmed that in the case of a long dwell time, the vapor cloud expands in the form of a hollow cylinder. The density profiles in this thesis are in

agreement with this experimental evidence. Further confirmation of the validity of the model is obtained from strip photographs of exploding wires. Photographs by Francis Webb et al (1962) confirm that the highest intensity flashes occur with restrike phenomena. The model of this thesis corresponds to an exploding wire without restrike. Webb reports that streak photographs show that the emitted light decreases with time to a very low intensity. The extreme limb darkening that is observed on these photographs indicates that a hot interior is formed which is surrounded by a cold outer shell. This is, of course, the precise character of the calculated results.

Recommendations for Future Improvements

While qualitative comparisons are good, there are some uncertainties in the results. In particular, there are two major errors that may be very important. These raise significant questions which concern the behavior of the cold plasma at high density in the shell that forms around the hot core. First, without doubt, the equation of state is invalid for the densities and temperatures that occur in the shell. Second, an energy transfer mechanism has been omitted in the exploding plasma calculation. This mechanism is the energy transfer that is associated with plasma oscillations. These deficiencies suggest only two of the several ways in which the model may be improved. Future improvements should at least include consideration of improvements in the following areas:

A. Equation of State

1. Add three-body interactions to the cluster integrals.
2. Include quantum corrections for high density plasmas

3. Improve the plasma oscillation energy component

B. Flow Solution

1. Add plasma oscillation energy transfer mechanism

2. Improve the transport coefficients

C. Spectra

1. Improve the approximation of the photoionization cross-sections.

These suggestions will improve the accuracy of the calculation and are expected to result in better correlation between the analytical results and the proposed laboratory experiments. Likewise, the spectra calculation would be performed with greater accuracy and reliability.

Conclusion

A reasonable method has been suggested for calculating the gross properties of an exploding plasma sphere. While the model shows good qualitative agreement, the data herein should be considered no better than a crude approximation of the solution of the real problem. This thesis does, however, present a considerably more accurate solution over a wider range of pressures and temperatures than has been attempted by anyone else in the published literature.

SELECTED BIBLIOGRAPHY

Ables, J. G. "A Computer Solution for a Spherically Exploding Plasma." (Unpublished M. S. Thesis, Oklahoma State University, 1963.)

Alexander, W. M. Private Communication. 1962.

Aller, L. H. Astrophysics, Vol. I, The Atmospheres of the Sun and Stars. Philadelphia: Ronald Press, 1953.

Bohm, D. and E. P. Gross. Phys. Rev. Vol. 75. (1949) 1864.

Brout, R. and P. Caruthers. Lectures on the Many-Electron Problem. New York: Interscience Publishers, 1963.

Bruce, R. and F. C. Todd. Proc. of the Okla. Acad. of Sci. for 1963. Vol. 44 (1964). 94.

Charters, A. C. Scientific America. Vol. 203. (October, 1960) 128.

Clark, G. L., J. J. Hickey, R. J. Kingsley and R. F. Wuerker. "Exploding-Wire-Driven Shock Waves." Exploding Wires. Vol. 2, Ed. W. G. Chance and H. K. Moore. New York: Plenum Press, 1962.

Conrant, R. and K. O. Friedricks. Supersonic Flow and Shock Waves. New York: Interscience Publishers, 1948.

Debye, P. and H. Hückel. Physik. Vol. 24. (1923) 185.

Ditchburn, R. W. and U. Öpik. "Photoionization Processes." Atomic and Molecular Processes. Ed. D. R. Bates. New York: Academic Press, 1962.

Dittmer, A. F. Phys. Rev. Vol. 28. (1926) 507.

Drummond, J. E. Plasma Physics. New York: McGraw-Hill Book Company, Inc., 1961.

Duclos, D. P. and A. B. Cambel. "Equation of State of an Ionized Gas." Prog. in Intern. Research on Thermodynamic and Transport Properties. New York: Academic Press, 1962.

Ecker, G. and W. Kröll. Physics of Fluids. Vol. 6. (1963) 62.

Ecker, G. and W. Weitzel. Ann. Physik. Vol. 117. (1956) 126.

Fowler, R. H. Statistical Mechanics. London: Cambridge University Press, 1936.

Fowler, R. H. and E. A. Guggenheim. Statistical Thermodynamics. London: Cambridge University Press, 1956.

Friedman, H. L. Ionic Solution Theory. New York: Interscience Publishers, 1962.

Gabor, D. Proc. Roy. Soc. (London). Vol. A213. (1952) 73.

Huang, K. Statistical Mechanics. New York: McGraw-Hill Book Company, Inc., 1963.

Hulthen, L. and K. V. Laurikainen, Rev. of Mod. Phys. Vol. 23. (1951) 1.

Kahn, B. and G. E. Uhlenbeck. Physica. Vol. 5. (1938) 399.

Kelly, D. "Structure of Spectral Lines from Plasma." H. Margenau and M. Lewis. Rev. Mod. Phys. Vol. 31. (1959) 596.

Kunth, E. L. Physics of Fluids. Vol. 2. (1959) 339.

Lake, H. R. "Digital Computer Solution for Propagation of a Spherical Shock Wave in Aluminum." (Unpublished M. S. Thesis, Oklahoma State University, 1962.)

Landau, L. J. Phys. (U.S.S.R.). Vol. 10. (1946) 25.

Landau, L. D. and E. M. Lifshitz. Statistical Physics. Reading, Mass.: Addison Publishing Co. Inc., 1959.

Larine, S. and H. E. Wrigley. Discussions Faraday Soc. Vol. 24. (1957) 43.

Liboff, R. L. Physics of Fluids. Vol. 2. (1959) 40.

Mayer, J. E. J. Chem. Physics. Vol. 18. (1950) 1426.

Mayer, J. E. and M. G. Mayer. Statistical Mechanics. New York: John Wiley and Sons, 1940.

McDongall, J. and E. C. Stoner. Philosophical Transactions of the Royal Society of London. Vol. 237. (1939) 67.

Meeron, E. J. Chem. Phys. Vol. 26. (1957) 804.

Menzel, D. H. and C. L. Pekeris. Monthly Not. Roy. Astron. Soc. Vol. 96. (1935) 77.

Milne, W. E. Numerical Solution of Differential Equation. New York: John Wiley and Sons, 1953.

Müller, W. Z. Physik. Vol. 149. (1957) 397.

Mustel, E. R. "Part I." Theoretical Astrophysics. Ed. V. A. Ambartsumyan. New York: Pergamon Press, 1956.

Pai, Shih-I. Magnetogdynamics and Plasma Dynamics. Vienna: Springer-Verlag, 1962.

Poirier, J. C. J. Chem. Phys. Vol. 89. (1952) 641.

Richtmyer, R. D. Difference Methods of Initial-Value Problems. New York: Interscience Publisher, 1957.

Riordan, J. Introduction to Combinatorial Analysis. New York: John Wiley and Sons, 1958.

Robinson, R. A. and R. H. Stokes. Electrolytic Solutions. New York: Academic Press Inc., 1955.

Roseland, S. Theoretical Astrophysics. Oxford: Clarendon Press, 1936.

Ronse, C. A. Astrophysical J. Vol. 135. (1962) 599.

Rouse, C. A. Astrophysical J. Vol. 136. (1963) 636.

Samaras, D. G. Theory of Ion-Flow Dynamics. Englewood Cliffs, New Jersey: Prentice-Hall, Inc., 1962.

Scarborough, J. B. Numerical Mathematical Analysis, 2nd ed. Baltimore: John Hopkins Press, 1950.

Schwarzschild, M. Structure and Evolution of the Stars. Princeton: Princeton University Press, 1958.

Sodek, Benard. Private communication. (1965)

Stoner, E. C. Philosophical Magazine. Vol. 28. (September, 1939) 257.

Tonks, L. and J. Langmuir. Phys. Rev. Vol. 33. (1929) 990.

Webb, Francis H., P. H. Levine, H. H. Helton and A. V. Tollestrup. "The Electrical and Optical Properties of Rapidly Exploded Wires. Exploding Wires. Vol. 2. Ed. W. G. Chance and H. K. Moore. New York: Plenum Press, 1962.

Williams, F. A. American Journal of Physics. Vol. 26. (1958) 467-469.

APPENDIX I

SET NOTATION

Let N specify the set of all particles of the system (at present we are considering a one component system). Let m specify any subset of the particles of the system; i.e., any collection of part of the system from 1 particle to N particles. To specify m as a subset of N one writes

$$m \leq N \, , \tag{A1.1}$$

In a similar manner $\{N\}$ represents the set of all coordinates of the N particles and if $\{m\}$ is a subset of the coordinate set, then one writes

$$\{m\} \subseteq \{N\} \, ; \tag{A1.2}$$

$\{m\}$ is the set of coordinates for m of the N particles. Note that for each particle, there are three coordinates. If m = 3 then

$$\{m\} = \{\{x_1, y_1, z_1\}; \{x_2, y_2, z_2\}; \{x_3, y_3, z_3\}\}$$

and the coordinates for these three particles are contained in the set $\{N\}$.

Multicomponent Notation - Composition Set:

$\underline{N}$ is called the composition set. It is an ordered set of numerals, each numeral representing the number of particles of a particular species in the total system. For example, a system containing σ species has a coordinate set, $\underline{N}$, with σ elements, i.e.,

$$\underline{N} = n_1, \, n_2, \, n_3, \ldots\ldots\ldots\ldots, \, n_\sigma \, . \tag{A1.3}$$

where n_1 = number of particles of species 1 in the system, n_2 = number of particles of the 2 species in the system, etc. N (not $\underline{N}$) is the total number of particles in the system:

$$N = n_1 + n_2 + n_3 + \ldots\ldots\ldots + n \, . \tag{A1.4}$$

A subset of the composition set is represented by $\underline{m}$ and is indicated by

$$\underline{m} \leq \underline{N} \ , \tag{A1.5}$$

This means that the elements of $\underline{m}$ are made up of parts of $\underline{N}$. As an example, if $\underline{m}$ is a subset of the σ component system which is represented by $\underline{N}$, written $\underline{m} \leq \underline{N}$ then the elements of $\underline{m}$,

$$\underline{m} = m_1, m_2, m_3, \ldots\ldots\ldots\ldots, m_\sigma, \tag{A1.6}$$

are related to the elements of $\underline{N}$ by

$$m_1 \leq n_1, m_2 \leq n_2, \ldots\ldots\ldots\ldots, m_\sigma \leq n_\sigma \ . \tag{A1.7}$$

Similar to equation A1.4,

$$m = m_1 + m_2 + m_3 + \ldots\ldots\ldots + m \ , \tag{A1.8}$$

where m (not $\underline{m}$) is the total number of particles in the subset.

Coordinate Set: $\{\underline{N}\}$

In a manner similar to the above, the coordinate set $\{\underline{N}\}$ of a multicomponent system is the ordered collection of all coordinates of all particles in the system. The elements of the set are the 3N coordinates of the particles in the system, i.e.

$$\{\underline{N}\} = \{x_1, y_1, z_1\}; \{x_2, y_2, z_2\}; \ldots; \{x_{n_1}, y_{n_1}, z_{n_1}\}; \ldots; \{x_{n_\sigma}, y_{n_\sigma}, z_{n_\sigma}\} \ , \tag{A1.9}$$

where the notation x_{i_j} stands for the x component of the jth particle of the i^{th} species.

More briefly this set is written as

$$\{\underline{N}\} = \{1\}; \{2\}; \ldots; \{n_1\}; \{1_2\}; \ldots; \{n_\sigma\} \ , \tag{A1.10}$$

where m_s stands for the 3 coordinates of the m^{th} particle of the s^{th}

species.

Coordinate Subset: $\{\underline{m}\}$

$\{\underline{m}\}$ represents a subset of the coordinate set and is indicated by

$$\{\underline{m}\} \subseteq \{\underline{N}\} . \tag{A1.11}$$

The elements of $\{\underline{m}\}$ are made up of elements of $\{\underline{N}\}$. If the relation

$$\{\underline{m}\} \subseteq \{\underline{N}\}$$

exists between the coordinates sets $\{\underline{m}\}$ and $\{\underline{N}\}$ then $\underline{m} \leq \underline{N}$ specifies the relation between their corresponding composition sets. It should be noted that the above subsets may consist of the entire system.

Other Set Notation

It is apparent that the preceding notation is a more efficient way of representing complicated systems which would be laborous to write out in detail. There are several other set symbols that are used to conserve labor and space.

Concentration Set $\underline{C}$:

If $C_s = n_s/V$, the number density of the s^{th} species, then the concentration set is defined by

$$\underline{C} = n_1/V, n_2/V, \cdots, n_\sigma/V, \tag{A1.13a}$$

or

$$\underline{C} = C_1, C_2, \cdots, C_\sigma . \tag{A1.13b}$$

The elements of the concentration set are the number densities of the various species. (Note in all of the above sets, zero is an allowed element.) It is obvious that the total concentration C, (not $\underline{C}$) is given by

$$C = C_1 + C_2 + \cdots + C_\sigma \,. \qquad \text{(A1.14)}$$

Chemical Potential Set $\underline{\mu}$:

The elements of are the chemical potentials of each of the species, i.e.

$$\underline{\mu} = \mu_1, \mu_2, \cdots, \mu_\sigma \,. \qquad \text{(A1.15)}$$

Other Definitions:

$\underline{n}! = (n_1!)(n_2!)\cdots(n_\sigma!)$; (Product of factionals of elements of $\underline{n}$);

$\underline{C}^{\underline{n}} = C_1^{n_1} C_2^{n_2} \cdots C_\sigma^{n_\sigma}$; (Product of elements of c, each raised to power of corresponding elements of composition set);

$$\underline{\mu} \cdot \underline{n} = \underline{n} \cdot \underline{\mu} = n_1\mu_1 + n_2\mu_2 + \cdots + n_\sigma\mu_\sigma \,,$$

and

$$\underline{C}^{\underline{m}+\underline{n}} = \underline{C}^{\underline{m}} \cdot \underline{C}^{\underline{n}} = C_1^{n_1} C_2^{n_2} \cdots C_\sigma^{n_\sigma} C_1^{m_1} \cdots C_\sigma^{m_\sigma} \,.$$

Notation:

$f(\underline{n})$ = function which is dependent upon the composition set, i.e., upon the n particles of which n_1 are of species one, n_2 of species two, etc. In other words, the function may not only depend upon the total number of particles but also upon their distribution by species.

$\sum f(\underline{n})$ = sum of $f(\underline{n})$, as defined above, over all of the composition for which $n \geq 0$. (n = total number of particles in $\underline{n}$).

$\sum' f(\underline{n})$ = as above, except $n \geq 1$.

$\sum''$ f(n) = as above except $n \geq 2$. Note in these, the sum is generally over all possible subsets for each n; i.e., if there are 4 different species and n = 2, then there are 10 different terms.

$f(\{m\})$ = function dependent upon the 3m different coordinates of the m particles. The function may also be dependent upon the species involved.

$\sum_{\underline{m} \leq \underline{n}} f(\underline{m})$ = sum over all possible subsets $\underline{m}$ of the set $\underline{n}$ as m goes from 0 to n.

$\sum_{\{\underline{m}\} \subseteq \{\underline{n}\}} f(\{\underline{m}\})$ = same as above, except concerns coordinate subsets.

Binomial Expression $\left(\frac{a}{b}\right)$:

The binomial expression $\left(\frac{a}{b}\right)$ is defined by

$$\left(\frac{\underline{a}}{\underline{b}}\right) = \prod_{s=1}^{\sigma} \binom{a_s}{b_s} = \prod_{s=1}^{\sigma} \frac{a_s!}{b_s!(a_s - b_s)!} \quad . \tag{A1.16}$$

Examples

$$\int f(\{\underline{m}\})\, d\{\underline{m}\} = \int \cdots \int f(x_1, y_1, z_1, \ldots, x_{\sigma_n}, y_{\sigma_n}, z_{\sigma_n})\, dx_1 \cdots dz_{\sigma_n} \quad . \tag{A1.17}$$

In A1.17 the integrand is dependent upon 3n coordinates and must be integrated for 3n different coordinates (unless otherwise noted, the integral is over the entire space).

Partitions

Consider the coordinate set $\{\underline{n}\}$ as being composed of three disjoint sets:

$$\{\underline{n}\} = \{\underline{a}\} + \{\underline{b}\} + \{\underline{c}\} \quad . \tag{A1.18}$$

The inverse, splitting $\{\underline{n}\}$ into the three disjoint sets, is a partition of the set $\{\underline{n}\}$.

For present purposes, one may consider a partition of the set $\{\underline{n}\}$ as any splitting of $\{\underline{n}\}$ into disjoint sets. One may define the "partitian set" as the set of numerals, zero or one, which designates the absence or presence of a particular subset in the partition. As an example, the partition set for A1.18 would be

$$P = 1_{\{a\}}, 1_{\{b\}}, 1_{\{c\}}, 0_{\{d\}}, \ldots 0_{\{m\}}. \qquad \text{(A1.19)}$$

Each partition set defines a particular partition. In Appendix II a partition set for a coordinate set is written

$$P\,]\{n\}$$

and one of its elements would be noted by $P_{\{k\}}$

A partition set for the composition set differs somewhat from the above. It is possible that the three coordinate subsets in A1.18 might represent identical composition subsets. With this possibility in mind, it is apparent that the elements of the partition set (of the composition set $\underline{n}$), written

$$P\,]\,\underline{n}$$

will be the number of times the particular composition subset appears in the partition.

In general

$$\underline{n} = \sum_i \underline{n}_i \; ; \qquad \text{(A1.20)}$$

the total composition is the sum of the subset compositions. The elements of the partition set,

$$P = P_{n_1}, P_{n_2}, \ldots \qquad \text{(A1.21)}$$

indicates the number of times that the composition subset $\underline{n}_i$ appears in the partition: i.e., $P_{\underline{n}_i}$ may be any positive integer including zero. As a result

$$\sum_{\underline{n}_i \leq \underline{n}} \underline{n}_i P_{\underline{n}_i} = \underline{n} \quad , \tag{A1.22}$$

where the product $\underline{m}\ p_{\underline{m}}$ is defined by

$$\underline{m} P_{\underline{m}} = \underline{m} + \underline{m} + m + \cdots \quad , \tag{A1.23}$$

with $p_{\underline{m}}$ terms on right.

If

$$\underline{m} = m_1, m_2, \cdots, m_\sigma \quad , \tag{A1.24}$$

then

$$\underline{m} P_{\underline{m}} = P_{\underline{m}} m_1, P_{\underline{m}} m_2, P_{\underline{m}} m_3, \cdots \tag{A1.25}$$

which is the same as A1.23.

As a matter of notation

$$\sum_{P \rbrack \{\underline{n}\}} \underline{a}_P \quad = \text{sum of } \underline{a}_P \text{ for all partitions of } \{\underline{n}\}$$

and

$$\sum_{P \rbrack \underline{n}} \underline{a}_P \quad = \text{sum of } \underline{a}_P \text{ for all partitions of } \underline{n}.$$

APPENDIX II

CLUSTER THEORY

Cluster theory is a statistical method for obtaining the thermodynamic properties of a system through consideration of the interaction potentials of atoms or molecules composing the system. The process is one of calculating the "configuration integral". From an expansion of the configuration integram, the excess free energy of the system may be obtained directly. By "excess free energy," one means the excess of free energy over that of a perfect gas system. From the excess free energy, the corrections to other equilibrium properties are calculable.

It should be noted that the cluster theory is not exclusively devoted to the calculation of thermodynamic properties. The theory may be used for almost any type of system for which a configuration integral is to be calculated in attempting a solution to the many-body problem. In some cases it has replaced the second quantization method.

In the following section the theory will be applied to a very simple system to illustrate the method. In conclusion, a review is presented of the difficulties that are encountered with the theory and with their solution.

No attempt will be made to completely develop the theory. The most complete development of the theory is found in "Ionic Solutions Theory" by Harold L. Freidman (1962). In fact, this appendix is an incomplete summary of the first 165 pages of this text. The original theory as applied to non-ionic solutions may be found in Mayer and Mayer's text (1940). Mayer's original method for extension to ionic solutions (1950) and Poirier's evaluation (1952) of the cluster integrals are reviewed in Chapter II of the thesis. Very readable discussions of the theory are found in "Statistical Mechanics" by Huang (1963) and "The Many Electron Problems" by Brout and Caruthers (1963).

In the following text, only the general scheme of the development is outlined. In particular, all of the difficult combinational analysis is omitted. Analysis and evaluation of all combinational factors is given in the preceding references.

1. Simple System:

First, a simple one component will be considered. The configuration integral of such a system (N identical particles) is defined by

$$Z(N,V,T) \equiv V^{-N} \int \exp\left[-U(\{N\})/kT\right] d\{N\}, \qquad \text{(A2.1)}$$

where the total potential energy of the system, $U(\{N\})$, is a function of the center of mass corrdinates of the N particles of the system, $\{N\}$. The total potential may be expressed as the sum of the pair interactions between particles:

$$U(\{N\}) = \sum_{pairs} u(r_{ij}) . \qquad \text{(A2.2)}$$

A2.1, using A2.2, is expanded in terms of the cluster function,

$$f_{ij} \equiv \exp\left[-u(r_{ij})/kT\right] - 1 , \qquad \text{(A2.3)}$$

to give

$$V^N Z(N,V,T) = \int d\{N\} \left[1 + \sum_{pairs} f_{ij} + \sum_{trips} (f_{ij} f_{jk} + f_{jk} f_{ik} + f_{ij} f_{ik} + f_{ij} f_{jk} f_{ki}) + \cdots\right]. \qquad \text{(A2.4)}$$

Thus, the original configuration integral is replaced by an infinite sum of integrals. The leading terms of the expansion are easy to evaluate. The first integral is simply

$$\int d\{N\} = V^N ,$$

the second is

$$\int \sum_{pair} f_{ij}\, d\{N\} = \frac{N(N-1)}{2}\, V^{N-2} \int f_{ij}\, d\{i,j\}\ .$$

Some of the integrals are reducible to other forms. As an example, the third term of equation 4 reduces as follows (neglecting combinational factors):

$$\int f_{ij} f_{ij}\, d\{i,j,k\} = \int d\{j\}\left[\int f_{ij}\, d\{i\}\right]\left[\int f_{jk}\, d\{k\}\right]$$

$$= \int d\{j\}\left[\int f_{ij}\, d\{i\}\right]^2 = \left[\int f_{ij}\, d\{i,j\}\right]^2 / V.$$

This is essentially the second term squared, divided by the volume.

To calculate the equilibrium properties, the volume (with a constant concentration of particles) is allowed to become infinite. It is obvious that any term containing a factor V should be neglected (when compared to the other terms of the expansion without the factor). It developes that all integrals for non-ALDC graphs are negligible. When at least two bonds are connected to each vertex in the graph, the graph is not negligible. All other graphs have a factor of at least V^{-1} in the integrals. To illustrate the graph technique, the f-bond is represented by a line between two vertices on a skeleton of N vertices: Figure A1,a. The triple $f_{ij}f_{ik}$ is represented by Figure A1,b. A more complicated combination of bonds is shown in Figure A1,c; it is $f_{ij}f_{jk}f_{kl}f_{il}f_{ik}$. Figure A1,c is an ALDC graph (at least doubly connected). The exception to the rule is the f_2-bond (f_{ij}), Figure A1,a, which is also considered ALDC since its integral does not contain a factor V. Note that Figure A1,c is ALDC on a subset of 4 vertices; not N vertices).

Z(N,V,T) can be expressed in terms of the irreducible cluster integrals (integrals over the ALDC graphs):

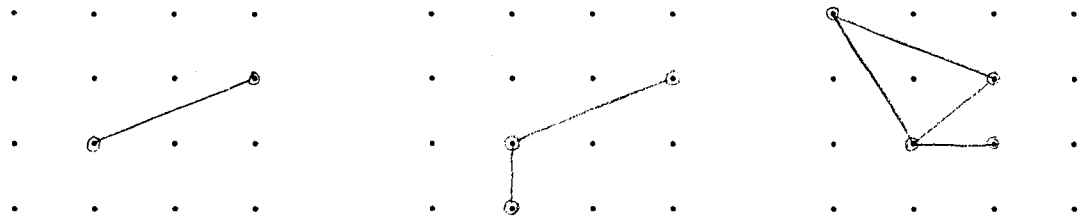

1,a - f_{ij} 1,b - $f_{ij}f_{jk}$ 1,c - $f_{ij}f_{jk}f_{kl}$ $f_{il}f_{ik}$

Figure A.1. Illustrations of several types of fbond graphs on a skeleton of N (16) vertices. There are 16 x 15/2 different ways the f_{ij} bond could be drawn on the skeleton (1a). Graphs 1a and 1c are ALDC graphs on subsets of 2 vertices and 4 vertices respectively.

$$Z(N,V,T) = \sum_{m} \binom{N}{m} V^{-m} \sum_{\tau} A_{m,\tau} I_{m,\tau} \; , \qquad \text{(A2.5)}$$

where the binomial coefficient, $\binom{N}{m}$, is the number of ways one obtains the same graphs, $A_{m,\tau}$ is the combinational factor indicating the number of distinguishable graphs obtained by numbering the verticies and $I_{m,\tau}$ is the specific integral over the graph on m vertices with topology τ.

The term $\binom{N}{m}V^{-m}$ is evaluated to C^m/m in the limit $N\to\infty$. Defining $\sum_{\tau} A_{m,\tau}I_{m,\tau}$ for a specific m as β_m the expansion may be quickly simplified.

For all non-negligible terms of the cluster expansion, the configuration integral may be written as

$$Z(N,V,T) = \exp\left[\sum{}'' C^n \beta_n\right] = 1 + \sum{}'' C^n \beta_n + \left[\sum{}'' C^n \beta_n\right]^2/2 + \cdots \; , \qquad \text{(A2.5)}$$

in which β_n represents a specified integral on a subset of n vertices and c is the concentration: c = N/V. The first three β_n's are:

$$\beta_2 \equiv \frac{1}{2!}\int f_{ij}\, d\{i,j\}\,;$$

$$\beta_3 \equiv \frac{1}{3!}\int f_{ij} f_{jk} f_{ij}\, d\{i,j,k\}$$

$$\beta_4 \equiv \frac{3}{4!}\int f_{ij} f_{jk} f_{kl} f_{il}\, d\{i,j,k,l\} + \frac{6}{4!}\int f_{ij} f_{jk} f_{kl} f_{il} f_{ik}\, d\{i,j,k,l\} + \frac{1}{4!}\int f_{ij} f_{jk} f_{kl} f_{ik} f_{jl}\, d\{i,j,k,l\}. \tag{A2.6}$$

From the relation

$$Z(N,V,T) = \exp\left[-A_{IN}/kT\right], \tag{A2.7}$$

in which A_{in} is the excess free energy of the system, one obtains

$$-F_{IN} = kT\sum{}'' c^n \beta_n, \tag{A2.8}$$

in which F_{in} is the excess free energy per unit volume and B_n is defined by the limit

$$B_n = \lim_{V\to\infty} \beta_n/V. \tag{A2.9}$$

The sum in A2.8 is defined as $\mathcal{G}$:

$$\mathcal{G} = \sum{}'' c^n \beta_n \tag{A2.10}$$

Examination of the preceding equations shows that the important quantity to calculate is B_n. The remainder of this section will be concerned with this calculation.

2. General Difficulties with the Theory:

Three of the major difficulties that arise in the use of cluster integrals should be examined. They may be summarized as follows:

1) Adequacy of the pair potentials to describe the system;

2) Complexities introduced by multicomponent systems;

3) Divergences encountered with coulomb potentials. Each of these difficulties will be considered in the following section.

3. Generalized Potentials - Potentials of Average Force

In this section, the functional dependence of the total potential energy of the systems will be examined. In Section 1 of this Appendix, it was assumed that the potential energy could be expressed as the sum of all pair interactions:

$$U(\{N\}) = \sum_{pairs} u(r_{ij}) . \qquad \text{(A2.11)}$$

In some cases this assumption may not be quite correct.

Consider a closed system of interacting particles, of composition set $\underline{N}$, in the equilibrium state. (The set notation is outlined in Appendix A I.) The potential energy of the system may not only be a function of the 3N centers of mass coordinates but may also be a function of the $3N_i$ internal coordinates of the particles. The probability of such a system is proportional to

$$\exp\left[-U(\{\underline{N}\},\{\underline{N_i}\})/kT\right] ,$$

where the total internal energy, U, is a function of both the center of mass coordinate set, $\{\underline{N}\}$, and the internal coordinate set, $\{\underline{N_i}\}$. The probability of a configuration specified only the the coordinate set may be defined as

$$\exp\left[-U(\{\underline{N}\})/kT\right] = \frac{\int \exp\left[-U(\{\underline{N}\},\{\underline{N_i}\})/kT\right] d\{\underline{N_i}\}}{\int d\{\underline{N_i}\}} . \qquad \text{(A2.12)}$$

This equation also serves as a definition of $U(\{\underline{N}\})$, the direct potential. It is clear from equation A2.12 that the direct potential is not simply the potential energy of the system.

The physical meaning of $U(\{\underline{N}\})$ may be seen by obtaining its negative gradient with respect to the spatial coordinate of a specific particle. The total force on the m^{th} particle is given by

$$\vec{F}_m = -\nabla_m U(\{\underline{N}\}, \{\underline{N}_i\}). \tag{A2.13}$$

Noting that

$$\nabla_m \exp\left[-U(\{\underline{N}\})/kT\right] = \frac{1}{kT} \exp\left[-U(\{\underline{N}\})/kT\right] \nabla_m U(\{\underline{N}\}), \tag{A2.14}$$

differentiation of A2.12 leads to

$$\langle \vec{F}_m \rangle = -\nabla_m U(\{\underline{N}\}) = \frac{\int \vec{F}_m \exp\left[-U(\{\underline{N}\},\{\underline{N}_i\})/kT\right] d\{\underline{N}_i\}}{\int \exp\left[-U(\{\underline{N}\},\{\underline{N}_i\})/kT\right] d\{\underline{N}_i\}}, \tag{A2.15}$$

where $\langle \vec{F}_m \rangle$ is the force on the m^{th} particle, averaged over internal coordinates. Therefore, the potential $U(\{\underline{N}\})$ represents the potential of the average force. It is called alternately the "direct potential," or the "potential of average force."

Kahn and Uhlenbeck (1938) introduced a general expansion of the direct potential :

$$\begin{aligned} U_N(\{\underline{N}\}) &= \sum_{\{\underline{n}\} \le \{\underline{N}\}}'' u_{\underline{n}}(\{\underline{n}\}) \\ &= \sum_{pair} u_{ij}(\{i,j,k\}) + \sum_{trip} u_{ijk}(\{i,j,k\}) + \cdots . \end{aligned} \tag{A2.16}$$

In A2.16, the $u_{\underline{n}}(\{\underline{n}\})$ are called the component potentials. The higher order component potentials, $n > 2$, arise from averaging over internal

coordinates in the definition of $U_{\underline{N}}(\{\underline{N}\})$. The component potentials can be defined by taking the inverse of A2.16:

$$u_{\underline{n}}(\{n\}) = \sum_{\{N\}\subseteq\{n\}} (-1)^{N} U_{\underline{N}}(\{N\})$$

$$= U_{\underline{n}}(\{\underline{n}\}) - \sum_{\{m\}\subseteq\{a\};\, m=1} U_{\underline{n}-\underline{m}}(\{\underline{n}-\underline{m}\}) + \sum_{\{m\}\subseteq\{n\};\, m=2} \cdots , \tag{A2.17}$$

where $U_{\underline{N}}(\{\underline{N}\})$ are the direct potentials.

For n = 2

$$u_{ij}(\{i,j\}) = U_{ij}(\{i,j\}) , \tag{A2.18}$$

and for n = 3

$$u_{ijk}(\{i,j,k\}) = U_{ijk}(\{i,j,k\}) - u_{ij}(\{i,j\}) - u_{jk}(\{j,k\}) - u_{ik}(\{i,k\}). \tag{A2.19}$$

The n=3 component is the difference between the direct potential for the 3 bodies, and the sum of the three pair potentials. The n=4 component potential would be the resultant of the sum of the four-body direct potential and all of the pair potentials minus all of the three body component potentials.

In terms of the component potentials, the cluster function is defined as

$$f_{\underline{m}}(\{m\}) \equiv \exp\left[-u_{\underline{m}}(\{m\})/kT\right] - 1 , \tag{A2.20}$$

where $\{\underline{m}\}$ is a coordinate subject of the coordinate set $\{\underline{N}\}$; $\underline{m}$ is the corresponding composition subset.

Details of the higher order component potentials and of their respective cluster functions will be outlined in the following sections. It should be noted that the $u_{\underline{m}}(\{\underline{m}\})$, m>2., are very short range and have an effect only at very high particle densities. In the remainder

of this chapter, the $f_{\underline{m}}(\{\underline{m}\})$ cluster function will be termed the $f_{\underline{m}}$-bond.

MULTICOMPONENT SYSTEMS

Multicomponent systems require many more terms than simple, one component systems. This is best illustrated by considering the expansion of the system's potential in terms of the cluster function

$$\exp\left[-U(\{N\})/kT\right] = 1 + \sum_{pairs} f_{ij} + \cdots \quad . \tag{A2.21}$$

When the summation over all pairs is made, all possible combinations of particle assignments for i and j occur. Since the f_2-bond represents a pair potential, potentials involving different species for i and j can differ. In other words, if there are 5 different species in the system, the integral $\int \sum_{pairs} f_{ij}\, d\{N\}$, will be replaced by 15 different integrals which reflect the different possible combinations of pairs. Apparently there is no simple anaylic expression that will replace the labor of writing out each separate integral; however, the set notation simplifies the form of equations. The set notation is outlined in Appendix A I. Use will be made of the composition set, $\underline{N}$, and coordinate set, $\{\underline{N}\}$.

$$Z(\underline{N}, V, T) \equiv \int \exp\left[U_{\underline{N}}(\{\underline{N}\})/kT\right] d\{\underline{N}\} \,, \tag{A2.22}$$

in which the set notation indicates that the different species must be considered. The expansion of the potential becomes

$$U_{\underline{N}}(\{\underline{N}\}) = \sum_{\{\underline{m}\} \subseteq \{\underline{N}\}}'' u_{\underline{m}}(\{\underline{m}\}) \,. \tag{A2.23}$$

A word of explanation is necessary. $u_{\underline{m}}(\{m\})$ is the component potential for m particles and is a function of their coordinates. In addition, the set notation $\underline{m}$ indicates that the potential is also a function of the composition of the m particles. The symbol $\sum''_{\{m\}\subseteq\{N\}}$ means that the summation is over all possible coordinate subsets for $m \geq 2$. If m=2, there is one term in the sum for each possible pair of particles. Species of particles must be considered.

The corresponding cluster function is defined by

$$f_{\underline{m}}(\{m\}) \equiv \exp\left[u_{\underline{m}}(\{m\})/kT\right] - 1 . \tag{A2.24}$$

The generalized symbol $f_{\underline{m}}(\{\underline{m}\})$ will be termed the $f_{\underline{m}}$-bond for m particles of compositon $\underline{m}$.

The expansion in terms of the cluster functions becomes

$$\begin{aligned}\exp\left[U_N(\{N\})/kT\right] &= \prod_{\{m\}\subseteq\{N\}} \left[1 + f_{\underline{m}}(\{m\})\right] \\ &= 1 + \sum_{\{i,j\}\subseteq\{N\}} f_{ij}(\{i,j\}) + \sum_{\{i,j,k\}\subseteq\{N\}} \left[f_{ij}f_{jk} + f_{ij}f_{ik} + f_{jk}f_{ik} + f_{ij}f_{jk}f_{ik}\right. \\ &\quad \left. + f_{ijk} + f_{ijk}f_{ij} + \cdots\cdots + f_{ijk}f_{ij}f_{jk}f_{ik}\right] + \cdots .\end{aligned} \tag{A2.25}$$

It is apparent that a substantial problem exists in determining and collecting terms of the expansion. One way to insure that all terms are considered is to use graphical techniques. By this method, each term of the expansion is represented by a graph on an unlabeled skeleton of vertices, as in Figure A.1. The difference between the procedure outlined in Figure A.1 and that which must now be used is the additional terms that are required by the different species involved.

General Procedure - Graphical Techniques:

Each cluster term which is generated by Equation A2.17 may be represented by a unique graph on a skeleton of N vertices. For the purposes of clarity, the f_{ij} bond is represented by a line between two vertices on the graph. Figure A.2a; the f_{ijk}-bond is represented by a hatched area between three vertices, Figure A.2b; the f_{ijkl}-bond is represented by a tetrahedron connecting the vertices i, j, k and l. Because of drafting difficulties, the f_{ijkl}-bond will not be illustrated.

Figure A.3 shows the graphs associated with the m=2, m=3 and some of the m=4 terms. It should be noted that the species occupying the vertices are not specified. There will be one such graph for each different possible combination of species occupying the vertices.

Any graph on a skeleton of k vertices for which all k vertices are not connected together by bonds may be considered as the sums of other graphs on smaller subsets. See Figure A.4 for an illustration. Those graphs, in which all the vertices are connected together by bonds, are called "at least singly connected" (ALSC); i.e., one can go from any vertex to any other of the skeleton along bonds, as in Figure A.4b or A.4f.

To express the configuration integral in terms of graphs, define $s_{\underline{n}}(\{\underline{n}\})$ as the sum of all cluster terms that correspond to ALSC graphs on a skeleton of n, labeled vertices of composition $\underline{n}$. There is one term of $s_{\underline{n}}$ for every possible, distinguishable ALSC graph on the skeleton $\underline{n}$. As an example, for n=3 and $\underline{n} = 1_a, 1_b, 1_c$ (one particle of each species a, b, and c) $s_{\underline{3}}$ would include all graphs shown in Figure A.3 for m=3 with vertices designated by $\underline{n}$. There is one collection of graphs for each distinct composition. The expansion of the potential

A2,a. f_2-bond A2,b. $_3$-bond

Figure A,2. Illustration of graph notation of f_2 and f_3 bonds.

Subset	Graphs	Expansion Term	Comments
m=2		(1) f_{ij}	ALDC
m=3		(3) $f_{ij}f_{jk}$	Not ALDC
		(1) $f_{ij}f_{jk}f_{ik}$	ALDC
		(1) f_{ijk}	Not ALDC
		(3) $f_{ijk}f_{ij}$	Not ALDC
		(3) $f_{ijk}f_{ij}f_{jk}$	ALDC
		(1) $f_{ijk}f_{ij}f_{jk}f_{ik}$	ALDC
m=4		(3) $f_{ij}f_{kl}$	Not ALDC
		(1) $f_{ij}f_{jk}f_{kl}f_{il}$	ALDC
		(6) $f_{ij}f_{jk}f_{kl}f_{il}f_{jl}$	ALDC
		(12) $f_{ijk}f_{kl}$	Not ALDC
		(24) $f_{ijk}f_{jk}f_{kl}f_{il}$	ALDC

Figure A,3. Some of the graphs associated with terms of the expansion in equation A2.25. All terms for m=2 and m=3 are shown. Only a few of the m=4 terms are shown. The numbers in parenthesis are the number of different graphs produced by numbering the vertices.

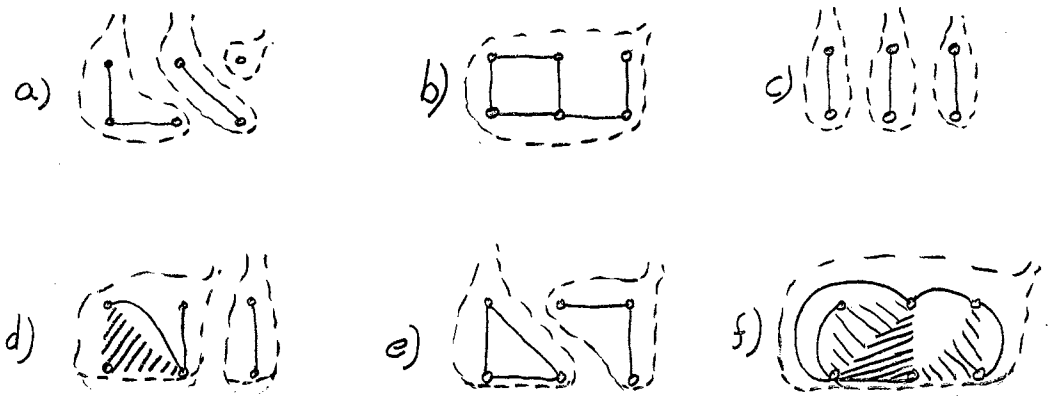

Figure A,4. Some examples of graphs on a skeleton of 6 vertices that are not singly connected. The dotted lines partition the skeleton into reducible clusters: i.e., graphs that are at least singly connected (ALSC). Graphs b and f are ALSC on the skeleton. Nobe b is not ALDC but f is ALDC.

may, consequently, be put in terms of $s_{\underline{n}}$, considering all possible composition subsets. Another way of saying this is that all possible partitions of the coordinate subset must be considered (See Appendix A.1). Consider the expression

$$\exp\left[-U_{\underline{N}}(\{\underline{N}\})/kT\right] = \sum_{p}\prod_{\{\underline{N}\}}\left[s_{\underline{k}}(\{\underline{k}\})\right]^{p_{\{\underline{k}\}}}, \qquad \text{(A2.26)}$$

where the element $p_{\{\underline{k}\}}$ is 0 or 1 depending upon whether or not the graph on $\{\underline{k}\}$ is a cluster of the partition p. Equation A2.26 has the following explanation. The coordinates for the N particles are all labeled. A partition of the coordinates is made and all of the cluster terms which corresponds to that partition are multiplied together. A second partition is made and all the cluster terms $s_{\underline{k}}(\{\underline{k}\})$ contained in that partition are multiplied together. The terms of the second partition are added to the first. Additional partitions add additional terms, each of which is a product of $s_{\underline{k}}(\{\underline{k}\})$ terms. All possible partitions of $\underline{N}$ are made.

The reducible cluster integral is defined as

$$b_k \equiv \left[\frac{1}{V\,\underline{k}!}\right] \int_V s_k(\{\underline{k}\})\, d\{\underline{k}\} \; ; \; b_1 \equiv 1 \; . \qquad \text{(A2.27)}$$

Integration of equation A2.26, over the product of $s_{\underline{k}}(\{\underline{k}\})$ simply leads to the corresponding product of integrals because each factor $s_{\underline{k}}(\{\underline{k}\})$ involves a disjoint subset of $\{N\}$. It is further noted that every partition $\underline{p}] \{\underline{N}\}$ which corresponds to the same partition, $\underline{p}] \underline{N}$, gives the same result upon integration. This is the number of ways of separating N distinguishable objects, of composition $\underline{N}$, into separate collections, each of distinct composition, with no restriction either on the order of the collections or of the objects in the collections. Thus, the partition of the coordinate set can be changed to a partition of the composition set. There will be

$$(\underline{N}!/\underline{p}!) \prod_{\underline{k}<\underline{N}} [\underline{K}!]^{p_{\underline{k}}}$$

identical partitions $\underline{p}]\{\underline{N}\}$ for each partition $\underline{p}] \underline{N}$. (J. Riordan, 1958) As a consequence, integration of A.2.26 yields

$$V^N Z(\underline{N}, V, T) = N! \sum_{\underline{p}] \underline{N}} \prod_{\underline{k}<\underline{N}} \left[V b_{\underline{k}}\right]^{p_{\underline{k}}} / p_{\underline{k}}! \qquad \text{(A2.28}$$

in terms of the partition of the composition set. It is simply the sum of the integral products corresponding to all possible, distinct ALSC graphs on $\{\underline{N}\}$.

As illustrated in the first section, some of the integrals reduce to terms with a factor of V in the denominator. All graphs that are not ALDC are so reducible and may be neglected. Figure A.3 indicates which graphs are ALDC for the m=3.

Since only ALDC graphs produce a result in the calculations, define

$S_{\underline{k}}(\{\underline{k}\})$ = sum of all cluster terms that correspond to ALDC graphs on a skeleton k vertices of composition $\underline{k}$. (A2.29)

Define the "irreducible cluster integral" as

$$B_{\underline{k}} \equiv \left[V \underline{k}!\right]^{-1} \int_V S_{\underline{k}}(\{\underline{k}\})\, d\{\underline{k}\} . \tag{A2.30}$$

Equation A2.28, defining $Z(\underline{N}, V, T)$, can be expressed in terms of $B_{\underline{k}}$. By partitioning the f-bonds, an ALSC graph is decomposed into ALDC graph. Thus one may think of the ALDC graph subsets as forming a covering of the ALSC graph set. In this manner $s_{\underline{n}}(\{\underline{n}\})$ is related to $S_{\underline{k}}(\{\underline{k}\})$ by

$$s_{\underline{n}}(\{\underline{n}\}) = \sum_{t\{\underline{n}\}} \prod_{\{\underline{k}\}\subseteq\{\underline{n}\}} \left[S_{\underline{k}}(\{\underline{k}\})\right]^{t_{\underline{k}}} \tag{A2.31}$$

where $\sum_{t\{\underline{n}\}}$ may be considered the sum of all distinguishable partitions of the f-bonds on the set $\{\underline{n}\}$ that produce ALDC graphs, and the elements $t_{\underline{k}}$ is 0, or 1, depending upon the presence of the particular graph in the partition.

No attempt will be made to carry the derivationfurther. To do so would require considerable space to derive and explain combinational factors that are more adequately explained in standard reference texts. For the complete development of the theory, reference should be made to "Ionic Solution Theory" by H. L. Friedman (1962), or Mayer and Mayer's original text, "Statistical Mechanics" (1940). Somewhat simpler derivation of the art found in "Lectures on the Many-Electron Problem" by R. Brout and P. Carruthers (1963), and "Statistical Mechanics" by Kerson Huang (1963).

Integration of both sides of equation A2.31 leads to a relation between $b_{\underline{k}}$ and $B_{\underline{k}}$ which contains a combinational factor called the tree coefficient. Evaluation of this coefficient is the intricate part of the derivation of the theory. The result is that $\mathcal{G}$ may be expressed rigerously in the limit of infinite volume, as

$$\mathcal{G} = \sum_{\underline{n}}'' \underline{c}^{\underline{n}} B_{\underline{n}} \; , \qquad \text{(A2.32)}$$

which is related to the thermodynamic variables by equation A2.8.

The procedure for determining the thermodynamic properties of a multicomponent system by cluster integrals is summarized below:

1. Make a drawing of all possible ALDC graphs on an unlabeled skeleton. Start with m=2. Continue the process for m=3, m=4, etc.
2. Determine all possible compositions of the vertices for each m.
3. For each different composition, all ALDC graphs for a given $\underline{k}$ correspond to $S_{\underline{k}}(\{\underline{k}\})$.
4. Determine all $S_{\underline{k}}(\{\underline{k}\})$ for k=2.
5. Determine and collect all $S_{\underline{k}}(\{\underline{k}\})$ integrals for k=3.
6. Continue in this manner, collecting terms and evaluating the various B_n's.
7. Use the B_n to determine equilibrium properties. The degree of accuracy of the calculated properties depends upon the number of terms used and upon the ability of the model to adequately describe the system; i.e., the accuracy of the component potentials.

COULOMB POTENTIALS - SIMPLE SYSTEMS

For this section, all particles are considered identical except for + or - charges of equal magnitude. Only Coulomb potentials are considered in the model. If the integral

$$2B_2 = \lim_{V\to\infty} \int_V f_{ij}\, d\{i,j\}/V \tag{A2.33}$$

is evaluated for the Coulomb potential, one obtains

$$2B_2 = \lim_{R\to\infty} \int_0^R \left[e^{-\varepsilon^2/kTr} - 1\right] 4\pi r^2 dr, \tag{A2.34}$$

which by series expansion becomes

$$2B_2 = \sum_{n\geq 1} [-\lambda]^n \lim_{R\to\infty} \int_0^R [4\pi r]^{1-n} r\, dr/n!, \tag{A2.35}$$

where $\lambda = 4\pi\varepsilon^2/kT$. Observation of A2.35 indicates that the integral diverges for $n<4$ as $R\to\infty$. To overcome this difficulty, a different method of collecting terms is necessary. Every f_{ij}-bond is expanded by series expansion into powers of 1/r bonds. This is equivalent to expanding every ALDC graph into an infinite sum of graphs. To obtain convergence, the first term of every expanded B_n, $n>2$, is added to the second term of the B_2 expansion. For purposes of clarity, the 1/r bond is called a g-bond and the sum of the recollected terms (integrals) is called $\mathfrak{S}_c$. $\mathfrak{S}_c$ is the collection of all terms consisting of simple cycles of g-bonds (the most divergent terms).

$$\mathfrak{S}_c = \sum_n {}'' \frac{[-c\lambda]\,[n-1]!}{n!\,2} \int g_{12} g_{23} \cdots g_{n-1,n} g_{n,1}\, d\vec{r}_{12} \cdots d\vec{r}_{1n}, \tag{A2.36}$$

where

$$g_{ij} = \frac{1}{4\pi r_{ij}}. \tag{A2.37}$$

The integral A2.36 is over the infinite volume for 3 (N-1) Cartesian coordinates. By use of the convolution theorum, and Fourier transforms (see "Ionic Solution Theory" Section 12, Chapter III) $\mathcal{G}_c$ is evaluated as

$$\mathcal{G}_c = \varkappa^3/12\pi \tag{A2.38}$$

where

$$\varkappa^3 \equiv \lambda C . \tag{A2.39}$$

Coulomb Potentials - for Multicomponent Systems:

For more general systems, start with

$$\mathcal{G} = \sum_{\underline{m}}{}'' \underline{\zeta}^{\underline{m}} B_{\underline{m}} . \tag{A2.40}$$

One must now rearrange terms of the cluster expansion to obtain modified, irreducible cluster integrals that do not diverge as $V \to \infty$ when Coulomb potentials are present. The ring graphs must be collected and summed separately to obtain convergence. The remainder of the terms are then collected and summed. Prior to this summation, the form of the pair component potential should be examined.

In the general case, both long and short range potentials are present. The Coulomb potential is certainly long range and is given by

$$u_c(\{i,j\}) = -z_i z_j \lambda g(r_{ij}) , \tag{A2.41}$$

where Z_i is a dimensionless charge parameter and (ε is the electronic charge)

$$\lambda = 4\pi\varepsilon^2/DkT ; \tag{A2.42}$$

$$g(r_{ij}) = g_{ij} = [4\pi r_{ij}]^{-1} . \tag{A2.43}$$

D is the dielectric constant (assumed to be 1 in CGS units). The short

range potential is usually indicated by u_{ij}^* in the literature. The most general expression for u_{ij}^* is given by a power series expansion starting with r^{-4} (as determined by Lavine and Wrigley (1957).

$$u_{ij}^*(r_{ij}) = A/r_{ij}^4 + B/r_{ij}^5 + C/r_{ij}^6 + \cdots \qquad \text{(A2.44)}$$

An expansion of this type certainly would include the Leonard-Jones potential,

$$u_{LJ}(r_{ij}) = B_{ij}/r_{ij}^{12} - A_{ij}/r_{ij}^6, \qquad \text{(A2.45)}$$

or any of its modifications. Potentials, including exponential functions which modify the Leonard-Jones potential, are equally well described by A2.44 since the exponential itself is expandable as a power series.

For the present discussion, no specifications are made on u_{ij}^*. All equations will be left in a form adaptable to any short range potential.

To cluster function for the pair potentials is defined by

$$f_{ij}(r_{ij}) = \exp\left[-u_{ij}^*/kT - z_i z_j \lambda g_{ij}\right] - 1 ; \qquad \text{(A2.46)}$$

by defining

$$k_{ij} \equiv \exp\left[u_{ij}^*/kT\right] - 1 \qquad \text{(A2.47)}$$

and expanding the Coulomb potential

$$\exp\left[-z_i z_j \lambda g_{ij}\right] = \sum_{\rho \geq 0} \frac{(-z_i z_j \lambda g_{ij})^\rho}{\rho!}, \qquad \text{(A2.48)}$$

one obtains for the cluster function

$$f_{ij} = k_{ij} + k_{ij}\left[\sum_{\rho} \frac{(-z_i z_j \lambda g_{ij})^\rho}{\rho!}\right] + \left[\sum_{\rho \geq 1} \frac{(-z_i z_j \lambda g_{ij})^\rho}{\rho!}\right]. \qquad \text{(A2.49)}$$

The graph of this expansion of the f_2-bonds is shown in Figure A.5. In order to prevent divergence of the integrals, one regroups the terms of the cluster function expansion,

$$\exp\left[-U_N(\{N\})/kT\right] = \prod_{\{m\}\subseteq\{N\}} \left[1 + f_m(\{m\})\right] \qquad \text{(A2.50)}$$

so that a sum over simple cycles of g-bonds may be made first.

Equation A2.50 is the same as equation A2.25 except that each f_{ij} bond is to be expanded into an infinite number of bonds. The graphs resulting from A2.49 are called expanded graphs.

In order to regroup the terms of the expanded graphs, two definitions seem advisable:

a) g-bonds node ≡ vertex in an expanded graph at a junction of exactly 2 g-bonds.

b) g-bond chain ≡ a sequence of g-bonds connected by g-bond nodes.

The rearrangement is accomplished by noting that equation A2.48 is summed over all possible composition sets. In the expanded graphs, some of the m particles will form g-bond nodes. Let $\underline{n}$ be the subset of $\underline{m}$ that is composed of g-bond nodes and g-bonds for n=2. Then

$$\underline{m} = \underline{n} + \underline{u} \qquad \text{(A2.51)}$$

where $\underline{u}$ is the part of $\underline{m}$ not forming g-bond nodes. Define $\mathcal{G}_l$ = sum over all terms corresponding to 2 vertices connected by 1 g-bond.

$\mathcal{G}_c$ = sum over all terms corresponding to simple cycles of g-bonds, i.e., over the subset $\underline{n}$.

Equation A2.48 becomes

$$\mathcal{G} = \mathcal{G}_l + \mathcal{G}_c + \sum_{\underline{u}}{}'' c^{\underline{u}} B_{\underline{u}} . \qquad \text{(A2.52)}$$

Evaluation of A2.52 results in $\mathcal{G}_\rho \approx \sum z_s c_s = 0$ and $\mathcal{G}_c$ as defined in equation A2.38. Thus

$$\mathcal{G} = \frac{\chi^3}{12\pi} + \sum_{\underline{u}} \underline{c}^{\underline{u}} B_{\underline{u}} \qquad \text{(A2.53)}$$

The first term $x^3/12$ is the Debye-Huckel correction term.

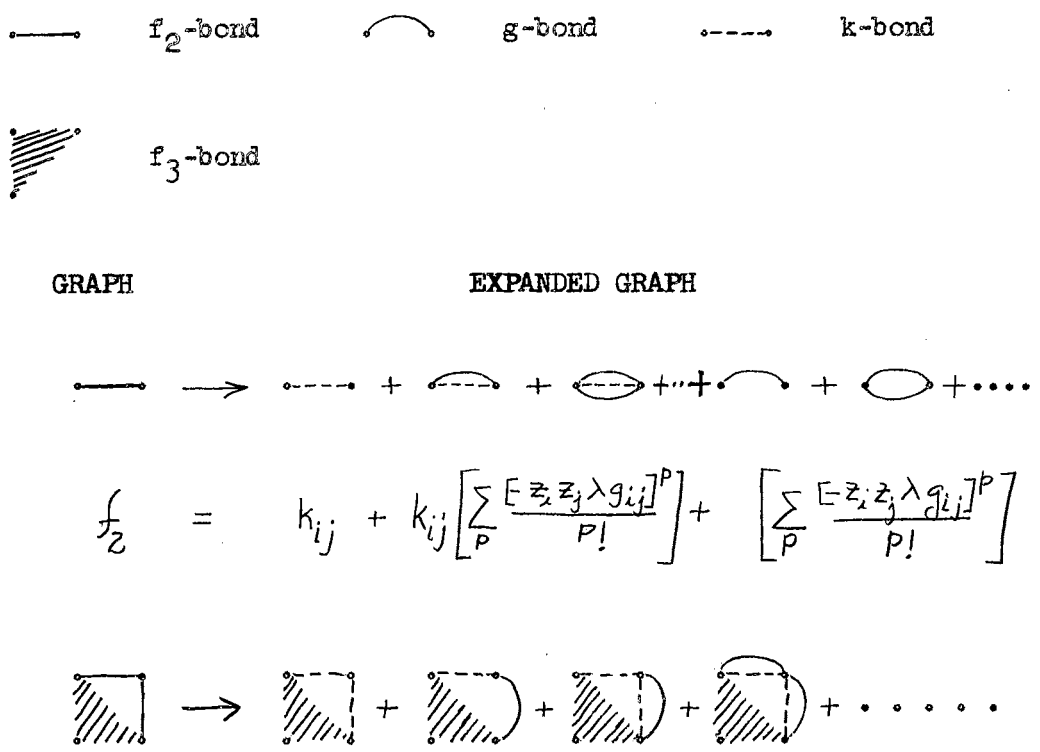

Figure A.5. Expansion of the f_2-bond defined by equation A2.49

7. Summary of development of terms of $\sum_{\underline{u}} \underline{c}^{\underline{u}} B_{\underline{u}}$:

All terms entering $\sum_{\underline{u}} \underline{c}^{\underline{u}} B_{\underline{u}}$ correspond to ALDC graphs, equation A2.30. In evaluating the individual $B_{\underline{u}}$, care must be taken to include all terms produced by the expansion of the f_2-bond. Extensions of the basic graph on u must be made by g-bonds so that all graphs on m will be included. To do this, a careful procedure must be followed.

It is convenient to define

Protograph ≡ a specification of the number and interconnection

of k, f_u and g-bonds on a skeleton $\mathcal{u}$. (One also considers the empty skeleton $\mathcal{u}$ as a protograph.)

Elements of Protograph ≡ number of topologically <u>different</u> graphs obtained by numbering the $\mathcal{u}$ vertices.

Let each protograph be represented by the symbol $\mathcal{T}$ and its elements by $\mathcal{T}_i$. To collect all terms of the sum, the following procedure is followed.

1. Write down the finite number of protographs, $\mathcal{T}$, on the skeleton u for each $u \geq 2$.
2. Determine the elements of each protograph $\mathcal{T}_i$.
3. Assign species to each vertex - i.e., compositon $\underline{\mathcal{u}}$.
4. Add all possible numbers of g-bond chains between pairs of vertices of the protographs. If there are u vertices, there are u(u-1)/2 pairs.

Define $\underline{\mathcal{l}}$ = set of g-bond chains on a particular protograph. The elements of $\underline{\mathcal{l}}$ specify the number and connection of g-bond chains: $\mathcal{l}_j$ = number of g-bond chains between the j^{th} pair.

The set of $\underline{\mathcal{u}}, \mathcal{T}_i, \underline{\mathcal{l}}$ specifies the quantity that Mayer defined as a Prototype. It should be noted in the above that $\underline{\mathcal{l}}$ does not specify the length nor the composition of g-bond chains, only their number and end points; i.e., terminal pairs. There is a restriction on the minimum number of g-bond chains. This results from the requirement that all graphs be ALDC. In general, the smallest $\underline{\mathcal{l}}$ is not $\underline{\mathcal{l}} = \underline{0}$, which only occurs when the protograph is already ALDC. The composition and langth of g-bond chains is specified by the matrix

$$\langle n_s^{(\alpha)} \rangle = \begin{matrix} n_1^1 & n_2^1 & \cdots & n_\sigma^1 \\ n_1^2 & \cdots & \cdots & n_\sigma^2 \\ \cdots & \cdots & \cdots & \cdots \\ n_1^\nu & n_2^\nu & \cdots & n_\sigma^\nu \end{matrix} \quad . \qquad \text{(A2.54)}$$

The rows specify the composition of each of the g-bond chains. The symbol, n_s^α, indicates the number of species, s, in the α-th chain.

The specification of $\underline{u}, \tau_i, \underline{\nu}, \langle n_s^{(\alpha)} \rangle$ and the order of species in each chain designates a particular expanded graph which is a particular term of $B_{\underline{m}}$, $\underline{m} = \underline{n} + \underline{u}$. All expanded graphs which differ only in the order of species in the g-bond chains are the same after integration over $d\{m\}$.

Summary of terms

τ = protograph (type of bonds and number of vertices - no g-bonds).

τ_i = elements of protograph (permutation caused by numbering vertices).

$\underline{\nu}$ = specification of composition of all g-bond chains.

$\langle n_s^{(\alpha)} \rangle$ = specification of number of g-bond chains between each pair of vertices in protograph.

If one specified

a) $\underline{u}, \tau_i, \underline{\nu} \rightarrow$ define a particular prototype;

b) $\underline{u}, \tau_i, \underline{\nu}, \langle n_s^{(\alpha)} \rangle$ define a particular class of graphs;

c) $\underline{u}, \tau_i, \underline{\nu}, \langle n_s^{(\alpha)} \rangle$, order of species in chains $\underline{\nu}$ define expanded graphs which is a particular term of $B_{\underline{m}}$. $B_{\underline{u}}(x)$ may be defined in terms of the collection of graphs:

$$V B_{\underline{u}}(\varkappa) = \sum_{\tau_i} \sum_{\underline{\nu}} \sum_{\langle n_s^{(\alpha)} \rangle} \subseteq^{n} K(\underline{u}, \tau_i, \underline{\nu}, \langle n_s^{(\alpha)} \rangle) I(\underline{u}, \tau_i, \underline{\nu}, \langle n_s^{(\alpha)} \rangle) , \qquad \text{(A2.55)}$$

where $K(\underline{u}, \tau_i, \underline{\nu}, \langle n_s^{(\alpha)} \rangle)$ = combinational factor ;

$I(\underline{u}, \tau_i, \underline{\nu}, \langle n_s^{(\alpha)} \rangle)$ = integral, $\int d\{\underline{n}+\underline{u}\}$ of a specified class of graphs.

The sum over τ_i is essentially two sums:

$$\sum_{\tau_i} = \sum_{\tau} \sum_{\tau_i} ,$$

which means sum over all distinguishable protographs, then over all elements of each. $B_{\underline{u}}$ is replaced by $B_{\underline{u}}(\varkappa)$ because its value is dependent upon the composition of the added g-bond chains.

Fortunately considerable simplification can be made in the calculation of $B_{\underline{u}}(\varkappa)$. Equation A2.55 reduces to a much simpler form. After simplification, one obtains

$$V \underline{u}! B_{\underline{u}}(\varkappa) = \sum_{\tau_i} \sum_{\underline{\nu}} \int_V F_{\tau_i}(\underline{u}) \left[\prod_j (q_{ij})^{\nu_j} / \nu_j! \right] d\{\underline{u}\} , \qquad \text{(A2.56)}$$

in which

$F_{\tau_i}(\underline{u})$ = product of k and $f_{\underline{u}}$-bonds corresponding to the element of the protograph τ ; (A2.57)

and

$$q_j = q_{ab} \equiv -\lambda z_a z_b g(r, V) \qquad \text{(A2.58)}$$

and

$$g(r, V) = e^{-\varkappa r} / 4\pi r \qquad (\varkappa \text{ defined as} = \lambda c) . \qquad \text{(A2.59)}$$

Further simplification can be made by noting that

$$\prod_j e^{q_j} = \sum_{\underline{\nu}} \prod_j q_j^{\nu_j}/\nu_j! \qquad \text{(A2.60)}$$

and evaluating $B_{\underline{u}}(\chi)$ for $u \geq 2$. For u = 2 there are only two protographs; one with a k-bond and one without. There is only one element of each protograph.

$$B_{ab}(\chi) = \left[V\,(a,b)!\right]^{-1} \int_V \left[\sum_\nu q_{ab}^\nu/\nu! + k_{ab}\sum_\nu q_{ab}^\nu/\nu!\right] d\{a,b\}. \qquad \text{(A2.61)}$$

The range of ν in each of the two sums is different. To obtain an ALDC graph, sum over $\nu \geq 3$. (Note that $\nu = 1$ and $\nu = 2$ were already summed over in $\mathfrak{S}_f$ and $\mathfrak{S}_c$.) In the second sum, the ALDC condition is met with $\nu \geq 0$. Therefore

$$B_{ab}(\chi) = \left[V(a,b)!\right]^{-1} \int \left[(1+k_{ab})e^{q_{ab}} - 1 - q_{ab} - q_{ab}^2/2\right] d\{a,b\}, \qquad \text{(A2.62)}$$

or

$$B_{ab}(\chi) = \left[V\,(a,b)!\right]^{-1} \int \Phi_{ab}^{III}\, d\{a,b\}. \qquad \text{(A2.63)}$$

Equation A2.62 defines Φ_{ab}^{III} . It should be noted that (a,b)! is 1 if $a \neq b$, and 2 if a = b.

A similar simplification can be made for $u \geq 3$. It is simpler to define the results of the simplification in terms of ϕ -bonds:

$$\Phi_{ab} = \left[1 + k_{ab}\right] e^{q_{ab}} = \exp\left[-u_{ab}^*/kT - \left(\lambda z_a z_b e^{-\chi r_{ab}}/4\pi r_{ab}\right)\right]; \qquad \text{(A2.64)}$$

$$\Phi'_{ab} = \Phi_{ab} - 1 \qquad \text{(A2.65)}$$

$$\phi''_{ab} = \phi_{ab} - 1 - q_{ab} \; ; \tag{A2.66}$$

and

$$\phi'''_{ab} = \phi''_{ab} - q^2_{ab}/2 \; . \tag{A2.67}$$

Define

$$B_{\underline{u}}(x) \equiv [\underline{u}!\, V]^{-1} \int_V S_{\underline{u}}(x, \{\underline{u}\})\, d\{\underline{u}\}, \tag{A2.68}$$

where

$S_{\underline{u}}(x,\{\underline{u}\})$ = sum of terms corresponding, one-to-one, to all of the distinguishable graphs on the skeleton $\underline{u}$ that may be formed by q-bonds, ϕ'' bonds, f_3-bonds.....and a $f_{\underline{u}}$-bond subject to the following:

1. Every graph is AKDC on $\underline{u}$,
2. There are no q-bonds nodes,
3. On a given pair of vertices there may be one q-bond or one ϕ''-bond but not both. On any m vertices, there may be at most one f_m-bond.

A systematic way to specify the graphs that enter into the definition of the terms of $S_{\underline{u}}(x,\{\underline{u}\})$ is the following ($u > 2$).

1. Form all distinguishable configurations of f_3, f_4....f_u-bonds on a skeleton of u unlabeled vertices beginning with the empty skeleton itself.
2. In each graph produced by (1), every pair of vertices that is at least doubly connected by edges of f_m-bonds must now be connected by a ϕ-bond.
3. Every pair of vertices which remains without a direct connection may be either left this way, connected by a q-bond, or connected by a ϕ''-bond.

Every ALDC graph on u unlabeled vertices by the above procedure is called a "Kappagraph." The group of elements of a kappagraph is the collection of distinguishable graphs that are formed by numbering the vertices. The terms of $S_{\underline{u}}(x,\{\underline{u}\})$ are obtained by assigning species of the composition set, $\underline{u}$, to the numbered vertices of the elements of the kappagraphs on u.

With this method for obtaining $S_{\underline{u}}(x,\{\underline{u}\})$ the integral

$$B_{\underline{u}}(x) = [\underline{u}!v]^{-1} \int S_{\underline{u}}(x,\{\underline{u}\})\, d\{\underline{u}\} \qquad \text{(A2.69)}$$

may be evaluated and, consequently,

$$G = \frac{x^3}{12\pi} + \sum_{\underline{u}}'' c^{\underline{u}}\, B_{\underline{u}}(x) \qquad \text{(A2.70)}$$

is evaluated.

APPENDIX III

THE CONTINUOUS ABSORPTION COEFFICIENTS FOR HYDROGEN

The absorption coefficient for hydrogen-like-atoms can be computed rather accurately. If the atom in an excited level n, absorbs a quantum of energy, $h\nu$,

$$|h\nu| > |\chi_e - E_n| \tag{A3.1}$$

(where χ_e is the ionization potential and E_n is the excitationenergy of the level n), the photoejected electron will have momentum given by Einstein's equation,

$$\frac{1}{2} m_e v^2 + \frac{hR}{n^2} = h\nu , \tag{A3.2}$$

(where m_e is the mass of the electron, v its velocity and h is Planck's constant) since the energy of the level n is hR/n^2 (referring to the ionized atom as zero). R is Rydberg's constant:

$$R = \frac{2\pi\varepsilon^4 m_e}{h^3} \tag{A3.3}$$

where ε is the charge of the electron.

The Bohr equation for the frequency, ν, absorbed takes the form

$$\nu = RZ^2\left(\frac{1}{n^2} - \frac{1}{(n'')^2}\right), \tag{A3.4}$$

where Z is the atomic number and n'' is a complex number. Menzel and Pekeris (1935) suggested for the continum,

$$n'' = ik , \tag{A3.5}$$

where k is a real but not necessarily integral quantum number and $i = \sqrt{-1}$. With this consideration A3.4 takes the following form,

$$\nu = RZ^2\left(\frac{1}{n^2} + \frac{1}{k^2}\right), \tag{A3.6}$$

and k is defined by means of the relations,

$$hRZ^2/k^2 = m_e v^2/2 , \tag{A3.7a}$$

and its derivative

$$-(2hRz^2/k^3)dk = m_e v dv = h d\nu \quad . \tag{A3.7b}$$

Now one attempts to obtain the expression for the absorption coefficient per atom for the continuum. By virtue of

$$\int \alpha_\nu d\nu = \frac{\pi e^2}{mc} f \quad , \tag{A3.8}$$

where α_ν is the absorption coefficient per atom, c is the velocity of light and f is the oscillator strength (f-number), α_ν may be expressed as

$$\alpha_\nu = \frac{\pi e^2}{mc} \frac{df}{d\nu} \quad . \tag{A3.9}$$

Since the absorption coefficient is continuous over the series limit, the f-number may be defined for unit frequency interval. On the red side of the series limit, there will be Δ n lines of mean oscillator strength, f, for unit frequency interval. Just to the opposite side of the limit, the f-number per unit frequency interval will be $f\Delta k$. Thus

$$df = f dk \tag{A3.10}$$

and

$$\alpha_\nu = \frac{\pi e^2}{mc} \frac{df}{dk} \frac{dk}{d\nu} = \frac{\pi e^2}{mc} f \frac{dk}{d\nu} \quad . \tag{A3.11}$$

Substituting $dk/d\nu$ as defined by A3.7b in A3.11 and dropping the negative sign, the following relation is found

$$\alpha_\nu = \frac{\pi e^2}{mc} f \frac{k^3}{2Rz^2} \quad . \tag{A3.12}$$

The f-number for a given transition in hydrogen may be calculated from

$$f_{nn'} = \frac{Z^6}{3\pi\sqrt{3}} \frac{1}{g_n'} \frac{1}{\left[\left(\frac{1}{n'}\right)^2 - \left(\frac{1}{n}\right)^2\right]^3} \left| \frac{1}{n^3} \cdot \frac{1}{(n')^3} \right| g' \, , \qquad \text{(A3.13)}$$

where g' is the Gaunt correction term, which according to Menzel and Pekeris is given by

$$g' \approx 1 - .1728 \left(\frac{\nu}{RZ^2}\right)^{1/3} \left[\frac{Z}{n^2}\left(\frac{RZ^2}{\nu}\right) - 1\right] ,$$

$g_{n'}$ is the statistical weight of the level, n' (given by $2(n')^2$) and n and n' are the quantum numbers of the levels. For the case where n' = k the oscillator strength f_{nk} is given by

$$f_{nk} = \frac{32}{3\pi\sqrt{3}} \frac{1}{2n^2} \frac{1}{\left[\left(\frac{1}{n}\right)^2 - \left(\frac{1}{k}\right)^2\right]^3} \left| \frac{1}{n^3} \frac{1}{k^3} \right| g' \, , \qquad \text{(A3.14)}$$

which, when substituted into A3.12 along with A3.6 and the definition of R, gives the absorption coefficient per atom in the n^{th} level:

$$\alpha_n(\nu) = \frac{32}{3\sqrt{3}} \frac{\pi^2 \varepsilon^6}{ch^3} \frac{RZ^4}{n^5 \nu^3} g' . \qquad \text{(A3.15)}$$

At the series limit the absorption coefficient is 1.38×10^{-17} cgs units per atom in the second level.

The total absorption coefficient per gram of hydrogen is computed for a particular temperature by summing over all levels that can produce absorption at the particular wavelength. For 4000 Å transitions from the third and higher levels are considered; the first level need not be considered until the wavelength is shorter than 912 Å. The temperature enters the computation of the mass absorption coefficient through the dependence of the distribution of the atoms in their various excitation levels upon temperature. It is assumed that this distribution is given by Boltzmann's law (under the condition of temperature equilibrium):

$$\frac{n_{r,n}}{n_{r,1}} = \frac{g_{r,n}}{g_{r,1}} e^{-E_{rn}/kT} , \qquad \text{(A3.16)}$$

where n_{rn} and n_{r1} are the number of r times ionized atoms in the levels n and 1 (where 1 is the ground state), g_{rn} and g_{r1} are the statistical weights (2J + 1) of each level, E_{rn} is the excitation energy between the two levels, k is Boltzmann's constant and T is the temperature. Figure A.6 shows the dependence of the mass absorption coefficient of hydrogen on temperature and frequency. Notice that between the successive series limits the coefficient falls off as ν^3, rises anew at each series limit and falls off again as ν increases.

Where n is the number of atoms, dh is the thickness, α_ν is the absorption coefficient per atom, then

$$dI_\nu = -I_\nu \alpha_\nu n \, dh . \qquad \text{(A3.17)}$$

Using A3.15 and A3.16, the absorbing effect of atoms at frequency , due to the n^{th} absorption band is:

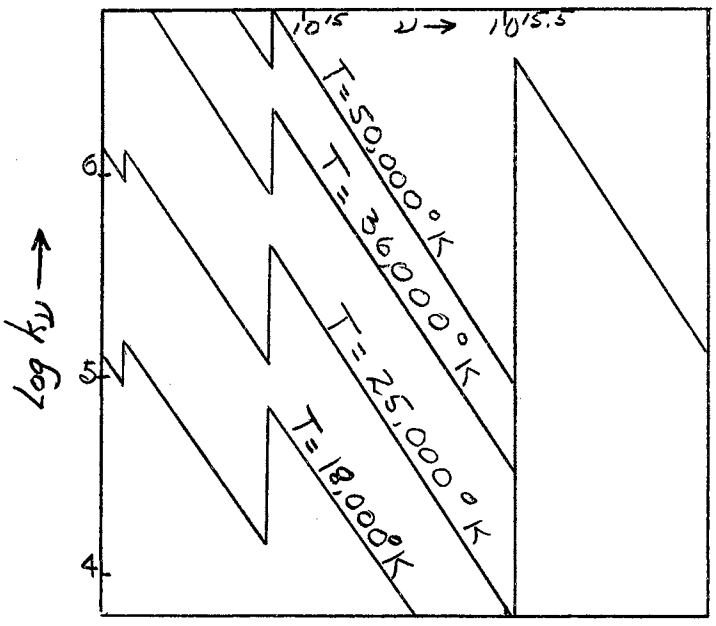

Figure A.6. Atomic Hydrogen's Absorption Coefficient

$$dI_\nu^{(n)} = -I_\nu \alpha_n(\nu)\, n_{rn}\, dh = -I_\nu \frac{32\pi^2 \varepsilon^6 R Z^4 g' n_{r1} g_{rn}}{3\sqrt{3}\, c\, h^3 \nu^3 n^5 g_{r1}} e^{-E_{rn}/kT}. \quad \text{(A3.18)}$$

The total absorption is the summation over n.

$$dI_\nu = \sum_{n=n_o}^{\infty} dI_\nu^{(n)}, \quad \text{(A3.19)}$$

where the sum begins at the first band, which corresponds to n_o, to the violet of ν. The total number of atoms in one cm^3, n_{rn}, must be summed over all quantum numbers n = 1 to n = ∞.

$$n_r = \sum_{n=1}^{\infty} n_{r,n} = \frac{n_{r1}}{g_{r1}} \sum_{n=1}^{\infty} g_{rn} e^{-E_{rn}/kT} = \frac{n_{r1}\, \mathcal{U}_r}{g_{r1}}, \quad \text{(A3.20)}$$

where $\mathcal{U}_r$ is the partition function for r times ionized atoms which is defined by

$$\mathcal{U}_r(T) = \sum_{n=1}^{\infty} g_{rn} e^{-E_{rn}/kT}. \quad \text{(A3.21)}$$

Introducing Saha's ionization equation,

$$\frac{n_{r+1}}{n_r} p_e = \frac{\mathcal{U}_{r+1}}{\mathcal{U}_r} \frac{2(2\pi m)^{3/2}(kT)^{5/2}}{h^3} e^{-\chi_r/kT}, \quad \text{(A3.22)}$$

where k is Boltzmann's constant, m is the mass of the electron, p_e is the partial electron pressure and where n_e is the number of electrons per cm^3,

$$p_e = n_e kT, \quad \text{(A3.23)}$$

one obtains

$$\frac{n_{r1}}{g_{r1}} = \frac{n_{r+1}}{\mathcal{U}_{r+1}(T)} p_e \frac{h^3 e^{\chi_r/kT}}{2(2\pi m)^{3/2}(kT)^{5/2}}. \quad \text{(A3.24)}$$

If A3.24 is put into A3.19 the total absorption is given by

$$dI_\nu = \sum_{n=n_o}^{\infty} dI_\nu^{(n)} = -I_\nu \frac{n_{r+1}}{\mathcal{U}_{r+1}(T)} \frac{2^4 \pi \varepsilon^6 R Z^4 dh}{3\sqrt{3}\, c (2\pi m)^{3/2} \nu^3 (kT)^{5/2}} \sum_{n_o}^{\infty} \frac{g_{rn} g'}{n^5} e^{-\left(E_{rn} - \chi_r\right)/kT}. \quad \text{(A3.25)}$$

For hydrogen-like-atoms

$$E_{rn} = hRz^2\left(1-\frac{1}{n^2}\right) = \chi_r - hRz^2/n^2 \qquad \text{(A3.26)}$$

is valid. Also u_{r+1} is equal to unity since only the nucleus is left and consequently the partition function reduces to one term: the statistical weight of the nucleus. Noting that g_{rn} is $2\,n^2$ for hydrogen type atoms, dI_ν becomes

$$dI_\nu = -I_\nu n_{r+1} Pe \frac{C_o z^2 T^{-3/2}}{\nu^3}\left[\frac{zhRz^2}{kT}\sum_{n=n_o}^{\infty}\frac{g'}{n^3} e^{\frac{hRz^2}{n^2kT}}\right]dh, \qquad \text{(A3.27)}$$

where

$$C_o = \frac{z^4\pi\varepsilon^6}{3\sqrt{3}\,ch}\frac{1}{(2\pi mk)^{3/2}} = 2.67\times10^{24}. \qquad \text{(A3.28)}$$

Unfortunately this expression is incomplete since neither the stimulated emission (negative absorption) nor free-free transitions have been considered. To get the correct coefficient, both must be included. To do this, one equates the stimulated emission coefficient to, the absorption coefficient through the process of detailed balancing and then corrects the results for free-free transmissions.

If there are n_k atoms per cm^3 in quantum state, k, and the number in a lower state "i" is n_i, then the number of transitions per cm^3 per second which produce $h\nu_{ik}$ is

$$n_{k\to i} = n_k\left(A_{ki} + u_{\nu_{ik}} B_{ki}\right), \qquad \text{(A3.29)}$$

where A_{ki} and B_{ki} are Einstein's transmission probability coefficients and $u_{\nu_{ik}}$ is the energy density of the desired frequency, given by

$$u_{\nu_{ij}} = \frac{1}{c}\int I_{\nu_{ij}}\, d\omega. \qquad \text{(A3.30)}$$

$u_{\nu_{ik}} B_{ki}$ corresponds to the stimulated transmissions which take place

under the action of the radiation field of density $u_{\nu_{ik}}$.

The number of converse transmissions, i--k, in one cm^3 per second absorbing $h\nu_{ik}$ is

$$n_{i\to k} = n_i u_{\nu_{ik}} B_{ik} \quad . \tag{A3.31}$$

It is assumed, of course that the radiation density is relatively constant in the neighborhood of ν_{ik}. Between the three transmission coefficients, the following relations hold

$$g_k B_{ki} = g_i B_{ik} \tag{A3.32}$$

and

$$A_{ki} = \frac{8\pi h(\nu_{ik})^3}{c^3} B_{ki} = \frac{8\pi h(\nu_{ik})^3}{c^3} \frac{g_i}{g_k} B_{ik} \quad . \tag{A3.33}$$

The latter may be used to express 3.29 as

$$n_{k\to i} = n_k A_{ki} \left(1 + \frac{c^3}{8\pi h(\nu_{ik})^3} u_{\nu_{ik}}\right) \quad . \tag{A3.34}$$

To modify the previously acquired atomic absorption coefficients, transmission coefficients for the recombination process must be introduced. Let $\alpha_n(\nu)$ be the atomic absorption coefficient corresponding to photoionizations from the n^{th} level for r times ionized atoms. The number of ionizations per cm^3 per second will be given by

$$n_{n\to k}\, d\nu = n_{rn} \alpha_n(\nu) \frac{d\nu}{h\nu} \int I\, d\omega \,, \tag{A3.35}$$

which is just the total energy absorbed divided by the energy absorbed per transmission ($h\nu$). The electron will be in some final state, k, after the transmission which corresponds to an electron of velocity v fixed by equation A3.2.

The converse of the photoionization process may be thought of

as a collision between an ion and an electron. Hence an effective "cross-section" for recombination, denoted by σ_{kn} is introduced. The number of recombinations per cm^3 per second are

$$n'_{k\to n} = n_{r+1}\,\sigma_{kn}\,v\,dn_e \qquad \text{(A3.36)}$$

where dn_e is the number of electrons per cm^3 having velocities in the range v to v + dv, n_{r+1} is the number of completely ionized atoms and dv and $d\nu$ are related by A3.2:

$$v\,dv = (h/m)\,d\nu. \qquad \text{(A3.37)}$$

It is noted that n_e may be expressed in terms of the Maxwellian velocity distribution since thermodynamic equilibrium is assumed:

$$dn_e = n_e 4\pi \left(\frac{m}{2\pi kT}\right)^{3/2} e^{-\frac{mv^2}{2kT}}\, v^2 dv, \qquad \text{(A3.38)}$$

where n_e is the number of electrons per cm^3, m is the mass of the electron and k is Boltzmann's constant.

Expression A3.36, expressing spontaneous recombinations, must be modified to account for the process of stimulated recombination- equation A3.34 - if the medium is in a field of radiation of density u_ν. Modifying A3.34 by A3.36 obtain

$$n_{k\to n}\,d\nu = n_{r+1}\,\sigma_{kn}\,v\left(1+\frac{c^3}{8\pi h\nu^3}u_\nu\right)dn_e \qquad \text{(A3.39)}$$

The coefficient σ_{kn} in A3.39 is related to $\alpha_{n(\nu)}$ in A3.35. By the principle of detailed balancing, which states that for thermodynamic equilibrium a process can take place exactly as often as its converse occurs, A3.39 and A3.35 may be equated (using equation A3.30)

$$n_{rn}\alpha_n(\nu)\frac{c\,d\nu}{h\nu}u_\nu = n_{r+1}\sigma_{kn}\,\nu\left(1+\frac{c^3 u_\nu}{8\pi h\nu^3}\right)dn_e \qquad \text{(A3.40)}$$

Substituting for u_ν,

$$u_\nu = \frac{8\pi h\nu^3}{c^2}\frac{1}{\exp[h\nu/kT]-1}\,, \qquad \text{(A3.41)}$$

since thermodynamic equilibrium is assumed, and for dn_e, defined by A3.38, and noting A3.37, equation A3.40 becomes

$$n_{rn}\alpha_n(\nu)\left(\frac{2\nu^2}{c^2}\right) = n_e n_{r+1}\sigma_{kn}\,e^{\frac{h\nu-m\nu^2/2}{kT}}\left(\frac{m}{2\pi kT}\right)^{3/2}\frac{\nu^2 h}{m}\,. \qquad \text{(A3.42)}$$

Using the fact that the numerator of the exponential term is χ_r and the relation (obtained from A3.16 and A3.20)

$$n_{rn} = n_{r1}\frac{g_{rn}}{g_{r1}}e^{-E_{rn}/kT} = \frac{n_r}{u_r(T)}g_{rn}e^{-E_{rn}/kT}\,, \qquad \text{(A3.45)}$$

equation A3.42 may be written as

$$\frac{n_r}{u_r(T)}g_{rn}e^{-\chi_r/kT}\alpha(\nu) = n_e n_{r+1}\sigma_{kn}\frac{\nu^2 c^2 h}{2m\nu^2}\left(\frac{m}{2\pi kT}\right)^{3/2}. \qquad \text{(A3.44)}$$

Finally, using the relationship between n_r and n_{r+1} as defined by A3.22 and using A3.23, the correspondance between $\alpha(\nu)$ and σ_{kn} is determined:

$$\sigma_{kn} = \frac{g_{rn}}{u_{r+1}(T)}\frac{\nu^2 h^2}{c^2 m^2\nu^2}\alpha(\nu)\,, \qquad \text{(A3.45)}$$

which is further simplified because $u_{r+1} = 1$ for hydrogen-like-atoms.

To obtain the absorption coefficient k_ν the equation of transfer must be considered:

$$\cos\theta\frac{dI_\nu(\theta)}{dh}d\nu d\omega = I_\nu(\theta)k'_\nu\rho\,d\nu d\omega - j_\nu(\theta)\rho\,d\nu d\omega\,, \qquad \text{(A3.46)}$$

where k'_ν indicates an absorption coefficient taking account of only ordinary absorption. To see the dependence of j_ν on Θ, express A3.30 for a pencil beam,

$$(u_{ik})_{d\omega} = I_{\nu ik}(\Theta)\,\frac{d\omega}{c} \qquad \text{(A3.47)}$$

and note that j_ν includes the stimulated emission. In other words j_ν will be a function of the radiation density which is in turn a function of Θ. Using A3.31, rewitten for a pencil beam (using A3.46 and A3.33),

$$(n_{k\to i})_{d\omega} = n_k A_{ki}\left(\frac{1}{4\pi} + \frac{c^3}{(8\pi h\nu_{ij}^3)}\cdot\frac{I_{\nu ik}(\Theta)}{c}\right)d\omega, \qquad \text{(A3.48)}$$

and equation A3.39 one may write

$$j_\nu(\Theta)_\rho\, d\nu\, d\omega = n_{r+1}\sigma_{kn}\nu\left(\frac{1}{4\pi} + \frac{c^3}{8\pi h\nu^3}\cdot\frac{I_\nu\Theta}{c}\right)h\nu\, dn_e\, d\omega, \qquad \text{(A3.49)}$$

since $h\nu$ is emitted in every recombination and only $d\omega/4\pi$ of the total radiation is in the beam $d\omega$. Using A3.22, A3.47 and the definition, $\chi_r - E_{rn} = \chi_{rn}$, the right side of A3.49 is changed to

$$\frac{n_{rn}}{g_{rn}}\cdot\frac{u_{r+1}}{P_e}\cdot e^{\chi_{rn}/kT}\cdot\frac{2(2\pi m)^{3/2}(kT)^{3/2}}{h^2}\,\sigma_{kn}\nu\left(\frac{1}{4\pi} + \frac{c^2 I_\nu(\Theta)}{8\pi h\nu^3}\right)h\nu\, dn_e\, d\omega.$$

Further substitution with equations A3.38, A3.23 and A3.45, followed by use of

$$m\nu\, d\nu = h\, d\nu \quad \text{and} \quad \chi_{rn} + m\nu^2/2 = h\nu$$

yields

$$j_\nu(\Theta)_\rho\, d\nu\, d\omega = n_{rn}e^{-\frac{h\nu}{kT}}\alpha(\nu)\left[\frac{2h\nu}{c^2} + I_\nu(\Theta)\right]d\omega\, d\nu. \qquad \text{(A3.50)}$$

Replacing ah $h\nu^3/c^2$ in A3.50 with its equivalent from Planck's law gives:

$$j_\nu(\Theta)\rho\, d\nu d\omega = n_{rn}\,\alpha(\nu)\left\{\left(1-e^{-h\nu/kT}\right)B_\nu(T) + e^{-\frac{h\nu}{kT}}\, I_\nu(\Theta)\right\} d\omega d\nu. \quad \text{(A3.51)}$$

The form of the absorption coefficient is now shown by introducing equation A3.51 into the equation of transfer, A3.46 where the quantity $k_\nu \rho$ is replaced by $[\alpha(\nu)\, n_{rn}]$:

$$\cos\Theta \frac{dI_\nu(\Theta)}{dh} = n_{rn}\alpha(\nu) I_\nu(\Theta)\left(1-e^{-h\nu/kT}\right) - n_{rn}\alpha(\nu) B_\nu(T)\left(1-e^{-h\nu/kT}\right),$$

$$= n_{rn}\alpha(\nu)\left(1-e^{-h\nu/kT}\right)\left[I_\nu(\Theta) - B_\nu(T)\right]. \quad \text{(A3.52)}$$

By letting

$$k_\nu^* = \left(1-e^{-h\nu/kT}\right)\alpha(\nu), \quad \text{(A3.53)}$$

the equation of transfer becomes

$$\cos\Theta \frac{dI_\nu(\Theta)}{dh} = n_{rn}\, k_\nu^* \left[I_\nu(\Theta) - B_\nu(T)\right], \quad \text{(A3.54)}$$

and introducing the absorption coefficient per unit mass,

$$K_\nu = \frac{n_{rn}}{\rho}\, k_\nu^* = k_\nu^*/m_H, \quad \text{(A3.55)}$$

where m_H is the mass of one hydrogen atom, one obtains the equation of transfer in its original form:

$$\cos\Theta \frac{dI_\nu(\Theta)}{dh} = \rho\, k_\nu \left[I_\nu(\Theta) - B_\nu(T)\right]. \quad \text{(A3.56)}$$

It is clear that when using the equation of transfer, A3.56, the absorption coefficient, which takes into account the stimulated emission only, must be modified by A3.53. It should be noted that A3.53 presupposes thermodynamic equilibrium. Also that the same expression may be obtained by considering only discrete transitions between different quantum orbits of the electron (E. R. Mustel', 1956).

Finally, the absorption coefficient for one (r + 1) times ionized atoms is given by (using A3.53 and A3.27)

$$k_\nu^* = \frac{C_0 Z^2 P_e}{T^{3/2} \nu^3} \left(\frac{2hRZ^2}{kT} \sum_{n_0}^{\infty} \frac{g}{n^3} e^{\frac{hRZ^2}{n^2 kT}} \right) \left(1 - e^{-h\nu/kT}\right) . \quad \text{(A3.57)}$$

VITA

Rufus Elbridge Bruce, Jr.

Candidate for the Degree of

Doctor of Philosophy

Thesis: A MODEL AND CALCULATIONS FOR THE PROPERTIES OF AN EXPLODING PLASMA SPHERE

Major Field: Physics

Biographical:

Personal Data: Born in New Orleans, Louisiana, March 20, 1926, the son of Rufus E. and Lucy Salles Bruce.

Education: Graduated from New Orleans, Louisiana Public High Schools, 1943; received Bachelor of Science degree from Louisiana State University, with a major in Physics, in August, 1949. Attended Louisiana State University Graduate School for one year ending 1950; received the Master of Science degree at Oklahoma State University in May, 1962; completed requirements for the Doctor of Philosophy degree in May, 1966.

Professional Experience: Teaching Assistantship at Louisiana State University, 1950, followed by eight years of commercial and management experience with teaching experience at Northeast Louisiana State College, prior to attending Oklahoma State University in 1960. Research on this problem began in 1962.